

**“Structure - gas permeation property correlations in
polybenzimidazoles and related polymers”**

Thesis submitted to the

UNIVERSITY OF PUNE

For the degree of

DOCTOR OF PHILOSOPHY

IN CHEMISTRY

BY

SANTOSH C. KUMBHARKAR

Research Guide

Dr. Ulhas K. Kharul

POLYMER SCIENCE AND ENGINEERING DIVISION

NATIONAL CHEMICAL LABORATORY

PUNE-411 008, INDIA

November 2008

Dedicated to my mother

Acknowledgements

I would like to take this opportunity to express my sincere gratitude to my research supervisor, Dr. Ulhas K. Kharul for providing me an opportunity to initiate my carrier as a Ph.D. student and offering valuable suggestions and encouragement in more stressful times. He taught me useful skills for research work as well as technical writing during the course of work.

I am grateful to Dr. S. Sivaram, Director, NCL, Dr. B. D. Kulkarni, Deputy Director, NCL and Dr. M. G. Kulkarni, Head, Polymer Science and Engineering Division for the opportunity I got to work in this prestigious institute and help during various stages of my stay at NCL. I duly acknowledged CSIR, New Delhi for valuable support in the form of a Senior Research Fellowship.

It gives me great pleasure to thank Dr. P. P. Wadgaonkar, Dr. (Mrs.) J. P. Jog, Mr. K. V. Pandare, Dr. C. Ramesh, Dr. Selvraj, Dr. J. M. Gadgil and Mrs. Dhoble for their valuable suggestions and allowing me to use facilities. I would also like to acknowledge valuable assistance of Mr. Vivek Borkar for data acquisition in sorption measurements.

The wonderful moments of my life spent with my close friends Yogesh and Harshada are unforgettable. Our friendship was very important to our collective success. It was my great pleasure to have friends like them, with whom I could share most of the things.

I would like to thank my friends Ganesh, Minakshi, Manisha, Sachin, Wasif, Aniruddha, Pinak, Avinash, Vijay, Rahul, Santosh Wanjale and Prasad Karadkar. It is difficult to forget the support I got from my lab mates Sandeep Kothawade, Yogesh Chendake, Shubhangi, Mrunal, Soumya, Prerna, Manoj Patil, Alkesh, Rupesh and Yogesh. I am thankful to them for their co-operation.

A special thanks to Mr. Soraj Singh, not only for his assistance during my work but also for encouragement.

I would like to thanks Dr. Dangat for his moral support and encouragement throughout my education.

I am forever grateful to my mother who taught me how to attempt the problems so that I could achieve the impossible. She showed me how to dream and make these dreams come true. I would not have made it without her love, efforts and blessings of my late father. I would like to thanks my Didi and Jiju for their love, prayer and assistance that have aided me to this point of my life.

Finally, I am grateful to the God, 'Shree Swami Samarth', for my continuous source of inspiration.

Certificate of Guide

Certified that the work incorporated in the thesis entitled “**Structure - gas permeation property correlations in polybenzimidazoles and related polymers**” submitted by Santosh Chandrakant Kumbharkar was carried out under my supervision. Such material as has been obtained from other sources has been duly acknowledged in this thesis.

November, 2008
National Chemical Laboratory
Pune 411 008

U. K. Kharul
(Research Guide)

Declaration by the Candidate

I declare that the thesis entitled “**Structure - gas permeation property correlations in polybenzimidazoles and related polymers**” is my own work conducted under the supervision of Dr. U. K. Kharul, at Polymer Science and Engineering Division, National Chemical Laboratory, Pune. I further declare that to the best of my knowledge, this thesis does not contain any part of work, which has been submitted for the award of any degree either of this University or any other University without proper citation.

Research Guide
(Dr. U. K. Kharul)

Research Student
(S. C. Kumbharkar)

Contents

❖	List of Schemes	i
❖	List of Figures	ii
❖	List of Tables	v

Chapter 1. Introduction

1.1.	General considerations	1
	<i>1.1.1. Advantages of membrane based gas separation processes</i>	1
	<i>1.1.2. Applications of membranes for various gas separations</i>	2
	<i>1.1.3. Membrane materials</i>	7
	<i>1.1.4. Different types of membranes</i>	9
	<i>1.1.5. Membrane modules</i>	11
1.2.	Rationale of the work	12
	<i>1.2.1. Requirements of a polymer as a membrane material</i>	12
	<i>1.2.2. Potentials of polybenzimidazole (PBI) as a membrane material</i>	13
1.3.	Scope of the work	14
1.4.	Aims and objectives	14
1.5.	Organization of thesis	15

Chapter 2. Literature survey

2.1.	Gas permeation properties: Theoretical considerations	17
	<i>2.1.1. Transport in rubbery polymers</i>	19
	<i>2.1.2. Transport in glassy polymers</i>	20
2.2.	Factors affecting gas permeation properties	25
	<i>2.2.1. Properties of gas</i>	25
	<i>2.2.2. Physical properties of polymer</i>	26
	<i>2.2.3. Operational conditions</i>	30
	<i>2.2.4. Membrane preparation parameters</i>	31
2.3.	Structure-property correlation in polymers	32

2.3.1.	<i>Substitution by non polar alkyl groups</i>	33
2.3.2.	<i>Substitution by hexafluoroisopropylidene group</i>	34
2.3.3.	<i>Substitution by polar groups</i>	35
2.3.4.	<i>Effect of isomerism</i>	36
2.3.5.	<i>Substitution by trimethylsilyl group</i>	36
2.4.	CO₂ sorption and permeation: promising materials	37
2.4.1.	<i>CO₂ separation using alkanol amine</i>	37
2.4.2.	<i>CO₂ separation using ionic liquids</i>	38
2.4.3.	<i>CO₂ separation using poly(ionic liquid)s</i>	39
2.5.	Properties and applications of polybenzimidazole (PBI)	41
2.6.	Permeation properties of PBI	44
2.7.	Structural variations in PBI	45
2.7.1.	<i>Variations in diamine and diacid moiety</i>	
2.7.2.	<i>PBI modification</i>	49
2.8.	Synthetic routes of PBI	51
2.8.1.	<i>Melt and solid-state polymerization</i>	51
2.8.2.	<i>Low and high-temperature solution polymerization</i>	52

Chapter 3. Experimental

3.1.	Monomers and materials	57
3.2.	Synthesis of PBIs based on 3,3'-diaminobenzidine (DAB) and aromatic dicarboxylic acids	57
3.3.	Synthesis of poly(2,5-benzimidazole) (ABPBI)	58
3.4.	N-substitution of promising PBIs	60
3.4.1.	<i>N-substitution of PBI based on isophthalic acid (PBI-I) and 5-tert-butyl isophthalic acid (PBI-BuI)</i>	60
3.4.2.	<i>N-substitution of ABPBI</i>	61
3.5.	PBI quaternization and subsequent ion-exchange to obtain PIL	62
3.5.1.	<i>N-quaternization of PBI-I and PBI-BuI</i>	62
3.5.2.	<i>N-quaternization of ABPBI</i>	62
3.5.3.	<i>Anion exchange of N-quaternized PBIs</i>	64
3.6.	Dense membrane preparation	65

3.7. Polymer characterizations	65
3.8. Gas sorption and permeation analysis	67

Chapter 4. Variations in acid moiety of PBI based on DAB: Synthesis, characterization and investigation of gas permeation properties

4.1. Synthesis	71
4.2. Physical properties	72
4.2.1. <i>Solubility and spectral characterizations</i>	72
4.2.2. <i>Density and free volume</i>	77
4.2.3. <i>Thermal stability</i>	79
4.2.4. <i>Water sorption</i>	81
4.3. Gas permeation properties	81
4.3.1. <i>Initial explorations on gas permeation properties of PBIs based on different dicarboxylic acids</i>	81
4.3.2. <i>Sorption properties</i>	84
4.3.3. <i>Gas permeability</i>	88
4.3.4. <i>Gas diffusivity</i>	89
4.3.5. <i>Comparison of permeation properties</i>	93

Chapter 5. Effects of N-substitution of PBI on physical and gas permeation properties of resulting polybenzimidazoles

5.1. Synthesis, FT-IR and ¹H-NMR characterization	95
5.2. Physical Properties	101
5.2.1. <i>Solvent solubility and viscosity</i>	101
5.2.2. <i>Packing density parameters</i>	103
5.2.3. <i>Thermal properties</i>	105
5.3. Permeation properties	107
5.3.1. <i>Sorption Properties</i>	107
5.3.2. <i>Gas permeability</i>	116
5.3.3. <i>Diffusion properties</i>	117

Chapter 6. Investigations in polymeric forms of ionic liquids (PILs) based on polybenzimidazoles: Emphasis on CO₂ permeation properties

6.1. Synthesis	122
6.1.1. <i>N</i> -quaternization of PBI to obtain polymeric forms of ionic liquids (PIL)s	122
6.1.2. Estimation of degree of substitution	123
6.1.3. Anion exchange	125
6.2. Physical properties	126
6.2.1. Solvent solubility	126
6.2.2. Spectral characterizations and density	128
6.2.3. Solution viscosity	132
6.2.4. Thermal properties	135
6.3. Permeation properties	136
6.3.1. Sorption properties	136
6.3.2. Gas permeability and diffusivity	141

Chapter 7. Conclusions

References 151

Synopsis

Publications

List of Schemes

- Scheme 2.1.** General structure of polybenzimidazole (PBI)
- Scheme 3.1.** Synthesis of PBI by condensation of DAB with aromatic dicarboxylic acids
- Scheme 3.2.** Synthesis of ABPBI
- Scheme 3.3.** *N*-substitution of (a) PBI-I and (b) PBI-BuI
- Scheme 3.4.** *N*-substitution of ABPBI
- Scheme 3.5.** *N*-quaternization of (a) PBI-I and (b) PBI-BuI
- Scheme 3.6.** *N*-quaternization of ABPBI

List of Figures

- Figure 2.1.** Time-lag measurement of gas permeation
- Figure 2.2.** Schematic representation of dual-mode sorption
- Figure 2.3.** Theoretical pressure dependence of permeability coefficient obeying to partial immobilization model [Paul (1976)]
- Figure 3.1.** Gas sorption equipment
- Figure 3.2.** Gas permeation equipment
- Figure 4.1.** FTIR spectra of polybenzimidazoles (a: PBI-I, b: PBI-T, c: PBI-BuI, d: PBI-HFA, e: PBI-BrT, f: PBI-DBrT, g: PBI-2,6Py)
- Figure 4.2.** ^1H -NMR spectra of polybenzimidazoles (a: PBI-I, b: PBI-T, c: PBI-BuI, d: PBI-HFA, e: PBI-BrT, f: PBI-DBrT)
- Figure 4.3.** WAXD spectra of polybenzimidazoles (a: PBI-I, b: PBI-T, c: PBI-BuI, d: PBI-HFA, e: PBI-BrT, f: PBI-DBrT, g: PBI-2,6Py)
- Figure 4.4.** TGA spectra of polybenzimidazoles (a: PBI-I, b: PBI-T, c: PBI-BuI, d: PBI-HFA, e: PBI-BrT, f: PBI-DBrT, g: PBI-2,6Py)
- Figure 4.5.** Equilibrium sorption isotherm for polybenzimidazoles investigated at 35 °C (Δ : H_2 , \circ : N_2 , +: O_2 , \times : CH_4 , \square : CO_2)
- Figure 4.6.** Correlation of solubility coefficient (S), with Lennard-Jones force constant, (ϵ/κ) (--- : PBI-I; — : PBI-BuI; - - - - : PBI-HFA)
- Figure 4.7.** Correlation of solubility coefficient (S) with fractional free volume, v_f (\circ : N_2 , +: O_2 , \times : CH_4 , \square : CO_2)
- Figure 4.8.** Correlation of diffusion coefficient (D) with (a) kinetic diameter (--- : PBI-I; — : PBI-BuI; - - - - : PBI-HFA) and (b) with v_f (Δ : H_2 , \circ : N_2 , +: O_2 , \times : CH_4 , \square : CO_2) for gases at 35 °C
- Figure 4.9.** Correlation of diffusion coefficient (D) with solubility parameter (δ) (Δ : H_2 , \circ : N_2 , +: O_2 , \times : CH_4 , \square : CO_2)
- Figure 4.10.** Occurrence of polybenzimidazoles on Robeson upper bound [Robeson (1991)] (\diamond : PBI-I, Δ : PBI-BuI, \square : PBI-HFA)

- Figure 5.1.** FT-IR spectra of *N*-substituted polybenzimidazoles at (a) ambient and (b) higher temperature (150/250 °C)
- Figure 5.2.** ¹H-NMR spectra of *N*-substituted PBI-I
- Figure 5.3.** ¹H-NMR spectra of *N*-substituted PBI-BuI
- Figure 5.4.** ¹H-NMR spectra of SABPBI
- Figure 5.5.** WAXD spectra of *N*-substituted polybenzimidazoles
- Figure 5.6.** TGA spectra of *N*-substituted polybenzimidazoles
- Figure 5.7.** Sorption isotherms for *N*-substituted PBI-I at 35 °C (Δ: H₂, ○: N₂, +: O₂, ×: CH₄, □: CO₂)
- Figure 5.8.** Sorption isotherms for *N*-substituted PBI-BuI at 35 °C (Δ: H₂, ○: N₂, +: O₂, ×: CH₄, □: CO₂)
- Figure 5.9.** Sorption isotherms for *N*-substituted ABPBI at 35 °C (Δ: H₂, ○: N₂, +: O₂, ×: CH₄, □: CO₂)
- Figure 5.10.** Correlation of Langmuir saturation constant (C'_H) with Tg-35 (°C) (○: N₂, ×: CH₄, □: CO₂)
- Figure 5.11.** Correlation of solubility coefficient (S) at 20 atm with Lennard-Jones force constant (ϵ/k)
- Figure 5.12.** Correlation of permeability coefficient (P) with fractional free volume (v_f) (Δ: H₂, ○: N₂, +: O₂, ×: CH₄, □: CO₂)
- Figure 5.13.** Correlation of Diffusion coefficient of gases in *N*-substituted PBI with (a) v_f (Δ: H₂, ○: N₂, +: O₂, ×: CH₄, □: CO₂) and (b) kinetic diameter of H₂, CO₂, O₂, N₂ and CH₄
- Figure 6.1.** ¹H-NMR spectra of PILs
- Figure 6.2.** FT-IR spectra of PILs at (a) ambient and (b) 150 °C
- Figure 6.3.** Wide angle X-ray diffraction spectra of PILs
- Figure 6.4.** Viscosity of PILs as a function of polymer concentration in DMSO at 35 °C
- Figure 6.5.** Fuoss plot of PILs in DMSO at 35 °C
- Figure 6.6.** TGA spectra of PILs (a: TMPBI-I·I; b: TMPBI-I·BF₄; c: TMPBI-I·Tf₂N;

d: TMPBI-BuI·I; e: TMPBI-I·BF₄; f: TMPBI-I·Tf₂N; g: DMABPBI-I·I; h: DMABPBI-I·BF₄)

Figure 6.7. Sorption isotherms for PILs at 35 °C (Δ : H₂, \circ : N₂, \times : CH₄, \square : CO₂)

Figure 6.8. Correlation of diffusion coefficient with kinetic diameter (Å) of gases in PILs at 35 °C

Figure 6.9. Occurrence of PBI-I based PILs(\blacksquare) and PBI-BuI based PILs (\square) on Robeson's plot [Robeson (1991)] (a) PBI-I; (b) TMPBI-I·BF₄; (c) TMPBI-I·Tf₂N; (d) PBI-BuI; (e) TMPBI-BuI·BF₄; (f) TMPBI-BuI·Tf₂N

List of Tables

- Table 2.1.** Permeation properties of PBI based on isophthalic acid
- Table 2.2.** Different tetramines used for the synthesis of PBI
- Table 2.3.** Different dicarboxylic acids/derivatives used for the synthesis of PBI based on DAB
- Table 4.1.** Reaction parameters for polybenzimidazole synthesis
- Table 4.2.** Solubility of polybenzimidazoles in solvents
- Table 4.3.** Physical properties of polybenzimidazoles
- Table 4.4.** H₂ and O₂ permeability (P)^a and selectivity (α)^b of polybenzimidazoles
- Table 4.5.** Dual-mode sorption parameters^a for polybenzimidazoles
- Table 4.6.** Solubility coefficient^a and solubility selectivity of polybenzimidazoles
- Table 4.7.** Permeability coefficient^a and permselectivity of polybenzimidazoles
- Table 4.8.** Diffusivity coefficient^a and diffusivity selectivity of polybenzimidazoles
- Table 5.1.** Solubility of *N*-substituted PBI in common solvents
- Table 5.2.** Physical properties of *N*-substituted PBI
- Table 5.3a.** Dual-mode sorption parameters^a for *N*-substituted PBI-I
- Table 5.3b.** Dual-mode sorption parameters^a for *N*-substituted PBI-BuI
- Table 5.3c.** Dual-mode sorption parameters^a for *N*-substituted ABPBI
- Table 5.4.** Solubility coefficient (S)^a and solubility selectivity (S_A/S_B) of *N*-substituted PBI
- Table 5.5.** Permeability coefficient (P)^a and permselectivity (P_A/P_B)^b of *N*-substituted PBI
- Table 5.6.** Diffusivity coefficient (D)^a and diffusivity selectivity (D_A/D_B) of *N*-substituted PBI
- Table 6.1.** Solvent solubility of PILs
- Table 6.2.** Physical properties of PILs
- Table 6.3.** Dual-mode sorption parameters^a
- Table 6.4.** Solubility coefficient (S)^a and solubility selectivity (S_A/S_B) of PILs
- Table 6.5.** Permeability coefficient (P)^a and permselectivity (P_A/P_B)^b of PILs
- Table 6.6.** Diffusivity coefficient (D)^a and diffusivity selectivity (D_A/D_B) of PILs

Chapter 1

Introduction

1.1. General considerations

Industrial scale gas separations rely mainly on cryogenic distillation, adsorption and membrane based processes. The separation of gas mixtures with membranes has emerged from being a laboratory curiosity to the successful industrial operation, which is growing rapidly owing to demand based newer material developments and advancement of engineering aspects. The first generation Prism membrane demonstrated the feasibility of the membrane process for H₂ recovery from ammonia purge gas in 1980 [Zolandz (1992), Paul (1993)]. This was followed by the newer material developments leading to the successful demonstration of various separations, viz., CO₂/hydrocarbon, O₂/N₂, H₂/hydrocarbon, H₂/N₂ and H₂O/hydrocarbon separation [Nunes (2001)]. These applications are economically competitive over conventional technologies owing to inherent advantages of membrane process [Strathman (1981), Paul (1993), Stern (1994), Mulder (1998), Scholes (2008)]. Though a large fraction of overall requirement of industrial gas separation is still met by conventional processes (cryogenic distillation or pressure swing adsorption), membranes are gaining increasing importance owing to such inherent process advantages. This ultimately becomes a major thrust for advancement of membrane technology on all aspects, including membrane material development, to meet newer challenges those bring economical benefits for newer applications.

1.1.1. Advantages of membrane based gas separation processes

Gas separation using polymeric membrane is becoming highly competitive over conventional technologies owing to following advantages.

i) Lower capital and operating cost

Membrane systems are skid mounted. Therefore, scope, cost and time taken for site preparation are minimal. Their installation costs are significantly lower. Membrane units do not require additional gadgets (solvent storage, water treatment, etc.) [Aaron (2005)]. The only major cost is for membrane replacement, which is significantly lower than the solvent replacement and energy costs associated with traditional technologies.

ii) Operational simplicity and high reliability

Membrane based systems are simple to operate and can be operated unattended for longer periods [Dortmundt (1999), Aaron (2005)]. Conversely, absorption /adsorption require regeneration of solvent/sorbents. These separation processes are carried out in cycles involving complicated operations, which necessitates well trained manpower.

iii) Weight and space efficiency

Due to the compact nature of membrane devices, they are usually less voluminous [Li (2005)]. Skid construction can be easily optimized to fit multiple elements into tubes to increase space efficiency. This space efficiency is especially important for offshore operations where energy and space management gains prime importance. This makes membranes more attractive for remote locations.

iv) Easy scale-up

The modularity of membrane modules makes the design simple and easy to be scaled up linearly [Li (2005)].

vi) Design efficiency

Membrane and pretreatment systems integrate certain operations such as dehydration, CO₂ and H₂S removal, dew point control, etc. Usually, traditional CO₂ removal technologies require these operations as separate processes [Dortmundt (1999)].

vii) Environment friendly

Membrane processes rely on physical separation and thus do not involve handling of solvents or other chemicals for separation. Thus, they are environment friendly.

v) Easy adaptability for various feed CO₂ concentration

Since membrane area is dictated by the percentage of CO₂ removal rather than absolute CO₂ removal, small variation in feed CO₂ content can hardly change the sales-gas CO₂ specification [Dortmundt (1999)].

1.1.2. Applications of membranes for various gas separations

Membrane based gas separations find wide applicability as discussed below.

I) Hydrogen separations

Hydrogen recovery was among the first wide-scale commercial applications of membranes [Koros (2000)]. H₂ has reasonably high selectivity over other components of gaseous mixture, with which it is commonly associated. Most of the H₂ recovery falls in

to one of the three broad categories; a) Syn gas ratio adjustment; b) H₂ recovery from hydroprocessing purge streams; c) H₂ recovery from ammonia plant purge streams and other petrochemical plant streams.

a) *Syngas ratio adjustment*

Syngas contains H₂ and CO along with impurities such as CO₂, CH₄, N₂ and water. It can be used as the mixture with desired composition or separated in to a high purity component. Syngas is generally produced from hydrocarbons by (i) reforming natural gas or light hydrocarbons and (ii) partial oxidation of heavy oils [Kesting (1993)]. The H₂/CO ratio of the feed varies depending on its source, whereas the desired ratio for the product depends on the synthesis in which the gas is to be used. Syngas made via steam reforming has 3:1 H₂/CO ratio, whereas typical application requires a ratio of between 0 and 2.1 [Zolandz (1992)]. Membranes are ideally suited for stripping H₂ out of the syngas in order to reduce the H₂/CO ratio [Zolandz (1992)].

b) *H₂ recovery from hydroprocessing purge streams*

In petroleum refining, H₂ is increasingly needed to process heavy and sour crudes. Various purge and off gases are produced, where H₂ content of these streams ranges from 15 to 80%. A purity of 90 to 95% is required to recycle the H₂ to a processing unit, which is achieved by membranes as H₂ rich permeate stream [Zolandz (1992)].

c) *H₂ recovery from ammonia and methanol plant purge streams*

This was the first wide spread use of gas separation membranes, using Permea's PrismTM system. In the ammonia process, H₂ and N₂ are reacted directly to produce ammonia. Argon, arriving with the N₂ from air and methane arriving with the H₂, accumulate as inerts within the ammonia reactor. Ammonia is produced along with a gas that contains approximately 60% H₂, 5% Ar, 15% CH₄ and 20% N₂ [Zolandz (1992)]. This gas can be recycled to the reactor, but a purge is required to prevent the build up of inerts. Without a separation process, all of the H₂ in this purge stream is lost from the process and must be replaced by H₂ generated from methane or obtained from other sources. Membrane system processing this high-pressure (excess of 100 atmospheres) purge typically recover over 90% of the H₂ from these purge gas [Zolandz (1992)].

Membranes are also used to recover H_2 from methanol plant purge gas. The recovered H_2 is recycled back to the reactor, leading to higher yield and lower operating costs [Zolandz (1992)].

II) Helium separations

Helium is used as a diluent in breathing gas mixtures used by deep sea divers. Membranes can be used to recover He from spent gas [Zolandz (1992)].

III) Oxygen and nitrogen enrichment

Generation of N_2 and N_2 -rich atmospheres has become one of the largest uses for gas separation membranes [Nunes (2001)]. The process involves passing compressed air across the membrane. Since O_2 permeate faster, reject stream is enriched in N_2 .

The primary utility for N_2 is an inerting atmosphere, typically for fire suppression. The critical O_2 concentration (minimum level of O_2 to sustain combustion), is typically below 12% for many hydrocarbons and organic compounds [Nunes (2001)]. Thus membrane-generated N_2 with minimal O_2 concentration (below 3%) finds ready application where flammable materials are stored, processed or handled. Many fruits, vegetables and their products are also preserved by maintaining low O_2 atmosphere [Nunes (2001)]. Besides, membrane-generated N_2 also finds application for inerting metal process furnaces in metal industry, for blanketing of fuel tanks and as a replacement for compressed air for tyre inflation [Nunes (2001)].

O_2 enrichment finds applications for medical purposes as well as for enhanced combustion purposes. Commercial-scale market for the later application is yet to reach its full potential. Current membranes are not capable of economically producing comparable purity, and only a limited number of applications that can utilize low-purity O_2 (25 - 50%) are served by polymeric membranes [Koros (2000)].

IV) Acid gas separation

Commercial acid gas removal applications include pipeline grade natural gas production, CO_2 recovery and recycle in enhanced oil recovery (EOR), methane recovery from landfill and biogas and CO_2 recovery from flue gases.

a) Natural gas production

Natural gas is a complex mixture containing desirable gaseous hydrocarbons and non-hydrocarbon components such as H_2S , CO_2 and water. Removal of H_2S and CO_2

from the desired lower hydrocarbons is an important processing operation, since they can corrode pipelines as well as reduce the energy content of the gas [Koros (2000)]. The pipeline specifications for these components are $< 2\%$ for CO_2 and < 4 ppm for H_2S [Bhide (1998)]. In combination with water, they are highly corrosive. In LNG plants, CO_2 must be removed to prevent freezing in the low-temperature chillers.

b) *Enhanced oil recovery (EOR)*

In the EOR process, CO_2 is injected in to the oil bearing strata at pressures in excess of 1000 psi [Zolandz (1992)]. CO_2 dissolves the oil and carries it to the producing wells. The overhead offgas consists of CO_2 , CH_4 and other hydrocarbons, N_2 and often H_2S . For economic and environmental reasons, removal of CO_2 ($\sim 95\%$ purity to maintain its solvent power) from the offgas is done by membrane based processes.

c) *Biogas processing*

Membrane can be used to recover CH_4 from biogases such as landfill gas, which contains typically 40 to 45% CO_2 , 50 - 56% CH_4 and 0.5 - 1% other contaminants [Zolandz (1992)]. In this recovery, membrane produce enriched CH_4 at the elevated feed pressure and a low pressure CO_2 as the by-product.

d) *CO₂ separation from flue gases*

Out of the total CO_2 emitted to the earth's atmosphere, its large portion comes from fossil fuel power plants [Aaron (2005)]. Flue gases typically contain N_2 , CO_2 , H_2O , NO_x , SO_x , CO , O_2 and particulate matter [Aaron (2005)]. N_2 , CO_2 , and water vapor are generally the major components, accounting for $>90\%$ of this stream [Huang (2008)]. The capture and storage of CO_2 has been identified as a potential solution to greenhouse gas driven climate changes. Membrane based gas separation is competitive over conventional technologies for CO_2 capture [Scholes (2008)]. A wide range of polymeric membranes with reasonable permeability and selectivity to CO_2 are known. Some patented polymeric membranes which have performance around Robeson's upper bound are based on polyamides, polysemicarbazides, polycarbonates, polyarylates, poly(phenylene oxide), polyaniline and polypyrrolones [Scholes (2008)]. However, most of the commercially available membranes are not suitable for high-temperature and high-humidity operation, which is required in the direct CO_2 capture from the flue gas in power plants [Koros (2000), Bredsen (2004)]. For the specific application of CO_2 capture

from the flue gas, a CO₂/N₂ selectivity of >70 and a minimum CO₂ permeability of 100 Barrers (a permeance of 1000 GPU) are required for the economic operation [Hirayama (1999)]. In an another approach, Guo et al. (2006) reported the stainless-steel-net-imbedded silicalite-1 zeolite membrane. Such membranes showed increase in CO₂/N₂ separation factor from 68.7 to 75 when the temperature was decreased from 20 to 0 °C.

e) CO₂/H₂ separation

H₂ is usually produced via steam reforming of hydrocarbons and is contaminated with CO₂. In order to obtain high purity hydrogen from either syngas or the products of the water-gas shift reaction, separation of H₂ from either CO or CO₂ is necessary [Lu (2007)]. Although polymeric membranes have been used for H₂ separation, particularly for low temperature applications for many years, the high temperature stability issue limits the applications of these membranes for H₂ production [Lu (2007)]. However, inorganic membrane systems for H₂ separation and for membrane reactors involving the removal of H₂ show promises. H₂-permeable inorganic membranes composed of either a porous ceramic or dense metal have been reported [Armor (1989)]. They show promises in membrane reactor involving water-gas shift reaction due to their high temperature stability and durability in harsh environment [Lu (2007)]. Besides this, H₂ separation membranes designed for chemically harsh, high-temperature processes, such as H₂S dehydrogenation are also reported [Edlund (1993), Ohashi (1998)].

V) Emerging applications

a) Gas dehydration and separation of organic vapors

Membranes can also be used for gas dehydration. Moist pressurized air is fed to one side of the membrane, while dry gas at approximately ambient pressure on the opposite side. Membranes can also be used to separate organic vapors from air. Rubbery polymers show extremely high permeation rates for many solvents, which results in high solvent-to-air selectivities.

b) Reverse selective membranes

Highly efficient membrane materials which are more permeable to large impurity molecules, CO₂, than to H₂ produce purified H₂ at high pressure. This, so-called reverse selective behavior is opposite to that exhibited by the vast majority of polymers [Lin

(2004)]. Materials based on poly(ethylene glycol)diacrylate showed CO₂/H₂ selectivity from 19 to 40 and CO₂ permeability from 6.6 to 52 Barrers at 253 K [Lin (2004)].

c) Membrane reactor

The water–gas shift reaction is one of the most important industrial reactions that can be used to produce H₂ for ammonia synthesis, adjust the H₂-CO ratio of synthesis gas and to produce H₂ for fuel cell applications [Lu (2007)]. By extracting H₂ from the reaction mixture through membrane, a reaction is shifted towards the products, thus giving a higher conversion with respect to the equilibrium values. The unique H₂ selective ability of membranes have significant potential in membrane reactors where constant removal of reaction products could lead to catalyst reductions, reduced operation size, reduced expenses and improved temperature and pressure conditions. Membranes are excellent candidates for H₂ purification, especially when incorporated with membrane reactor combining reaction/separation in a single unit [Lu (2007)].

1.1.3. Membrane materials

Synthetic membranes can be categorized in to polymeric and inorganic in nature.

i) Polymeric membranes

Non-porous polymeric membranes based on solution-diffusion mechanism have been intensively employed in current commercial membrane devices [Spillman (1989), Meindersma (1996)]. Majority of commercial membranes are made from synthetic polymers and can be glassy or rubbery in nature, depending upon the target gas separation. Typically, polymers have advantages of desirable mechanical properties and economical processing capabilities. Out of a large number of polymers described in the literature proposed for gas separation, choice of a polymer as the membrane material is not arbitrary, but is based on very specific properties, originating from structural factors. Most commonly used glassy polymeric membranes for gas separation are cellulose acetate (CA), polyimide (PI), polysulfone (PSF), polycarbonate (PC); whereas; polydimethylsiloxane (PDMS) is the commonly used rubbery polymers for vapor separation. Effects of structural variations in polymer backbone on permeation properties are elaborated in Section 2.3. The ultra-high free volume polymers aroused much interest in membrane research after the publication of physical properties of poly(*I*-

trimethylsilyl-1-propyne) (PTMSP) in 1983 [Masuda (1983)]. PTMSP though is a glassy polymer, showed permeabilities more than 10 times higher than rubbery PDMS. Besides this, Du pont's Teflon AF2400® and poly(4-methyl-2-pentyne) (PMP) were also developed. The theoretical aspect of permeation in polymeric materials is elaborated in Section 2.3.

ii) Inorganic membranes

Different types of inorganic membranes frequently used may be distinguished as ceramic membranes; glass membranes; metallic membranes and zeolitic membranes. Ceramics are formed by combination of a metal (eg. aluminium, titanium, silicium or zirconium) with a non-metal in the form of an oxide, nitride or carbide. They possess superior chemical and thermal stability relative to polymeric membranes. Nevertheless, their use as membrane material has been limited due to disadvantages such as brittleness and high cost, although a growing interest can now be observed. The main obstacle is said to be their high price and reproducible large-scale production [Nunes (2001)]. Palladium based alloys are the only class of inorganic membrane materials, which are currently used on commercial scale for ultra-pure H₂ generation.

Porous ceramic, particularly microporous membranes possess high permeability, chemical and thermal stability. Thus, they are attractive for H₂ production reactions. Carbon molecular sieve membranes are reported for refiner gas separation and hydrogen recovery. They have demonstrated in pilot scale studies that carbon molecular sieve membranes can be very efficient for separating H₂ from refiner gas streams [Lu (2007)]. Air products and Chemicals Inc. has employed such technology for H₂ enrichment to 56 - 60% prior to PSA to produce 99.99% H₂ [Lu (2007)]. Molecular sieves such as zeolites or carbon molecular sieves show higher selectivity for many gas mixtures than polymeric membranes due to their defined pore sizes. There are reviews describing recent progresses in the preparation, characterization and applications of various zeolitic membranes of the types MFI, LTA, MOR, FER and FAU [Cot (2000), Caro (2000)]. The separation of gases was shown to be based on differences of adsorption or diffusion rates, rather than on size exclusion like in LTA- or MFI-type zeolite membranes.

1.1.4. Different types of membranes

Gas separation membranes can be classified in to different types as follows.

i) Dense membranes

Membranes prepared by solution casting method are usually dense membranes. This method involves evaporation of solvent from the polymer solution. Such membranes are of academic interest and are prepared for investigation of structure-gas permeability correlation. In order to have high flux, usual choice is to make a selective layer as thin as possible to increase the permeability. However, reduced thickness also reduces the mechanical strength and therefore is unusable as such. A solution to this problem with an introduction of asymmetric membrane allowed to break this limitation.

ii) Asymmetric membranes

These membranes consists of a very dense top layer (thickness $< 0.5 \mu\text{m}$) supported by a porous sub layer (thickness 50-200 μm) [Loeb (1962)]. The top layer or skin determines the transport rate, while the porous sublayer of the same polymeric material acts as a support. Drawbacks that they are composed of only one material, are costly to make out of exotic, customized polymers (which often can be produced only in small amounts) are overcome by producing a composite membrane.

iii) Composite membranes

Composite membranes consist of a thin toplayer and porous sublayer originating from different polymeric materials. Their advantage is that each layer can be independently optimized to obtain optimal membrane performance with respect to selectivity, permeation rate and thermo-chemical stability. Several techniques can be used to apply thin top layer upon a support, such as dip coating, spray coating, spin coating, interfacial polymerization, plasma polymerization, grafting etc. Major limitations for composite membrane preparation include (i) porous materials compatibility with the processing conditions used in applying the selective layer and (ii) difficulty of adhesion of the skin to the porous support owing to differences with respect to their thermal, mechanical, shrinkage, solvent swelling properties. This leads to cracking/delamination of the top skin layer. Issue of adhesion can be overcome by using porous support of the same class of polymer. Du Pont applied a speciality polymer (polyimide) as a thin layer on a polyimide support made of commercial low cost polyimide polymer [Nunes (2001)].

iv) Mixed matrix membranes

Molecular sieves such as zeolites or carbon molecular sieves show a much higher selectivity for many gas mixtures than polymeric membranes due to their defined pore sizes. The preparation of defect-free zeolite layers on a large scale is extremely difficult. However, the combination of the superior gas selectivities of molecular sieves with the processibility of polymeric membranes is one of the new approaches for gas separation membrane and has attracted many researchers. Such hybrid membranes are referred to as mixed matrix membranes. In spite of studies on many conventional polymers, only a few attempts to increase gas separation membrane performance with dense film mixed matrices of zeolite and rubbery or glassy polymers have been reported [Kulprathipanja (1988), Jia (1991), Duval (1993), Gür (1994), Zimmerman (1997)]. However, material selection for both matrix and sieve phases is a key aspect in the development of mixed-matrix membranes [Zimmerman (1997)]. The matrix polymer selected must provide a commercially acceptable performance, and this limits the choice of candidate materials greatly [Mahajan (2000)].

v) Supported liquid membranes (SLMs)

SLMs contain liquids (carbonates or alkanol amine solutions) impregnated into pores of the membrane. The separation is governed by the liquid, whereas the porous membrane acts as a support. This type of configuration provides high surface area for the separation per unit contact volume. Microporous PTFE-hollow fiber membrane absorbers were used for separation of CO₂-N₂ mixture [Kim (2000)]. The absorbents used were monoethanolamine, methyl-diethanolamine and 2-amino-2-methyl-1-propanol. Selective removal of acid gases from a contaminated gas stream uses diethylenetriamine (DETA), diaminoethane (DAE), diethylamine (DEYA), and bis(2-ethylhexyl)-amine (BEHA) as immobilized liquids in a facilitated transport membrane [Al Marzouqi (2005)]. For CO₂/N₂ mixtures, use of glycerol carbonate [Kovvali (2002)], sodium carbonate-glycerol [Chen (2000, 2001)], dendrimer and solutions of Na₂CO₃-glycerol [Kovvali (2001)] in an immobilized liquid membrane configuration are proposed. Industrial applications of SLMs are scarce due to poor stability and long-term performance [Kemperman (1996)]. These effects were attributed to the loss of solvent from the supporting membrane, either by evaporation or dissolution/dispersion [Takeuchi (1987)]. Approaches to minimize

instability include use of mild operating conditions, protection of the SLM with a gel layer [Kemperman (1998)], adequate design of supporting membranes and the contacting phases [Danesi (1987)].

1.1.5. Membrane modules

For practical application, large membrane areas are required. The smallest unit to which the membrane area is packed is called a module. A number of module designs are possible and all are based on two types of membrane configurations: flat and tubular. Plate-and-frame and spiral-wound modules involve flat membranes; whereas tubular, capillary and hollow fiber modules are based on tubular membrane configurations.

i) Plate-and-frame module

In this module, two membranes are sandwiched so that their feed sides face each other. In each feed and permeate compartment, a suitable spacer is placed. Number of such sets needed for a given membrane area furnished with sealing rings and two end plates builds up a plate-and-frame module. The packing density (membrane surface per module volume) of such modules is about 100-400 m²/m³ [Mulder (1998)].

ii) Spiral-wound module

In this arrangement, two flat sheet membrane with a permeate spacer in between are glued along three of their sides to form an envelope (or *leaf*), that is open at one end. Many of these envelopes are separated by feed spacers and wrapped around a permeate tube with their open ends facing the permeate tube. Feed gas enters along the side of the membrane and passes through the feed spacers separating the envelopes. As the gas travels between the envelopes, highly permeable species permeate into the envelope. The packing density of this type of modules is 300-1000 m²/m³ [Mulder (1998)].

iii) Tubular module

The difference between modules based on tubular configuration arises mainly from the dimensions of the tubes employed. The dimensions of the pore diameter is > 10 mm for tubular module, 0.5-10 mm for capillary module and < 0.5 mm for hollow fiber module. Tubular membranes are placed inside a porous stainless steel, ceramic or plastic tube. The packing density of tubular module is rather low < 300 m²/m³ [Mulder (1998)].

iv) Capillary module

This module consists of a large number of capillaries assembled together. Free ends of fibers are potted with epoxy resins, polyurethanes or silicone rubber. Unlike tubular membranes, these membranes are self supporting. A packing density for these modules is about 600-1200 m²/m³ [Mulder (1998)]. Two types of module design can be distinguished, whether the feed fluid passes through bore of the capillary (tube-side feed) or it enters the module from the shell (external) side of capillaries (shell-side feed).

v) Hollow fiber module

In hollow fiber, the feed can enter inside the fiber (inside-in) or from the outside (outside-in) as in capillary modules. This type of module has the highest packing density, which can attain values of 30,000 m²/m³ [Mulder (1998)]. In gas separation, the module with outside-in design is used to avoid high pressure losses inside the fiber and to attain a high membrane area.

1.2. Rationale of the work

1.2.1. Requirements of a polymer as a membrane material

Commercial viability of a membrane is largely dictated by its flux and selectivity towards desired component of a gas mixture. The intrinsic permeability and selectivity of the polymer which was used for the membrane preparation are governed by its physical properties. These include chain packing density, segmental motions (glass transition and sub-T_g relaxations) and interactions with penetrants. In view of long term sustainability of the membrane, polymer material used for membrane preparation should be resistant to plasticization (caused usually by acid gases and organic vapors) under high operational pressure. In order to resist plasticization, the polymer chains should be highly rigid, which can also be brought up by crosslinking.

Applicability of polymeric membranes for gas separation is largely confined to near ambient temperatures. This is due to loss of selectivity by increased segmental motion as the temperature increases. In order to widen the applicability of polymeric membranes at higher operational temperatures, polymeric materials that have lower segmental motion combined with high thermal stability are required. The rigidity in the polymer matrix is brought either by incorporating aromatic groups, substitution of rigid

and bulky groups on the polymer backbone or by crosslinking of polymer chains. Increasing aromaticity increases thermal stability of a polymer in addition to increase in the glass transition temperature, T_g , which is not necessarily always obeyed by crosslinking, since it also depends on nature of crosslinker as well.

Some of the glassy polymers like polycarbonate, polyarylate, polyamides, etc. are known for structure-gas permeation property relationship and are well explored for near ambient temperature applications. Wholly aromatic poly(ether ketone) is one of the thermoplastics with excellent mechanical property, high thermal stability, solvent resistance and considerable toughness [Chivers (1994)]. Effects of structural variations in polysulfone on their gas permeation and physical properties are reported [Mchattie (1991a, 1992)]. Polyimides also have excellent thermo-chemical stability, mechanical strength and are investigated widely for effects of structural variations in diamine/dianhydride moiety on gas permeation properties [Kim (1988), Stern (1994), etc.]. Poly(ether ether ketone)s by alkyl group substitution are known to increase gas permeability [Handa (1997)]. Polytriazole combine good thermal stability and chemical resistance with processability. The gas permeation properties of aromatic poly-1,2,4-triazole and poly-1,3,4-oxadiazole have been investigated [Hensema (1994)].

1.2.2. Potentials of polybenzimidazole (PBI) as a membrane material

Aromatic polybenzimidazoles, a class of heteroaromatic polymers have rigid molecular structure, excellent thermo-oxidative stability, high T_g , high chemical resistance and retention of its mechanical properties at high temperature [Vogel (1961, 1963), Földes (2000)]. Due to high thermo-oxidative stability, it finds applications in aerospace and has also been well explored as the proton exchange membrane (PEM) material for fuel cell application. These characteristics suggest the potential of PBI to be used as the gas separation membrane material, where harsher chemical / temperature environments are involved. At the time of beginning this work, only a single report was available on the gas permeability of polybenzimidazole based on 3,3'-diaminobenzidine (DAB) and isophthalic acid (IPA) [Pesiri (2003)]. Subsequently, Klaehn et al. (2005) and He et al. (2006) reported permeability of this polymer.

1.3. Scope of the work

Investigation on gas permeation properties of polybenzimidazoles as a family of polymers is almost unaddressed in the literature. PBI based on DAB and IPA, the only member of this family is investigated for gas permeability [Pesiri (2003), Klaehn (2005), He (2006)]. The monomers of this polymer, i.e. tetramine and dicarboxylic acid can suitably be substituted by an appropriate group prior to the polymer synthesis. Alternatively, polymer modification using convenient groups can also be possible. It was thought that through appropriate structural architecture, it could be possible to enhance gas permeability and solvent solubility without major compromise in thermal properties, and thus became the objective of this work.

It has been reported in the literature that ionic liquids (IL) possess exceptionally high CO₂ sorption. Most of these ILs are based on imidazolium as the cationic species. It was thought to extend this characteristic of ILs having high CO₂ sorption to the polymeric forms of ionic liquids based on polybenzimidazole after appropriate structural variations. PBI substituted with suitable alkyl group can be converted into these polymeric forms of ionic liquids (PILs). This synthesis is to be followed by determination of physical properties, gas sorption and permeation analysis; where CO₂ permeation characteristic could be a focused objective.

1.4. Aims and objectives

In view of excellent thermochemical properties but very low gas permeability of PBI, the objective of this work became to investigate permeation properties of modified polybenzimidazoles and related polymers based on quaternized PBI (polymeric forms of ionic liquids, PILs) obtained by following promising methodologies:

a) Structural variation at monomer level

The objective was to investigate effects of variations in substitution site, substituent polarity and its bulk on the acid moiety and to examine the gas permeation characteristics of resulting polybenzimidazoles. The substitution on acid moiety with bulky groups such as *tert*-butyl, hexafluoroisopropylidene, polar groups like bromo and isomerism effect of dicarboxylic acid could be promising to enhance permeability.

Investigations of physical properties of resulting polybenzimidazoles were to be correlated with gas permeation properties.

b) *Modification of polybenzimidazoles by N-substitution*

N-substitution of the benzimidazole ring by various bulky alkyl groups was thought to be the first step to obtain PILs. This kind of substitution by itself could be a promising approach for structural variations in PBI, which could also offer some directives for PIL synthesis. It was anticipated that *N*-substitution could lead to the higher free volume in the polymer matrix, leading to increased permeability without seriously affecting their mechanical and thermal stability.

c) *N-quaternization of imidazole ring of PBI to offer polymeric forms of ionic liquids (PILs)*

Following this approach, polybenzimidazoles could be quaternized by *N*-substitution with methyl iodide. These PBIs containing iodide counterion, after undergone through ion exchange with selected anions such as tetrafluoro borate [BF_4^-] and bis(trifluoromethane)sulfonimide [Tf_2N^-] were thought to evaluate for CO_2 and related gas sorption and permeation characteristics.

1.5. Organization of thesis

Thesis aims at investigation of gas permeation properties of polybenzimidazoles and related polymers. PBI after appropriate structural variation followed by gas permeation analysis provided an insight towards structure-gas permeation property correlation in this family of polymers. Work done towards defined objectives is presented in 7 chapters.

Chapter 1: This chapter briefly reviews applications of gas separation using polymeric membranes and their advantages over the conventional processes. Rationale of the work is followed by scope, aims and objectives. This chapter ends with organization of the thesis.

Chapter 2: Theoretical aspects of gas permeation and factors affecting gas permeation properties in polymeric membranes are briefly described at the beginning of this chapter. This is followed by effects of systematic structural variation on gas permeation properties in different families of polymers. In view of importance of CO_2

separation in current scenario and possible applicability of PBI for this purpose, related materials, especially ionic liquids demonstrating high CO₂ sorption are discussed. At the end of the chapter, permeation and physical properties of PBI and synthetic aspects are reviewed.

Chapter 3: Experimental procedures for synthesis, polymer characterization, sorption and gas permeation analysis are detailed in this chapter. Optimization during synthesis of different PBIs with structural variations in acid moiety while keeping diamine same, viz., 3,3'-diaminobenzidine (DAB) is described. The experimental protocol set for the preparation of *N*-substituted PBIs and subsequent exchange of iodide anion is given. Dense membrane preparation, methods used for characterization of physical properties, gas sorption and permeation properties is presented.

Results and discussion is divided into 3 chapters as follows.

Chapter 4: This chapter begins with results obtained and discussions on the initial structure-permeability explorations with select gases (H₂ and O₂) for a series of PBI obtained by variation in acid moiety. Based on these results, further explorations with PBI based on isophthalic acid (PBI-I), 5-*tert*-butylisophthalic acid (PBI-BuI) and 4,4'-(hexafluoroisopropylidene)bis(benzoic acid) (PBI-HFA) is presented.

Chapter 5: This chapter deals with *N*-substitution of three promising PBIs [PBI-I (base case), PBI-BuI (bulky substitution) and ABPBI (rigid backbone)] by appropriately chosen alkyl halides. Gas sorption and permeation properties are correlated with physical properties.

Chapter 6: This chapter deals with polymeric forms of ionic liquids (PIL). PBI was converted in to PIL by *N*-quaternization of imidazole ring of PBI, followed by anion exchange. These PILs were based on three promising PBIs (PBI-I, PBI-BuI and ABPBI), while anions studied were iodide [I⁻.], tetrafluoro borate [BF₄⁻.] and bis(trifluoromethane)sulfonimide [Tf₂N⁻.]. Results and discussion on synthetic aspects, physical properties, gas sorption and permeation properties revealing promises of PIL are presented.

Chapter 7: The results obtained and conclusions drawn are summarized in this chapter.

Chapter 2

Literature Survey

2.1. Gas permeation properties: Theoretical considerations

Gas permeation through a nonporous polymeric membrane is a complex process, first noted by Graham in 1866 [Baker (2004)]. Separation through dense polymeric membranes occurs by solution-diffusion mechanism. In the 1940s to 1950s, Barrer and others [Barrer (1951)], Van Amerongen [Van Amerongen (1950)], Stern [Stern (1966)], Meares [Meares (1954)] laid the foundation of the modern theories of gas permeation. The solution-diffusion model of gas permeation developed then is still the accepted model for gas transport through membranes. Application of gas pressure at one interface of a membrane results in the following sequence of events: (a) solution of gas into the membrane (sorption) at that interface, (b) molecular diffusion of the gas in and through the membrane, and (c) release of the gas from solution (desorption) at the opposite interface. Gas flux through the membrane normally follows Fick's first law.

$$Q_A = -D_A \left(\frac{dC_A}{dx} \right) \quad (2.1)$$

where D_A is the diffusivity and C_A is the local concentration of a gas in the membrane. The diffusivity normally is concentration independent with some deviations in the case of highly soluble gases. The permeability, which is the flux of a penetrant normalized by the pressure-driving force and thickness, is given by equation,

$$P_A = \frac{Q_A}{\Delta p_A / \ell} \quad (2.2)$$

where P_A is the permeability of component A, Δp_A is the pressure as driving force across the membrane, and ℓ is the thickness of the membrane. This equation is valid for ideal components, which allows the driving force to be described by the difference in partial pressures. In nonideal cases, the difference in partial pressure of components is replaced with their corresponding fugacities. Permeability coefficient is given by the relation,

$$P_A = D_A S_A \quad (2.3)$$

where D_A and S_A are diffusivity and solubility coefficients for the component A, respectively. The S_A is thermodynamic in nature and gives a measure of the amount of penetrant sorbed by the membrane under equilibrium conditions. Gas solubility may be affected by (i) the polymer penetrant interactions, (ii) the inherent condensability of the penetrant and (iii) the free volume in the polymer [Ghosal (1994)]. The average diffusion coefficient D_A is a kinetic parameter, which indicates how fast the penetrant is transferred through a membrane and is largely determined by polymer-penetrant dynamics.

Both, P and D (and thus S) can be determined in a single experiment by measuring the “time lag” for pressure increase on the low pressure side of the membrane.

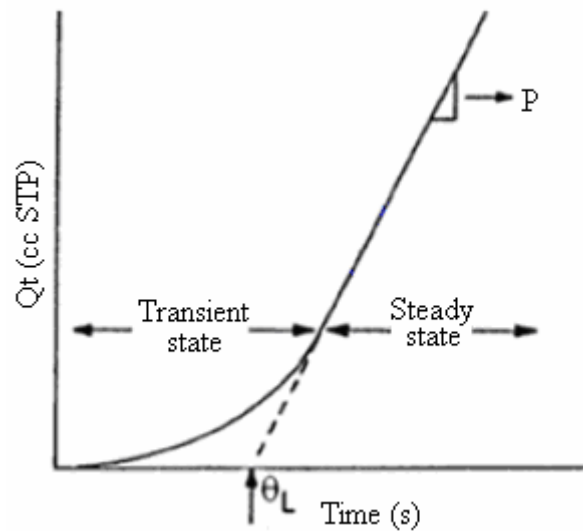


Figure 2.1. Time-lag measurement of gas permeation

The time lag, θ , obtained by extrapolating the linear portion of the pressure versus time function back to the time axis (Figure 2.1) is given by:

$$\theta = \frac{\ell^2}{6D} \quad (2.4)$$

Permeability is given by slope of the function and solubility can be calculated by Equation 2.7. To express permeability, commonly used units are: barrer ($10^{-10} \text{ cm}^3(\text{STP})\text{cm}\cdot\text{s}^{-1}\text{cm}^{-2}\text{cmHg}^{-1}$) and gas permeation unit ($\text{GPU} = 10^{-6} \text{ cm}^3(\text{STP})\text{cm}^{-2} \text{ s}^{-1}\text{cmHg}^{-1}$), molar permeability ($\text{mol m s}^{-1} \text{ m}^{-2} \text{ Pa}^{-1}$).

Selectivity is a membrane's ability to separate a desired component from the feed mixture. Selectivity is often calculated as permselectivity (ratio of permeation of single

gases) or as a separation factor ‘ α ’ for a mixture. The permselectivity ($\alpha_{A/B}$) is the product of the diffusivity selectivity and sorption selectivity as given in Equation 2.5.

$$\alpha_{A/B} = \frac{P_A}{P_B} = \left(\frac{D_A}{D_B} \right) \left(\frac{S_A}{S_B} \right) \quad (2.5)$$

The diffusivity selectivity term relates to the ability of polymer matrix to selectively separate penetrants based on molecular size. As a result, it is governed by the chain backbone rigidity and intersegmental packing. The sorption selectivity favors more condensable penetrants and is affected by the relative affinity between the penetrants and the polymer matrix [Hellum (1989), Ghosal (1994)].

2.1.1. Transport in rubbery polymers

The sorption of low molecular weight penetrants in rubbery materials is typically described by Henry’s law for cases in which the sorbed concentrations are low.

$$C = k_D p \quad (2.6)$$

where, C is the gas concentration, k_D is the Henry’s law coefficient, and p is the penetrant pressure. The permeability coefficient, independent of feed pressure, is given by,

$$P = k_D D \quad (2.7)$$

However, deviations from Henry’s law are observed for rubbery polymers in the presence of high activity gases or vapors. The Henry’s law constant, k_D , appearing in Equations 2.6 and 2.7 can be related to the Lennard-Jone’s force constant, that provides a measure of the ease of condensation of the gas [Michaels (1961), Uhlmann (1976)]. Alternatively, critical point or boiling point of the gas can also be chosen as a correlating parameter, with equally good results [Stern (1969)].

Diffusion coefficient for gases in rubber can be described by Equation 2.8,

$$D = D_0 \cdot \exp(-E^* / RT) \quad (2.8)$$

The activation energy E^* , is an energy that must be concentrated in the polymer adjacent to diffusing molecule to open a passage of enough free volume, to allow the penetrant to execute diffusional jump. The concept of “free-volume” or “empty” volume used to describe the transport of gases and liquids in polymers have been reviewed in the literature [Berry (1968), Kumins (1968), Stern (1981)].

2.1.2. Transport in Glassy polymers

Glassy polymers offer enhanced diffusivity based selectivity as compared to rubbery polymers due to the more restricted segmental motion in glassy polymer matrix. They are able to discriminate effectively between extremely small differences in molecular dimensions of gases (e.g., 0.2 to 0.5Å) [Zolanz (1992)]. Gas permeation has been explained by various models, some of which are briefly discussed below.

i) Dual mode model

Gas solubility in glassy polymers is often described by the dual-mode sorption model (Equation 2.9). It is the concept of sorption in to two idealized environments. One population of sorption is viewed as arising from uptake into a dissolved environment, similar to sorption in low molecular weight liquids and rubbery polymers, described by Henry's law. Second population of sorption is due to uptake in unrelaxed volume present in glassy polymers. This population is described as Langmuir "hole-filling" process.

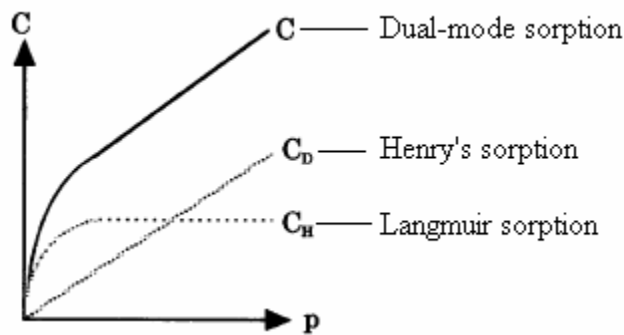


Figure 2.2. Schematic representation of dual-mode sorption

Dual-mode sorption is described by the sum of populations in the Henry's Law dissolution and sorption in Langmuir environment (Figure 2.2).

$$C = C_D + C_H = k_D p + \frac{C'_H b p}{(1 + b p)} \quad (2.9)$$

where, the Henry's Law concentration, C_D , accounts for penetrants in the dissolved state similar to the sorption environment in rubbery polymers. The Langmuir concentration, C_H , accounts for the molecules sorbed into microvoids that are characteristic of non-equilibrium glassy polymers. Parameter k_D is Henry's Law coefficient, b is the Langmuir

affinity constant, and C'_H is the Langmuir capacity constant. The sorption coefficient of the penetrant A, S_A , is the secant slope of the sorption isotherm and is given by equation,

$$S_A = \frac{C}{p} = K_D + \frac{C'_H b}{(1 + bp)} \quad (2.10)$$

At low pressures Equation 2.9 reduces to,

$$C = k_D p + C'_H b p = K p \quad (2.11)$$

$$K = k_D + C'_H b \quad (2.12)$$

At low pressure, overall solubility constant K has two components: k_D and $C'_H b$. The later is usually much larger than k_D . Hence at low pressures, hole filling is more important than Henry's law dissolution. Similarly, at high pressures, Equation 2.9 reduces to,

$$C = k_D p + C'_H = K' p \quad (2.13)$$

$$K' = k_D + C'_H / p \cong k_D \quad (2.14)$$

At high pressure, hole filling is less important and ordinary dissolution becomes dominant.

ii) *Partial immobilization model*

This model is based on the independent dual diffusion of the Henry and Langmuir modes. Partial immobilization assumes that the Langmuir mode species can mobilize partly in glassy polymeric membranes, in contrast to the basic dual-mode model, where the Langmuir mode species is considered not to be mobile. The equation for partial immobilization model is

$$\bar{P} = k_D D_D \left[1 + \frac{FK}{1 + bp} \right] \quad (2.15)$$

$$K = \frac{bC'_H}{k_D} \text{ and } F = \frac{D_H}{D_D} \quad (2.16)$$

where, D_D is the diffusion coefficient due to the Henry mode species, D_H is the diffusion coefficient due to Langmuir mode species, F is the ratio of the two diffusion coefficients (D_H/D_D), or the mobile fraction of the Langmuir mode species and \bar{P} is the average permeability coefficient. The parameter F in Equation 2.16, as mentioned previously, has the physical meaning of a mobile fraction of the Langmuir mode species. If we assume $F=0$, Equation 2.16 reduces to the immobilization model, which is represented by

diffusion of the Henry mode species only. In such cases, $\bar{P} = k_D D_D$ corresponds to the permeability coefficient of rubbery polymeric membranes. The theoretical pressure dependence of the permeability coefficient obeying the partial immobilization model is drawn for different F values in Figure 2.2. The permeability coefficient of the partial immobilization model decreases gradually with an increase in the applied pressure, and then it levels off to the value of $k_D D_D$, irrespective of the value of F .

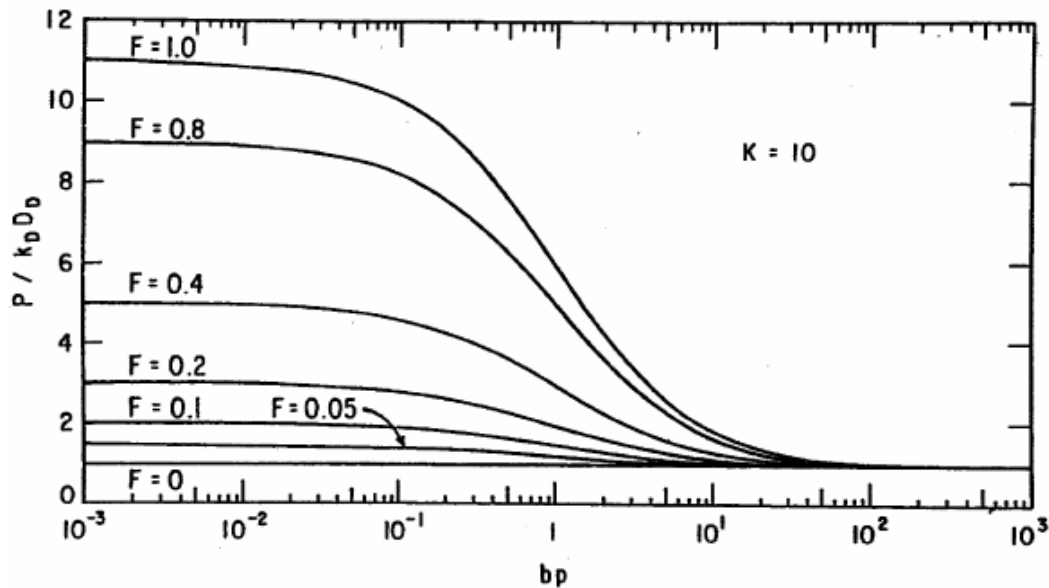


Figure 2.3. Theoretical pressure dependence of permeability coefficient obeying to partial immobilization model [Paul (1976)]

Increase in permeability coefficient at low pressure is caused by a contribution of the diffusion due to the Langmuir mode species. The permeability coefficient is enhanced, notably by the increase in the value of F . However, such an immobile mechanism is not applied to glassy polymeric membranes, but rather the concept that the Langmuir sorbed molecule is slightly mobile is accepted for the gas permeation.

iv) Modified mobility model

Sada et al. (1988) reported that the dual-mode model failed to explain the pressure dependence for various gas polymer systems. It was suggested that the gas molecules sorbed in the glassy polymer matrix by Henry's law mode (D) and Langmuir mode (H) may execute four kinds of diffusion steps viz., $D \rightarrow D$, $D \rightarrow H$, $H \rightarrow D$ and $H \rightarrow H$

[Barrer (1984)]. Sada et al. (1987) derived two modified mobility models, one based on the concentration gradient analogous to that derived by Paul et al. (1976) and another based on the chemical potential gradient approach put forth by Petropoulos (1970). Pressure dependence of the mean permeability coefficient was given by,

$$P = K_D D_{DD} + \left[\frac{2K_D D_{DH}}{b(p_2 - p_1)} \right] \ln \left[\frac{(1 + bp_2)}{(1 + bp_1)} \right] + \left[C'_H b(D_{HH} + D_{HD}) - \frac{K_D D_{DH}}{(1 + bp_2)(1 + bp_1)} \right] \quad (2.17)$$

v) **Concentration dependent transport model**

The interpretations of the permeation behavior of gases in glassy polymers based on dual-sorption model have assumed that the diffusion coefficient of the penetrant is independent of the concentration. The results therefore are applicable to those gases which exhibit a low solubility in polymers, for example, N₂, CH₄, etc. However, the diffusion coefficient of plasticizing gases and diluents could be highly concentration dependent [Stern (1980)]. According to this model, the effective or apparent diffusion coefficient, D_{eff} is given by,

$$D_{\text{eff}} = D(0) \exp \left[\beta \cdot c_D \left(1 + \frac{FK}{(1 + \alpha C_D)} \right) \right] \cdot \left\{ \frac{[1 + (FK/(1 + \alpha C_D)^2)]}{[1 + (K/(1 + \alpha C_D)^2)]} \right\} \quad (2.18)$$

where, D(0) is the diffusion coefficient in the limit C_m → 0, C_m is the concentration of the mobile part of the penetrant gas, β is an empirical constant, which depends on the nature of the penetrant-polymer system, K=C'_H.b/k_D, α=b/k_D and F is fraction of the gas in the Langmuir mode which has a finite mobility.

For the transport of gas across planar non-porous membrane of thickness l, maintained at upstream pressure p₂ and downstream pressure p₁ → 0, P_{eff} is given as,

$$P_{\text{eff}} = D(0)/\beta(0_2) \left\{ \exp[\beta k_D p_2 (1 + FK/(1 + bp_2))] - 1 \right\} \quad (2.19)$$

The transport model incorporating a concentration dependent diffusion coefficient can be exploited to predict the optimum conditions under which selective permeation of gaseous mixture can be anticipated. The ideal pressure for the separation of the multicomponent mixture will be dependent on the relative positions and magnitude of minima in P_{eff} vs p₂ curves, as well as on the composition of the mixture.

vi) **Gas-polymer-matrix model**

It has been suggested that there is only one population of sorbed gas molecules in the polymers at any pressure and the sorbed gas alters the sorption and transport characteristics as a result of the change in the co-operative main chain motions in the polymer [Sefcik (1983)]. It was also proposed that the gas-polymer interaction reduces the interchain potential of the polymer, and hence decrease the activation energy for the polymer chain separation as well as for the diffusion [Raucher (1983)]. Since the gas-polymer interaction alters the interchain energy, solubility coefficients also vary as the structure and the dynamics of the polymer matrix changes. The gas-polymer matrix model is based on the experimental evidence put forth by the authors that even permanent gases interact with polymeric chains, resulting in changes in the solubility and diffusivity coefficient as a function of pressure.

According to this model, the concentration of sorbed gas is given by,

$$c = \sigma_0 \cdot p / (1 + \gamma^* \cdot c) \quad (2.20)$$

where, σ_0 is the solubility coefficient in the zero-concentration limit. γ^* is a constant relating $\sigma^* k$ to the concentration c , σ^* is a constant relating excess free energy of mixing to the depression of T_g of the polymer by the gas. k is defined by,

$$k = [T_{g(0)} - T_{g(c)}] \quad (2.21)$$

where, $T_{g(0)}$ and $T_{g(c)}$ are the T_g s of the pure polymer and polymer-gas mixture.

The diffusion coefficient D is given by Equation 2.22, which was formulated using the diffusion model of Pace et al. (1979) and the theory of corresponding states [Houde (1991)].

$$D = D_0 (1 + \beta^* \cdot k) \exp(\beta^* \cdot k) \quad (2.22)$$

where, D_0 is the diffusion coefficient in zero concentration limit, and β^* is a constant relating the excess activation energy of chain separation to the depression of the T_g of the polymer by the gas. The permeability constant P was given by,

$$P = D_0 \cdot \sigma_0 [(1 + \beta^* \cdot c) / (1 + \gamma^* \cdot c)] \quad (2.23)$$

At pressure less than 1 atm, the matrix model predicts a strong apparent pressure dependence of permeability. However, the dual-mode model predicts only a weak dependence.

2.2. Factors affecting gas permeation properties

Various polymer properties, experimental conditions, processing history of membrane affect gas permeation properties. These factors are briefly discussed below.

2.2.1. Properties of gas

i) *Size and shape of penetrant molecules*

Diffusion coefficients generally decrease as volume and shape of the penetrant gas molecule increases. In glassy polymers, the diffusivity is usually dominant and permeability falls with increasing permeate size. In rubbery polymers, the solubility coefficient is usually dominant and permeability increases with increasing permeate size [Baker (2004)]. Most of the glassy gas separation membrane materials achieve high permselectivity as a result of high diffusivity selectivity. As the difference in kinetic diameter of the gases to be separated increases, the diffusivity selectivity increases due to easy discrimination by the polymer between penetrants. The van der Waals volume is one of the methods to express penetrant size. However, it does not account for the shape of the penetrant. The diffusivity of linear or oblong penetrant molecules such as CO₂ is higher than the diffusivities of spherical molecules of equivalent molecular volume. The van der Waals volumes of CO₂ and CH₄ are estimated to be 17.5 and 17.2 cm³/mole. These molecular volumes yield equivalent spherical diameters of 3.33 and 3.31 Å for CO₂ and CH₄ respectively. Thus, kinetic diameter (3.3 Å for CO₂ and 3.8 Å for CH₄) is frequently used to characterize the penetrant size [Ghosal (1994)]. Ease of condensation of penetrant gas molecule determines the solubility. Thus, solubility of organic vapors increases with increase in size due to increase in their condensabilities in the same order.

ii) *Condensability of gas molecules*

The solubility coefficient in polymer matrix generally increases with increasing gas condensability. The gas condensability is usually expressed in terms of its critical temperature (T_c), boiling temperature (T_b) or Lennard-Jones force constant (ε/k). These are found to correlate well with the solubility coefficients of the gases in polymers [Ghosal (1994)]. Some of the industrially important gases, viz., He, H₂, N₂, O₂ and Ar are non-interacting gases, while CO₂ and hydrocarbon gases are considered as interacting gases with the polymer and thus have higher solubilities than the non-interacting gases.

2.2.2. Physical properties of polymer

Physical properties of polymers affecting gas permeability are packing density, chain and sub-group mobility, polarity, presence of crystallinity and crosslink sites.

i) Chain packing density

Chain packing density is one of the most important variables affecting the permeability [Stern (1989)]. Both, d -spacing (d_{sp} , average intersegmental distance) and fractional free volume (v_f or FFV) are used as indices of the degree of openness of the polymer matrix. Effects of decreasing packing density of polymer matrix on increasing diffusivity and permeability has been shown in several types of polymers [Chern (1987), Kim (1988), Stern (1989), Charati (1991)]. The d_{sp} is obtained from wide-angle X-ray diffraction spectra. Sometimes d_{sp} has limitations as measures of the extent of ‘openness’ of the matrix, since it measures only the distance between the centres of masses of neighboring chains [Hellums (1989)]. X-ray spectra reflect scattering features than the average distance between polymer chains and thus have limited usefulness for interpreting transport properties. WAXD has been demonstrated in the literature as a probe to measure d_{sp} and interpret permeation characteristics successfully for various types of polymers such as poly(methyl methacrylate), cellulose acetate, polysulfones, poly(ether sulfone), polystyrene, polycarbonates, polyarylates, polyimides, etc.

Fractional free volume is a fraction of the total polymer specific volume that is not occupied by the polymer molecules. The excess or “unrelaxed volume” is thought to be the result of trapped non-equilibrium chain conformations in quenched glasses, which result from the extraordinarily long relaxation time for segmental motions in the glassy state. The excess volume allows accommodation of the additional penetrant above that observed in low molecular weight liquid and rubbers. Generally, with increase in v_f , increase in gas permeability has been observed for many polymers, viz., polycarbonate [Hellums (1989)], polyimide [Coleman (1990)], polyarylate [Pixton (1995a)], polysulfone [Mchattie (1991a)] etc. A commonly used method to determine fractional free volume (v_f) is based on semiempirical calculation using experimentally determined density of the polymer and van der Waals volume (V_w) by group additivity [Bondi (1964)]. The positron annihilation lifetime spectroscopy, photochromic and fluorescence technique are also used for determining the free volume [Victor (1987)].

The diffusion coefficient (D) of a gas is related to v_f by the equation,

$$D = A \exp(-B/v_f) \quad (2.24)$$

where, constants A and B are characteristics of the polymer-penetrant system [Ghosal (1994, 1996)]. Constant A is related to size and shape of the diffusing molecule, while B is related to the minimum hole size necessary for a diffusional jump [Barbari (1997)]. Though solubility coefficient can be correlated with v_f , it is a weaker function [Ghosal (1994, 1996)].

ii) Chain and subgroup mobility

Chain and subgroup mobility (expressed by various transition temperatures) has direct relationship with penetrant permeability and inverse relationship with selectivity. Emphasis on new material development for gas separation is based on improving selectivity with marginal effects on permeability. Structural alterations which inhibit chain packing while simultaneously inhibiting rotational motion about flexible linkages on polymer backbone tend to increase permeability while maintaining or increasing selectivity [Coleman (1990)]. Introduction of rigid linkages such as aromatic group decrease the torsional mobility and reduce penetrant mobility [Ghosal (1994)]. Inhibition of the segmental and sub-segmental mobility can be judged by increase in glass transition (T_g) or sub- T_g temperatures. Typical methods to characterize torsional mobility include dynamic mechanical relaxation spectroscopy, differential scanning calorimetry, dipole relaxation spectroscopy and nuclear magnetic resonance [Ghosal (1994)].

iii) Polarity

Polarity results from the uneven distribution of electrons about atoms and molecules. Since polarity leads to net forces of attraction between macromolecules, d_{sp} and v_f in polar polymers tend to be smaller. Attempts to influence solubility component of permeability via the introduction of polar groups are made [Van Amerongen (1950), Koros (1985), Ghosal (1992), Story (1991)]. It is proving more advantageous to increase v_f in a polar and therefore selective polymer, than to increase selectivity in nonpolar polymer. For gases such as CO_2 , which has a quadrupole moment, are in general, more soluble in polar polymers [Hirayama (1999)]. Presence of polar groups like bromo, chloro, nitro, sulfonic/carboxylic acid group and their salts, etc. generally lead to a decrease in permeability and increase in selectivity. This was observed for various types

of polymers such as poly(phenylene oxide) [Bhole (2007a)], polysulfone [Ghosal (1992)], polyarylate [Murugandam (1987), Kharul (2002)], etc.

Polymer polarity affects quantifiable parameters such as dielectric constant and solubility parameter. The solubility parameter (δ) is defined as the square root of the cohesive energy density of the polymer per unit volume [Seymour (1984)]. It can be experimentally determined by either solvent solubility or swelling experiments. It can also be estimated by semi-empirical method [Burrell (1975)] as follows;

$$\delta = \frac{\rho \Sigma G}{M} \quad (2.25)$$

where, ρ is the mass density of the polymer, M is molar mass of the repeat unit and ΣG is the molar attraction constant obtained by the group additivity method.

iv) Molecular weight

It is known that the polymer molecular weight (MW) significantly influences the transport processes. As polymer MW increases, the number of chain ends decreases. The chain ends represent a discontinuity and may form sites for permeant molecules to be sorbed in to glassy polymers. For instance, for a series of polystyrene samples, the diffusivity of a range of organic vapours (acetone, benzene, etc.) decreased by a factor of almost 10 as MW increased from 10,000 to 300,000 [Berens (1982)]. Smid et al. (1991) reported that increase in MW of PPO makes it possible to produce membranes with higher permeability, whereas the selectivity remains the same. Polotskaya et al. (1996) reported that for PPO, increase in MW increases N_2 and O_2 permeability, while permselectivity was independent of MW. Mikawa et al. (2002) reported that MW of polyimide had a great influence on CO_2 permeation stability and was one of the important factors determining the plasticization of the membrane [Mikawa (2002)].

iv) Crystallinity

The diffusion of gases takes place primarily through amorphous region, where as the crystalline region acts as barrier to gases. Generally, with increase in crystallinity for a given polymer, gas permeability decreases. The diffusion coefficient can be expressed as a function of the crystallinity [Mulder (1998)],

$$D_i = D_{i,0} \left(\frac{\psi_c^n}{B} \right) \quad (2.26)$$

where, ψ_c is the fraction of crystalline material present, B is a constant and n is an exponential factor ($n < 1$). When the crystallinity is low, diffusion resistance is quite low and consequently, the effect of crystallinity on the permeation rate is often very small.

Various techniques have been employed to assess the relative and absolute degree of crystallinity, including X-ray diffraction, density methods, thermal analysis, nuclear magnetic resonance (NMR) and infrared (IR) spectroscopy [He (2000)]. Mcgonigle et al. (2004) reported that additional constraints resulting from increased crystallinity improved gas barrier performance of the polyester [Mcgonigle (2004)]. The H₂ and CO₂ transport properties of poly(ethylene-2,6-dicarboxylatenaphthalene) decreased for thermally crystallized samples [Hardy (2003)]. No change in the sorption properties of the amorphous phase was noticed as a function of the thermal treatment and the evaluation of the diffusion coefficient was related to the tortuosity effect because of crystalline entities.

v) ***Crosslinking***

Crosslinking provides an additional constraint and significantly reduces the polymer segmental mobility and thus the diffusion coefficients typically decrease. It also stabilizes the polymer against thermal and chemical degradation, as well as impacting the gas transport [Dudley (2001)]. Gases with larger molecular diameters are more severely impacted than those with smaller diameters. Thus, crosslinking can lead to improved separation selectivity, usually at the expense of reduced gas permeation rates. Plasticization is a major issue that is always encountered for gas separation in glassy polymers, especially for the separation of CO₂/CH₄ [Staudt-Bickel (1999), Ismail (2002)]. There are various ways to crosslink a polymer matrix such as photochemical, thermal or chemical crosslinking. Photochemical cross-linking by UV irradiation [McCaig (1999), Liu (1999), Dudley (2001)] and thermal cross-linking at elevated temperatures [Dudley (2001), Ismail (2002), Chung (2003)] were used to enhance polymers anti-plasticization properties. Staudt-Bickel et al. (1999) chemically crosslinked polyimide with ethyleneglycol to improve CO₂/CH₄ selectivity.

2.2.3. Operational conditions

i) Temperature

As the diffusion in polymers is an activated process, when temperature is increased, the diffusion coefficient increases yielding a positive activation energy for diffusion (energy required for a penetrant to make a diffusive jump from one equilibrium site to another). The variation of diffusivity, sorption and permeability coefficients with temperature follows Arrhenius behavior [Barrer (1939), Kim (1989), Gülmüs (2007)]. The permeability, diffusivity and solubility coefficients of gases were studied in natural rubber in the range of 25 to 50 °C [Zolanz (1992)]. The diffusion coefficients were changed by 200 to 300%, where as solubility coefficients were found to vary by less than 30%. The temperature dependence of gas permeation in various glassy polymers is well reported in the literature [Kim (1989), Costello (1994), Gülmüs (2007), de Sales (2008)], where increase in permeability with increase in temperature was observed. The solubility coefficient for a given penetrant generally decreases with temperature; however, this decrease is overcome by the substantial increase in the diffusion coefficients, producing a net increase in the permeability coefficient. The permselectivity generally decreases with increase in temperature. The dependence of permselectivity on temperature is larger for gas pairs with high difference in activation energies of gas pairs [de Sales (2008)].

ii) Pressure

Diffusivity, solubility and, in turn, permeability may vary appreciably as the pressure of penetrant in contact with the polymer changes. Low sorbing penetrants such as He, H₂, N₂, O₂ and other permanent gases in either rubbery or glassy polymers show small decrease in permeability with an increase in pressure [Ghosal (1994)]. On the other hand, for penetrants which have considerably high sorption in polymers (such as CO₂) generally show monotonic decrease in permeability with increasing pressure [Ghosal (1994), Lin (2001)]. This phenomenon of pressure dependence on permeability is consistent with the dual-mode transport model used to describe gas transport behavior of glassy polymers (represented as the sum of the Henry mode and the Langmuir mode). In general, the Langmuir mode, which is associated with the “excess” free volume formed in the glassy state, makes a large contribution to the pressure dependence on the permeability in glassy polymers. The permeability of a rubbery polymer to an organic

vapor shows a monotonic increase in permeability and is related to concomitant increases in penetrant solubility and diffusivity with increasing pressure [Stern (1983), Ghosal (1994)]. A combination of these two behaviors is typical of the isotherm characterizing the permeability of a glassy polymer to a plasticizing penetrant such as an organic vapor [Chern (1991)]. The polymer permeation properties in such cases exhibit dual-mode behavior at low pressures and penetrant-induced plasticization at high pressures. At high pressure, dual-mode behavior diminishes due to onset of the segmental motions after plasticization of polymer chains.

2.2.4. Membrane preparation parameters

Since glassy state is a nonequilibrium condition, v_f , chain orientation or crystallinity (if present) of the membrane can be influenced by physical treatments such as sub- T_g annealing, thermal quenching and CO_2 pressure conditioning. These can also be effective for the control of microvoid formation in glassy state, and thus sorption and permeation of small molecules [Tsuji (2003)]. These are briefly described below.

i) Sub- T_g annealing

Sub- T_g annealing can lead to decrease in microvoids of glassy polymers. It is done at sub- T_g temperature since annealing at supra- T_g temperature would increase chain segment mobility to effect expansion or free-volume increase. This is then frozen in to glass upon quenching to sub- T_g temperature [Kesting (1993)]. Hachisuka et al. (1988) studied the CO_2 sorption of as cast and sub- T_g annealed copoly(vinylidene cyanide-vinyl acetate) from standpoint of sorption mechanism and the change in microvoids. CO_2 sorption was decreased with increasing sub- T_g annealing period as a result of decrease in the specific volume [Hachisuka (1988)]. Increasing annealing period of PC decreased permeability and increased selectivity for various gas pairs [Hacarlioglu (2003)].

ii) Quenching

A very rapid quenching of a polymer from a rubbery state to the glassy state can lead to enhanced microvoid formation. The amount of CO_2 sorption in PC films quenched from various temperatures above the T_g was increased with increasing holding temperature above T_g , and was larger than that in PC film cooled slowly from a

temperature above T_g [Hachisuka (1991)]. This increase in sorption was due to increase in Langmuir capacity constant (C'_H) explained in terms of increase in frozen free volume.

iii) Pressure conditioning

CO₂ plasticizes various polymers at high pressures. PC was exposed to high pressure CO₂ and liquid N₂, which led to increase in microvoid content and hence the sorption [Hachisuka (1991)]. The amount of sorption in pressure-conditioned PC films was more than that in quenched films. Tsujita et al. (2003) reviewed that the dual-mode sorption parameter (C'_H); as well as the CO₂ permeability coefficient of polyamic acid (a precursor of polyimide), partially imidized polyimide, polyimide, poly(2,6-dimethyl phenylene oxide), and polycarbonate increased markedly by thermal quenching and CO₂ pressure conditioning. CO₂ pressure conditioning was more effective in enhancing the sorption and permeability than the thermal quenching.

iv) Solvent effect

Properties of solvent used for the membrane preparation affects membrane morphology and its performance. Polysulfone cast from different solvent with increasing volatility resulted in increased v_f and increase in permeability [Hu (2003)]. It was shown that boiling point, surface tension and viscosity of the solvents used for casting poly(phenyleneoxide) membranes affected the gas permeation [Khulbe (1997)]. An increase in permeability and decrease in selectivity (O₂/N₂, CO₂/CH₄) was observed with increase in boiling point of solvent. Presence of the residual solvent in membrane can also have significant effect on the permeation properties [Joly (1999)]. Besides physical properties of the solvent, other factors such as solution concentration, solution and casting temperature, humidity of the casting environment, etc. are also of considerable importance in determining membrane morphology and performance. Using different casting methods like mercury floated casting or knife-casting can cause some differences in the final film because of molecular orientations [Kesting (1993)].

2.3. Structure-property relationship in polymers

In order to improve gas separation properties, structure of the polymer to be used as a membrane material can be systematically designed. Variation in structure of monomers by appropriate substitution is one of the ways. Several investigations with

different families of glassy polymers like polysulfones, polycarbonates, polyimides, polyarylates, etc. describe effects of structural modifications by different groups on physical properties and their correlation with gas permeation properties. Such modifications provide insight towards consequences of substitution by various substituents (size, polarity, flexibility, etc.) on the permeation properties of thus modified polymers. In view of investigations of PBI structural modifications on permeability as one of the objectives of this thesis, reviewing aspects of various types of substitutions provided inputs towards aimed PBI structure architecture.

2.3.1. Substitution by non polar alkyl groups

It has been shown that the tetramethyl substitution on the bisphenol rings in various polymers such as polysulfones [McHattie (1991a)], polycarbonates [Muruganandam (1987)], polyarylates [Pixton (1995a), Kharul (1997, 1998)], led to increased permeability while retaining selectivity as that of respective unsubstituted case. Substitution of *tert*-butyl group on isophthalic acid increased gas permeability by 2 - 6 folds, but lowered selectivity in polyarylates obtained from various bisphenols [Pixton (1995a)]. Polyarylates prepared using a silicon-diacid and dimethyl substituted bisphenol showed good combination of O₂ permeability (1.2 - 1.7 barrer) and high O₂/N₂ selectivity (8.-9.3) [Jadhav (1997)]. In case of copolyarylates based on 4,4'-(hexafluoroisopropylidene)diphenol and a mixture of isophthaloyl dichloride and 5-*tert*-butylisophthaloyl dichloride, gas permeability increased with the extent of bulky *tert*-butyl group, attributable to increased free volume [Loría-Bastarrachea (2007)]. The simultaneous decrease in selectivity was small.

Almost fourfold enhancement in CO₂ permeability of TMPSF (tetramethyl substitution on bisphenol-A) relative to the unsubstituted PSF was observed without an appreciable decrease in selectivity [McHattie (1992)]. Dimethyl substitution on bisphenol in polysulfone (DMPSF) resulted in a lower free volume, more selective but less permeable polymer [McHattie (1991a)].

In tetramethylpolycarbonate (TMPC), the permeability to CO₂ was approximately three times higher than that of unsubstituted PC with marginal increase in CO₂/CH₄

selectivity [Muruganandam (1987)]. This increase was due to substantial increase in CO₂ solubility coupled with nearly two fold increase in CO₂ diffusivity.

In case of polyimide prepared from methyl-substituted phenylenediamines and 2,2-bis(3,4-dicarboxyphenyl)hexafluoropropane dianhydride (6FDA), the pendant methyl group on diamine restricted intramolecular rotation while maintaining a highly rigid structure [Tanaka (1992)]. In case of PPO with the substitution like alkynylation [Bonfanti (1994)], fullerene substitution [Sterescu (2004)] led to the increase in gas permeability. Sterescu et al. (2004) showed that the PPO-bonded C₆₀ membranes exhibited significantly higher gas permeability (up to 80%) in comparison to unsubstituted PPO, without compromise on selectivity.

2.3.2. Substitution by hexafluoroisopropylidene group

Substitution by hexafluoroisopropylidene group (-C(CF₃)₂-) rendered loose chain packing and enhanced gas permeation properties in various families of polymers such as polysulphone [McHattie (1991b, 1992)], polycarbonate [Hellums (1989)], polyimide [Stern (1989), Coleman (1990)], polyarylate [Kharul (1994)], etc.

Polysulfone with (-C(CF₃)₂-) group (HFPSF) was more permeable than PSF with comparable selectivity [McHattie (1991b)]. The -C(CF₃)₂- group sterically hindered both, the bond rotation as well as the intersegmental packing. It was said that the packing of HFPSF could also be inhibited by intermolecular repulsive forces between fluorine atoms, which are areas of high electron density. Hellums et al. (1989) studied gas transport properties of polycarbonates (PC) containing -C(CF₃)₂- moiety at the bisphenol bridge position (TMHFPC). This polymer exhibited CO₂ permeability of 110 barrer vis-à-vis 6.8 barrer for unsubstituted PC, coupled with a 26% increase in selectivity. Incorporation of the bulky -C(CF₃)₂- group markedly increased fractional free volume and stiffening of polymer chains, as judged by increase in T_g. Relative to unsubstituted PC, CO₂ diffusivity in TMHFPC was higher by a factor of almost 7. The solubility of CO₂ was 2.5 times higher as well, than in unsubstituted PC.

Polyimides containing -C(CF₃)₂- group in its dianhydride unit inhibited efficient chain packing, reduced local segmental mobility and increased both, selectivity and permeability [Kim (1988), Cao (2002)]. The -C(CF₃)₂- groups not only increase chain

stiffness, but also act as molecular spacer to decrease chain packing, resulting in greater free volume [Stern (1994)]. As a result of reduced chain packing, a tendency to form charge transfer complexes (CTCs) also weakened, as could be detected by the disappearance of color of the formed polymer [Stern (1994)], leading to increased permeability. Dianhydrides with $-\text{C}(\text{CF}_3)_2-$ are generally more effective at enhancing selectivity versus comparable diamines containing $-\text{C}(\text{CF}_3)_2-$ groups [Stern (1994)].

2.3.3. Substitution by polar groups

In various types of polymers, presence of polar groups like bromo, chloro, nitro, carboxyl, sulfonic acid/salt, etc. generally leads to decrease in permeability and increase in selectivity [Muruganandam (1987), Kawakami (1991), Story (1992), Polotskaya (1997), Kharul (1998), Chowdhury (2000), Kharul (2002), Bhole (2007a, 2007b)]. This is due to closer chain packing of the polymer molecules caused by intermolecular interaction. The decrease in permeability by chloro or bromo substitution on PC was a consequence of the introduction of stronger cohesive forces owing to polarity, that might resulted in more dense packing and reduced rates of certain group motions [Muruganandam (1987)]. The increased cohesive energy density of the chloro and bromo substituted PC relative to TMPC lowers the diffusivity and increases the mobility selectivity with little difference in solubility or solubility selectivity [Koros (1993)]. Tetrabromination of bisphenols either maintained or increased permeability with increase in O_2/N_2 selectivity as compared to the nonbrominated analog [Pixton (1995b)]. The increase in permselectivity was due to more size selective nature of the brominated polymers. Combined effects of polarity and bulk was observed for polyarylate based on dinitrodimethyl substitution, which offered high O_2 permeability (4.4 barrer) than dimethyl substituted (2.4 barrer) polyarylate, without variation in O_2/N_2 selectivity [Chen (1993)]. Gas permeability of dibromodimethyl bisphenol-A (DBrDMbisA) based polyarylates were higher than for tetrabrominated analog, but were lower than that for tetramethyl substituted analog [Pixton (1995a), Kharul 1998]. The selectivity observed for various gas pairs were higher than either of the tetrabromo- or tetramethylsubstituted polyarylates.

In the case of PPO, bromination [Chern (1987), Story (1992)], carboxylation [Chowdhury (2000), Story (1992)], sulfonation [Polotskaya (1997), Chowdhury (2000)], nitration [Ghosal (1992)], etc. improved selectivities with a general decrease in gas permeability. Sulfonated polyimide displayed higher selectivity of H₂ over CH₄ without loss of H₂ permeability [Tanaka (2006)].

2.3.4. Effect of isomerism

A meta-substitution in the diamine of polyimides decreased permeability and increased selectivity due to impeded intra and intersegmental motions than the para-isomer [Coleman (1990), Kawakami (1995)]. A comparison between PMDA-4,4'-ODA (para) and PMDA-3,3'-ODA (meta-substitution) showed that the para-isomer exhibited T_g of 400 °C, vis-à-vis 287 °C for the meta-isomer and was twice as permeable as its meta-isomer [Mi (1993)]. Pessan et al. (1993) studied the effect of isomerism in dicarboxylic acid on resulting polyarylates. The one based on isophthalic acid showed lower permeability and higher permselectivity than that based on terephthalic acid.

2.3.5. Substitution by trimethylsilyl group

The introduction of -Si(CH₃)₃ group on the backbone led to a large increase in gas permeability coefficients for various polymers. Lower the permeability of the unsubstituted polymer, more drastic the effect introduced by -Si(CH₃)₃ group [Paul (1993)]. This was due to large increase in free volume after the substitution of -Si(CH₃)₃.

Dai et al. (2004) reported the modification of hexafluoro polysulfone and tetramethylhexafluoro-polysulfone by trimethylsilyl group (-Si(CH₃)₃). This modification resulted in 8 - 9 folds increase in CO₂ and O₂ permeability with no reduction in CO₂/N₂ selectivity and only a moderate reduction in O₂/N₂ selectivity as compared to the base polymer, hexafluoropolysulfone. Polyimides bearing a *tert*-butylphenyl or trimethylsilyl phenyl groups showed O₂ permeability coefficient and permselectivity of O₂ to N₂ in the ranges of 31 - 110 barrer and 2.8 - 4.3, respectively [Kim (2003)]. In case of PPO, -Si(CH₃)₃ substitution increased gas permeability [Zhang (1994)]. The -Si(CH₃)₃ substituted on the phenylene of the backbone contributed more to

the increase of gas permeability than the group substituted on the lateral methyl group. The gas permeability was also found to increase with the rise in degree of substitution.

2.4. CO₂ sorption and permeation: promising materials

CO₂ removal from major emission sources such as power stations, steel industries and chemical industries is becoming very essential. Reduction of CO₂ emissions through sequestration of CO₂ either in geologic formations or in terrestrial ecosystems can be part of the solution to the problem of global warming [Litynski (2006)]. The first step in sequestration is CO₂ capture and then its storage in “sinks”, which will eliminate its release to the atmosphere. Following section briefs various methods popularly used for the CO₂ separation.

2.4.1. CO₂ separation using alkanol amines

In CO₂ absorption processes, a solvent is used that preferably dissolves CO₂, but not O₂, N₂, or any other components of a flue gas stream. The CO₂-rich solution is typically pumped to a regeneration column, where CO₂ is stripped from the solution and the solvent recycled for a new batch of flue gas. The traditional solvent used for CO₂ absorption are monoethanolamine (MEA), diethanolamine (DEA), di-2-propanolamine (DIPA), triethanolamine (TEA) and methyldiethanolamine (MDEA) [Blauwhoff (1984), Versteeg (1988), Vaidya (2007)]. The primary and secondary alkanolamines react directly and reversibly with the CO₂ through the formation of a zwitterion intermediate which is deprotonated by the bases present in the solution to form a stable carbamate as in Equation 2.27 and 2.28 [Blauwhoff (1984), Versteeg (1988), Vaidya (2007)].



where R₁ is an alkyl group and R₂ is H for primary amines and an alkyl group for secondary amines; B is a base that could be an amine, OH⁻ or H₂O.

Both, primary and secondary amines react fairly strongly with CO₂ to form stable carbamates and their heats of reactions are substantial. Consequently, these amines require substantial energy for regeneration. Also, the loading limit is ~ 0.5 mole of CO₂

per mol of amine [Benamour (2005), Ramchandran (2006)]. Tertiary amines have a high CO₂ loading capacity of 1 mole of CO₂ per mole of amine, but low rates of CO₂ absorption limit their use [Sartori (1983)]. The CO₂ absorption rates of tertiary amines can be enhanced by the addition of small amounts of primary or secondary amines [Chakraborty (1986)] An another class of amine, sterically hindered amines such as 2-amino-2-methyl-1-propanol (AMP), 2-piperidineethanol (PE) have been proposed for acid-gas purification. They have not only greater capacity for CO₂, but also a lower tendency to form carbamate and an appreciable absorption rate for CO₂ [Sartori (1983), Chakraborty (1986), Hook (1997), Vaidya (2007)]. Blends of primary or secondary amines with a tertiary or sterically hindered amine combine the higher CO₂ reaction rates of the primary or secondary amine with the higher CO₂ loading capacity of the tertiary or sterically hindered amine [Ali (2002), Mandal (2003)].

2.4.2. CO₂ separation using ionic liquids

Ionic liquids (ILs) are inorganic or organic molten salts that are liquid over a wide range of temperatures near and at room temperature. If melting point is below room temperature (25 °C), the IL is called as room-temperature ionic liquid (RTIL) [Thomas (1999)]. They are found to possess high CO₂ sorption. Recent literature deals with RTILs made of a bulky N- or P-containing organic cation such as alkyl-imidazolium, pyridinium or pyrrolidinium, ammonium or phosphonium; and a variety of anions such as, triflate, dicyanamide, acetate, trifluoroacetate, trifluoromethylsulfate, bromide, chloride, nitrate, perchlorate, chloroaluminate, tetrafluoroborate, or hexafluorophosphate, etc. [Liu (2005), Berthod (2008)]. The growing interest in using RTILs as gas-separation media [Pez (1988), Blanchard (1999), Scurto (2002), Scovazzo (2004)] stems from their exceptional properties, such as negligible vapor pressure, high thermal stability and tunability of various other properties with the structural changes. Due to the Coulombic attraction between ions of these liquids, they exhibit no measurable vapor pressure up to their thermal decomposition, generally > 300 °C. A lack of vapor pressure makes them highly attractive for gas processing. CO₂ solubility in ILs is higher than other gases like N₂, O₂ or lower hydrocarbons which make them more CO₂ selective. Imidazolium-based ILs are well known for their remarkable CO₂ solubility [Blanchard (1999), Bates (2002), Cadena (2004), Scovazo (2004), Anderson (2007)]. Bates et al. (2002) reported task specific ILs

to sequester CO₂. Bara et al. (2007a) reported imidazolium-based RTILs with one, two, or three oligo(ethylene glycol), which showed similar levels of CO₂ solubility but lower solubilities of N₂ and CH₄ with 30 - 75% higher solubility selectivities for CO₂/N₂ and CO₂/CH₄ than that of corresponding alkyl analogues [Bara (2007a)]. ILs are also used as an alternative solvent in green chemistry [Olivier-Bourbigou (2002)], catalysis [Olivier-Bourbigou (2002)], electrochemical devices [Caja (2000, 2006)], analytical chemistry [Liu (2005), Berthod (2008)] besides for gas separation [Blanchard (1999), Scurto (2002), Scovazzo (2004)].

ILs are non-volatile, have possibility of tailoring their physicochemical properties by an adequate selection of the cation, its substituents and the anion to have high CO₂ sorption [Scovazzo (2004)]. Additionally, ILs are immiscible with many organic solvents, possess relatively high viscosities and interfacial tensions, and may exhibit a reduced solubility in water. These properties made use of ILs very attractive to obtain stable supported ionic liquid membranes (SILM) for gas separation [Fortunato (2004)]. These contacting devices show promises over the conventional CO₂ separation processes due to advantages like high surface area per unit contact volume, independent control of gas-liquid interfacial area, etc. [Gabelman (1999), Kim (2000), Wang (2004)]. In a membrane contactor, the gas flows on one side of the membrane and the absorbent liquid flows on the other without phase dispersion. The commonly used absorbents are aqueous solutions of amines such as MEA, DEA, etc. [Kim (2000), Wang (2004), Al Marzouqi (2005)] or strongly alkaline salts such as K₂CO₃ [Quinn (1995)]. Conventional SLMs are associated with problems such as the loss of liquid through vaporization or dissolution in contacting phases and their loading limits [Takeuchi (1987), Scovazzo (2004), Zao (2006)]. Several approaches have been proposed to minimize instability problems, such as the use of mild operating conditions, protection of the SLM with a gel layer [Kemperman (1998)], and adequate design of both the supporting membranes and the contacting phases [Danesi (1987)].

2.4.3. CO₂ separation using poly(ionic liquids)

Polymeric forms of ionic liquids or poly(ionic liquids) (PILs), are polymers that are usually made from ionic liquid monomers. Reports on PILs first appeared in the literature relating to conductivity in thin films [Washiro (2004), Ohno (2004), Nakajima

(2005)]. Their investigations as gas separations materials began soon after, reporting enhanced CO₂ uptake [Tang (2005a, 2005b), Hu (2006)]. Subsequently, enhanced CO₂ solubility and selectivity was demonstrated [Blasig (2007a), Bara (2007a, 2007b, 2008)]. These polymers mainly consist of poly(acrylate) or poly(styrene) backbones with imidazolium or ammonium cations tethered as side chains. Such PILs were found to exhibit not only higher CO₂ sorption capacity, but also higher sorption-desorption rates than their corresponding IL monomers. [Tang (2005a, 2005b)] Poly[*p*-vinylbenzyltrimethyl-ammonium tetrafluoroborate] (P[VBTMA][BF₄]) and poly[2-(methylacryloyloxy)ethyl-trimethyl-ammonium tetrafluoroborate] P[MATMA][BF₄] though exhibit high CO₂ sorption, were too brittle to form good membranes. In a study by Hu et al. (2006), PIL based membranes were prepared by grafting polyethylene glycol (PEG) onto the glassy P[VBTMA][BF₄] and P[MATMA][BF₄]. Membranes made of P[VBTMA][BF₄]-g-PEG and P[MATMA][BF₄]-g-PEG were CO₂ selective over CH₄ and N₂, and were less brittle than those made of pure P[VBTMA][BF₄] and P[MATMA][BF₄]. Blasig et al. (2007a) reported effects of cation type on CO₂ sorption in PIL. CO₂ solubility in poly(*p*-vinylbenzyltrimethyl ammonium tetrafluoroborate) was higher than that in poly(1-(*p*-vinylbenzyl)-3-methyl-imidazolium tetrafluoroborate). In case of P[VBTMA][BF₄], the CO₂ solubility was found to be higher than that in P[MATMA][BF₄] [Blasig (2007b)].

Bara et al. (2007b) reported gas permeation of single component PILs. Five simple RTIL monomers with either acrylate or styrene-based polymerizable groups were evaluated. CO₂ permeability increased from 7 to 32 Barrers as the alkyl group was varied from methyl to *n*-hexyl in the styrene-based backbone. CO₂/N₂ selectivity varied from 37-28. Functionalized poly(RTIL)s using imidazolium-based monomers containing either oligo(ethylene glycol) or alkyl-terminated nitrile groups with improved CO₂ selectivity are reported [Bara et al. (2008a)]. Composite membrane prepared by the incorporation of 20 mol% free RTIL in the poly(RTIL) improved CO₂ permeability by 400% with a 33% increase in CO₂/N₂ selectivity relative to the analogous membrane lacking any free ion pairs [Bara (2008b)]. Cross-linked gemini RTIL-polymer membranes showed lower gas permeabilities than previously reported poly(RTIL) membranes [Bara (2008c)].

2.5. Properties and applications of polybenzimidazole (PBI)

Polybenzimidazole (PBI) is one of the classes of heteroaromatic polymers known for many years following the early work of Marvel and coworkers [Vogel (1961)]. PBI is known as high performance material due to its remarkable thermal, mechanical and chemical stability. These properties are retained at elevated and cryogenic temperatures. The limiting oxygen index (minimum O₂ concentration at which a given sample can be induced to burn) of PBI is 48% [Belohlav (1974)] which is much better than for other common polymers such as Nomex®, Kapton®, etc. A remarkable moisture regain by PBI proved to be of interest in its applications such as protective clothing which compares favorably in this respect with both, cotton and other synthetic fibers [Belohlav (1974)]. Coexistence of these properties in PBI makes it useful in many other applications such as fuel cell membrane material, in aerospace industry, molecular composites, sorbents, etc.

i) Proton exchange membrane(PEM) for Fuel cell

One of the member of PBI family, commonly termed as PBI, prepared using 3,3'-diaminobenzidine and isophthalic acid as monomers is gaining increasing importance as the PEM material due to its unique thermochemical and mechanical stability. Fuel cell based on its membrane can be operated up to 200 °C [Li (2003, 2004)], has high CO tolerance [Li (2001, 2004a)], low fuel crossover [Wainright (1995), Li (2004)], almost zero osmotic drag coefficient [Wainright (1995)] and proton conductivity comparable to the well established Nafion membrane [Wainright (1995), Li (2003, 2004)]. This highly basic material is characterized by high density [Földes (2000), Mecerreyes (2004)], high T_g [Földes (2000)], H₃PO₄ uptake of ~ 14 moles/repeat unit (mol/RU) and 3.4-3.6 mol/RU of water sorption [Li (2001)]. The imidazole group, like water acts as a solvating agent for the proton [Kreuer (1998)]. It donates free electrons to the protons (from strong acids) to form stable complex. Bouchet et al. (1999) using infrared spectroscopy showed that the interaction between PBI and strong acids involved protonation rendering the stability to acid-doped PBI membranes.

ii) Miscible blends with enhanced properties

Because of the properties of PBI such as high T_g, chemical resistance, and retention of mechanical properties at both high and cryogenic temperatures, it is currently being examined as the primary material in high performance polymer blends. Because of

the ability of PBI to form hydrogen bonding it forms miscible blends with various polyimides, polyarylate, polyvinylpyrrolidone, etc. [Choe (1996)]. The miscibility increases with increasing polymer polarity. Enhanced rate of thermal degradation of miscible blend of PBI and polyimidesulfone is known [Choe (1996)].

iii) Molecular composites

Molecular composites are miscible blend containing two or more components dispersed at the molecular level at a scale no greater than few nanometers. Films were made from ABPBI blends with rigid-rod polymers such as poly(*p*-phenylene benzobisthiazole) (PBT) at the ratio of 70/30%. Above a critical concentration, the blend showed a phase separation of aggregated PBT crystallites (10 nm) in a ABPBI matrix. Below a critical concentration, the blend formed a homogeneous solution, and the fibers and films prepared from the blend contained crystallites of both PBT and ABPBI with size of crystallites < 3 nm, thus forming a molecular composites. The fiber properties of the molecular composite were higher than the phase separated fibers [Choe (1996)].

iv) PBI performance parts

PBI performance parts produced by either hot compression-molding or a direct forming process are marketed under the trade name of Celazole® by Hoechst Celanese Corporation [Choe (1996)]. Molded PBI possesses outstanding mechanical and dielectric properties at elevated temperatures or after heat aging in air. PBI moldings have found use as structural components in automotive, aeronautical and electrical engineering applications where these properties are of importance [Neuse (1982)]. PBI molded resin produced by hot-compression has a compressive strength of 58 Kpsi, a tensile strength of 23 Kpsi and a density of 1.3 g/cc. An excellent property retention at elevated temperature above 371 °C, combined with excellent chemical and hydrolysis resistance made Celazole precision parts useful for chemical processes and oil recovery industries. It is also applicable where hardness, low friction, high compressive strength, and thermal, chemical and dimensional stabilities are required; for example, bearings, sleeves and rollers [Choe (1996)]. Developmental emphasis has been placed on PBI composite materials made of fiber reinforced laminates [Kalnin (1978)]. Both glass and quartz fiber materials have been employed for reinforcement [Neuse (1982)].

v) ***As catalyst support***

PBI was used as a support for preparation of polymer-supported catalysts in reduction-oxidation reactions [Choe (1996)]. High thermal stability of PBI support at elevated temperatures is an extremely valuable feature for this application. PBI-supported molybdenum (VI) was used for the epoxidation of propene using *tert*-butylhydroperoxide [Leinonen (1999)]. PBI was complexed with PdCl₂ and reduced to PBI/Pd⁰ using H₂ and methanol/NaOH in nitrobenzene. PBI/Pd⁰ is highly active, thermally stable, recyclable and is very effective in the reduction of nitro compounds to corresponding amines or alkenes to corresponding alkanes [Choe (1996)].

vi) ***Metal sorbents***

Chemically modified PBIs with chelating ligands via epoxidation have been used for metal-selective sorbants. For example, PBI epoxidised-dimethylglyoxime exhibited a high sorption capacity for UO₂²⁺ and Fe³⁺ [Chanda (1989a)]. Epoxidized PBI resin with immobilized dithiooxamide exhibited high sorption for Pd(II) and Pt(IV) [Chanda (1990a)]. PBI resin modified with mercaptoacetic acid resulted in a significant improvements in its sorption capacity for precious metals such as silver and gold [(Chanda (1987a)]. PBI protonated with mercaptoacetic acid exhibited higher sorption capacity for Hg(II) [Chanda (1987b)].

vii) ***Membrane***

Reverse osmosis membranes prepared from PBI (21% DMAc solution containing 2% LiCl) showed a flux of 16 g/ft²/d and salt rejection of 95% [Belohlav (1974)]. PBI has affinity for acidic compounds and thus was used for separation of acidic compounds from a mixture of acid and phenols in dilute solution [Choe (1996)]. Microporous PBI was used for sorption of SO₂ and sulfonated PBI for separation of CO₂ [Choe (1996)].

viii) ***Fibers and fabrics***

PBI is most conveniently made into fibers by dry-spinning from DMAc solution containing a few percent LiCl for solubility improvement [Belohlav (1974)]. The washed and dried yarns are generally drawn for enhanced orientation and strength, drawing temperatures for high-performance materials being as high as 400 - 500 °C. Drawn filaments may typically possess tenacities of 4.5 - 6 g/den and elongations of 19 - 27% (for comparison, average values for regular grade of cotton fiber are 2 - 3 g/den and

elongation of 5 - 10%), and these properties do not change markedly at temperatures up to about 300 °C [Neuse (1982)]. In addition to being nonflammable, the fibers show an outstanding moisture regain (water content in equilibrium with surrounding air of 65% relative humidity at 21 °C) of 13%, most favorably contrasting with acrylics (2%) or Nylons (4.5%). Furthermore, fabrics woven from PBI yarns are comfortable to wear. It is for these reasons that PBI textiles are being used advantageously for protective clothing, for example, in special fire-fighting suits [Neuse (1982)].

ix) Structural adhesives

PBI possess excellent bonding characteristics not only at high temperatures, but even in the cryogenic region down to - 196 °C and lower, where most organic adhesives undergo strong embrittlement [Neuse (1982)]. However, the applications have been restricted to military and aircraft component design, due to the cost issue.

x) Electro-insulation materials

The retention of dielectric properties in a high temperature environment, coupled with good corrosion resistance in contact with certain reactive chemicals makes PBI suitable for use in electrical insulation and other dielectric applications (such as special cable and wire insulation, as battery and electrolytic cell separators, etc.) at high temperature or in aggressive chemical environments [Neuse (1982)].

2.6. Permeation properties of PBI

Investigation on gas permeation properties of polybenzimidazoles as a family of polymers is almost unexplored in the literature. Only few reports available on gas permeability of PBI based on DAB and isophthalic acid (PBI-I) indicated that it possesses very low gas permeability [Pesiri (2003), Jorgensen (2004), Klaehn (2005), He (2006)]. Jorgensen et al. (2004) has disclosed the crosslinking of PBI by α,α' -dibromo-*p*-xylene and compared the gas permeation properties of crosslinked and non-crosslinked membranes. The PBI permeability above 80 °C is reported by He et al. (2006) in relation to its fuel cell applicability. Klaehn et al. (2005) has reported N-substitution of PBI by methyl, phenyl vinyl and allyl groups and evaluated allyl-PBI for gas permeation. With an exception of H₂, permeability for other gases was 2 - 7 times higher than that of the parent PBI. However, detailed investigations on gas permeation properties of *N*-

substituted PBI were not available. A compilation of PBI permeability data reported in the literature is given in Table 2.1 below.

Pesiri et al. (2003) reported gas permeation properties of PBI at high temperature. The permeance of H₂ increased from 0.09 Barrer at room temperature to over 18 Barrer at 340 °C. The CO₂ transport was also increased significantly with increased temperature, from 0.01 Barrer at 25 °C to 4 Barrer at 340 °C. The selectivity of the CO₂/CH₄ gas pair was reported to be 33 at 250 °C, which is excellent as far as the reducing selectivity with increase in temperature known for common polymeric materials. Gas permeation properties of PBI based on aliphatic dicarboxylic acid was reported [Zhang (1995)]. A series of polyalkylenebenzimidazole having longer flexible chain showed higher gas permeability, but lower selectivity than the polymer containing shorter flexible chain.

Table 2.1. Permeation properties of PBI based on isophthalic acid

References	Temp. (°C)	H ₂	Ar	O ₂	N ₂	CH ₄	CO ₂
He (2006)	25	-	-	-	-	-	-
	80	4.78	-	0.149	-	-	-
	120	8.97	-	0.179	-	-	-
	180	12.85	-	0.299	-	-	-
Klaehn (2005)	30	3.9	0.073	0.086	0.049	0.04	0.07
	55	5.7	0.07	0.31	0.09	0.11	0.25
Jorgensen (2004)	23	5.117	-	-	0.026	0.307	0.017
	23*	11.187	-	-	0.011	0.011 at 89 °C	0.699
	313	171.18			2.19	1.70	7.57
Pesiri (2003)	25	0.09	-	-	-	-	0.01
	340	18	-	-	-	-	4

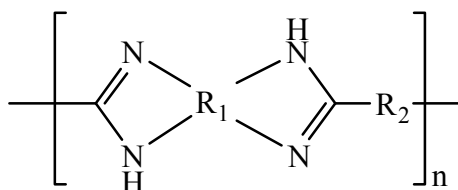
* Data for crosslinked PBI

2.7. Structural variations in PBI

2.7.1. Variation in diamine and diacid moiety

PBI have the general structure as shown in Scheme 2.1. Where R₁ group is from aromatic tetraamine and R₂ can be aliphatic or aromatic group is from dicarboxylic acid

used for PBI synthesis. Many aromatic PBIs have been reviewed [Levine (1969), Cassidy (1980), Neuse (1982), Choe (1996)]. A general overview of PBI synthesis was published in 1996 [Choe (1996)]. PBIs were prepared by different polycondensation methods such as melt/solid-state polycondensation, solution polymerization and suspension utilizing bis(*o*-diamines) and difunctional acids or derivatives or by nucleophilic substitution reactions of AB monomers.



Scheme 2.1. General structure of polybenzimidazole (PBI)

Different tetraamines amines and dicarboxylic acids used for PBI synthesis are given in Table 2.2 and 2.3 below. Tetraamines can be used in free form or in the form of salts with mineral acids [Iwakura (1964a, 1964b, 1964c, 1967)].

Table 2.2. Different tetraamines used for the synthesis of PBI

Tetraamines	Reference
	X= nill: Vogel (1963), Tsur (1974) X= -O-: Foster (1965), Hedberg (1974), Banihashemi (1980), Tsur (1974) X= -SO ₂ -: Narayan (1967) X= -S-: Choe (1996) X= -CO-: Hedberg (1974), Banihashemi (1980) X= -CH ₂ -: Tsur (1974)
	Vogel (1961), Banihashemi (1980)
 • 3HCl	Gerber (1973)
	R=Ph: Vogel (1963) R=CH ₃ : Mitsuhashi (1965)
	Dawans (1964)

Table 2.2 continued...

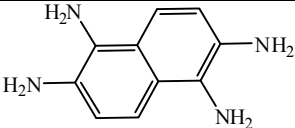
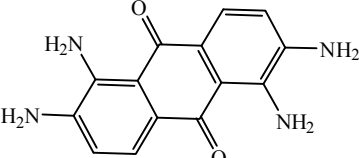
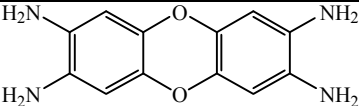
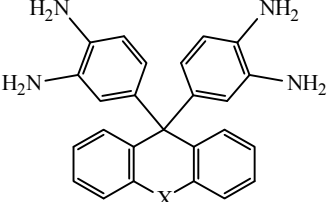
Tetraamines	Reference
	Choe (1996)
	Banihashemi (1980)
	Choe (1996)
	X= nill, -CO-: Srinivasan (1982)

Table 2.3. Different dicarboxylic acids/derivatives used for the synthesis of PBI based on DAB

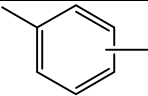
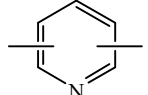
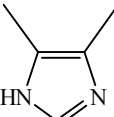
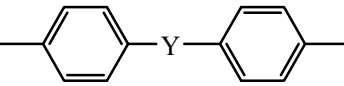
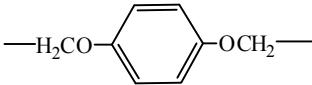
'Ar' in HOOC-Ar-COOH	Reference
	Hedberg (1974), Vogel (1963)
	Brock (1991), Xiao (2005), Vogel (1961)
	Brock (1991), Plummer (1964), Vogel (1961)
	Y= nill: Vogel (1961); Y= -C(CF ₃) ₂ -: Saegusa (1997), Chuang (2007); Y= -O-: Foster (1965); Y= -Si(Ph) ₂ -: Kovacs (1968)
	Scariah (1987)

Table 2.3 continued...

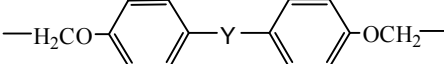
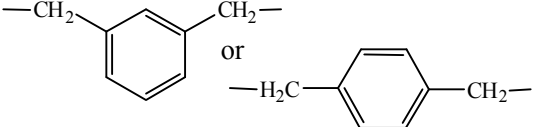
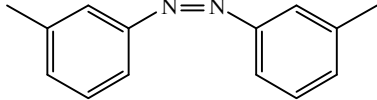
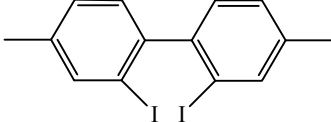
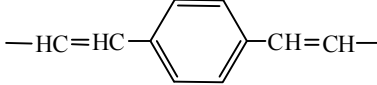
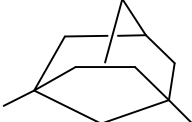
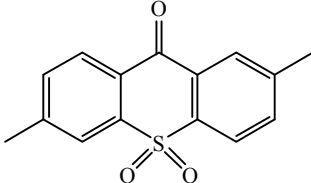
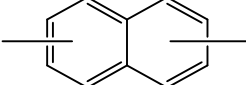
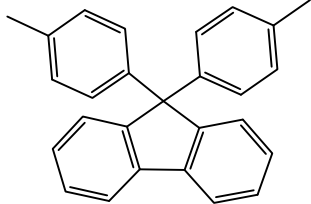
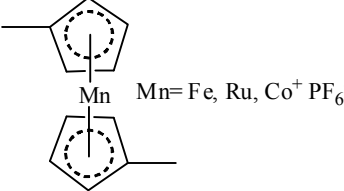
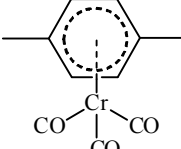
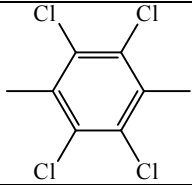
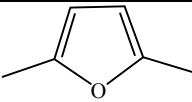
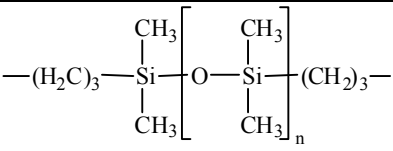
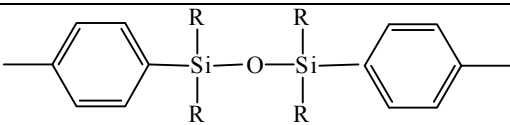
'Ar' in HOOC-Ar-COOH	Reference
	Y = -C(CH ₃) ₂ -, -SO ₂ -; Scariah (1987); Y = -SO ₂ -; Scariah (1987)
	Tsur (1974)
	Srinivasan (1982)
	Banihashemi (1980)
	Neuse (1982)
	Moon (1970)
	Reddy (1988)
	Plummer (1964)
	Srinivasan (1982)
	Plummer (1964)
	Neuse (1982)

Table 2.3 continued...

'Ar' in HOOC-Ar-COOH	Reference
	Neuse (1982)
	Vogel (1961)
---CH=CH---	Plummer (1964), Varma (1976)
	Nakajima (1969)
	R= -CH ₃ : Mulvaney (1961); R= -C ₆ H ₅ : Breed (1976)
$\text{---(CH}_2\text{)}_n\text{---}$	n= 2, 3: Vogel (1963); n= 2, 4, 6, 8: Tsur (1974); n= 4, 7, 8, 11, 20: Iwakura (1964b); n= 3, 8: Trischler (1967); n= 0-4, 8: Adrova (1965)
$\text{---(CF}_2\text{)}_n\text{---}$ n=3 and 6	Plummer (1964)

2.7.2. PBI modification

PBI though is known for variety of applications due to its unique thermo-chemical and mechanical stability as discussed in the Section 2.5; has very poor solubility in organic solvents, leading to processibility issues. It is soluble only after heating in highly polar, aprotic organic solvents (DMSO, DMAc, DMF NMP). Limited solubility of PBI was attributed to interchain hydrogen bonding and to the polarity of the benzimidazole ring [Hu (1993)]. To improve solubility, its modification either at monomer level or after polymer formation can be done conveniently. Efforts reported in the literature on monomer modifications are summarized in Section 2.8. Various strategies followed for post-modification include sulfonation [Jouanneau (2007), Qing (2005a, 2005b, 2006)], nitration [Lyo (2000)], *N*-substitution by alkyl group [Hu (1993), Klaehn (2005, 2007), Yamaguchi (2000)], copolymerization [Gordon (1988), Brock (1991)], etc.

The sulfonated PBI was obtained using sulfonated tetraamine [Jouanneau (2007)] or sulfonated dicarboxylic acid [Qing (2005a, 2005b, 2006), Jouanneau (2007)]. Post-sulfonation of PBI using H_2SO_4 , rendered insolubility due to the crosslinking by sulfonyl groups or, the formation of a strongly hydrogen-bonded network of the sulfonated polymer [Ariza (2002)]. Peron et al. (2008) reported direct sulfonation of PBI in H_2SO_4 under milder conditions. *N*-substitution of PBI with alkyl [Gieselman (1992)] or aryl group [Glipa (1997)] bearing sulfonated group was reported. *N*-substitution of PBI with sodium 4-(bromomethyl)benzenesulfonate, 2-propanesultone and 1,4-butanedisulfone transformed the PBI into new water soluble polymer derivatives [Gieselman (1992, 1993), Dang (1994)].

Nitration of PBI with a mixture of HNO_3 and H_2SO_4 improved its solubility [Lyo (2000)]. PBI with the maximum degree of substitution of 2, was soluble in DMAc and NMP. Cabasso et al. (2005) disclosed the functionalisation of polybenzimidazole by direct grafting via radical phosphonylation of phosphonated ester groups using a dialkylphosphite and an initiator.

N-hydroxyethylation, *N*-cyanoethylation and *N*-carboxyethylation to improve hydrophilicity of aliphatic PBI was reported [Trischler (1969, 1971)]. Introduction of long side chains (polyrotaxanes) by *N*-substitution imparted solubility in CHCl_3 , THF and acetone [Yamaguchi (1997)]. *N*-alkylated polybenzimidazole rotaxanes were synthesized by choosing β -cyclodextrin (β -CD) as the macrocyclic species and a reaction between an -ONa group and a crown ether [Yamaguchi (2000)].

Poly(*N*₁,*N*₃-dimethylbenzimidazolium) (PDMBI) salt and poly (*N*₁-methylbenzimidazole) (PMMBI) were synthesized by methylation of PBI [Hu (1993)]. PMMBI was soluble in NMP and PDMBI in DMSO at room temperature. Synthesis of poly(*N*-methylbenzimidazole) (PNMBI) and poly(*N*-ethylbenzimidazole) (PNEBI) with various alkylation degrees was performed by adding LiH and controlling the amount of substituting reactant [Pu (2005)]. PNMBI was soluble in NMP and PNEBI was soluble in DMAc and NMP at room temperature. *N*-substituted PBIs were obtained from tetraamine bis-carbamate derivative and a dicarboxylic acid with a gentle dehydrating agent polyphosphoric acid trimethylsilyl ester [Kane (1990)].

N-substitution of PBI with methyl, phenyl, vinyl and allyl halides offered improved solubility and thermal properties [Klaehn (2005)]. *N*-substituted organosilane PBI derivatives ($-\text{CH}_2\text{SiMe}_2\text{R}$; R= methyl, vinyl, allyl, hexyl, phenyl, and decyl), which were soluble in organic solvents are also reported [Klaehn (2007)].

PBI beads were *N*-substituted in an aqueous solution; however, the resulting substitution was simply a surface modification of the resin bead and not a fully substituted polymer backbone [Chanda (1987a, 1987b, 1990a, 1990b, 1991/92, 1992)]. The beads were reacted with epichlorohydrin and NaOH and the resulting product with pendant epoxy groups were further reacted with various chelating ligands such as ethylenediamine, diethanolamine, etc. [Chanda (1989b)].

2.8. Synthetic routes of PBI

Brinker and Robinson patented the first aliphatic PBI in 1959 [Chung (1997)]. Later aromatic PBI were synthesized by Vogel and Marvel [Vogel (1961, 1963, 1966)]. In 1983, Celanese Corporation commercialized PBI for textile and fire blocking applications [Chung (1997)]. Different routes used for the synthesis of PBI are summarized below.

2.8.1. Melt and solid-state polymerization

Marvel's pioneering approach for the synthesis of PBI involved melt polycondensation of 3,3'-diaminobenzidine (DAB) or 1,2,4,5-tetraaminobenzene (TAB) with diphenyl esters of aromatic dicarboxylic acids, such as isophthalic acid, terephthalic acid, 4,4'-biphenylene dicarboxylic acid, etc. [Vogel (1961)]. Polycondensations were carried out, generally in two stages, i.e., a combination of melt polymerization of DAB with diphenyl isophthalate (DPIP) [Vogel (1961, 1966), Chenevey (1969), Prince (1970a)], isophthalic acid (IPA), dimethyl isophthalate [Vogel (1961)], or isophthalonitrile [Ohfuji (1972)], followed by a second-stage solid-state polymerization at an elevated temperature. A single-stage melt polymerization of TAB with DPIP was also reported [Prince (1970b), Choe (1994)].

Marvel's initial procedure has been extended to additional monomers such as bis(3,4-tetraaminodiphenyl)ether, bis(3,4-tetraaminodiphenyl)ketone, bis(3,4-tetraaminodiphenyl)sulfone and 1,3-dianilino-4,6-diaminobenzene, as well as a large number of

additional bis(phenoxy carbonyl) derivatives of mono, di and trinuclear aromatic and heterocyclic dicarboxylic acids. A comprehensive listing of monomers is given in Levine's review [Neuse (1982)] and number of additional monomers used has been cited by Cassidy [Cassidy (1980)].

Effect of various catalysts to improve molecular weight and quality (in terms of viscosity and plugging value, a measure of solution filterability) of PBI based on IPA or DPIP and DAB using silicon and phosphorous based catalyst was explored [Choe (1994)]. Hydrochloric acid, ammonium chloride, *p*-toluenesulfonic acid, phosphoric acid, etc. were also explored. An entirely novel approach was proposed by Gray et al. (1967), where, DAB undergo melt condensation with 4-acetylacetophenone at 250 °C, to obtain polymeric intermediate through elimination of water. This prepolymer was readily aromatized to PBI with elimination of methane by heating at 300 °C [Gray (1967)].

ABPBI was synthesized by the melt polycondensation of phenyl-3,4-diaminobenzoate [Vogel 1961)]. Melt condensation of phenyl diaminobenzoate yielded a high molecular weight polymer with an inherent viscosity of 1.27 dL/g where as, methyl-3,4-diaminobenzoate led to its decomposition [Vogel (1961)].

Although PBIs prepared by melt polycondensation exhibited good performance characteristics, they do not lend themselves to processing by standard techniques other than spinning and film casting. They have been found to lack satisfactory solubility in non-corrosive solvents [Neuse (1982)]. Melt condensation limits the use of monomers to those stable enough to resist the high temperatures required. Monomers with free carboxylic acid groups, for example, 3,4-diaminobenzoic acid, is known to undergo decarboxylation at elevated temperatures rather than forming a linear polymer chain [Vogel (1961)].

2.8.2. Low and high-temperature solution polymerization

a) Solution polycondensation using polyphosphoric acid (PPA)

PPA has been widely used and proved to be a promising medium which acts as a solvent as well as dehydrating agent in PBI synthesis [Iwakura (1964a, 1964b, 1964c), Xiao (2003a, 2005), Zhang (2004), Sannigrahi (2007), Xu (2007), Jayakody (2007), Kim (2007a, 2008a)]. The polymerization reaction is homogeneous and occurs at temperature

of approximately 200 °C, which is considerably lower than that of the melt/solid-state polymerization. It is suited for monomers with limited thermal stability [Xiao (2003b)]. During polymerization, PPA solvates both, monomers (diacid and bis-*o*-diamines), and subsequently formed polymer. PPA activates both the functional groups towards the polycondensation and reacts with the condensation byproduct water to effectively dehydrate the system [Wolfe (1987)]. The resultant PBIs were identical with and possessed same properties as the corresponding products of melt condensation process [Vogel (1961)].

Polymerization of 3,4-diaminobenzoic acid (DABA) in refluxing dilute or concentrated phosphoric acid suspension produced only low molecular weight polymer (0.2 dL/g) [Philips (1930)]. Imai et al. (1965) used DABA and its salts in PPA to obtain ABPBI. Inherent viscosities of formed polymers were 0.78 - 1.95 dL/g. Most of the literature reports the synthesis of ABPBI by solution polycondensation method using PPA [Asensio (2004), Gómez-Romero (2005), Asensio (2005), Kim (2007b)]. ABPBI was also synthesized in a polymerization medium containing CH₃SO₃H and P₂O₅ [Kim (2004, 2008b)].

While PPA based solution polycondensation method presents a convenient means of synthesizing PBIs, it is not amenable to prepolymer isolation and processing. It is, therefore, restricted in its usefulness to such cases where the ultimate products can be utilized (e.g. in spinning or film casting). PPA is unsuitable for polymerization of monomers unstable in a hot acidic environment [Neuse (1977)]. It attacks glass leading to incorporation of silica into the polymer [Banihashemi (1969)]. Its susceptibility for promoting self condensation of amines is known [Banihashemi (1969)].

b) *Solution polycondensation using high boiling organic solvents*

Solution polymerization can also take place in high boiling organic solvents such as dimethyl acetamide, dimethyl sulfoxide, *N*-methylpyrrolidone, hexamethylphosphoramide, phenol and cresol [Kokelenberg (1970), Hedberg (1974)]. PBIs were prepared by a two stage solution polymerization of DAB with aromatic dialdehyde in DMAc [D'Alelio (1963), Neuse (1983)], with isophthalonitrile in DMF [Brand (1978)], and by a single-stage polycondensation of aromatic tetramines with isophthalaldehyde bis(bisulfite adduct) in refluxing DMAc [Higgins (1970)]. It can also be synthesized with

diphenyl isophthalate in a refluxing sulfone solvent, e.g., sulfolane or phenyl sulfone [Hedberg (1974)] and with bisorthoesters in DMSO [Dudgeon (1978)]. The amide solvents caused transamidation [Neuse (1982), Brock (1992)]. By use of sulfolane or diphenyl sulfone as solvents [Hedberg (1974)], smooth polymerization of bis(*o*-diamine)s and bis(phenyl ester)s could be accomplished without side effects as observed with poly(phosphoric acid) and the amide media [Neuse (1982)].

PBI preparation by solution polymerization of aromatic bis(*o*-diamine)s with free dialdehydes at preferably 100-125 °C is reported [D'Alelio (1963)] in DMAc or similar solvents, which permits use of thermally/chemically unstable monomers. Example of such monomers is tetrahaloterephthalaldehydes or crosslinkable 3-vinylisophthalaldehyde [Neuse (1982)]. PBIs were also prepared by the aromatic nucleophilic displacement reaction of di(hydroxyphenyl)benzimidazole monomers with activated aromatic dihalides or dinitro compounds [Inbasekaran (1993), Connell (1994, 1996, 1997), Wang (2008)]. The reactions are usually carried out in NMP or DMAc at elevated temperature in the presence of alkali metal bases (e.g. K₂CO₃). PBI can be synthesized within an hour or less at temperatures as low as 100 °C, using highly reactive bis(trialkyl ortho-ester)s in DMSO/pyridine mixture [Dudgeon (1978)].

c) Reductive cyclization

The term reductive polyheterocyclization means the occurrence of cyclization immediately after reduction [Korshak (1984)]. Use of bis(*o*-nitroaniline)s in place of tetraamines were demonstrated following this route. The intermediary poly(*o*-nitroamide)s are subjected to reductive cyclization in presence of activated iron and dry HCl [Korshak (1979)]. This process includes the addition of dicarboxylic acid dichloride to bis[*o*-nitro aniline] solution in NMP, mixing of the reaction solution for 10 - 12 h, saturation with gaseous HCl, and heating under N₂ and HCl at 170 °C - 180 °C for 1 h [Korshak (1984)]. High degrees of cyclization under milder synthesis conditions (170 °C - 180 °C, 1 h) is most important advantages of reductive polyheterocyclization. However incomplete reduction or incomplete cyclization of the reduced and partially reduced fragments can lead to lower thermal and chemical stability of the formed polymer due to chemical heterogeneity [Korshak (1984)].

The modified reductive polyheterocyclization differs from the previous processes [Korshak (1979, 1984)] in that the cyclization processes are separated by one or more reactions (usually acylation) from the nitro-group to amino group reduction stage [Korshak (1984)]. The modified reductive polyheterocyclization processes were accomplished as continuous processes in NMP using activated Fe/HCl as reducing agents and HCl as cyclization catalyst. An illustrative example of modified reductive polyheterocyclization is the synthesis of C-phenylsubstituted PBI by interaction of activated bis[(*o*-nitro)halogen]arylenes with aromatic diamines, reduction of the resulting poly[(*o*-nitro)imines] to poly[(*o*-amino)imines], benzoylation of the latter and cyclization of the poly[(*o*-benzamido)imines] [Korshak (1984)]. The synthesis of C-phenylsubstituted PBI is a simple process proceeding under mild conditions and contains no unreduced nitro groups and uncyclised fragments. It was also reported that at none of the process stages does the temperature exceeded 180°C. The presence of phenyl substituents determines the high solubility of PBI in dipolar aprotic and phenol solvents [Korshak (1984)].

d) *Interfacial polycondensation*

The low-temperature or interfacial polycondensation involving reaction of a bis(*o*-diamine) and the acid chloride of a dicarboxylic acid in an effort to form a soluble poly(aminoamide) intermediate is reported [Vogel (1961), Neuse (1982)]. However, attempts made towards this end remained unsuccessful, as the primary amidation step proved too fast to be selective. It caused an additional amidation at the *o*-amino group with resultant formation of the branching and, ultimately, three-dimensional crosslink formation: At the same time, it would prevent "imidazolization", i.e., closure of the five-membered heterocycle [Neuse (1982)]. However, various approaches have been reported in which the problem of multiple amidation and branching is overcome by the use of monomers having amino groups of different basicities, thus allowing for a more selective substitution and an enhanced degree of linearity. As an example, replacing tetraaminobenzene by 2,3,5,6-tetraaminopyridine gave soluble (aminoamide) intermediates that may be employed as prepolymers in a two-stage process [Gerber (1973, 1976)]. The two step synthesis can be carried out in a more controlled manner using bis(*o*-diamines); amino groups of which are partially blocked by removable

protecting groups. Instead of *1,2,4,5*-tetraaminobenzene, the *4,6*-bistosylated product was reacted with acid dichlorides in solution to obtain corresponding poly(amino)amides. After detosylation, these can be converted to PBI by cyclic dehydration in the solid phase [Rossbach (1991)].

e) PBI synthesis by non-aqueous suspension method

PBIs can be prepared in the form of small particles by reaction of bis(*o*-diamine) substituted compounds with dicarboxylic acids or of *o*-diamino-substituted carboxylic acids in the presence of an inert non-solvent liquid medium and polyphosphoric acid [Milford (1983)]. *3,4*-Diaminobenzoic acid was suspended in an inert organic continuous phase, e.g. paraffin oil. Polyphosphoric acid was then added to the stirred mixture forming a suspension. The dispersed phase consisted of the monomers dissolved in the acidic solvent and sodium dodecylbenzene sulphonate (SDBS) served as a surface active suspension stabilizer. Polycondensation was subsequently carried out by heating the reaction mixture to 200°C for several hours. This way, preparation of polybenzimidazole particulates in high yields and various particle sizes was reported [Milford (1983)]. Brock et al. (1992) reported the preparation of PBI beads in a similar way using a series of surface active suspension stabilizers, low molecular weight ones as well as polymeric dispersants [Brock (1992)]. The low molecular weight stabilizers such as *2*-dodecen-*1*-ylsuccinic anhydride, dodecylbenzene sulphonic acid sodium salt, etc. were used. Polymeric stabilizers such as poly (butadiene-*co*-acrylonitile) (carboxy terminated), polyisobutylene (epoxide or carboxy terminated), poly(ethylene-*co*-acrylic acid), poly(styrene-*co*-maleic anhydride), etc. were demonstrated.

Chapter 3

Experimental

3.1. Monomers and materials

Various solvents, viz., chloroform, 1,1,2,2-tetrachloroethane (TCE), methanol, carbon tetrachloride, toluene, cyclohexanone, acetone, acetonitrile, 1,4-dioxane, pyridine, *N,N*-dimethyl formamide (DMF), dry dimethyl sulphoxide (DMSO), *N*-methylpyrrolidinone (NMP), phosphoric acid (~ 88%), methane sulfonic acid (CH₃SO₃H), trifluoroacetic acid (CF₃COOH), methyl iodide, *n*-butyl iodide, potassium thiocyanate (KSCN), sodium chloride (NaCl) and formic acid (HCOOH-80%) were obtained from S.D. Fine Chemicals. 3,3'-diaminobenzidine (DAB), 3,4-diaminobenzoic acid (DABA), isophthalic acid (IPA), terephthalic acid (TPA), 4,4'-(hexafluoroisopropylidene)bis(benzoic acid) (HFA), 5-*tert*-butylisophthalic acid (BuI), 2-bromoterephthalic acid (BrTPA), 2,5-dibromoterephthalic acid (DBrTPA), 2,6-pyridinedicarboxylic acid (PyA), sodium hydride (60% dispersion in mineral oil), 4-*tert*-butylbenzyl bromide and (iodomethyl)trimethylsilane, silver tetrafluoroborate (AgBF₄), lithium bis(trifluoromethane)sulfonimide (Li-Tf₂N), silver nitrate (AgNO₃) were procured from Aldrich Chemicals. Polyphosphoric acid (PPA) was procured from Lancaster, *N,N*-dimethylacetamide (DMAc) and concentrated H₂SO₄ (98%) were procured from Merck. All these materials were AR/LR/GR grade and were used without further purification. Pure gases, viz., He, H₂, Ar, N₂, O₂ with minimum purity of 99.9% were procured from Inox Air Products Ltd., while CH₄ and CO₂ with purity of 99.995% were procured from Air Liquide.

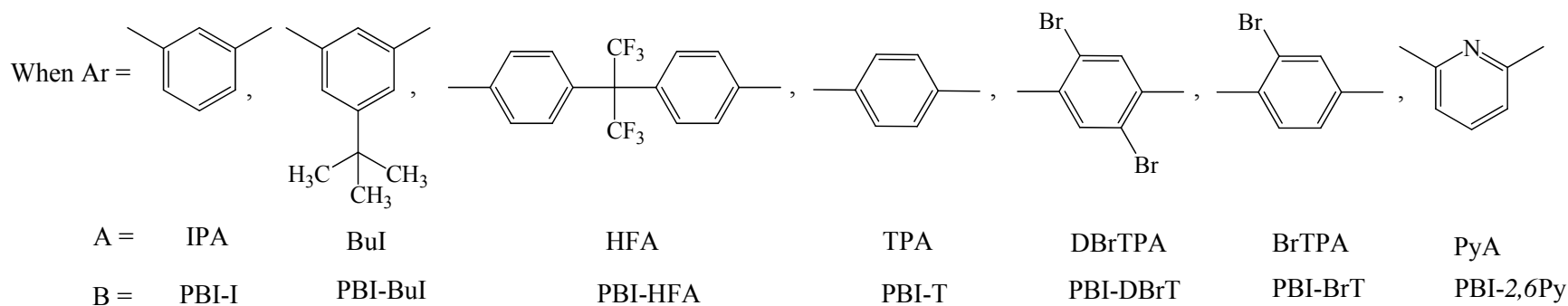
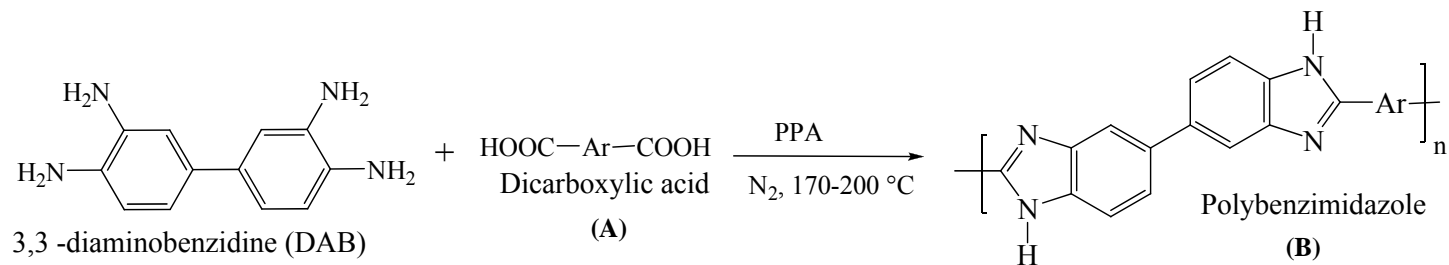
3.2. Synthesis of PBIs based on 3,3'-diaminobenzidine (DAB) and aromatic dicarboxylic acids

Polybenzimidazoles based on DAB and suitably chosen aromatic dicarboxylic acids were synthesized by solution polycondensation method using PPA, which acts as a solvent as well as condensation agent [Iwakura (1964c), Saegusa (1997)]. The reaction pathway is represented in Scheme 3.1. In a typical procedure, a three-necked flask

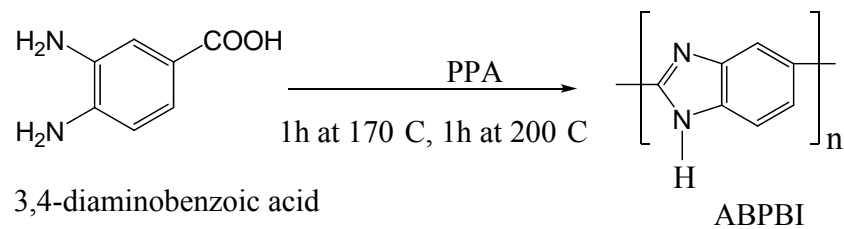
equipped with a mechanical stirrer, N₂ inlet and CaCl₂ drying tube was charged with 60 g of PPA, 2 g (0.0093 mol) of DAB and temperature was elevated to 140 °C. After complete dissolution of DAB, 0.0093 mol of respective dicarboxylic acid was added; temperature was slowly raised to 170 °C and maintained for 5 h under constant flow of nitrogen. The temperature was further raised to 200 °C and maintained for certain duration, depending upon the dicarboxylic acid used. The reasoning behind the need to vary this duration is explained in Chapter 4. After completion of the reaction, temperature was lowered and the highly viscous reaction mixture was poured on to the stirred water. The precipitated polymer was crushed and thoroughly washed with water till it was neutral to pH. The polymer was then kept overnight in 10% aqueous Na₂CO₃, washed with water until neutral to pH and soaked in acetone for 16 h to extract water. The dried polymer (100 °C, 3 days) was further purified by dissolving in DMAc, removing undissolved particles, if any, by centrifugation at 3000 rpm for 3 h and reprecipitation on to the stirred water. The polymer was finally dried at 60 °C for 24 h and then in vacuum oven at 100 °C for 3 days. Structures of obtained polymers along with their abbreviations used are given in Scheme 3.1.

3.3. Synthesis of poly(2,5-benzimidazole) (ABPBI)

Self condensation of 3,4-diaminobenzoic acid (DABA) to obtain ABPBI was performed as follows. The reaction mixture containing 5 g DABA in 100 g PPA was stirred at 170 °C for an hour and then at 200 °C for an additional hour (Scheme 3.2). Formed polymer after precipitating in water was crushed and washed with water till neutral to pH. It was then kept in 10% NaOH for 16 h, washed with water till neutral to pH, soaked in acetone for 5 h and dried at 100 °C under vacuum for 3 days. ABPBI could not be dissolved in common organic solvents and thus was used as such for further reactions of *N*-substitution or *N*-quaternization.



Scheme 3.1. Synthesis of PBI by condensation of DAB with aromatic dicarboxylic acids

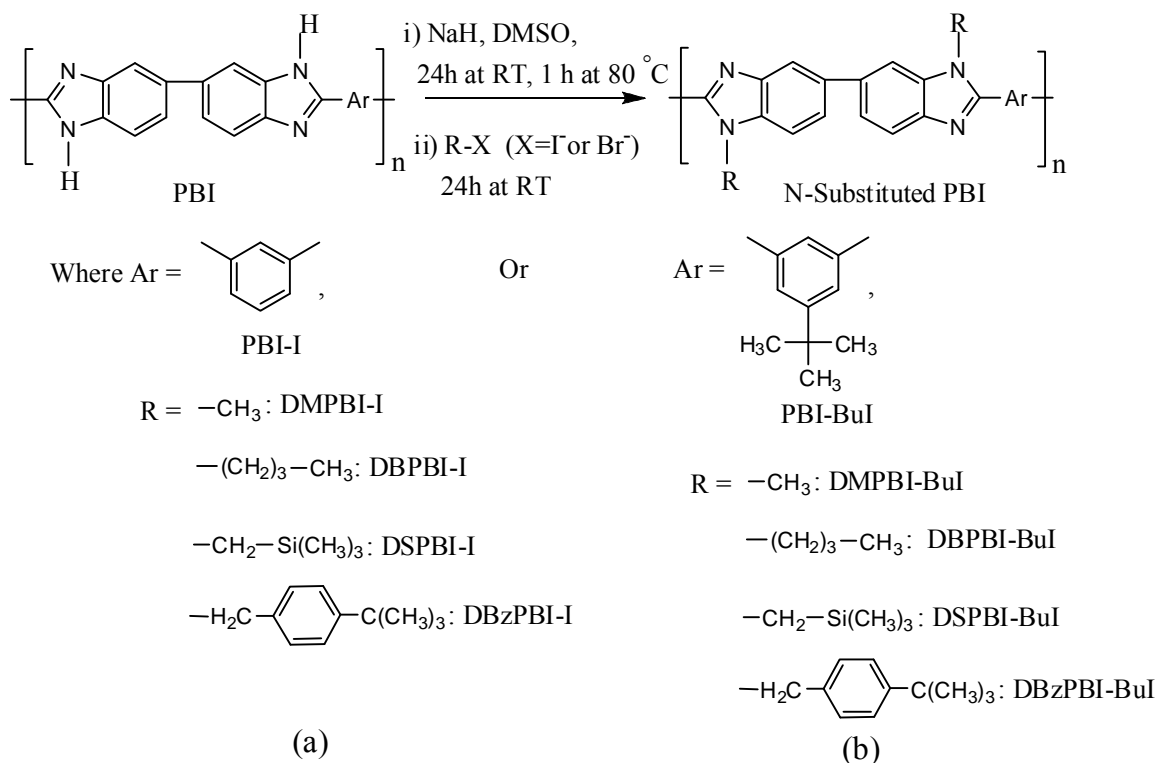


Scheme 3.2. Synthesis of ABPBI

3.4. N-substitution of promising PBIs

3.4.1. N-substitution of PBI based on isophthalic acid (PBI-I) and 5-tert-butyl isophthalic acid (PBI-BuI)

N-substitution of all PBIs was carried out in dry DMSO by preparing Na salt of PBI, followed by addition of the alkyl halide as shown in Scheme 3.3. To a three-necked round bottom flask equipped with N₂ balloon and a septum, charged 160 ml of dry DMSO, 0.0162 mol of PBI-I or PBI-BuI, 1.364 g of NaH (2.1 equivalents, 0.03409 mol) and stirred at ambient for 24 h. The reaction mixture was then heated at 80 °C for an hour. At this stage, a deep blood red colour developed after the complete dissolution of PBI. The solution was allowed to cool to ambient and 2 molar equivalents of alkyl iodide (methyl iodide, *n*-butyl iodide, 4-*tert*-butylbenzyl bromide or (iodomethyl)trimethylsilane dissolved in 10 ml of dry DMSO) was added in a dropwise manner for a period of 15 minutes. The reaction mixture got precipitated indicating formation of the *N*-substituted PBI. The reaction mixture was stirred further at ambient temperature for 12 h, and then was slowly poured on to the stirred water. The precipitated polymer was washed several times with water.

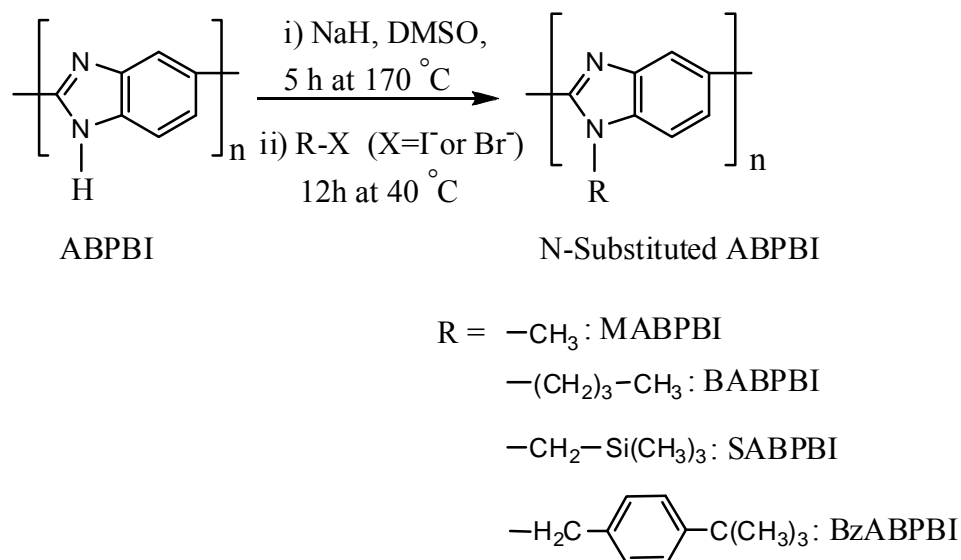


Scheme 3.3. N-substitution of (a) PBI-I and (b) PBI-BuI

Obtained polymers were purified by dissolving in DMAc (except for DMPBI-I, which was dissolved in NMP), followed by centrifugation at 3000 rpm for 3 h to remove undissolved particles, if any (< 1%), followed by precipitation in stirred water. The polymer was collected on the Buckner and was soaked in acetone for 5 h. After filtration, the polymer was dried at 80 °C for a week in a vacuum oven. The yield was almost quantitative (~ 95%) for all the *N*-substituted PBIs.

3.4.2. *N*-substitution of ABPBI

The reaction conditions in the case of ABPBI needed to be changed slightly, where, the reaction temperature during *N*-sodium salt formation was 170 °C for 5 h. A deep brown color developed yielding viscous homogeneous solution. The alkyl halide addition (1 molar equivalent) was then done at 40 °C. The reaction mixture was precipitated indicating formation of the *N*-substituted ABPBI. The reaction mixture was stirred further at ambient temperature for 12 h and then was slowly poured on to the stirred water. The precipitated polymer was washed several times with water. Chemical structures of polymers obtained along with their abbreviations are given in Scheme 3.4.



Scheme 3.4. *N*-substitution of ABPBI

N-substituted ABPBIs were purified by dissolving in formic acid (except SABPBI, which was dissolved in DMAc), followed by centrifugation at 3000 rpm for 3 h and precipitation in stirred water. To remove formic acid that was used as a solvent, these polymers were further treated with 10% NaHCO₃, followed by water wash. It was then soaked in acetone and dried at 100 °C, for a week in a vacuum oven.

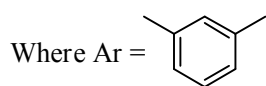
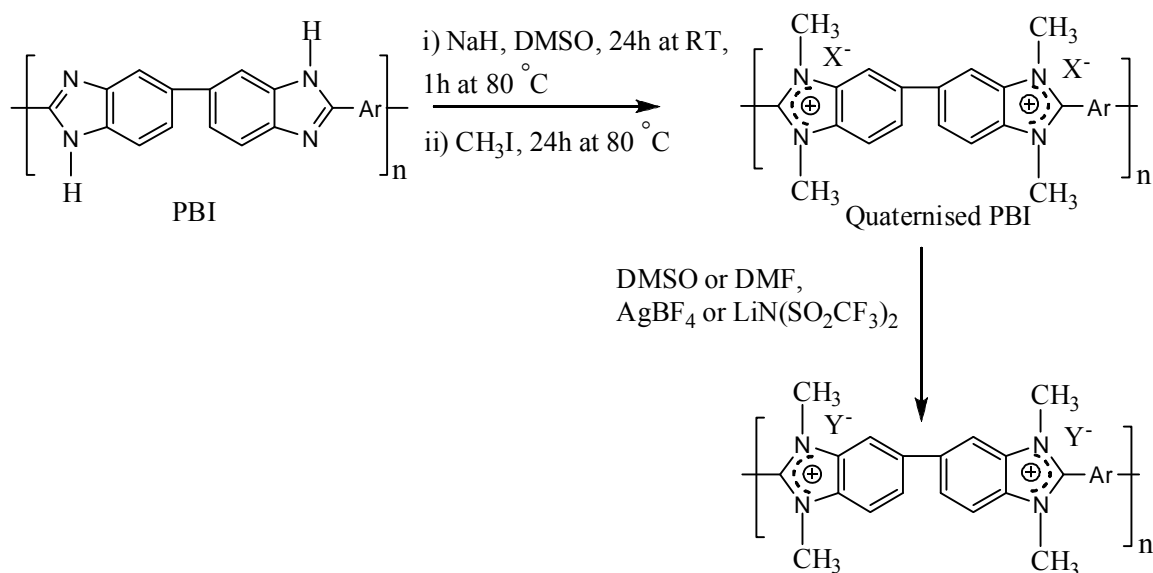
3.5. PBI quaternization and subsequent ion-exchange to obtain PIL

3.5.1. *N*-quaternization of PBI-I and PBI-BuI

The reactions of *N*-quaternization of PBI-I and PBI-BuI were carried out as given in Scheme 3.5. Typically, a 3-necked round bottom flask was charged with 160 ml of dry DMSO, 0.0162 mol of respective PBI, 1.364 g of NaH (2.1 equivalents, 0.03409 mol) and stirred under dry N₂ atmosphere at ambient for 24 h. The reaction mixture was further heated at 80 °C for an hour, where a deep blood red colour developed after complete dissolution of PBI, indicating formation of the *N*-sodium salt of PBI. The reaction mixture was cooled to the ambient and 4.3 ml (4.2 equivalents, 0.0682 mol) of methyl iodide was added slowly over a period of 15 minutes. A yellow precipitate was formed, which dissolved as the temperature was elevated to 80 °C. This temperature was maintained for 24 h. The reaction mixture after attaining ambient temperature was precipitated in a mixture of toluene and acetone (1:1). Obtained golden yellow fibrous precipitate was dried at 80 °C for 24 h. It was further purified by dissolving in DMSO and reprecipitating in toluene: acetone mixture. Obtained precipitate was dried at 60 °C for 24 h and then in vacuum oven at 80 °C for 3 days.

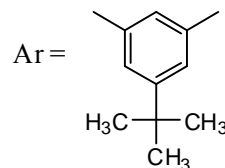
3.5.2. *N*-quaternization of ABPBI

The reaction conditions for *N*-quaternization of ABPBI were slightly different than that of PBI-I and PBI-BuI. The reaction temperature during *N*-sodium salt preparation needed was 170 °C (5 h), addition of methyl iodide (2.2 equivalents) was done at 40 °C, temperature was gradually raised to 80 °C and maintained for 24 h (Scheme 3.6). The reaction mixture was then precipitated in a mixture of toluene and acetone. Formed polymer was purified by dissolving in DMF and reprecipitating in methanol.

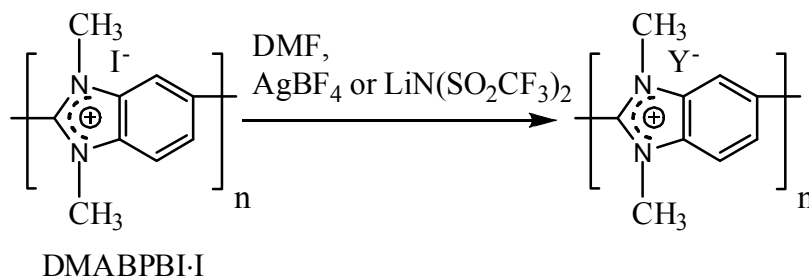


(a) PBI-I

Or



(b) PBI-BuI

 $X = \text{I}$: TMPBI-I-I, $Y = \text{BF}_4$: TMPBI-I-BF₄, $Y = \text{N}(\text{SO}_2\text{CF}_3)_2$: TMPBI-I-Tf₂N, $X = \text{I}$: TMPBI-BuI-I, $Y = \text{BF}_4$: TMPBI-BuI-BF₄, $Y = \text{N}(\text{SO}_2\text{CF}_3)_2$: TMPBI-BuI-Tf₂N,**Scheme 3.5.** N-quaternization of (a) PBI-I and (b) PBI-BuI

DMABPBI-I

Where $Y = \text{BF}_4$: DMABPBI-BF₄, $Y = \text{N}(\text{SO}_2\text{CF}_3)_2$: DMABPBI-Tf₂N**Scheme 3.6.** N-quaternization of ABPBI

3.5.3. Anion exchange of N-quaternized PBIs

An exchange of iodide anion of a quaternized PBI by tetrafluoroborate (BF_4^-) was performed by dissolving it in a suitable solvent (DMSO for TMPBI-I·I, DMAc for TMPBI-BuI·I and DMF for DMABPBI·I). Typically, a two necked round bottom flask equipped with a calcium chloride guard tube was charged with 50 ml of a desired solvent and 0.008 mol of quaternized PBI (PIL with iodide as the counterion). After complete dissolution of polymer while stirring, 0.016 mol of AgBF_4 (2 molar equivalents) was added. The formation of a fine precipitate of AgI began with the addition of AgBF_4 ; while the polymer remained in dissolved state. The reaction mixture was further stirred at ambient temperature for 24 h to ensure complete replacement of the anion. The reaction mixture was centrifuged at 3000 rpm for 5 h to separate the fine precipitate of AgI, which was recovered and was washed with the solvent, dried at 80 °C for 24 h and weighed to correlate the extent of anion exchange. The supernatant polymer solution after centrifugation was evaporated to recover the polymer, which was further purified by dissolving in DMF (10% w/w), precipitating in methanol and drying at 60 °C in vacuum oven for 3 days.

For the exchange of iodide (I^-) by bis(trifluoromethane)sulfonimide (Tf_2N^-), 0.008 mol of PIL with iodide as the counterion was dissolved in a desired solvent (DMSO for TMPBI-I·I, DMAc for TMPBI-BuI·I and DMF for DMABPBI·I) and 0.016 mol of Li- Tf_2N was added. A homogeneous solution was obtained, which was further stirred for 24 h. The byproduct, LiI was removed by precipitating the reaction mixture in deionized (DI) water at ambient temperature. The precipitate was further washed with water several times to remove LiI. The filtrate and washings were collected together and diluted to a known volume with DI water for iodide estimation by conductometric titrations (Section 3.7). All the precipitated polymers with Tf_2N^- as the counterion were purified by dissolving in DMAc (10% w/w), reprecipitating in water, followed by drying at 60 °C in vacuum oven for 48 h. Structures of these polymers obtained along with their abbreviations used are given in Schemes 3.5 and 3.6.

3.6. Dense membrane preparation

Dense membranes were prepared by solution casting method using 3% (w/v) polymer solution in appropriate solvent; prepared while stirring at 80 °C for 14-18 h under dry atmosphere. Formed membrane (~ 40 µm thick) was peeled off and soaked in water at 60 °C for 3 days in order to extract traces of solvent. Such membranes were finally dried in vacuum oven at 100 °C for a week and used for subsequent analyses. Membranes of PILs were not treated with water due to the possibility of partial dissolution of the polymer in water, instead they were kept in vacuum oven for longer duration of 10 days.

3.7. Polymer characterizations

The solubility of synthesized polymers in common solvents was determined with 1% polymer solution (w/v) as a criterion. Inherent viscosity (η_{inh}) of all the unsubstituted PBIs and *N*-substituted PBIs was determined using Ubbelohde viscometer with 0.2 g/dL polymer concentration in 98% H₂SO₄ at 35 °C. In the case of PILs, inherent viscosity (η_{inh}) was determined at different polymer concentrations (0.025 to 0.2 g/dL) in DMSO at 35 °C. The FT-IR spectra of polymers in thin film form (~ 10 µm) were recorded at ambient temperature on Perkin Elmer-16-PC FT-IR spectrophotometer. For disubstituted PBIs and PILs, temperature of analysis initially was ambient and then these samples were also analyzed at 150 °C on Perkin Elmer Spectrum GX spectrophotometer provided with high temperature assembly of Mettler Toledo make with FP90 central processor. The ¹H-NMR spectra were recorded on Bruker AC-200 using DMSO-*d*₆ as the solvent (except for *N*-substituted PBIs where a mixture of DMSO-*d*₆ and trifluoroacetic acid (TFA) in 1:0.5 (v/v) proportion was used). Wide angle X-ray diffraction (WAXD) spectra of polymers in film form were recorded using Rigaku X-ray diffractometer (D-max 2500) with Cu-K_α radiation. The average intersegmental *d*-spacing (*d*_{sp}) for the amorphous peak maxima was calculated using Bragg's equation ($n\lambda = 2d\sin\theta$). The reproducibility of the *d*_{sp} measurement was ± 0.04 Å.

The density (ρ) measurement was carried out at 35 °C by flotation method with ~ 100 µm thick films using a suitable non-solvent pairs. The non-solvents with negligible sorbtion in the membranes and appropriate density were used further. The density of one

of the non-solvent pairs should be higher than that of the polymer under investigation. Thus, for unsubstituted PBIs (except ABPBI) mixture of tetrachloroethane/iodomethane and cyclohexanone, for *N*-substituted PBIs (except for DSPBI-BuI) and PILs (except TMPBI-I·Tf₂N and TMPBI-BuI·Tf₂N) mixture of 1,2-dibromobenzene and cyclohexanone were used. The sorption of these non-solvents in the membranes of all the polymers, was negligible (< 1%) for a period of 2 h exposure duration sufficient for density determination. DSPBI-BuI swell considerably in 1,2-dibromobenzene. Thus, a mixture of carbon tetrachloride and decalin (which showed negligible sorption for a period of 2 h exposure) was used as a solvent pair for the determination of density. TMPBI-I·Tf₂N and TMPBI-BuI·Tf₂N dissolved in cyclohexanone, but showed no sorption of decalin with in 2 h. Thus, a mixture of decalin and 1,2-dibromobenzene was used as the solvent pair for their density determination. For ABPBI fibers and DMABPBI-I, density was determined using specific gravity bottle and decalin as the solvent. Measurements were repeated at least with five different membrane samples. The deviation in density measurements for a polymer was found to be $\pm 0.007 \text{ g/cm}^3$. Based on the density determination, fractional free volume (v_f) and solubility parameter (δ) were estimated by group contribution method [Vankrevelen (1997)] using following equations.

$$v_f = \left[\frac{V_{sp} - V_w}{V_{sp}} \right] \quad (3.1)$$

$$\delta = \left[\frac{E_{coh}}{V} \right]^{1/2} \quad (3.2)$$

where, V_{sp} = specific volume (ratio of molecular weight of the repeat unit and the polymer density), V_w = van der Waal's volume, E_{coh} = cohesive energy of the polymer and V = molar volume of the polymer.

Thermogravimetric analysis (TGA) was performed on Perkin Elmer TGA-7 and TGA-5000 (TA instruments, USA) in a N₂ atmosphere with a heating rate of 10 °C/minute. The glass transition temperature (T_g) was recorded on DSC Q-10 (TA instruments, USA) in N₂ atmosphere with a heating rate of 10 °C/minute.

The maximum amount of water sorption in all the virgin PBIs was determined gravimetrically by immersing vacuum dried membrane samples in water at 35 °C for 3 days. The water sorption was determined with 6 samples and data averaged. The percent sorption was calculated using following Equation 3.2.

$$\% \text{ water sorption} = \frac{W_f - W_i}{W_i} \times 100 \quad (3.3)$$

Where, W_f = weight of the membrane after sorption and W_i = initial weight of the vacuum dried membrane.

For PILs, iodide estimation was performed by volumetric titration [Volhard's method]; where, 0.1 g of PIL in powder form was stirred in 10 ml of 0.01M AgNO_3 solution for 12 h, an excess of unreacted AgNO_3 was titrated with 0.01 M KSCN , and from the amount of AgNO_3 consumed initially, iodide content in the polymer was determined.

Purified PILs with BF_4^- or Tf_2N^- as a counterion were evaluated for the residual iodide content (if any) by Volhard's method. The percentage of iodide exchange was also deduced as follows. In case of iodide exchange by BF_4^- using AgBF_4 , the precipitated AgI was washed with the solvent and weighed to correlate with anion exchange. In case of Tf_2N^- exchange (using $\text{Li-Tf}_2\text{N}$), such correlation was done by titrating the LiI present in the filtrate water (after polymer precipitation and water wash) by 0.01 M AgNO_3 . The end point was monitored by the conductometric titration. From the amount of AgNO_3 consumed, iodide content and thus the total amount of iodide that got exchanged with Tf_2N^- was estimated.

3.8. Gas sorption and permeation analysis

The equilibrium sorption isotherms for H_2 , N_2 , O_2 , CH_4 and CO_2 in present polymers was carried out at incremental pressures up to 20 atm and at 35 °C using the gas sorption equipment that consisted of dual-volume single-transducer set up based on the pressure decay method Vieth et al. (1966). The schematic of sorption equipment was as given in Figure 3.1. The design of the sorption cell, specifications, material of construction, etc. was as discussed elsewhere [Karadkar (2006)]. The polymer sample in film form was placed in the sorption cell, evacuated and flushed with gas several times.

The system was then evacuated to 0.00001 mbar using oil diffusion pump. The gas was introduced rapidly and initial pressure recorded. As the sorption proceeds, the pressure starts decreasing and ultimately remains constant after the equilibrium is established. To increase the efficiency of experimentation, sequential sorption runs were made by incremental raise in pressure of the equilibrated system until about 20 atm was attained. The amount of gas sorbed in the sample at each equilibrium pressure was determined from the initial and final pressure.

Variable volume method [Stern (1963)] was used for determination of the gas permeability at upstream gas pressure of 20 atm and at 35 °C, while maintaining the permeate side at the atmospheric pressure. The purity for the gases viz., He, H₂, Ar, N₂, O₂ was 99.9%, while that for CH₄ and CO₂, it was 99.995%. A schematic of permeation equipment is shown in Figure 3.2. The design of the permeation cell, specifications, material of construction, etc. was as discussed elsewhere [Houde (1991)]. One end of the feed side of the cell was connected through valve V₁ to the feed gas cylinder outlet and a pressure gauge (0-550 psi range). The valve V₂ was vent and used to control the feed pressure. On the permeate side of the permeation cell, a calibrated borosilicate glass capillary (I.D. = either 1.0 or 1.5 mm) containing a small mercury slug (~ 4-6 mm in length) was connected. The membrane cell assembly was kept in thermostat maintained at 35 °C. Displacement of the mercury slug was monitored against time using cathetometer. The permeability (P) was calculated using the Equation 3.1.

$$P = \frac{14.7 \times d \times \text{F.C.} \times \ell}{76 \times A \times t \times \Delta p} \quad (3.1)$$

where, d = distance traveled by mercury slug (cm), F.C. = flow meter constant [volume of the flow meter capillary per unit length (cm³/cm)], ℓ = thickness of the membrane (cm), A = effective membrane area (cm²), t = time t (sec), Δp = pressure difference across the membrane (psi). The permeation measurements were repeated with at least 3-5 different membrane samples prepared under identical conditions and the data was averaged. The variation in permeability measurement was upto ± 15% for different gases studied. The ideal selectivity of various gases was calculated using the Equation 2.5 described in Section 2.1.

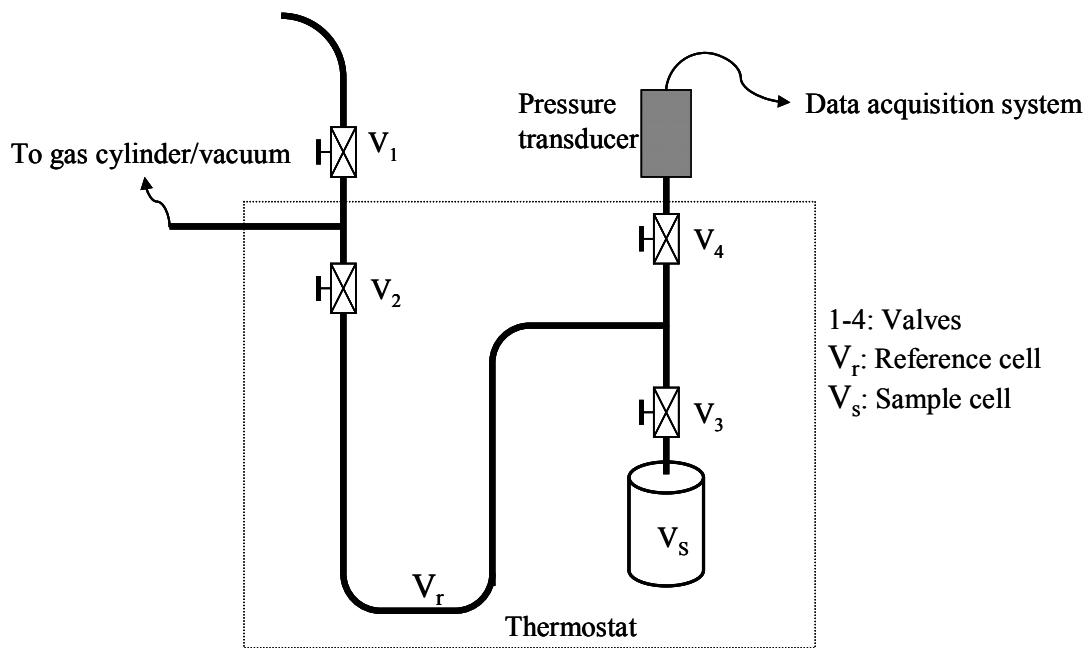


Figure 3.1. Gas sorption equipment

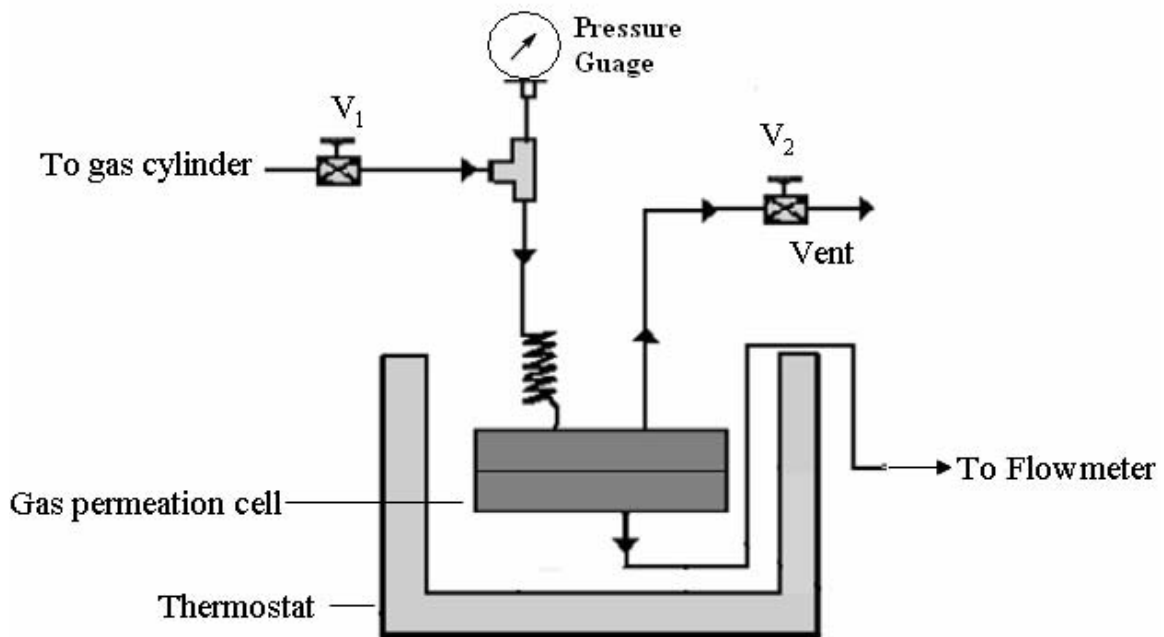


Figure 3.2. Gas permeation Equipment

Chapter 4

Variations in acid moiety of PBI based on DAB: Synthesis, characterization and investigation of gas permeation properties

4.1. Synthesis

The time of reaction at 200 °C was optimized for individual cases of PBI synthesis to achieve high enough inherent viscosity (~ 1 dL/g, Table 4.1). Reactions with *1,3*-substituted dicarboxylic acids (isophthalic, *5-tert*-butylisophthalic and *2,6*-pyridinedicarboxylic acid) took almost 12 h at 200 °C. This time was drastically reduced when *1,4*-substituted dicarboxylic acids (terephthalic, *2-bromo*terephthalic and *2,5*-dibromoterephthalic acid) were used. The difference in reactivity of these acids could be attributed to the substitution type. In latter cases, *para* (*1,4*-) substitution of –COOH groups leading to –I (inductive effect) effect could be responsible for enhanced reactivity by the nucleophilic substitution than for the former cases with *meta* (*1,3*-) substitution. Similar observations were reported by Iwakura et al. (1964c), wherein, the polycondensation reaction of terephthalic acid derivatives with *3,3'*-diaminobenzidine tetrahydrochloride proceeded faster than that in the case of isophthalic acid derivatives. Vogel and Marvel (1961) also have reported lesser reaction time for synthesizing PBI-T than for PBI-I by melt condensation using diphenyl ester of respective acids under similar temperature conditions. The reaction time required for DBrTPA was almost half than that required for the TPA. The presence of an electron withdrawing bromine on the acid moiety could be responsible for this enhanced reactivity. The reaction period for HFA was 6 h, indicating electron withdrawing nature of hexafluoroisopropylidene group enhanced the rate of reaction, than that of isophthalic acid case. Choi et al. (1997) have reported that the inductive effect of the electronegative fluorine would enhance the acid strength of HFA, leading to the higher reactivity of benzoyl group.

Poly(*2,5*-benzimidazole) (ABPBI) contain benzimidazole moiety in its structure and exhibit similar thermochemical properties as that of PBI-I. It has been explored as a

proton exchange membrane material (PEM) for fuel-cell [Kim (2004)]. As compared to PBI-I, the monomer used for ABPBI synthesis was much simpler and cheaper. ABPBI was synthesized by a self condensation of single monomer (DABA), whereas PBIs are synthesized from two functional monomers (DAB and dicarboxylic acid). In a short duration (170 °C/1 h, 200 °C/1 h), reaction mixture became very viscous due to increase in molecular weight of the polymer. Viscosity of the polymer obtained was also high as compared to that of other PBIs (Table 4.1). The ABPBI synthesis yielding high viscosity polymer was also observed by Carolla et al. (2006) and Asensio et al. (2005).

Table 4.1. Reaction parameters for polybenzimidazole synthesis

Polymers	Reaction time at 200 °C (h)	η_{inh}^a (dL/g)	Yield (%)
PBI-I	12	1.4	99
PBI-T	2	1.8	99
PBI-BuI	12	1.3	97
PBI-HFA	6	1.5	89
PBI-BrT	2	1.3	91
PBI-DBrT	1	1.3	98
PBI-2,6Py	12	0.9	95
ABPBI	1	2.9	99

^a Inherent viscosity using 0.2 g/dL solution in conc. H₂SO₄ at 35 °C.

4.2. Physical properties

4.2.1. Solubility and spectral characterizations

The solvent solubility of these PBIs was evaluated with 1% w/v polymer concentration as a criterion and the results are summarized in Table 4.2. All polymers were soluble in conc. H₂SO₄. Nature of the dicarboxylic acid used for synthesizing PBI had its own effect on the solubility. Presence of the bulky (*tert*-butyl, hexafluoroisopropylidene) or polar (-Br) group on dicarboxylic acid moiety of PBI enhanced the solvent solubility. Except for PBI-T, all other PBIs were soluble in DMAc, NMP, DMF and DMSO. PBI-T could be dissolved in DMAc only under heating. Lower solubility of PBI-T than that of PBI-I was reported by Vogel et al. (1961) and Iwakura et

al. (1964c); which was attributed to the polymer chain rigidity, symmetry and intermolecular attraction. An introduction of *tert*-butyl group in PBI-BuI, hexafluoroisopropylidene group in PBI-HFA, bromine in PBI-BrT and PBI-DBrT offered solubility also in formic acid (85%) at ambient temperature and within a short time of an hour. On the other hand, PBI-I needed prolonged stirring for 12 h under reflux condition. PBI-T and PBI-2,6Py were partially soluble in formic acid at reflux temperature for 24 h. PBI-HFA was found to be soluble in pyridine also.

Table 4.2. Solubility of polybenzimidazoles in solvents

Polymer	DMAc	NMP	DMF	DMSO	Pyridine	HCOOH	CH ₃ COOH	H ₂ SO ₄	H ₃ PO ₄
PBI-I	++	++	++	++	-	+	±	++	±
PBI-BuI	++	++	++	++	±	++	-	++	+
PBI-HFA	++	++	++	++	++	++	-	++	-
PBI-T	+	±	±	±	-	±	±	++	±
PBI-DBrT	+	++	++	++	-	++	-	++	++
PBI-BrT	++	++	++	++	-	++	-	++	++
PBI-2,6Py	++	++	++	+	-	±	-	++	±
ABPBI	-	-	-	-	-	±	±	++	++

++: Soluble at ambient temperature; +: Soluble at reflux temperature (120 °C in case of H₃PO₄); ±: Partially soluble or swelling after heating at reflux temperature in organic solvents; 120 °C in case of H₃PO₄; -: Insoluble even after heating.

Solubility of PBI-HFA in pyridine and formic acid (which are volatile and water miscible solvents) can be useful in transforming this material into required membrane type (thin film composite or asymmetric membranes) for gas separation and other membrane applications. Improved solubility of PBI-HFA in organic solvents and in acids is reported [Saegusa, (1997)]. Brominated PBIs were soluble in ~ 88% H₃PO₄. An introduction of a alkyl group like methyl [Korshak (1971), Hu (1993)] and polar group like nitro [Lyo (2000)] on PBI backbone is known to increase solvent solubility. ABPBI was soluble only in acidic solvents such as H₂SO₄ and H₃PO₄. All present PBIs were

insoluble in chloroform, dichloroethane, tetrachloroethane, 1,4-dioxane and tetrahydrofuran.

FT-IR spectra of these polymers were as given in Figure 4.1. The benzimidazole ring was characterized by the absorption at 1430, 1600, and 1620 cm^{-1} [Musto (1991, 1993)]. These peaks were common in all PBIs investigated. The region 1500 - 1650 cm^{-1} is the characteristic of benzimidazoles. These bands are derived from C=C and C=N stretching as well as ring modes, which are characteristic of conjugation between benzene and the imidazole rings [Musto (1991, 1993)]. The strong band at $\sim 3145 \text{ cm}^{-1}$ was ascribed to the hydrogen bonding of the type N-H---N, while the peak at $\sim 3410 \text{ cm}^{-1}$ was due to the free non-hydrogen bonded N-H stretching. The peak at 3050 cm^{-1} was attributed to stretching of the aromatic C-H bond. The peak at 2862 cm^{-1} in the IR spectrum of PBI-BuI could be ascribed to the presence of *tert*-butyl group on acid moiety. In case of PBI-HFA, the broad band at 1134 - 1294 cm^{-1} could be attributed to the C-F stretching vibrations [Choi (1997)]. For all PBIs, the peak at 3598 - 3628 cm^{-1} could be attributed to the O-H stretching of absorbed water. Such peak was also observed by Brook et al. (1993) and Li et al. (2004b) at 3620 cm^{-1} , which was said to be removed by heating at 120 °C.

Figure 4.2 shows $^1\text{H-NMR}$ signal assignments for the present polybenzimidazoles. In all these PBIs, the peak due to hydrogen of imidazole proton was observed as a singlet at δ 13.1 - 13.3, except for PBI-BrT, wherein it appeared as a doublet at δ 13.0 - 13.3. Aromatic protons appeared between δ 7.5 and 9.2. Protons due to -CH₃ group in PBI-BuI appeared at δ 1.4 as a singlet. The $^1\text{H-NMR}$ spectra of PBI-2,6Py could not be recorded due to its insolubility in DMSO-*d*₆ at ambient temperature.

WAXD analysis of these PBIs indicated that all of them were amorphous in nature (Figure 4.3). The *d*-spacing (d_{sp}) corresponding to the amorphous peak maxima in WAXD spectra are given in Table 4.3. It could be seen that PBI, in general, exhibited much lower d_{sp} than that of common polymers like polysulfone [McHattie (1991a), (1992)], polycarbonate [Hellums (1989)], polyarylate [Pixton (1995a)], etc. This behavior could be attributed to the presence of H-bonding in PBI that brings chains closer, resulting in efficient chain packing. PBI-BuI and PBI-HFA exhibited two amorphous peaks, indicating there could be two different types of predominant chain packing. A

peak corresponding to the lower d_{sp} of 4.05 Å could be dominated by H-bonded region, while the other peak corresponding to higher d_{sp} indicated looser chain packing dominated by bulky substitution (4.69 Å in case of PBI-BuI and 5.37 Å in case of PBI-HFA). PBI-T, PBI-BrT, PBI-DBrT and PBI-2,6Py exhibited higher chain packing density (lower d_{sp}) than that for PBI-I.

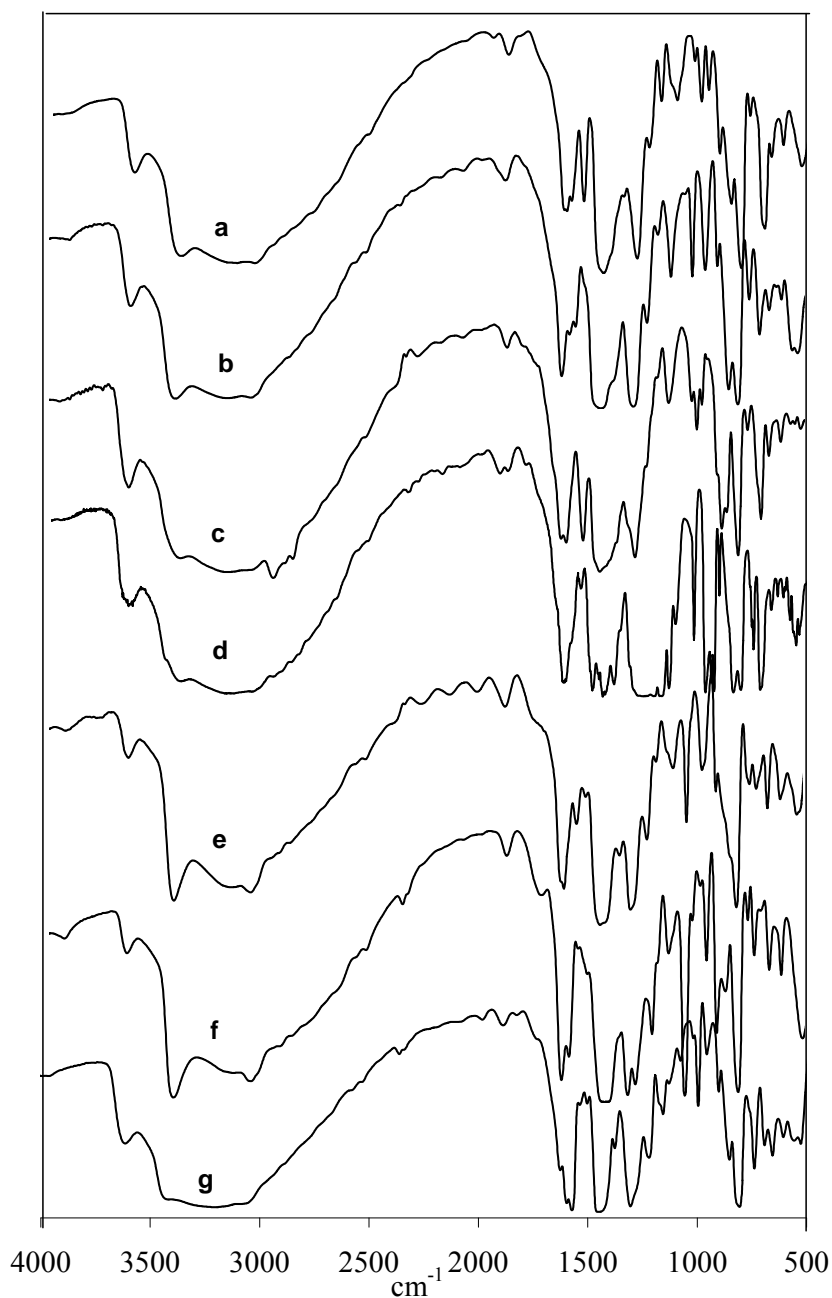


Figure 4.1. FTIR spectra of polybenzimidazoles (a: PBI-I, b: PBI-T, c: PBI-BuI, d: PBI-HFA, e: PBI-BrT, f: PBI-DBrT, g: PBI-2,6Py)

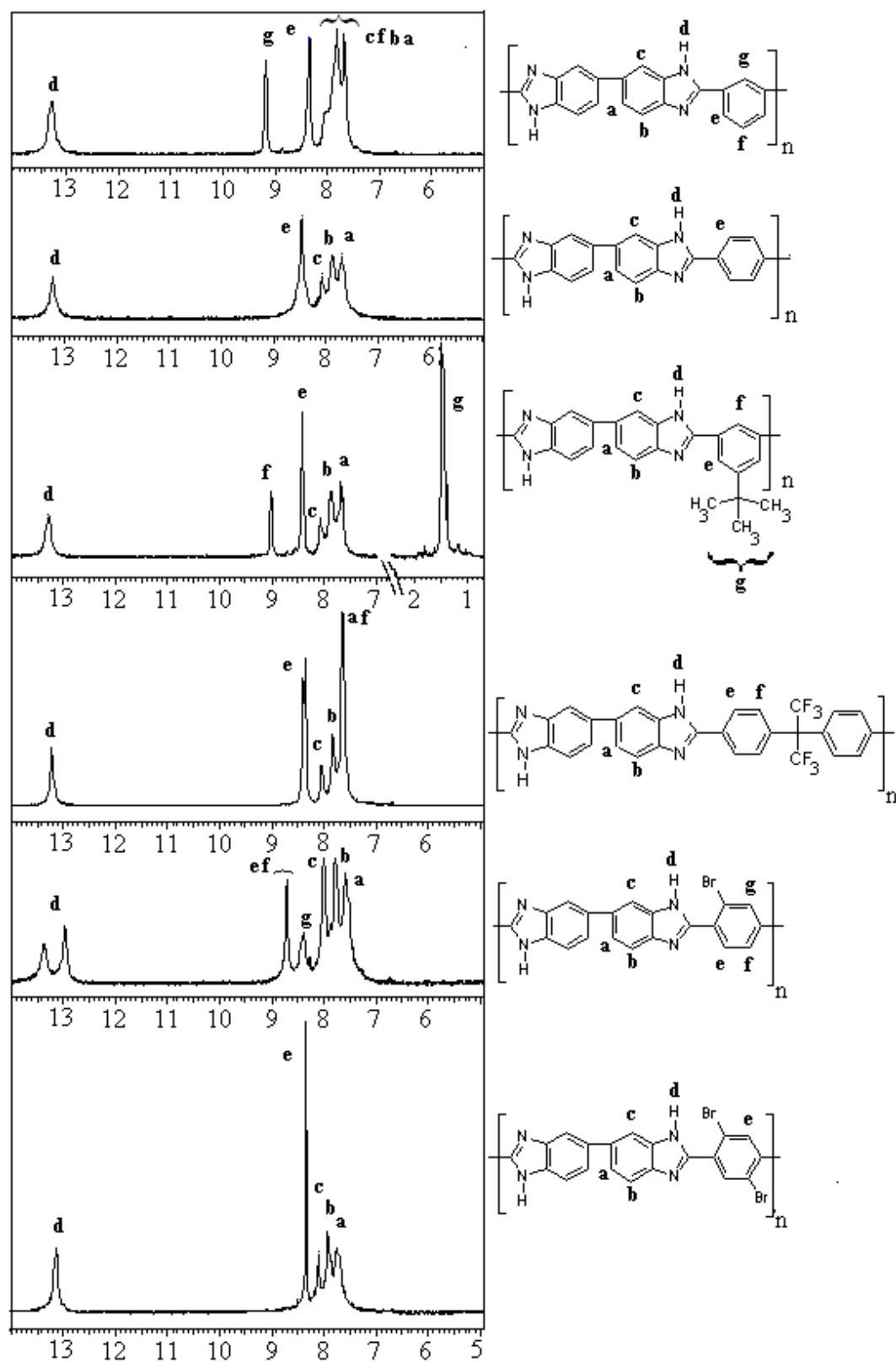


Figure 4.2. $^1\text{H-NMR}$ spectra of polybenzimidazoles (a: PBI-I, b: PBI-T, c: PBI-BuI, d: PBI-HFA, e: PBI-BrT, f: PBI-DBrT)

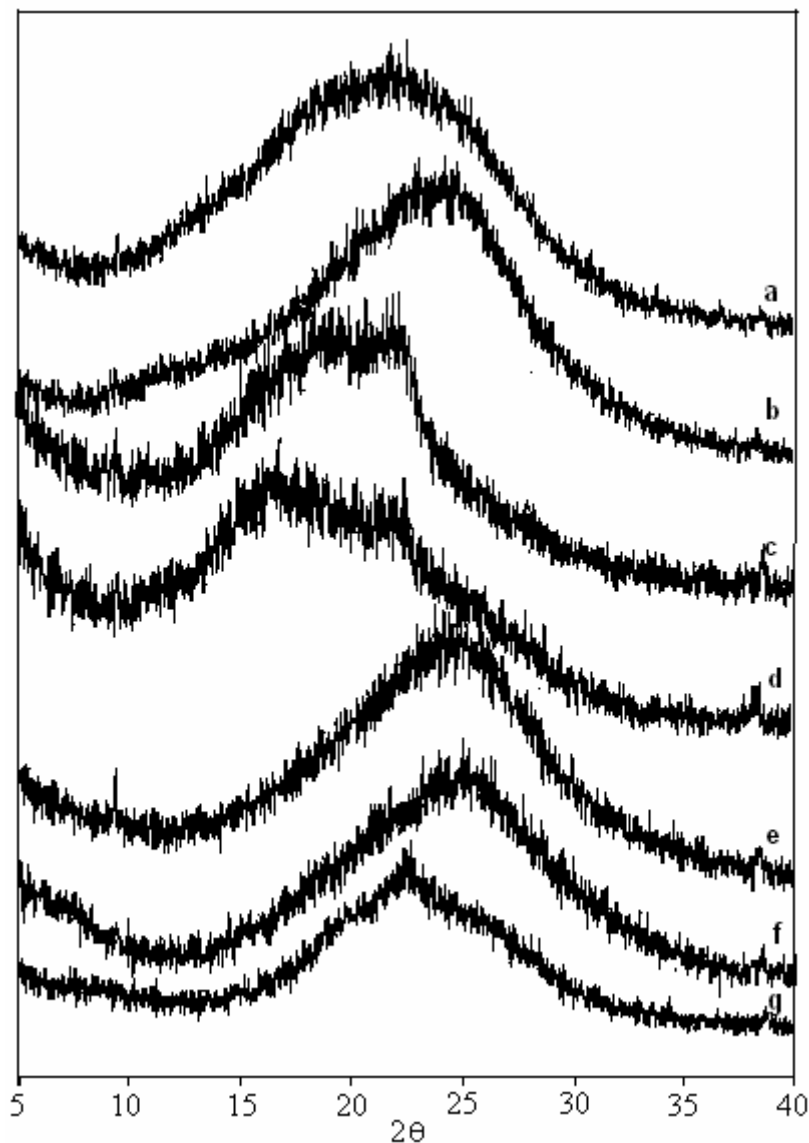


Figure 4.3. WAXD spectra of polybenzimidazoles (a: PBI-I, b: PBI-T, c: PBI-BuI, d: PBI-HFA, e: PBI-BrT, f: PBI-DBrT, g: PBI-2,6Py)

4.2.2. Density and free volume

Density (ρ) measurement of the dry PBI films was performed by floatation method. Since present PBIs sorb considerable amount of water (Table 4.3), use of aqueous solutions for density measurement would have led to erroneous results. Thus, organic solvents that have appropriate density and do not get sorbed in PBI were selected for the density measurement. To determine solvent sorption in PBI, a film of $\sim 100 \mu\text{m}$ thickness was dipped in these solvents for varying time. Iodomethane ($\rho = 2.275 \text{ g/cm}^3$),

tetrachloroethane ($\rho = 1.623 \text{ g/cm}^3$) and cyclohexanone ($\rho = 0.9465 \text{ g/cm}^3$) showed negligible sorption in all present PBIs ($< 1\% \text{ w/w}$) for 2 h dip time and at $35 \text{ }^\circ\text{C}$. This duration was sufficiently higher than the time required for density measurement. The amount of solvent sorbed did not increase considerably even after 24 h dipping, except for iodomethane in PBI-DBrT (2.34%) and for TCE in PBI-HFA (13%). Initially the density of PBI-I was determined and compared with the literature data. The density in the present investigation was found to be 1.331 g/cm^3 ; while literature values are 1.3 g/cm^3 [Tarasevich (2004)], 1.34 g/cm^3 [Mecerreyes (2004)] and 1.269 g/cm^3 [Földes (2000)]. In view of good agreement of measured density with the literature data, present method of the density estimation was extended for the density determination of other PBIs. Density of the halogenated PBIs (PBI-BrT/DBrT/HF) was higher than that of non-halogenated PBIs (PBI-I/T/2,6Py) (Table 4.3). Similar behavior was seen in other families of polymers such as polycarbonate [Hellums (1989)], polyarylate [Kharul (1994)], polysulfone [McHattie (1992)], etc.

Measured density was used to estimate fractional free volume (v_f) and solubility parameter (δ) using the group additivity method [Van Krevelen (1997)]. The results are given in Table 4.3. It was found that PBI-HFA exhibited the highest v_f among the series. Incorporation of *tert*-butyl group in PBI-BuI also led to an increase in v_f , indicating loose chain packing in comparison to the base case of PBI-I. These results are in agreement with the d_{sp} by WAXD, as discussed above. Incorporation of *tert*-butyl group or hexafluoroisopropylidene linkage in the main chain is known to render loose chain packing in cases of other polymers like polycarbonate [Hellums (1989)], polysulfone [McHattie (1992)], polyarylate [Kharul (1994), Pixton (1995a)], polyimide [Coleman (1990)], etc. It is interesting to note that PBI-T (*1,4*-substitution on the acid moiety) exhibited slightly lower d_{sp} as well as v_f than that of PBI-I (*1,3*-substitution). On the contrary, in case of other aromatic polymers like polyarylates [Pessan (1993)] or polyimides [Coleman (1990, 1994)], it is known that polymer with *1,3*-substitution leads to better chain packing than that of its isomer possessing *1,4*-substitution. Incorporation of hexafluoroisopropylidene group (PBI-HFA) and *tert*-butyl group (PBI-BuI) in polymer backbone led to the lowering in solubility parameter (δ); while, incorporation of bromine

(PBI-BrT and PBI-DBrT) and additional 'N' (PBI-2,6Py) increased the v_f and δ in comparison to unsubstituted cases of PBI-I and PBI-T (Table 4.3).

Table 4.3. Physical properties of polybenzimidazoles

Polymer	d_{sp}^a (Å)	ρ^b (g/cm ³)	Water uptake (mol/RU)	v_f^c (cm ³ .cm ⁻³)	δ^d (cal.cm ⁻³) ^{1/2}	TGA analysis		
						T_{wl}^e	IDT ^f (°C)	W_{900}^g (% wt)
PBI-I	4.05	1.331	3.5	0.3096	10.50	147	600	67
PBI-T	3.70	1.353	3.6	0.2982	10.59	179	620	82
PBI-BuI	4.69, 4.04	1.193	2.5	0.3393	9.63	136	525	65
PBI-HFA	5.37, 4.05	1.371	1.8	0.3605	9.19	128	535	61
PBI-BrT	3.70	1.553	2.6	0.3104	10.65	143	400	56
PBI-DBrT	3.63	1.717	2.2	0.3223	10.68	163	440	55
PBI-2,6Py	3.96	1.340	3.0	0.3226	10.57	187	600	78
ABPBI	3.01	1.437	-	0.279	13.41	-	620	44.7

^a: d -spacing obtained from WAXD spectra; ^b: Density measured at 35 °C ; ^c: Fractional free volume calculated using group contribution method [Van Krevelen (1997)]; ^d: Hildebrand solubility parameter estimated using group contribution method [Van Krevelen (1997)]; ^e: Temperature at which initial water loss occurred; ^f: Initial decomposition temperature; ^g: Char yield at 900 °C.

4.2.3. Thermal stability

Thermogravimetric analysis (Figure 4.4) revealed that all these PBI exhibited initial loss below ~ 190 °C, which is attributable to the absorbed water [Asensio (2002)]. The temperature at which this loss was completed (T_{wl}) is given in Table 4.3. It was observed that for PBIs with higher free volume (PBI-BuI and PBI-HFA), this temperature was lower than that for other polybenzimidazoles. This could be attributable to the looser chain packing (higher v_f and d_{sp} in the series), which would ease the diffusion of water molecules from the bulk. In case of PBI-2,6Py, this temperature was highest among the series. This could be attributed to the combined effect of tighter chain packing (lower v_f)

and the presence of additional nitrogen on the acid moiety, capable of providing additional H-bonding site to hold water molecules. PBI-I, PBI-T, PBI-2,6Py and ABPBI exhibited excellent thermal stability (≥ 600 °C, Table 4.3.). High thermal stability associated with PBI was earlier ascribed to the aromatic rigid structure in the backbone [Vogel (1961), Vogel (1963), Gerber (1973)] and could also be due to intermolecular H-bonding. This intermolecular H-bonding can be anticipated to be weaker in the case of PBI-BuI and PBI-HFA, as also indicated by their higher fractional free volume than that of other PBIs. Presence of the thermally labile group ($-\text{CF}_3$ or *tert*-butyl) and weaker H-bonding in these cases could be responsible for their observed lower thermal stability than that of PBI-I, PBI-T and PBI-2,6Py. The presence of *tert*-butyl group is known to lower the thermal stability [Schild (1994)] in polyesters. Bromine containing PBI (PBI-BrT and PBI-DBrT) exhibited considerably lower degradation temperature than that of other PBIs.

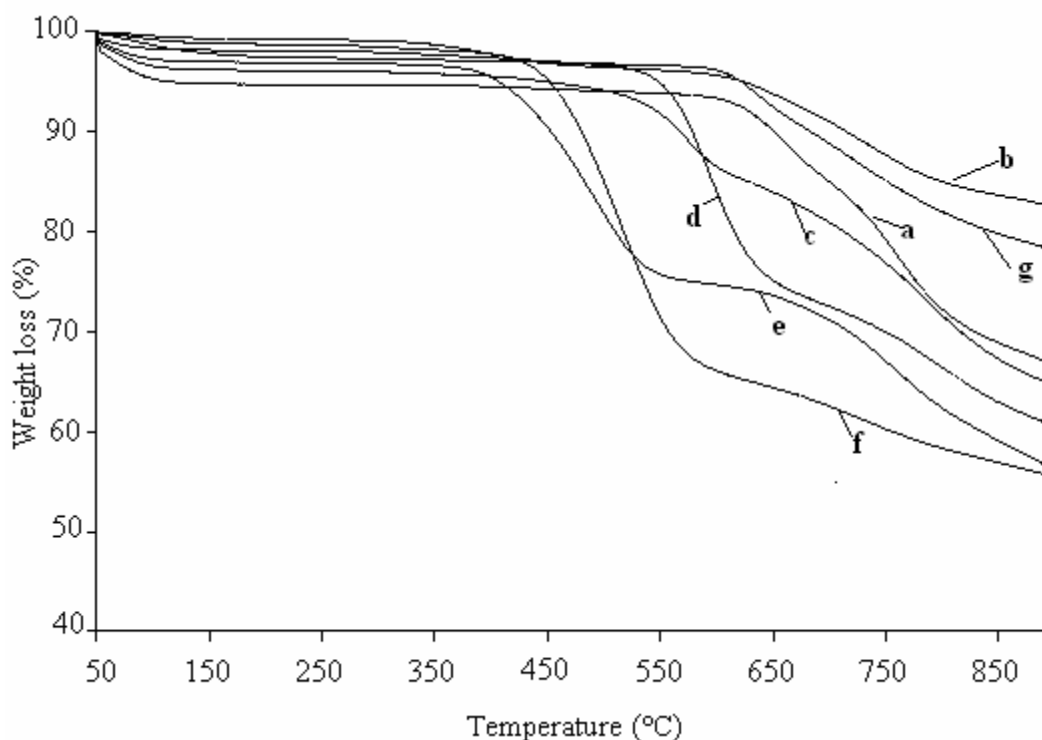


Figure 4.4. TGA spectra of polybenzimidazoles (a: PBI-I, b: PBI-T, c: PBI-BuI, d: PBI-HFA, e: PBI-BrT, f: PBI-DBrT, g: PBI-2,6Py)

4.2.4. Water sorption

The vacuum dried PBI membranes were immersed in water for 3 days at ambient temperature and amount of water sorbed was determined gravimetrically. The maximum amount of water sorbed in different PBIs was from 1.8 to 3.6 mol/RU (Table 4.3). These values were between the two limits as suggested by Brook et al. (1993). According to this model, the hydrogen bonding of H₂O with PBI can occur in two ways. The first possibility would occur if two water molecules were attached to each imidazole ring, so that one water molecule could act as a proton acceptor and the other as a proton donor. This would allow a maximum of four H₂O molecules to be attached to each polymer repeat unit. The second possibility involves, one water molecule attached to two neighboring imidazole rings from adjacent polymer chains. In this case, the water molecule would act as both, proton acceptor as well as donor, which would allow a maximum of two H₂O molecules per polymer repeat unit.

4.3. Gas permeation properties

4.3.1. Initial explorations on gas permeation properties of PBIs based on different dicarboxylic acids

It was thought to analyze the gas permeability coefficients and selectivities for H₂ and O₂ pair initially, to investigate the effect of added polarity, bulk and isomerism in the dicarboxylic acid moiety (Table 4.4). An interesting behavior in permeability and selectivity was noted. It was observed that PBI-T exhibited the lowest permeability, while PBI-HFA exhibited the highest. The permeability difference was 76 fold for H₂ and 150 fold for O₂. The low permeability of PBI-I [Pesiri (2003), Jorgensen (2004)] was attributed to the presence of H-bonding. Its rigid and closely packed structure (as indicated by lower d_{sp} of 3.01 Å) was responsible for observed low permeability. The increase in permeability was in the order: PBI-T < PBI-BrT < PBI-I < PBI-2,6Py < PBI-DBrT < PBI-BuI < PBI-HFA. The $\alpha(H_2/O_2)$ selectivity followed almost a reverse order, except for PBI-BrT and PBI-T. PBI-BrT showed the highest selectivity of 60 in the series, following a general trade-off relationship of permeation properties (structural modifications in a polymer backbone leading to the lowering in permeability increases selectivity and vice-versa). As expected, the bulky *tert*-butyl group in the case of PBI-BuI and hexafluoroisopropylidene group in the case of PBI-HFA leading to the inefficient

packing due to the bulk of these groups (higher v_f) was responsible for their higher permeabilities. PBI-HFA showed 19 and 40 times higher permeability for H_2 and O_2 , respectively, than that of PBI-I. The respective increase in permeability of PBI-BuI was 16.9 and 28 times. The behavior of increase in permeability by substitution of *tert*-butyl and hexafluoroisopropylidene group is well known in other families of polymers, such as polyarylate [Kharul (1994), Pixton (1995a)], polyimide [Coleman (1990)], polycarbonate [Hellums (1989)], etc. In present cases, similar increase in permeability was from 3.2 to 4.5 times, in comparison to the respective base unsubstituted polymer, selectivity being considerably lower than the PBI investigated in this work. A larger increase in permeability for PBI family by bulky group substitution could be explained on the basis of initial lower permeability of PBI-I. The presence of H-bonding reduces the available free volume and thus permeability (which was much lesser than the conventional polymers like PC, PSF, etc.). The substitution by bulky *tert*-butyl and hexafluoroisopropylidene groups disrupt this H-bonding to certain extent, as also supported by the appearance of two peaks in WAXD spectra and an increase in fractional free volume. On the other hand, higher selectivity can be explained based on the highly rigid structure of PBI. Higher T_g of PBI-I (430 °C) allowed better penetrant discriminating ability (and thus high selectivity) than shown by common polymers like PC (T_g of 150 °C) or PSF (T_g of 186 °C).

PBI-T (*1,4*-substitution on the acid moiety) exhibited lower permeability coefficient and higher selectivity in comparison with PBI-I (*1,3*-substitution in acid), which was attributable to its higher packing density as evident from its lower d_{sp} and v_f values. This trend in permeability and selectivity for these isomeric PBIs was reverse than the trend observed in cases of other polymers with *1,3*- and *1,4*-substituted isomers. For example, the isophthalic acid based polyarylates have less permeability and higher selectivity than the terephthalic acid based polyarylates, derived from the same bisphenol [Pessan (1993)]. In case of polyimides also, *1,3*-substituted polymer exhibited lower permeability and higher selectivity than its *1,4*-substituted analogue [Coleman (1990, 1994)].

The substitution of bromine in PBI-BrT elevated its v_f and thus gas permeability, in comparison to the unsubstituted PBI-T case. An increase in permeability by dibromo

substitution in PBI-DBrT was more than the case of monobromo substitution in PBI-BrT, which could be correlated to further increase in v_f by the dibromo substitution.

It would also be worth to compare the permeability and selectivity of these PBIs with widely investigated polymer materials for gas permeability like polysulfone and polyarylate. It can be seen from Table 4.4 that all these PBIs (except PBI-BuI and PBI-HFA) exhibited lower permeability, but order of magnitude higher selectivity than for polyarylate or polysulfone. Efforts of structural modification in PBI towards improving permeability, as in PBI-BuI and PBI-HFA elevated the H_2 permeability, which was closer to polyarylate or polysulfone, while O_2 permeability still remained lower. This led to 2 - 3 times higher selectivity for PBI-BuI and PBI-HFA than that for polyarylate or polysulfone. This behavior can be attributed to the rigid chain backbone of PBI (higher T_g) than other polymer families. In other words, though the structural modifications in these PBI (PBI-BuI and PBI-HFA) increased permeability, it retained its capability of better discrimination among different penetrants and thus can serve as better gas separation membrane materials. Thus, PBI-BuI and PBI-HFA were chosen for detailed gas sorption and permeation properties analysis using gases of interest viz., H_2 , He, N_2 , O_2 , CH_4 and CO_2 as given in following sections.

Table 4.4. H_2 and O_2 permeability (P)^a and selectivity (α)^b of polybenzimidazoles

Polymer	P(H_2)	P(O_2)	$\alpha(H_2/O_2)$
PBI-I	0.63	0.015	42
PBI-T	0.16	0.004	55
PBI-BuI	10.66	0.42	25.4
PBI-HFA	12.15	0.60	20.1
PBI-BrT	0.38	0.006	60
PBI-DBrT	1.89	0.07	28
PBI-2,6Py	1.38	0.045	31
Polyarylate ^c	13.4	1.3	10.3
Polysulphone ^d	14	1.4	10

^a: Pure gas permeability in Barrer (1 Barrer = $10^{-10}cm^3(STP).cmHg^{-1}.cm^{-1}.s^{-1}$); ^b: Ratio of pure gas permeability; ^c: From Ref. [Pixton (1995a)]; ^d: From Ref. [McHattie (1992)].

4.3.2. Sorption properties

The solubility coefficient, S , for a gas in glassy polymers is often described by the dual mode model [Veith (1976)];

$$S_A = \frac{C}{p} = k_D + \frac{C'_H b}{(1 + bp)} \quad (4.1)$$

where, C is the gas concentration in the polymer, p is the applied gas pressure, k_D is the Henry's solubility coefficient, C'_H is the Langmuir saturation constant and b is the Langmuir affinity constant. These constants were obtained by the nonlinear regression analysis of experimentally determined gas sorption by genetic algorithm, an optimization technique capable of searching global optima [Goldberg (1989)]. Equilibrium sorption isotherms for H_2 , N_2 , O_2 , CH_4 and CO_2 in PBI-I, PBI-HFA, and PBI-BuI at 35 °C are as shown in Figure 4.5 and exhibited dual mode sorption, as typically observed for glassy polymers. The order of sorption of different gases in these PBIs was found to be $H_2 < N_2 < O_2 < CH_4 < CO_2$.

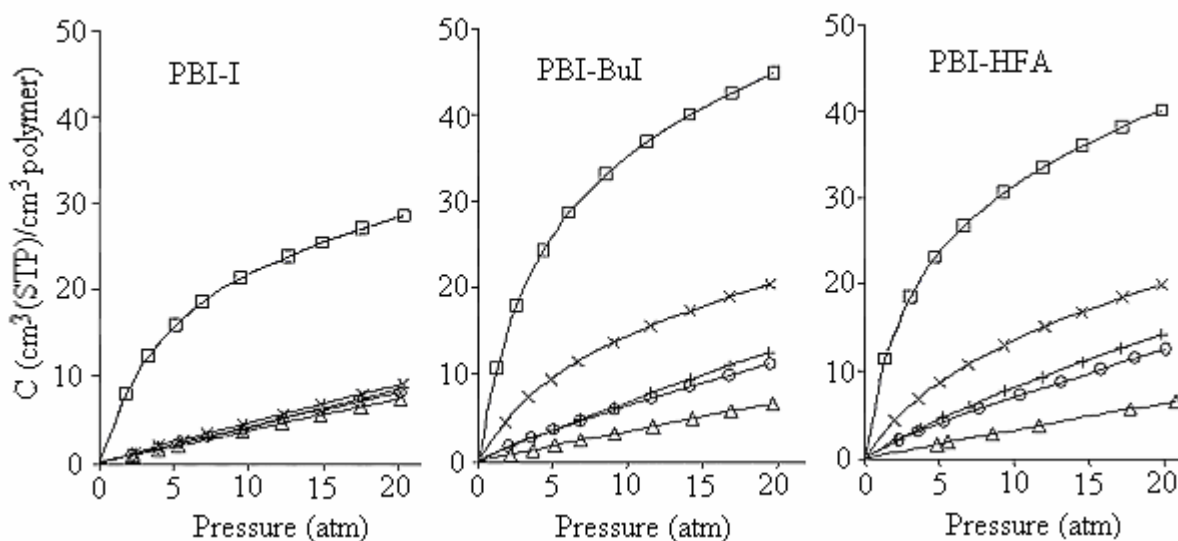


Figure 4.5. Equilibrium sorption isotherm for polybenzimidazoles investigated at 35 °C

(Δ : H_2 , \circ : N_2 , +: O_2 , \times : CH_4 , \square : CO_2)

In case of PBI-I, the sorption of CO_2 was considerably higher than that for other gases, which varied in a very narrow range. The sorption of all the gases increased in both cases; PBI-HFA and PBI-BuI, as a result of increased v_f . The sorption of CO_2 was

increased by 1.42 - 1.58 times in PBI-BuI or PBI-HFA than that of PBI-I; while sorption of N₂, O₂ and CH₄ was increased by 1.43 - 2.3 times at 20 atm. The estimated sorption parameters (Table 4.5) showed that the Henry's solubility coefficient k_D , equivalent to gas dissolution in rubbery polymers, was low for all the gases in all three PBIs and did not vary significantly. This can be attributed to the high T_g of these PBI. The rigid polymer matrix at investigation temperature (35 °C) may not sorb the gas largely by Henry's mode; leading to smaller k_D values, observed to be dependant of test gas only marginally. In case of PBI-HFA and PBI-BuI, Langmuir saturation constant C'_H was found to be increased for O₂, CH₄ and CO₂.

Table 4.5. Dual-mode sorption parameters^a for polybenzimidazoles

Gas	ε/κ (K)	PBI-I			PBI-BuI			PBI-HFA		
		k_D	C'_H	B	k_D	C'_H	b	k_D	C'_H	b
H ₂	33.3	0.348	1.89	0.011	0.333	0.42	0.0002	0.308	0.43	0.001
N ₂	126	0.397	3.56	0.001	0.456	3.01	0.132	0.496	3.36	0.132
O ₂	154	0.413	2.68	0.001	0.494	7.12	0.033	0.463	9.75	0.053
CH ₄	191	0.405	1.93	0.042	0.327	18.78	0.146	0.359	18.43	0.116
CO ₂	304	0.293	27.97	0.205	0.438	43.72	0.237	0.531	34.36	0.315

^a k_D is expressed in cm³ (STP)/cm³polymer.atm; C'_H is expressed in cm³(STP)/cm³polymer, while b is expressed in 1/atm.

The solubility coefficients for PBI-BuI and PBI-HFA correlated well ($R^2 > 0.97$) with Lennard-Jones force constant (ε/κ) of gases, as shown in Figure 4.6. In case of PBI-I, this correlation was weaker ($R^2 = 0.7$), but exclusion of S_{CO_2} elevated this correlation coefficient to 0.98. One of the reasons for this failure of CO₂ to correlate well could be due to its higher sorption than that of other gases in PBI-I as also seen from Figure 4.5. Figure 4.7 shows a correlation of solubility coefficient with v_f for O₂, N₂, CH₄ and CO₂.

As a result of increase in v_f , the gas solubility in case of PBI-HFA and PBI-BuI was higher than that for PBI-I for all gases, except for H_2 (Table 4.6). The reason for higher sorption of H_2 in PBI-I could not be explained and need more investigations. Though, the gas solubility is known to be a weak function of free volume [Ghosal (1993)], Figure 4.7 shows a good correlation of v_f with solubility coefficient for N_2 and O_2 ($R^2 \geq 0.96$) than with solubility coefficient for CH_4 or CO_2 ($R^2 \leq 0.85$). The extent of increase in CH_4 solubility was higher than that for other gases, as also reflected in reduced solubility selectivity: S_{CO_2}/S_{CH_4} and S_{N_2}/S_{CH_4} for PBI-HFA and PBI-BuI in comparison with the same for PBI-I (Table 4.6). The solubility selectivity for other gas pairs varied marginally.

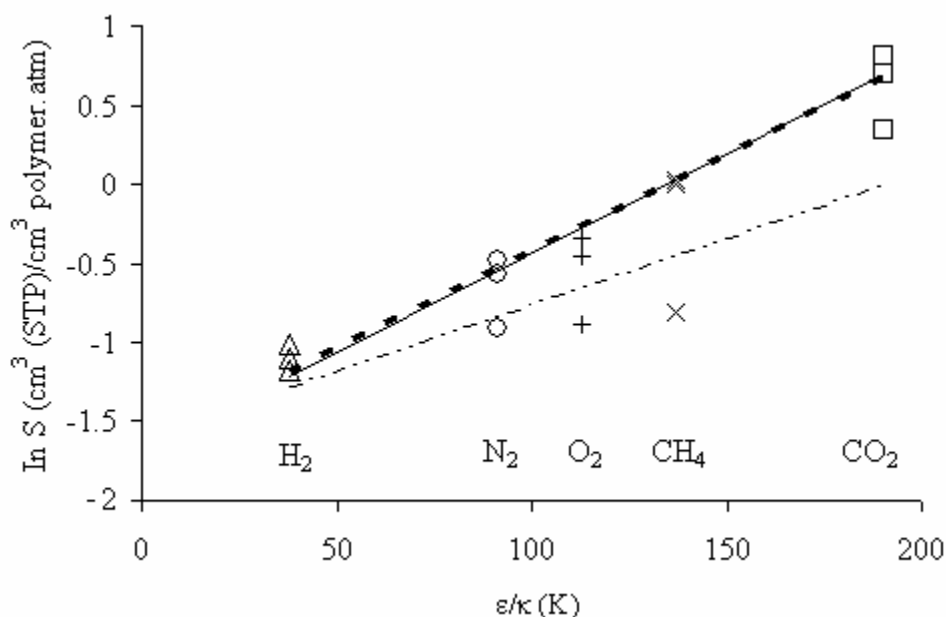


Figure 4.6. Correlation of solubility coefficient (S), with Lennard-Jones force constant, (ϵ/κ) (--- : PBI-I; — : PBI-BuI; - - - : PBI-HFA)

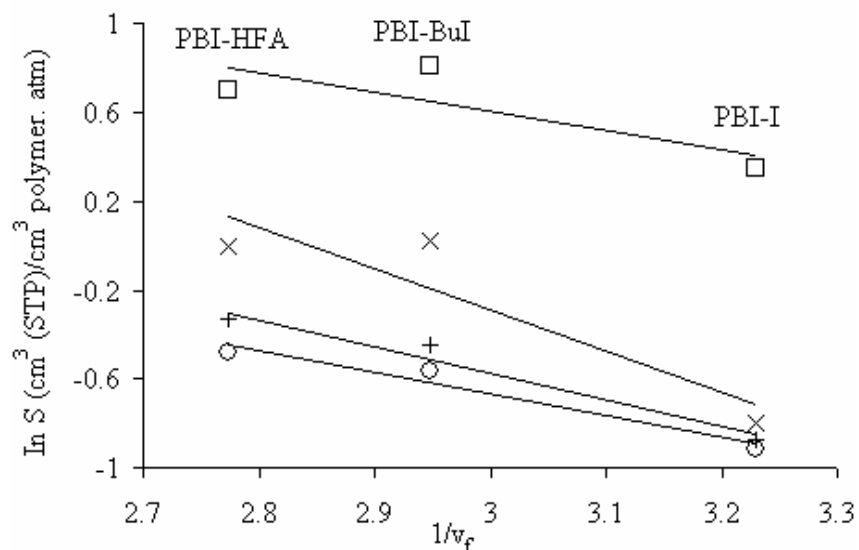


Figure 4.7. Correlation of solubility coefficient (S) with fractional free volume, v_f
(○: N_2 , +: O_2 , ×: CH_4 , □: CO_2)

Table 4.6. Solubility coefficient^a and solubility selectivity of polybenzimidazoles

Solubility coefficient (S)	PBI-I	PBI-BuI	PBI-HFA
S_{H_2}	0.37	0.33	0.31
S_{N_2}	0.40	0.57	0.62
S_{O_2}	0.42	0.64	0.71
S_{CH_4}	0.45	1.03	1.0
S_{CO_2}	1.42	2.24	2.01
Solubility selectivity (S_A/S_B)			
S_{H_2}/S_{N_2}	0.93	0.58	0.5
S_{H_2}/S_{CO_2}	0.26	0.15	0.15
S_{O_2}/S_{N_2}	1.04	1.13	1.16
S_{N_2}/S_{CH_4}	0.89	0.55	0.62
S_{CO_2}/S_{N_2}	3.53	3.97	3.26
S_{CO_2}/S_{CH_4}	3.16	2.19	2.01

^a Expressed in cm^3 (STP)/ cm^3 polymer.atm.

4.3.3. Gas permeability

The permeability of He, H₂, N₂, O₂, Ar, CH₄ and CO₂ in polybenzimidazoles (measured at 35 °C and at 20 atm upstream pressure) and ideal selectivity for various gas pairs are given in Table 4.7. The permeability of PBI-I was reported only for He, H₂ and O₂. It could not be measured accurately for other gases due to limitations of the variable volume method. Alternatively, the permeability of N₂, CH₄ and CO₂ in PBI-I was predicted based on correlation of diffusivity with kinetic diameter (Figure 4.8a) as discussed in following section separately. There are only few literature reports documenting permeability of PBI-I. He et al. (2006) reported the permeability of phosphoric acid doped and undoped PBI-I at higher temperatures in view of its applicability as a proton exchange membrane (PEM) material. Pesiri et al. (2003) reported permeability of H₂ (at room temperature) and CO₂ (at 25 °C), while Klaehn et al. (2005) reported permeability of H₂, N₂, Ar, O₂, CH₄ and CO₂ at 30 °C in PBI-I. For comparison, both these literature data are included in Table 4.7, since the temperature at which gas permeation was carried out in both these cases was nearer to the temperature of permeability measurement in the present study (35 °C). It could be seen from this table that there is a considerable scatter in the data. The experimental temperature difference may not be the only reason for this scatter, since the T_g of PBI is far above the test temperature.

The permeability of all gases in PBI-I was very low (Table 4.7) owing to the higher packing density (lower v_f and d_{sp}). The increase in packing density was as a result of H-bonding among the polymer chains containing two N-H groups per repeat unit. It is demonstrated in the literature that the increasing extent of H-bonding by increasing vinyl alcohol content in vinyl alcohol-vinyl butyral copolymers decreased CO₂ and CH₄ permeability [Reimers (1993)]. The low permeability in PBI-I was also associated with high selectivity of various gas pairs and the effect was more prominent in diffusivity based (He or H₂ based) selectivities.

Table 4.7. Permeability coefficient^a and permselectivity of polybenzimidazoles

Permeability coefficient (P)	PBI-I		PBI-BuI	PBI-HFA
	Reported	This work		
P _{He}	-	1.05	10.1	12.9
P _{H₂}	0.09 ^b / 3.9 ^c	0.6	10.7	12.2
P _{N₂}	0.049 ^c	0.0048 ^d	0.06	0.13
P _{Ar}	0.073 ^c	-	0.16	0.22
P _{O₂}	0.086 ^c	0.015	0.42	0.6
P _{CH₄}	0.04 ^c	0.0018 ^d	0.05	0.07
P _{CO₂}	0.01 ^b / 0.07 ^c	0.16 ^d	1.91	2.91
Permselectivity (P _A /P _B)				
P _{He} /P _{N₂}	-	219	168	99
P _{He} /P _{CH₄}	-	583	197	183
P _{H₂} /P _{N₂}	80	131	176	92
P _{H₂} /P _{CH₄}	98	350	208	173
P _{O₂} /P _{N₂}	1.8	3.1	7	4.6
P _{CO₂} /P _{N₂}	1.4	33	32	22
P _{CO₂} /P _{CH₄}	1.8	89	37	41

^a Determined at 20 atm upstream pressure, expressed in Barrer (1 Barrer = 10⁻¹⁰ cm³(STP).cm/cm².s.cm Hg); ^b Ref: [Pesiri (2003)]; ^c Ref: [Klaehn (2005)]; ^d Calculated based on predicted diffusivity (Figure 4.8a).

4.3.4. Gas diffusivity

The diffusivity coefficient (D_A) of a gas A was deduced from the experimentally determined intrinsic permeability (P_A) and the solubility coefficient (S_A) at 20 atm pressure using Equation 4.2.

$$P_A = D_A S_A \quad (4.2)$$

The variation in diffusion coefficient ($\ln D$) of penetrants as a function of their kinetic diameter as plotted in Figure 4.8a showed a good correlation for both polymers, PBI-HFA ($R^2 = 0.99$) and for PBI-BuI ($R^2 = 0.98$). A line joining $\ln D$ of H_2 and that of O_2 for PBI-I (slope = -6.54) was almost parallel to the lines corresponding to both, PBI-HFA and PBI-BuI (slope = -6.9 and -7.06 , respectively). Thus, the line for PBI-I was extrapolated to predict the diffusion coefficients for CO_2 , N_2 and CH_4 (encircled in Figure 4.8a), with an assumption that diffusivity coefficient of PBI-I has undeviating relation with kinetic diameter as that for PBI-HFA and PBI-BuI (in view of their observed parallel nature). Using these predicted diffusion coefficients along with respective solubility coefficient (Table 4.6), the permeability coefficient of CO_2 , N_2 and CH_4 for PBI-I was calculated using Equation 4.2 and are tabulated in Table 4.7.

The gas diffusivity, D , is often assumed to be dependant on polymer free volume as described by the Fujita relationship,

$$D = A \exp(-B/v_f) \quad (4.3)$$

where, constants A and B are the characteristics of the polymer-penetrant system [Ghosal (1993)]. Figure 4.8b represents a plot of diffusivity coefficient ($\ln D$) versus $1/v_f$ of PBI investigated for H_2 , N_2 , O_2 , CH_4 and CO_2 following Fujita's relationship. The plot of experimentally determined diffusivity coefficient of H_2 and O_2 with $1/v_f$ has coefficient of regression (R^2) as 0.89 and 0.90, respectively. The predicted diffusivity coefficient of CO_2 , N_2 and CH_4 in PBI-I from Figure 4.8a were used in Figure 4.8b (encircled). The coefficient of regression (R^2) for these gases (CO_2 , N_2 and CH_4) was found to be 0.96, 0.97 and 0.90, respectively, and provided a strong support for the predicted diffusivity coefficients.

The variation in diffusivity with solubility parameter (δ), a measure of the cohesive force between polymer chains, is as shown in Figure 4.9. The diffusivity of a particular gas in these PBIs decreased in the order: PBI-HFA > PBI-BuI > PBI-I, following the order of openness in the matrix, as supported by the decrease in d_{sp} and v_f in the same order. This is also an order of increasing N-H group density, which brings about closer chain packing and thus explain the order of decreasing diffusivity.

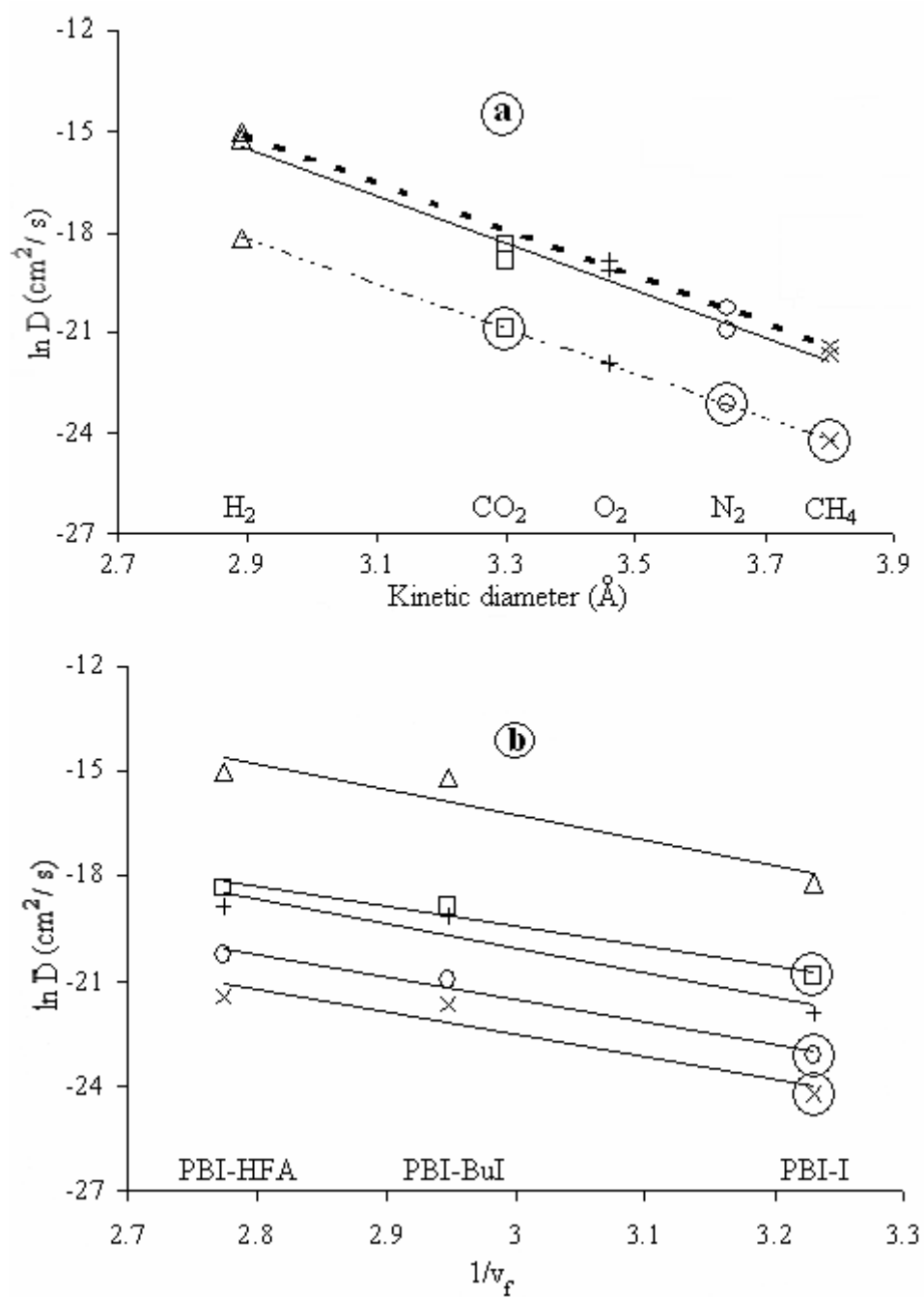


Figure 4.8. Correlation of diffusion coefficient (D) with (a) kinetic diameter (---) : PBI-I; — : PBI-BuI; - - - - : PBI-HFA and (b) with v_f (Δ : H_2 , \circ : N_2 , +: O_2 , \times : CH_4 , \square : CO_2) for gases at 35 °C.

Table 4.8. Diffusivity coefficient^a and diffusivity selectivity of polybenzimidazoles

Diffusivity coefficient (D)	PBI-I	PBI-BuI	PBI-HFA
D_{H_2}	1.25	24.45	30.06
D_{N_2}	0.009 ^b	0.08	0.16
D_{O_2}	0.03	0.50	0.64
D_{CH_4}	0.003 ^b	0.04	0.05
D_{CO_2}	0.085 ^b	0.65	1.10
Diffusivity selectivity (D_A/D_B)			
D_{H_2}/D_{N_2}	139	306	188
D_{H_2}/D_{CO_2}	14.7	37.8	27.4
D_{O_2}/D_{N_2}	3.3	6.2	4.0
D_{CO_2}/D_{N_2}	9.4	8.0	6.9
D_{CO_2}/D_{CH_4}	28	18	21

^a Expressed in $10^{-8} \text{ cm}^2/\text{s}$; ^b Predicted from Figure 4.8a.

A comparison of solubility and diffusivity coefficients (Table 4.6 and 4.8) for PBI-I with that for PBI-HFA or PBI-BuI indicated that the diffusivity coefficient increased to a larger extent than the solubility coefficient. This was affected by decreased packing density in later two cases as revealed by increased d_{sp} or v_f . The comparison of solubility selectivity of various gas pairs (Table 4.6) indicated that the solubility selectivity of different gas pairs was marginally affected by the incorporation of either hexafluoroisopropylidene or *tert*-butyl group in the PBI backbone. On the other hand, the diffusivity selectivity: D_{H_2}/D_{N_2} , D_{H_2}/D_{CO_2} and D_{O_2}/D_{N_2} increased considerably, while CO_2 based diffusivity selectivity: D_{CO_2}/D_{N_2} , D_{CO_2}/D_{CH_4} found to be decreased by the structural variation in PBI-I. As a result of these variations in solubility and diffusivity, the permeability coefficient of smaller gases (H_2 or He) increased by $\sim 10 - 20$ times, while the permeability enhancement in case of heavier gases (O_2 , N_2 , CH_4 , CO_2) was from 12 - 40 times for PBI-BuI or PBI-HFA, in comparison to the base case PBI-I (Table

4.7). This is associated with a general decrease of selectivity from $\sim 10 - 77\%$ for various gas pairs, except that for P_{O_2}/P_{N_2} , which was actually increased by 48% and 124% in case of PBI-HFA and PBI-BuI, respectively.

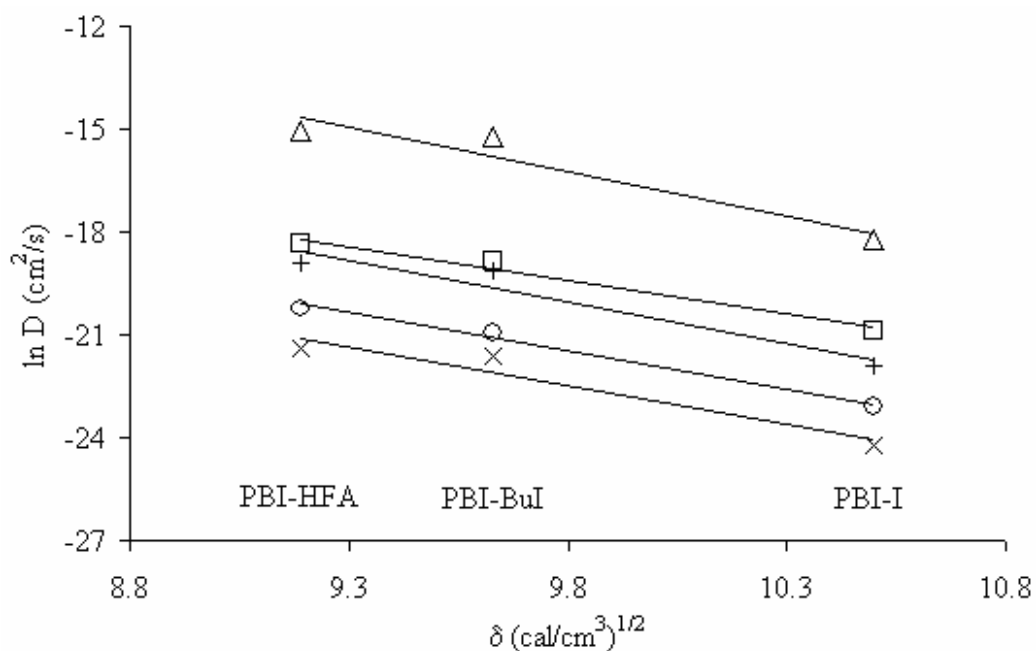


Figure 4.9. Correlation of diffusion coefficient (D) with solubility parameter (δ)
(Δ : H₂, \circ : N₂, +: O₂, \times : CH₄, \square : CO₂)

4.3.5. Comparison of permeation properties

The comparison of permeation properties between PBI-HFA and PBI-BuI indicated that the earlier exhibited slightly higher permeability and lower selectivity than for the later. This difference mainly stems from diffusivity term, rather than the solubility coefficient. As a result, for PBI-BuI, the diffusivity based selectivities (H₂ and He based) were appreciably higher (Table 4.7) than the solubility based selectivities (CO₂ based). The higher diffusivity based selectivity in PBI-BuI than that for PBI-HFA can be explained on the basis of higher chain rigidity for the former case. The *tert*-butyl group in PBI-BuI does not incorporate additional flexibility in the main chain of PBI, while in case of PBI-HFA, the hexafluoroisopropylidene group of HFA brings an additional flexibility about the bridge carbon. Thus, chain backbone of PBI-BuI was anticipated to be more rigid and thus capable of better discrimination among penetrants, than that of PBI-HFA.

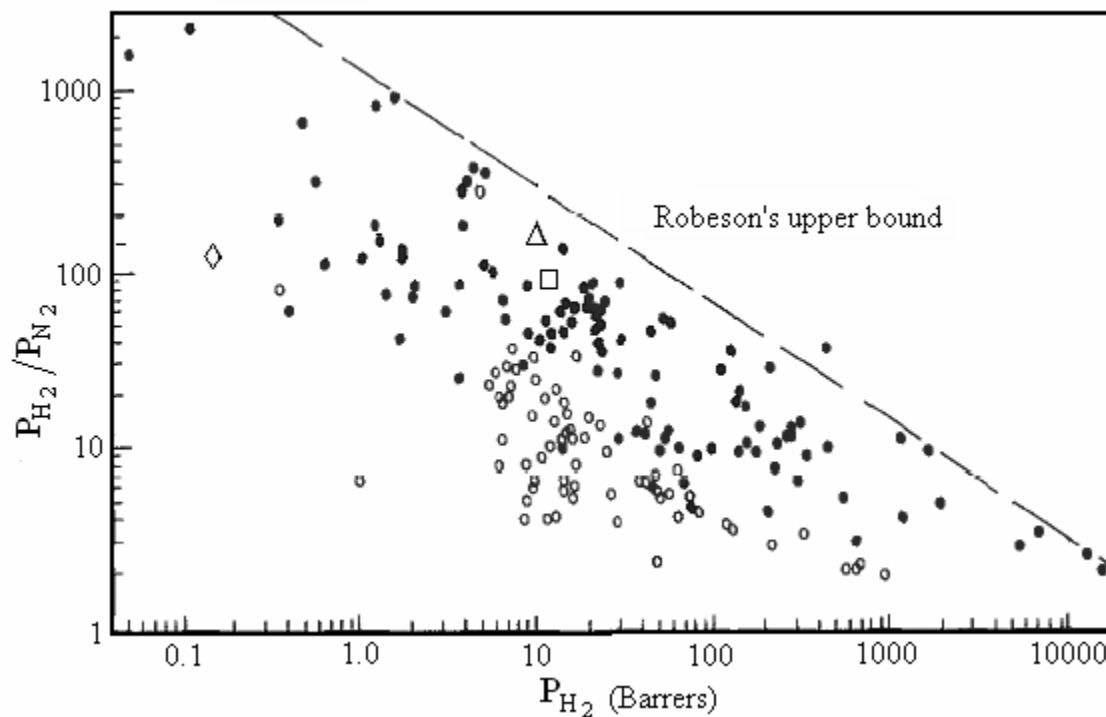


Figure 4.10. Occurrence of polybenzimidazoles on Robeson upper bound [Robeson (1991)] (\diamond : PBI-I, Δ : PBI-BuI, \square : PBI-HFA)

It is interesting to note that these PBI structural variations led these polymers to lie near Robeson's upper bound [Robeson (1991)]. As an example, incorporation of P_{H_2} and P_{H_2}/P_{N_2} of these PBIs in Robeson's upper bound curve is shown in Figure 4.10. Similar correlation for other cases, e.g., P_{He} and P_{He}/P_{CH_4} was also found. It could also be worth to compare permeation properties of present PBI family with that of other families of polymers involving similar types of substitutions. Incorporation of either hexafluoroisopropylidene or *tert*-butyl group in various families of polymers like polycarbonate, polyarylate, polysulfone or poly(aryletherketone) led to 2.3 to 6.2 times elevation in permeability with marginal changes in selectivity [Hellums (1989), Mchattie (1992), Kharul (1994), Pixton (1995a), Garcia (2002)]. On the other hand, PBI showed substantial enhancement in permeability of various gases by 10 - 40 times with just 10 - 77% decrease in selectivity for various gas pairs. This comparison also indicated that permeation properties of PBI were elevated by attempted structural modifications yielding excellent combination of gas permeability and selectivity.

Chapter 5

Effects of *N*-substitution on physical and gas permeation properties of resulting polybenzimidazoles

5.1. Synthesis, FT-IR and ¹H-NMR characterization

A synthetic route that describes the *N*-substitution reaction of chosen PBIs is given in Scheme 3.3 and 3.4. In case of PBI-I and PBI-BuI, after NaH addition, a typical deep blood red colour developed, indicating generation of the anion. In order to ensure completion of Na-salt formation, this homogeneous solution was further heated at 80 °C for an hour. *N*-alkylation of Na-salt of PBI was anticipated to occur at ambient temperature. Thus, the temperature of reaction mixture was lowered to the ambient temperature; alkyl halide (2 molar equivalents) was added over 15 minutes and was stirred further for 24 h. The addition of reaction mixture into the stirred water offered a pale yellow precipitate in all cases, except for the cases of *n*-butyl substitution, where a sticky brown mass was obtained.

In case of ABPBI, owing to its insolubility in most of the common organic solvents (Table 5.1), reaction conditions were slightly modified than that for PBI-I or PBI-BuI. ABPBI was suspended in DMSO, added NaH and the temperature was elevated to 170 °C and hold for 5 h. Elevated temperature was necessitated since at ambient, no reaction occurred (due to insolubility of ABPBI). As the temperature was slowly elevated to 170 °C, ABPBI started dissolving and within a period of 5 h, a homogeneous deep red coloured solution was formed. The temperature was lowered to 40 °C, where the solution still remained homogeneous. To this solution, alkyl halide (1 molar equivalent) added in a dropwise manner for a period of 15 minutes. The phase separation occurred after an hour. Stirring was further continued for 24 h in order to ensure completion of the reaction. Obtained polymer was recovered by addition of the reaction mixture into stirred water, followed by filtration, water washings and drying as given in Section 3.4.2.

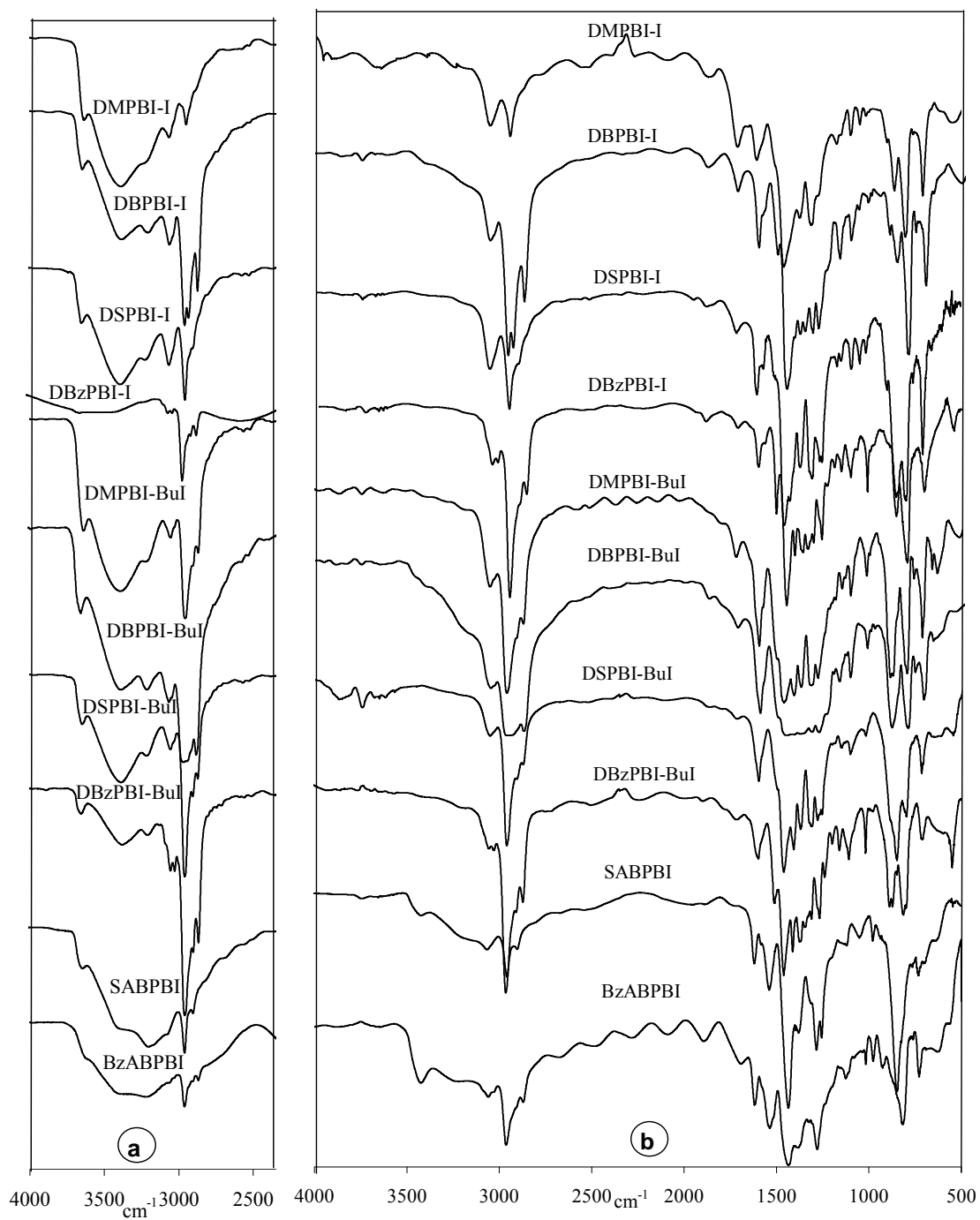


Figure 5.1. FT-IR spectra of *N*-substituted polybenzimidazoles at (a) ambient and (b) higher temperature (150/250 °C)

From FTIR analysis, it was seen that as a result of *N*-substitution, broad band in unsubstituted PBI at 2400 - 3500 cm^{-1} corresponding to N-H stretching disappeared. Though, a peak at $\sim 3300 \text{ cm}^{-1}$ attributable to sorbed moisture was seen, it showed decrease in intensity within a series of particular *N*-substituted PBI in the order of methyl > *n*-butyl > 4-*tert*-butylbenzyl substitution. This trend followed the order of hydrophobicity, which increased in the same order. This peak could be assigned to the hydrogen-bonding of the type N---H-O-H, i.e. H-bonding between imidazole '*N*' and hydrogen atom of water molecule. Though the films were vacuum dried prior to analysis, a small amount of moisture could be absorbed by the sample during handling. This was also seen from the peak at $\sim 3600 \text{ cm}^{-1}$ observed for all the polymers, attributable to the O-H stretching of absorbed water. However, except for BzABPBI and SABPBI, this peak completely disappeared when the samples were scanned at 150 °C as could be seen from Figure 5.1. Though, for BzABPBI and SABPBI though samples were scanned at even higher temperature of 250 °C, the broad peak at $\sim 3150 \text{ cm}^{-1}$ and sharp peak at $\sim 3400 \text{ cm}^{-1}$ did not disappear. The strong band at $\sim 3150 \text{ cm}^{-1}$ was ascribed to the hydrogen bonding of the type N-H---N, while the peak at $\sim 3410 \text{ cm}^{-1}$ was due to the free non-hydrogen bonded N-H stretching [Musto (1993), Pu (2003)]. These peaks in BzABPBI and SABPBI were assigned to the hydrogen bonded N-H stretching and the free non-hydrogen bonded N-H respectively. Presence of these peaks indicated that the reaction of *N*-substitution could not lead to completion, even after prolonged durations. Peaks in the range 2800 - 2900 cm^{-1} were ascribed to methylene or methyl group. Intensity of these peaks were least for the methyl substitution case and was increased as the number of methyl or methylene groups increased. The benzimidazole ring was characterized by the absorption at 1430, 1600, and 1620 cm^{-1} [Musto (1991, 1993)] in all PBIs investigated.

$^1\text{H-NMR}$ spectra (Figure 5.2 and 5.3) of all the *N*-substituted PBIs based on PBI-I and PBI-BuI showed disappearance of imidazole N-H protons that appeared at δ 13.2 ppm in cases of unsubstituted PBIs (Figure 4.2). Occurrence of N-H protons of PBI at δ 13.28 is also reported by Klaehn et al. (2007). In present cases, quantitative *N*-substitution was indicated by the disappearance of this peak as well as by the integration of peaks for the protons belonging to the added alkyl group. Except for the 4-*tert*-

butylbenzyl substitution, all *N*-substituted PBIs showed a peak at 4.23 to 4.6 ppm for methyl or methylene group attached to the nitrogen of the imidazole ring. In the case of 4-*tert*-butylbenzyl substitution, appearance of methylene protons shifted to further downfield ($\sim 5.37 - 5.39$ ppm) due to deshielding effect of the adjacent phenyl ring. Due to the insolubility of BzABPBI in DMSO- d_6 , it could not be analyzed. In the case of SABPBI, the peak at 13.28 ppm for the N-H appeared indicating incomplete degree of *N*-substitution (Figure 5.4). The degree of substitution was $\sim 60\%$ based on proton integration. These spectra are shown in Figure 5.2 - 5.4 and the peak assignments are as given below.

PBI-I: $^1\text{H-NMR } \delta$ (DMSO- d_6) = 13.28 (s, 2H), 7.68 - 9.17 (10H).

PBI-BuI: $^1\text{H-NMR } \delta$ (DMSO- d_6) = 13.28 (s, 2H), 7.67 - 9.0 (9H), 1.51 (s, 9H).

DMPBI-I: $^1\text{H-NMR } \delta$ (DMSO- d_6 + TFA) = 8.11 - 8.57 (10H, aromatic), 4.29 (6H, methyl).

DBPBI-I: $^1\text{H-NMR } \delta$ (DMSO- d_6 + TFA) = 8.16 - 8.94 (10H, aromatic), 4.73 (4H, methylene), 1.88 (4H, methylene), 1.32 (4H, methylene), 0.84 (6H, methyl).

DSPBI-I: $^1\text{H-NMR } \delta$ (DMSO- d_6 + TFA) = 7 - 8.23 (18H, aromatic), 4.41 (4H, methylene), 0.0 (9H, trimethylsilyl).

DBzPBI-I: $^1\text{H-NMR } \delta$ (DMSO- d_6 + TFA) = 6.53 - 8.23 (18H, aromatic), 5.7 (4H, methylene), 1.03 (18H, *tert*-butyl).

DMPBI-BuI: $^1\text{H-NMR } \delta$ (DMSO- d_6 + TFA) = 7.78 - 8.18 (9H, aromatic), 4.04 (6H, methyl), 1.47 (9H, *tert*-butyl).

DBPBI-BuI: $^1\text{H-NMR } \delta$ (DMSO- d_6 + TFA) = 8.16 - 8.81 (9H, aromatic), 4.69 (4H, methylene), 1.93, 1.54, 1.35 0.84 (23H, methylene and methyl).

DSPBI-BuI: $^1\text{H-NMR } \delta$ (DMSO- d_6 + TFA) = 8.29 - 8.78 (9H, aromatic), 4.36 (4H, methylene), 0.0 (9H, trimethylsilyl).

DBzPBI-BuI: $^1\text{H-NMR } \delta$ (DMSO- d_6 + TFA) = 7.08 - 8.54 (17H, aromatic), 5.83 (4H, methylene), 1.14 (27 H, *tert*-butyl).

SABPBI: $^1\text{H-NMR } \delta$ (DMSO- d_6) = 13.23, (N-H), 7.85 - 8.55 (3H, aromatic), 4.08 - 4.32 (methylene), -0.26 (9H, trimethylsilyl).

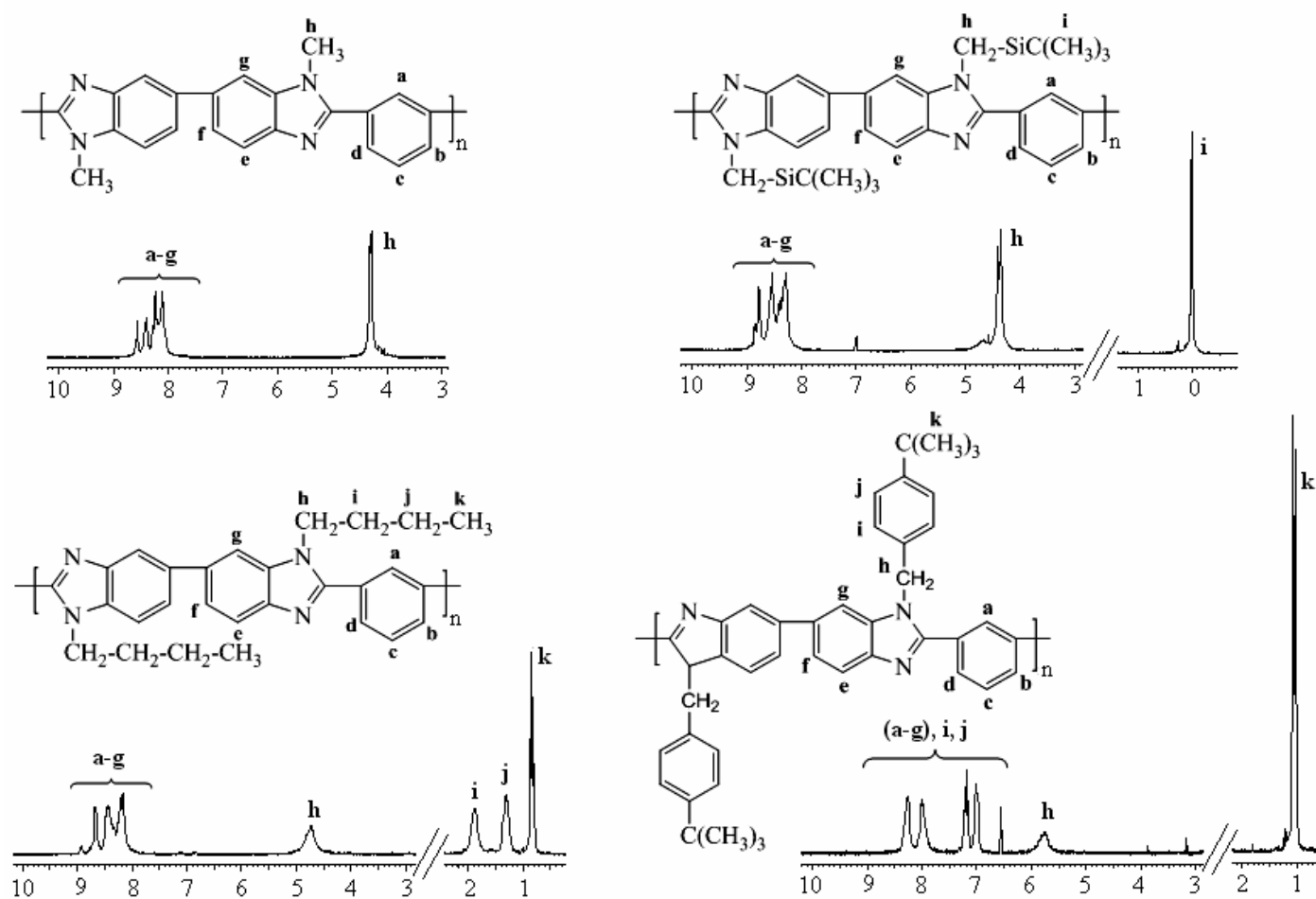


Figure 5.2. $^1\text{H-NMR}$ spectra of N -substituted PBI-I

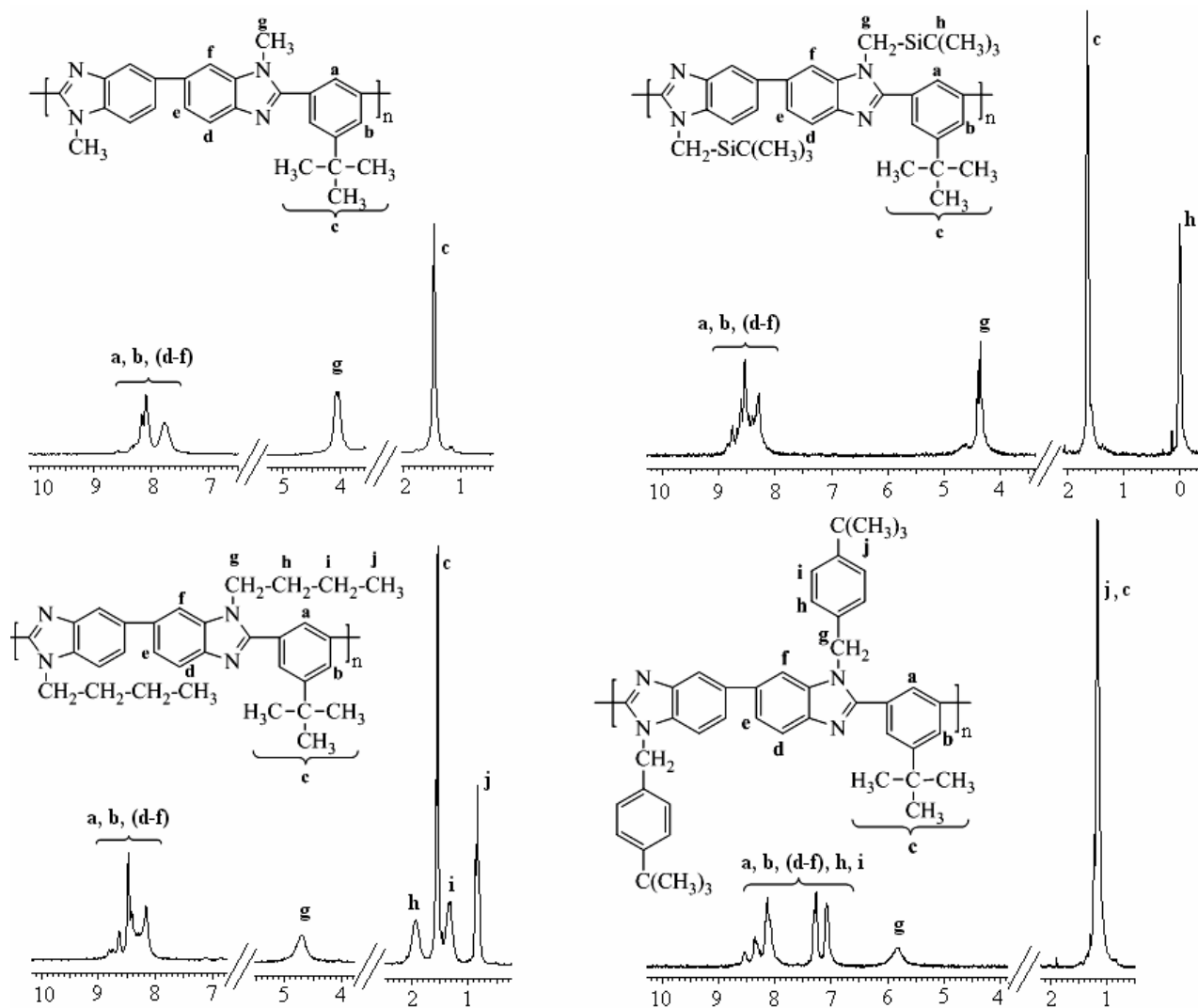


Figure 5.3. $^1\text{H-NMR}$ spectra of *N*-substituted PBI-BuI

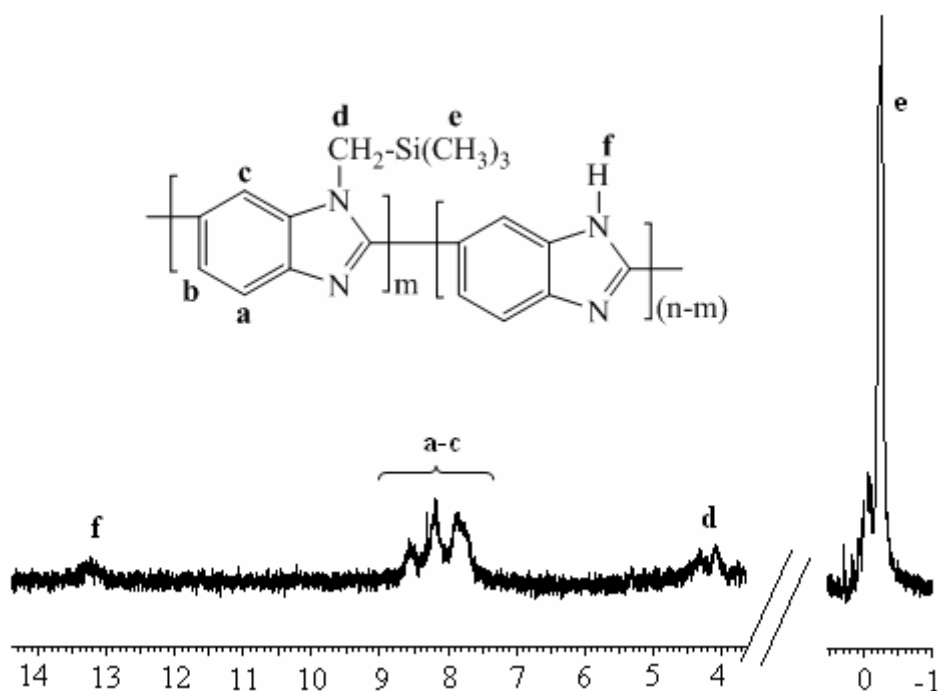


Figure 5.4. ^1H -NMR spectra of SABPBI

5.2. Physical Properties

5.2.1. Solvent solubility and viscosity

The solvent solubility of present polymers was as shown in Table 5.1. All *N*-substituted PBIs were easily soluble in H_2SO_4 , $\text{CH}_3\text{SO}_3\text{H}$, HCOOH and CF_3COOH . The methyl substitution on PBI-I did not show significant improvement in solubility as it dissolved only in NMP and acidic solvents. On the other hand, DMPBI-BuI was soluble in all solvents tested, except in THF. This enhanced solubility than that for DMPBI-I was attributed to the presence of *tert*-butyl group in the acid moiety of DMPBI-BuI. The substitution of 4-*tert*-butylbenzyl, methylene trimethylsilyl or *n*-butyl group on PBI-I and PBI-BuI rendered solubility even in chlorinated solvents (CHCl_3 and TCE). Though *N*-substitution in cases of PBI-I and PBI-BuI showed improved solubility, the same was not the case for ABPBI. SABPBI was soluble in DMAc, DMSO and NMP, where as BzABPBI was soluble only in H_2SO_4 , $\text{CH}_3\text{SO}_3\text{H}$, HCOOH and CF_3COOH , due to the backbone rigidity.

Table 5.1. Solubility of *N*-substituted PBI in common solvents

Solvent	DMPBI-I	DBPBI-I	DSPBI-I	DBzPBI-I	DMPBI-BuI	DBPBI-BuI	DSPBI-BuI	DBzPBI-BuI	ABPBI	SABPBI	BzABPBI
DMF	-	±	±	++	++	++	++	+	-	±	±
DMAc	-	++	++	++	++	++	++	+	-	++	±
DMSO	-	-	±	-	+	-	+	+	-	+	±
NMP	++	++	++	++	++	++	++	+	-	++	±
CHCl ₃	-	++	±	++	++	±	++	++	-	-	-
TCE	±	++	++	++	++	++	++	++	-	-	-
THF	-	±	-	++	-	±	±	±	-	-	-
H ₂ SO ₄	++	++	++	++	++	++	++	++	++	++	++
CH ₃ SO ₃ H	++	++	++	++	++	++	++	++	++	++	++
HCOOH	++	++	++	++	++	++	++	++	±	++	++
CF ₃ COOH	++	++	++	++	++	++	++	++	±	++	++

++: Soluble at room temperature; +: Soluble after heating at 80 °C for 24 h; ±: Partially soluble or swelling after heating at reflux temperature; -: Insoluble at reflux temperature.

After *N*-substitution, the inherent viscosity was found to be lowered than that of respective parent PBI (Table 5.2). This could be ascribed to the elimination of H-bonding interactions after *N*-alkylation. For a particular parent PBI, 4-*tert*-butylbenzyl substituted polymer showed the lowest viscosity than that of other substituted cases.

5.2.2. Packing density parameters

WAXD analysis indicated amorphous nature of these polymers (Figure 5.5). In many cases, there were more than one amorphous peaks present, indicating more than one type of chain packing arrangements in the polymer matrix. BzABPBI membrane was prepared with formic acid as the solvent, which could be responsible for inducing some crystallinity in it (Figure 5.5). It is known that formic acid induces crystalline character in PBI [Sannigrahi (2006)]. The d_{sp} was generally found to be increased after the alkyl group substitution. This could be expected based on the elimination of H-bonding interactions due to substitution and also due to the bulk of added alkyl group.

The density of PBI-I was higher than PBI-BuI indicating chains are closely packed in earlier case. This closer chain packing of PBI-I was correlated to its strong H-bonding (NH group density = 9.7%) in comparison to PBI-BuI (NH group density = 8.24%), where, the bulky *tert*-butyl group inhibits the closer chain packing. Due to insolubility of ABPBI in organic solvents, fibrous ABPBI were used for density determination using specific gravity bottle. The higher extent of H-bonding based on its higher N-H group density (12.9%) makes ABPBI a densely packed material. *N*-substitution led to lowering in density due to the elimination of H-bonding and addition of alkyl group which would disrupt chain packing in comparison to the parent PBI. Effect of *N*-substitution in decreasing the density was more prominent for densely packed ABPBI (16%) followed by PBI-I (4 - 15%) and the lowest for PBI-BuI (0.3 - 8%) in comparison to the respective unsubstituted PBI.

In case of PBI-I, fractional free volume, v_f was increased after *N*-substitution in the order of bulk of the substituent (methyl < *n*-butyl < 4-*tert*-butylbenzyl). Conversely, high initial v_f of PBI-BuI, decreased by methyl or *n*-butyl substitution, indicating bulk of these groups could have been accommodated in the available void space. Such examples of decreased v_f by substitution of small alkyl groups like methyl is known in the cases of

dimethylpolysulfone [Mchattie (1991a)], dimethylpolyarylate [Pixton (1995a)], etc. Wilks et al. (2006) observed that in case of rigid poly(norbornene) backbone, number of large free-volume elements decreased as length of the flexible aliphatic side chain increased. Pinnau et al. (2004) found a decrease in fractional free volume as length of the side chain substituent in poly(4-methyl-2-pentyne) increased by either one or two methylene groups. The bulky 4-*tert*-butylbenzyl substitution on PBI-BuI led to increased v_f . The v_f for methylene trimethylsilyl substituted PBIs could not be calculated due to unavailability of van der Waal's volume of $-\text{Si}(\text{CH}_3)_3$ group.

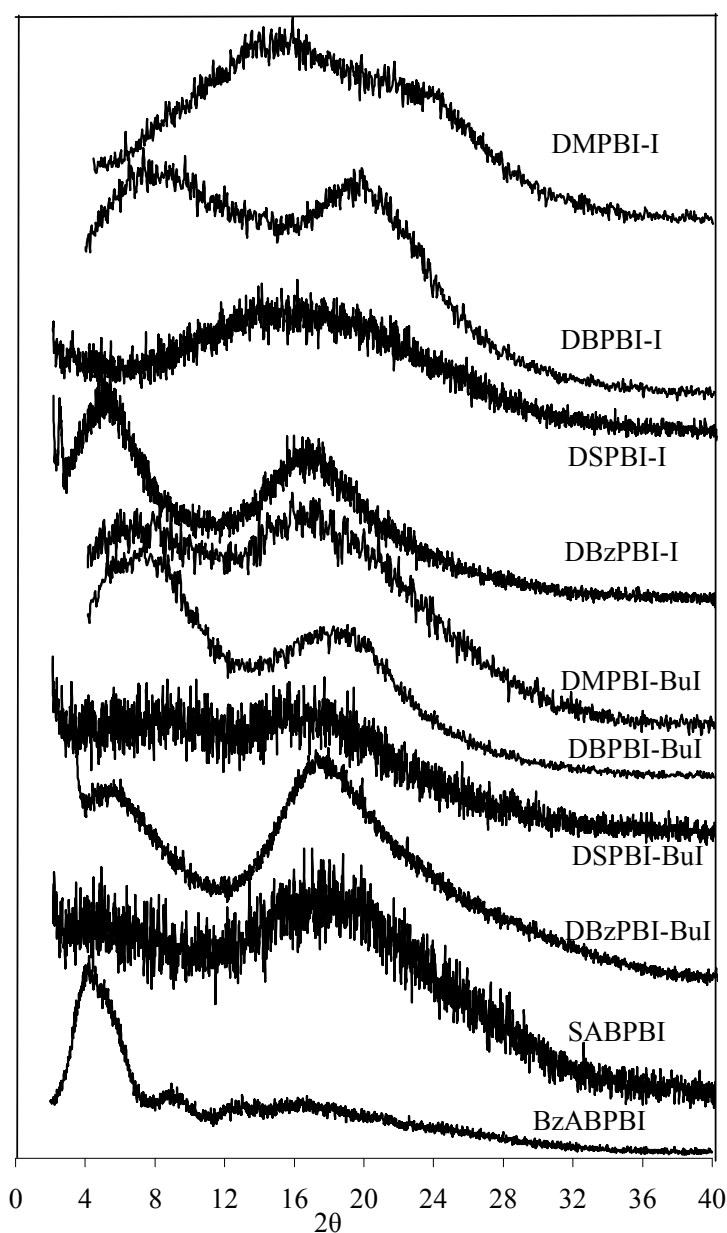


Figure 5.5. WAXD spectra of *N*-substituted polybenzimidazoles

5.2.3. Thermal properties

The T_g of *N*-substituted PBIs decreased after *N*-substitution owing to added flexibility of the substituent. The T_g of PBI-BuI and *N*-substituted ABPBI could not be detected even after repeated cycle of heating and cooling. In the case of *N*-substituted PBI-I and PBI-BuI, the extent of decrease in T_g by methyl group was less than by other substituents, which could be correlated to the higher flexibility of these groups. It was also observed that *N*-substitution of PBI-BuI with a particular alkyl group showed higher T_g than for its substitution on PBI-I. Thus it is indicative that PBI-BuI could have higher T_g than that of PBI-I.

Thermal stability of all PBIs was found to be decreased after *N*-substitution (Figure 5.6), as evident from lowered initial decomposition temperature (IDT of substituted PBIs) as given in Table 5.2. The decrease in thermal stability could be attributed to the elimination of H-bonding due to addition of flexible alkyl group, which also could be susceptible for degradation on the chain backbone. Methyl substituted PBI showed highest thermal stability in a series, whereas, *4-tert*-butylbenzyl substituted PBI were least stable. The char yields for all these *N*-substituted PBIs were high (45 - 73%).

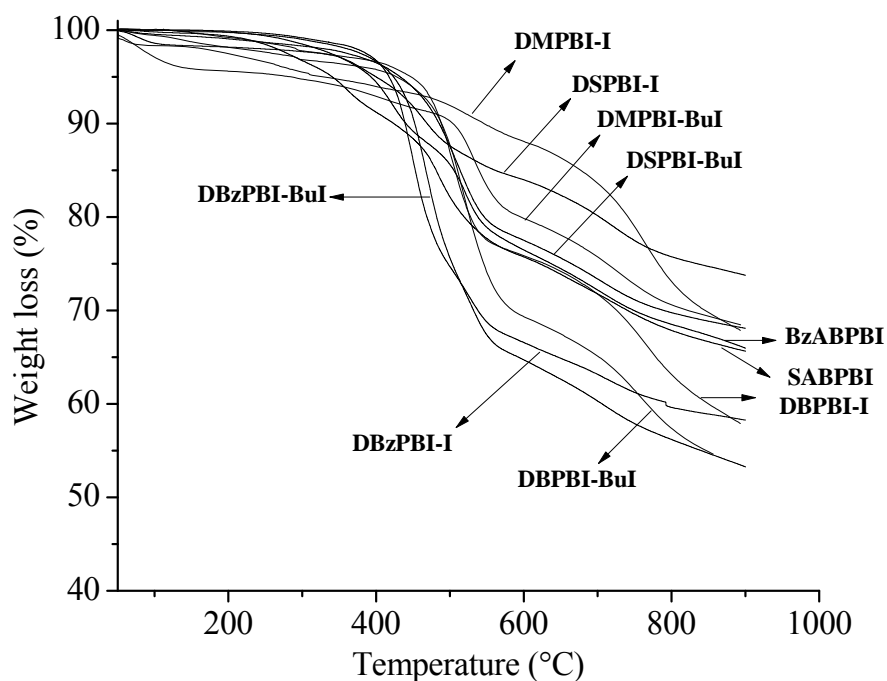


Figure 5.6. TGA spectra of *N*-substituted polybenzimidazoles

Table 5.2. Physical properties of *N*-substituted PBI

Polymer	η_{inh}^a (dL/g)	d_{sp}^b (Å)	ρ^c (g/cm ³)	v_f^d (cm ³ /cm ³)	δ^e (cal/cm ³) ^{1/2}	T_g^f (°C)	TGA analysis	
							IDT ^g (°C)	W ₉₀₀ ^h (%)
PBI-I	1.4	4.05	1.331	0.310	10.5	416	600	67
DMPBI-I	1.2	3.74, 6.24	1.279	0.317	11.54	341	480	67.9
DBPBI-I	1.1	4.44	1.168	0.330	10.82	233	420	57.9
DSPBI-I	1.1	5.68	1.214	-	11.42	294	375	73
DBzPBI-I	0.9	5.34	1.131	0.344	12.04	239	330	58
PBI-BuI	1.5	4.04, 4.69	1.193	0.339	9.63	-	525	65
DMPBI-BuI	1.4	5.22	1.196	0.325	10.87	361	500	68.4
DBPBI-BuI	1.2	4.67	1.124	0.332	10.40	270	440	54.6
DSPBI-BuI	1.3	5.28	1.146	-	10.93	324	404	68
DBzPBI-BuI	1.0	5.22	1.097	0.348	11.55	261	370	53
ABPBI	2.9	3.01	1.437	0.279	13.41	-	620	44.7
SABPBI	2.3	5.01	1.215	-	11.29	-	280	65
BzABPBI	2.4	5.37, 7.08, 9.83	1.224	0.288	12.03	-	390	65

^a: Inherent viscosity determined using 0.2 g/dL solution in conc. H₂SO₄ at 35 °C; ^b: *d*-spacing obtained from wide angle X-ray diffraction spectra; ^c: Density measured at 35 °C by floatation method; ^d: Fractional free volume calculated using group contribution method [Van Krevelen (1997)]; ^e: Hildebrand solubility parameter calculated using group contribution method [Van Krevelen (1997)]; ^f: Glass transition temperature; ^g: Initial decomposition temperature; ^h: Char yield at 900 °C.

5.3. Permeation properties

5.3.1. Sorption Properties

The equilibrium sorption isotherms for different *N*-substituted PBIs using H₂, N₂, O₂, CH₄ and CO₂ determined at 35 °C are shown in Figures 5.7 - 5.9. These isotherms showed a typical dual-mode nature, usually observed for glassy polymers [Veith (1976)] and described by Equation 4.1.

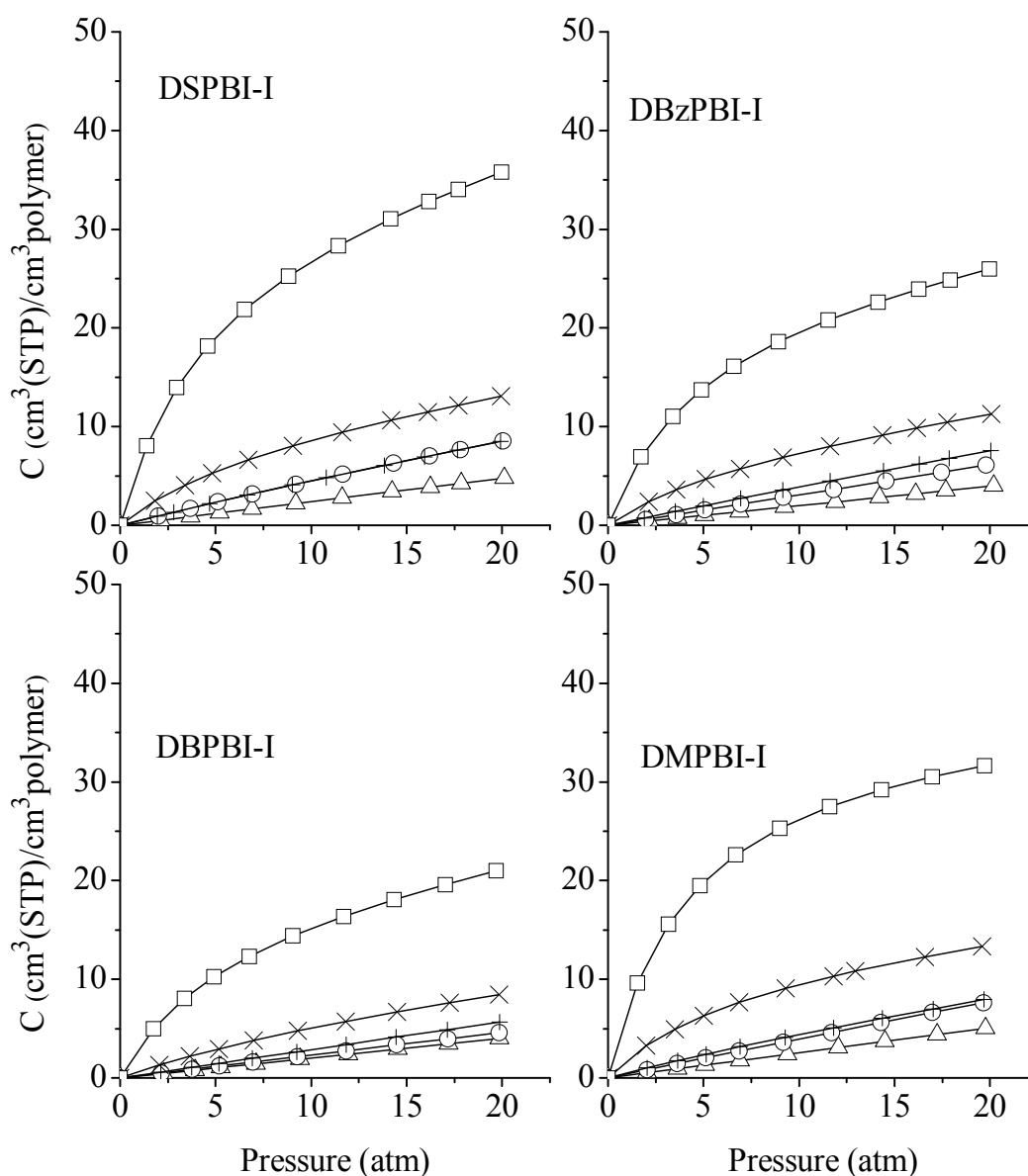


Figure 5.7. Sorption isotherms for *N*-substituted PBI-I at 35 °C (Δ : H₂, \circ : N₂, +: O₂,
 \times : CH₄, \square : CO₂)

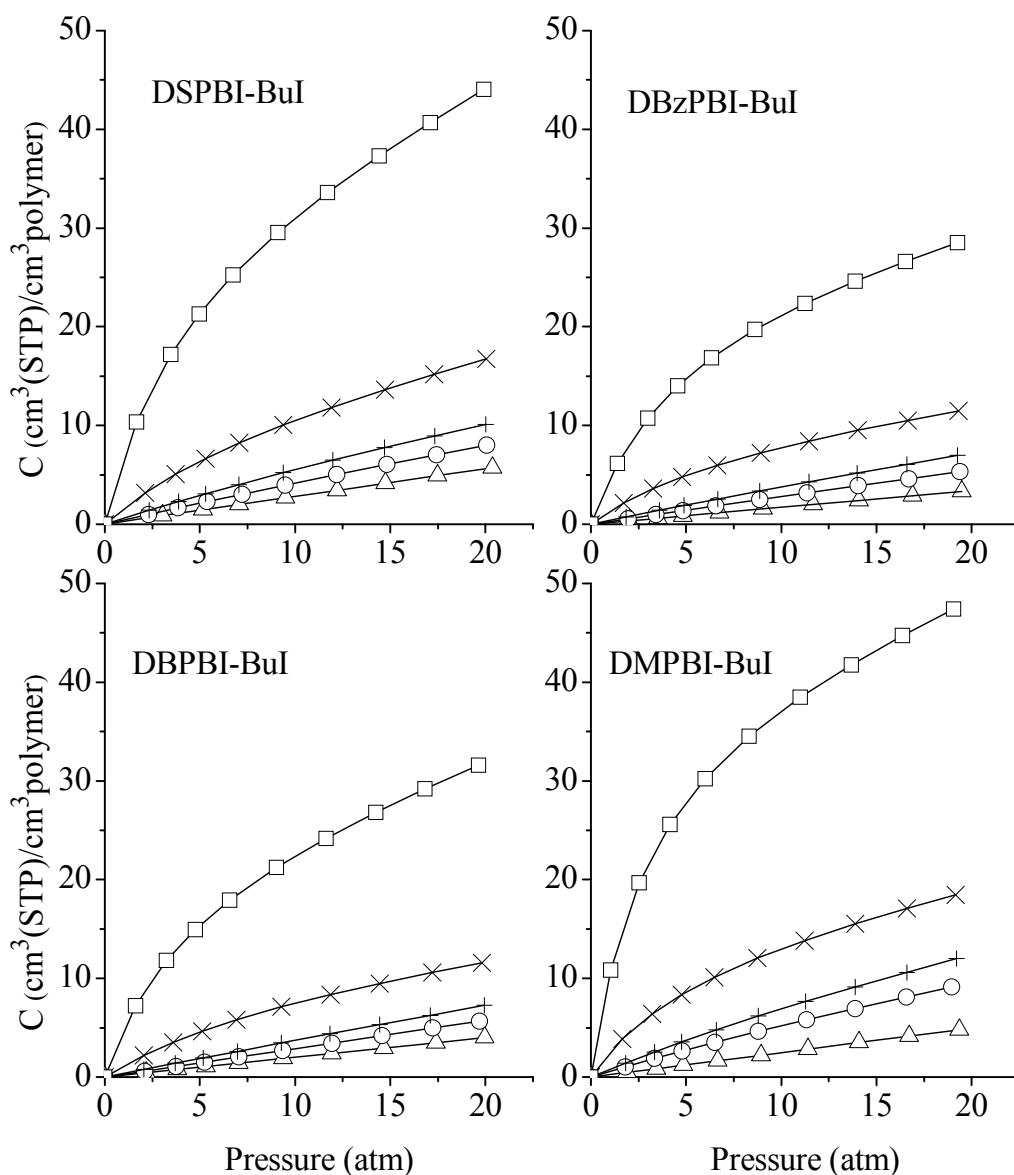


Figure 5.8. Sorption isotherms for *N*-substituted PBI-BuI at 35 °C (Δ : H₂, \circ : N₂, +: O₂, \times : CH₄, \square : CO₂)

The sorption of different gases increased in the sequence: H₂ < N₂ < O₂ < CH₄ < CO₂. This follows the trend of increasing order of inherent condensabilities of these gases. For example, critical temperature (T_c) for H₂, N₂, O₂, CH₄ and CO₂ increases in the order -239.95 °C < -146.95 °C < -118.55 °C < -82.55 °C < 31.05 °C, respectively [Wang (2002)].

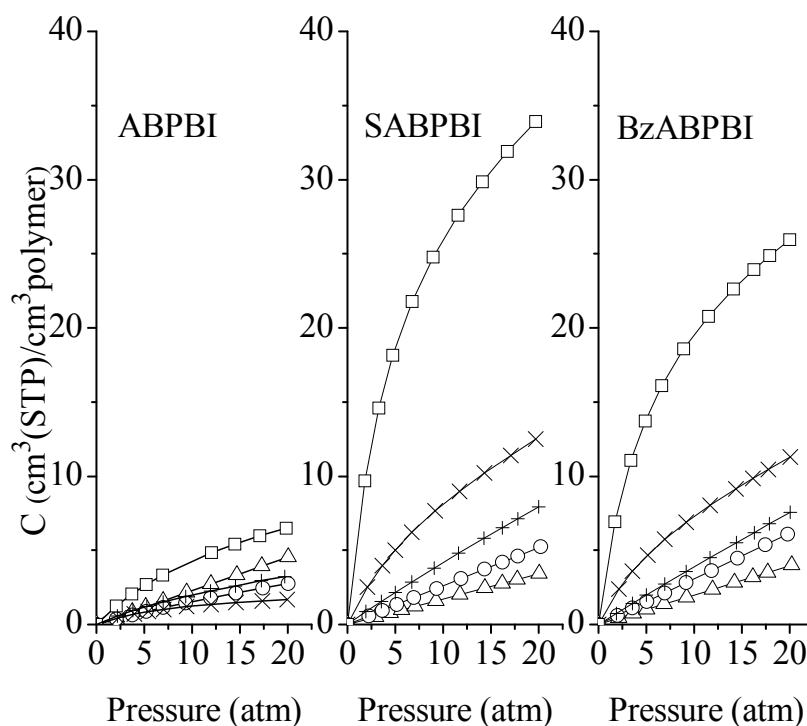


Figure 5.9. Sorption isotherms for *N*-substituted ABPBI at 35 °C (Δ : H₂, \circ : N₂, +: O₂, \times : CH₄, \square : CO₂)

The dual-mode sorption parameters k_D , C'_H and b were estimated by the non-linear regression analysis [Goldberg (1989)] of experimentally determined gas sorption at varying pressures upto 20 atm (Table 5.3a - 5.3c). The Henry's solubility coefficient k_D , ascribed to the gas dissolution in rubbery state was low for all gases in these *N*-substituted PBIs owing to their high T_g . The parameter k_D is also known to be a function of gas-polymer interactions [Barbari (1988)]. As a result, for a given polymer, this parameter for CO₂ is generally higher than the parameter for other gases. The Langmuir affinity constant, b , is the ratio of rate constants of sorption and desorption processes. The C'_H and b were increased in the order of increasing gas condensability for a particular PBI.

Table 5.3a. Dual-mode sorption parameters^a for *N*-substituted PBI-I

Gas	DMPBI-I			DBPBI-I			DSPBI-I			DBzPBI-I		
	k_D	C'_H	b	k_D	C'_H	b	k_D	C'_H	b	k_D	C'_H	b
H ₂	0.255	0.95	1.9E-06	0.201	1.41	5.8E-05	0.239	0.52	0.0002	0.198	0.18	3.05E-05
N ₂	0.355	1.81	0.028	0.231	2.88	0.0002	0.333	4.96	0.0314	0.307	0.33	0.0002
O ₂	0.285	3.54	0.085	0.283	5.35	0.0004	0.328	5.05	0.0314	0.329	2.80	0.026
CH ₄	0.222	11.94	0.153	0.241	6.12	0.075	0.310	9.36	0.1407	0.294	7.14	0.155
CO ₂	0.109	35.99	0.231	0.358	17.73	0.187	0.496	31.84	0.2168	0.321	24.33	0.205

^a k_D is expressed in cm³ (STP)/cm³ polymer. atm, C'_H is expressed in cm³ (STP)/cm³ polymer, while b is expressed in atm⁻¹.

Table 5.3b. Dual-mode sorption parameters^a for *N*-substituted PBI-BuI

Gas	DMPBI-BuI			DBPBI-BuI			DSPBI-BuI			DBzPBI-BuI		
	k_D	C'_H	b	k_D	C'_H	b	k_D	C'_H	b	k_D	C'_H	b
H ₂	0.248	0.32	0.00018	0.20	2.30	8.6E-05	0.282	0.45	6.1E-05	0.171	2.64	1.12E-05
N ₂	0.331	6.60	0.039	0.288	2.68	0.00013	0.309	6.46	0.019	0.243	3.46	0.011
O ₂	0.361	11.90	0.039	0.307	4.39	0.017	0.318	9.44	0.033	0.280	4.91	0.025
CH ₄	0.394	14.10	0.178	0.257	9.61	0.104	0.435	11.44	0.116	0.267	8.59	0.144
CO ₂	0.739	38.53	0.337	0.675	22.41	0.231	0.947	30.44	0.242	0.458	24.66	0.206

^a k_D is expressed in cm³ (STP)/cm³ polymer. atm, C'_H is expressed in cm³ (STP)/cm³ polymer, while b is expressed in atm⁻¹.

Table 5.3c. Dual-mode sorption parameters^a for *N*-substituted ABPBI

Gas	ABPBI			SABPBI			BzABPBI		
	k_D	C'_H	b	k_D	C'_H	b	k_D	C'_H	b
H ₂	0.226	0.059	1.0E-03	0.171	0.21	3.1E-05	0.307	0.64	2 E-04
N ₂	0.103	1.12	0.083	0.259	1.15	0.001	0.317	6.47	0.019
O ₂	0.095	2.05	0.103	0.291	6.55	0.024	0.307	9.94	0.032
CH ₄	3x10 ⁻¹¹	2.57	0.094	0.315	8.70	0.133	0.362	10.36	0.141
CO ₂	0.08	8.22	0.073	0.391	32.49	0.212	0.388	35.67	0.237

^a k_D is expressed in cm³ (STP)/cm³ polymer. atm, C'_H is expressed in cm³ (STP)/cm³ polymer, while b is expressed in atm⁻¹.

Owing to the presence of microvoids (unrelaxed free volume), sorption in glassy polymer is majorly dominated by Langmuir saturation constant (C'_H). In case of PBI-I and PBI-BuI, gas sorption decreased after the *N*-substitution as seen from decrease in C'_H (for a particular gas) of substituted PBI in comparison to C'_H of the respective parent PBI (Section 4.3). One of the possible reasons could be explained based on the correlation of C'_H with difference between glass transition temperature (T_g) and experimental temperature (35 °C) as shown in Figure 5.10. The C'_H for N₂, CH₄ and CO₂ was found to decrease with decrease in T_g of different *N*-substituted PBIs. The extent of decrease in C'_H was more pronounced for condensable CO₂ (the slope for CO₂, CH₄ and N₂ are 0.141, 0.034 and 0.054, respectively). The linear correlation coefficient (R^2) values were 0.861 for CO₂, 0.943 for CH₄ and 0.552 for N₂. This suggests that the correlation holds better for the condensable gases, CH₄ and CO₂, than for non-condensable gas N₂. Similar observation was reported for CO₂ by Toi et al. (1982), where C'_H increased with increase in T_g of polymers. Kaneshahi et al. (2005) presented a data of several glassy polymers obeying similar trend of increasing C'_H with increase in T_g of polymers for CO₂, N₂ and CH₄, irrespective of their chemical structure. No direct correlation was observed between v_f and C'_H . Though sorption was decreased in *N*-substituted PBI-I and PBI-BuI, *N*-substitution in case of ABPBI showed opposite trend. The sorption of all gases (especially C'_H) after methylene trimethylsilyl and 4-*tert*-butylbenzyl substitution increased. This behavior could be explained on the basis of a large increase in free

volume after the substitution. In PBI-I and PBI-BuI substitution cases, absence of correlation of v_f with C'_H , which otherwise holds true for ABPBI case, indicated that the sorption is governed by predominant changes in physical properties after the substitution. In other words, variation in T_g was more predominant in controlling sorption for PBI-I and PBI-BuI substitutions, while variation in v_f was more predominant in cases of ABPBI substitution.

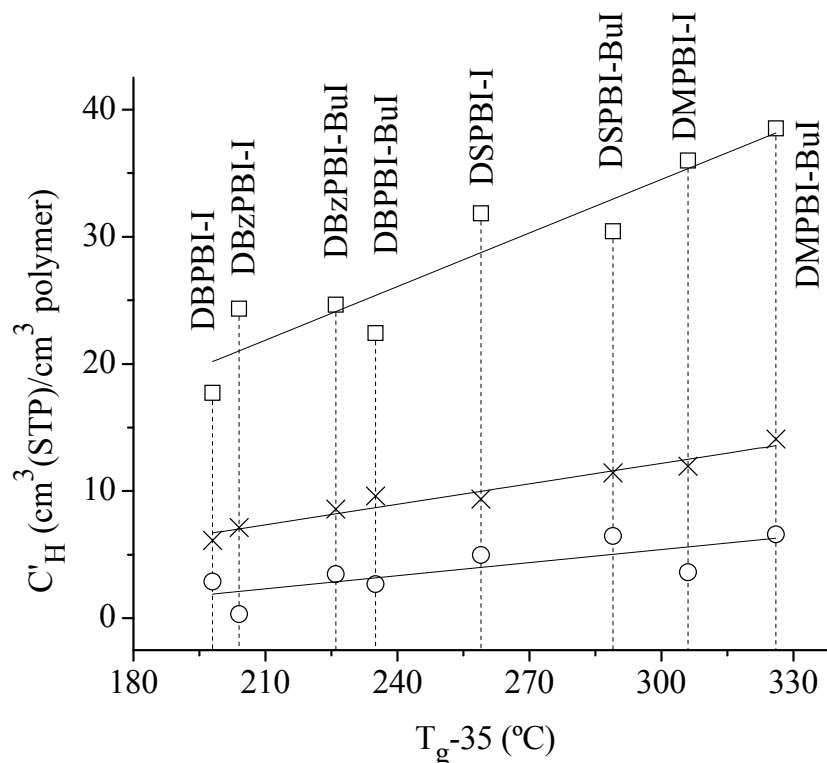


Figure 5.10. Correlation of Langmuir saturation constant (C'_H) with T_g-35 (°C) (○: N₂, ×: CH₄, □: CO₂)

Gas solubility and selectivity for various gas pairs at 20 atm is given in Table 5.4. *N*-substitution of PBI-I with methylene trimethylsilyl and 4-*tert*-butylbenzyl groups led to decrease in gas sorption of H₂, N₂ and O₂; while the same was increased for condensable gases, CH₄ and CO₂, (which increased upto 1.5 times in comparison to the base case of PBI-I). On the other hand, *N*-substitution with methylene trimethylsilyl and 4-*tert*-butylbenzyl groups in PBI-BuI led to a general decrease in gas sorption. Methyl group substitution in both, PBI-I and PBI-BuI did not show significant effect on gas sorption.

However, substitution with aliphatic *n*-butyl chain in both PBI-I and PBI-BuI led to a decrease in sorption for all gases. *N*-substitution of ABPBI led to increase in the sorption of all the gases. Gas permeability investigations using all gases for *N*-substituted ABPBIs were restricted only to SABPBI and BzABPBI. In case of methyl and *n*-butyl substituted ABPBI, helium permeability was low (0.88 and 1.58 Barrers, respectively) and thus, were not evaluated for further gas sorption and permeation properties.

N-substitution of PBI-I increased CH₄ and CO₂ solubility coefficient by 10 - 50% except for DBPBI-I, where, CH₄ sorption remained same and CO₂ sorption was decreased by 30% as compared to parent PBI-I (Table 5.4). This led to increase in $S_{\text{CO}_2}/S_{\text{N}_2}$ by 10 - 40% in *N*-substituted PBI-I. Where as, $S_{\text{CO}_2}/S_{\text{CH}_4}$ selectivity was decreased up to 25% as a result of larger increase in S_{CH_4} than S_{CO_2} . Solubility coefficient for other gases viz. H₂, N₂ and O₂ showed a decrease upto 50% and marginal changes in selectivities for various gas pairs. *N*-substitution in PBI-BuI showed a decrease in gas sorption for all the gases upto 50% except for CO₂. The extent of decrease in sorption of H₂, N₂, O₂ and CH₄ was more than for CO₂ sorption, which either remained same (as observed for DMPBI-BuI and DSPBI-BuI) or decreased by 30 - 40% for DBPBI-BuI and DBzPBI-BuI (Table 5.4). This led to increase in CO₂ based selectivities ($S_{\text{CO}_2}/S_{\text{N}_2}$ and $S_{\text{CO}_2}/S_{\text{CH}_4}$) by 13 - 41%.

Significant effects of *N*-substitution of ABPBI on their gas sorption were observed. As seen from Figure 5.9, sorption of all the gases was increased after *N*-substitution. Sorption for CH₄ and CO₂ was increased by 5.2 - 9.3 folds; while sorption for other gases was increased by 1.3 - 3.1 folds in comparison to parent ABPBI (Table 5.4). Though gas sorption is known to be a weak function of v_f [Ghosal (1996)], increased sorption for *N*-substituted ABPBI can be explained based on increased v_f . A dependence of sorption capacity on v_f , was observed previously in case of PBI (Section 4.3.2), polyarylate and PPO [Bhole (2007a), Karadkar (2007)]. The initial closely packed, compact and rigid backbone of ABPBI opens up after bulky group substitution (as also seen from increased d_{sp} and decrease in density by 16%) to accommodate more gases in thus created free volume domains. The dual-mode sorption parameters (Table 5.3c) also showed increase in C'_H in comparison to parent ABPBI. The extent of increase in CH₄

and CO₂ sorption was more, which results in high sorption based selectivity $S_{\text{CO}_2}/S_{\text{N}_2}$, which is 90 - 180% higher as compared to that of ABPBI. However, when sorption of CH₄ and CO₂ is compared, CH₄ sorption was increased by 7.9 - 9.3 folds and CO₂ sorption was increased by 5.2 - 5.6 folds. This resulted in decrease of $S_{\text{CO}_2}/S_{\text{CH}_4}$ selectivity by 61 - 66% for both the polymers, BzABPBI and SABPBI. This large increase in CH₄ sorption in comparison to CO₂ indicated that the effect of substitution in increasing v_f was more responsible for governing gas sorption properties.

The solubility coefficient (S) for all *N*-substituted PBIs correlated well with Lennard-Jones force constant (ϵ/k), a measure of condensability of gases, as shown in Figure 5.11. The correlation coefficient, R^2 for this correlation varied between 0.841 to 0.982, indicating a good correlation between S and ϵ/k .

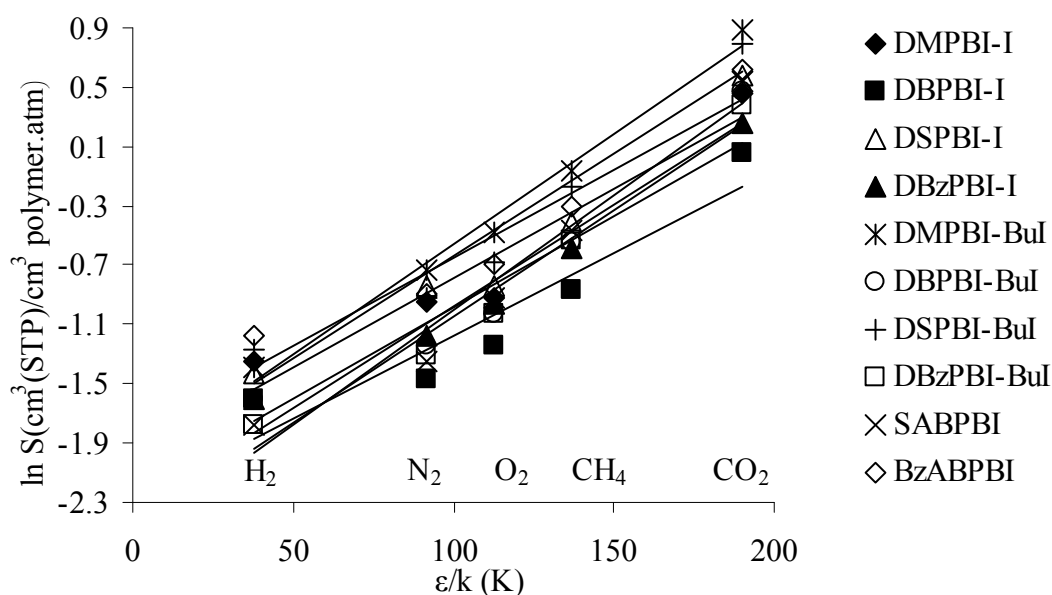


Figure 5.11. Correlation of solubility coefficient (S) at 20 atm with Lennard-Jones force constant (ϵ/k)

Table 5.4. Solubility coefficient (S)^a and solubility selectivity (S_A/S_B) of *N*-substituted PBI

Solubility Coefficient	PBI-I	DMPBI-I	DBPBI-I	DSPBI-I	DBzPBI-I	PBI-BuI	DMPBI-BuI	DBPBI-BuI	DSPBI-BuI	DBzPBI-BuI	ABPBI	SABPBI	BzABPBI
S_{H_2}	0.37	0.26	0.20	0.24	0.20	0.33	0.25	0.20	0.28	0.17	0.23	0.17	0.31
S_{N_2}	0.40	0.39	0.23	0.43	0.31	0.57	0.48	0.29	0.40	0.27	0.14	0.26	0.41
S_{O_2}	0.42	0.40	0.29	0.43	0.38	0.64	0.62	0.36	0.51	0.36	0.16	0.40	0.50
S_{CH_4}	0.45	0.67	0.42	0.66	0.56	1.04	0.94	0.58	0.84	0.59	0.08	0.63	0.74
S_{CO_2}	1.42	1.59	1.06	1.79	1.30	2.24	2.42	1.60	2.21	1.45	0.33	1.71	1.86
Solubility selectivity													
S_{H_2}/S_{N_2}	0.93	0.67	0.87	0.56	0.65	0.58	0.52	0.69	0.70	0.63	1.64	0.65	0.76
S_{H_2}/S_{CO_2}	0.26	0.16	0.19	0.13	0.15	0.15	0.10	0.13	0.13	0.12	0.70	0.10	0.17
S_{O_2}/S_{N_2}	1.04	1.03	1.26	1.00	1.23	1.13	1.29	1.24	1.28	1.33	1.14	1.54	1.22
S_{CO_2}/S_{N_2}	3.53	4.08	4.61	4.16	4.19	3.97	5.04	5.52	5.53	5.37	2.36	6.58	4.54
S_{CO_2}/S_{CH_4}	3.16	2.37	2.52	2.71	2.32	2.19	2.57	2.76	2.63	2.46	4.13	2.71	2.51

^a Expressed in cm^3 (STP)/ cm^3 polymer.atm.

5.3.2. Gas permeability

The pure gas permeability for He, H₂, Ar, N₂, O₂, CH₄ and CO₂ and ideal selectivity for various gas pairs are as given in Table 5.5. A trade off relationship between permeability and permselectivity i.e. with increase in permeability reduction in selectivity was observed. *N*-substitution of PBI-I led to 3 - 38 folds increase in permeability for smaller gases (He or H₂) and 10 - 129 folds increase for heavier gases (N₂, O₂, CH₄ and CO₂). On the other hand, *N*-substitution of PBI-BuI led to 1.2 - 4.3 folds increase in permeability for smaller gases and 4 - 27 folds increase for heavier gases. Though *4-tert*-butylbenzyl, methylene trimethylsilyl and *n*-butyl significantly enhanced gas permeability, methyl substitution did not have much effect on permeability for both PBI-I as well as PBI-BuI. It showed upto 3.6 times increase in gas permeability of various gases. The substituents remarkably increased the gas permeability for PBI-I than that for PBI-BuI. This could be attributed to initial higher v_f of the PBI-BuI than for PBI-I, wherein, the bulk of the added substituent was more efficient in creating additional free volume for less open structure of PBI-I. In case of PBI-BuI having higher initial v_f , the added bulk can be accommodated in available free space, at least to some extent. This was supported from the extent of decrease in density of *N*-substituted PBI-I, which was higher than for the same substitution in case of PBI-BuI.

In the present series of PBIs, extent of decrease in permselectivities was more for *4-tert*-butylbenzyl substitution than for any other substitution. This was due to large increase in v_f after *4-tert*-butylbenzyl substitution on PBI, which can not discriminate efficiently between penetrant gases. The permselectivities based on He or H₂ were decreased significantly (upto 87%) in both the *N*-substituted PBIs (PBI-I and PBI-BuI). They also showed a modest decrease for CO₂ based selectivities of upto 69% due to smaller increase in CO₂ permeability in comparison to the increase in permeability for other gases. It was interesting to note that P_{O_2}/P_{N_2} selectivities were increased by 29 - 65% for DBPBI-I, DSPBI-I and DBzPBI-I.

The gas permeabilities of *N*-substituted PBI and base materials were found to correlate well with fractional free volume. The relation between permeability and fractional free volume is given by Equation 5.1.

$$P = A \exp\left(\frac{-B}{v_f}\right) \quad (5.1)$$

where, A and B depends only on temperature and gas type [Pixton (1995a)]. Figure 5.12 represents a plot of permeability coefficient ($\ln P$) versus $1/v_f$. The correlation coefficients, R^2 were in the range 0.70 - 0.82 for H_2 , N_2 , O_2 , CH_4 and CO_2 .

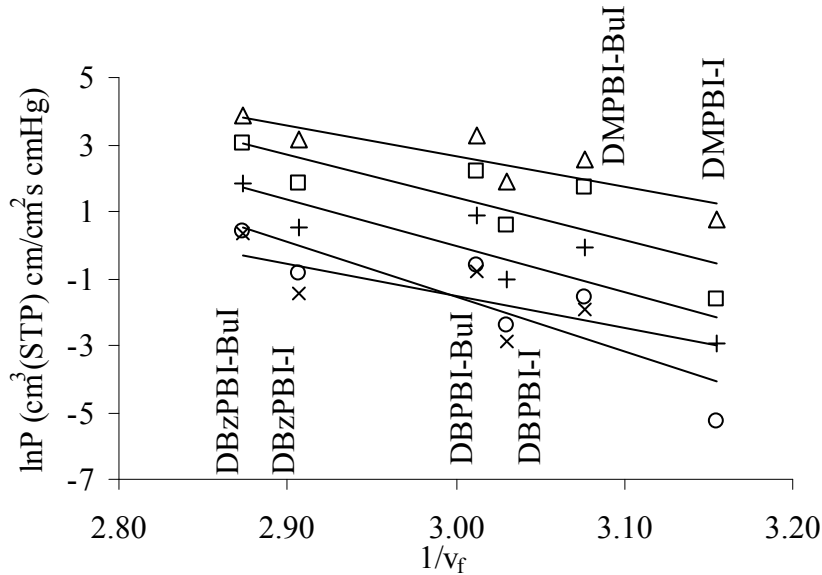


Figure 5.12. Correlation of permeability coefficient (P) with fractional free volume (v_f) (Δ : H_2 , \circ : N_2 , $+$: O_2 , \times : CH_4 , \square : CO_2)

5.3.3. Diffusion properties

Diffusivity coefficients were estimated from measured permeability coefficient and solubility coefficient at 20 atm and are tabulated in Table 5.6. Diffusion coefficient is a kinetic parameter, the magnitude of which depends on the size of penetrating gas molecules and the openness of the polymer matrix. Thus, the diffusion coefficient is usually well correlated with v_f and Kinetic diameter of the gases. The gas diffusivity, D , is often assumed to be a function of free volume as described by the Fujita relationship:

$$D = A \exp(-B/v_f) \quad (5.2)$$

where, constants A and B are the characteristics of the polymer-penetrant system [Ghosal (1996)].

Table 5.5. Permeability coefficient (P)^a and permselectivity (P_A/P_B)^b of *N*-substituted PBI

Permeability Coefficient	PBI-I	DMPBI-I	DBPBI-I	DSPBI-I	DBzPBI-I	PBI-BuI	DMPBI-BuI	DBPBI-BuI	DSPBI-BuI	DBzPBI-BuI	SABPBI	BzABPBI
P _{He}	1.05	3.11	6.63	6.43	17.96	10.1	11.76	21.26	26.64	38.28	13.53	6.05
P _{H₂}	0.6	2.18	6.54	6.81	22.85	10.7	13.06	26.9	39.16	46.45	15.9	5.12
P _{Ar}	-	0.009	0.17	0.15	0.83	0.16	0.37	1.29	1.70	3.24	0.62	0.17
P _{N₂}	0.0048	0.005	0.09	0.07	0.43	0.06	0.21	0.56	0.71	1.51	0.16	0.08
P _{O₂}	0.015	0.052	0.36	0.38	1.73	0.42	0.91	2.39	3.50	6.27	1.18	0.37
P _{CH₄}	0.0018	-	0.06	0.04	0.23	0.05	0.15	0.46	0.63	1.37	0.17	0.06
P _{CO₂}	0.16	0.193	1.79	1.62	6.24	1.91	5.62	9.11	7.81	21.32	5.28	0.94
Permselectivity												
P _{He} /P _{N₂}	219	625.9	73.9	87.9	41.6	168	56.9	38.1	37.4	25.4	84	75.2
P _{He} /P _{CH₄}	583	-	119.8	170.7	77.1	197	79.1	45.9	42.1	27.9	79.7	109
P _{H₂} /P _{N₂}	131	437.8	73	93.0	52.9	176	63.1	48.3	55.0	30.8	98.8	63.6
P _{H₂} /P _{CH₄}	350	-	118.4	180.7	98.1	208	87.8	58.1	61.9	33.9	93.7	92.3
P _{Ar} /P _{N₂}	-	1.8	1.8	2.0	1.9	2.7	1.8	2.3	2.4	2.2	3.9	2.1
P _{O₂} /P _{N₂}	3.1	10.5	4	5.2	4.01	7	4.4	4.3	4.9	4.2	7.3	4.6
P _{CO₂} /P _{N₂}	33	38.7	20	22.1	14.5	32	27.2	16.3	11	14.1	32.8	11.7
P _{CO₂} /P _{CH₄}	89	-	32.4	43	26.8	37	37.8	19.7	12.3	15.5	31.1	17.0

^a Determined at 20 atm upstream pressure, expressed in Barrer (1 Barrer = 10⁻¹⁰ cm³(STP).cm/cm².s.cm Hg)

^b Ratio of pure gas permeability.

Table 5.6. Diffusivity coefficient (D)^a and diffusivity selectivity (D_A/D_B) of *N*-substituted PBI

Diffusivity Coefficient	PBI-I	DMPBI-I	DBPBI-I	DSPBI-I	DBzPBI-I	PBI-BuI	DMPBI-BuI	DBPBI-BuI	DSPBI-BuI	DBzPBI-BuI	SABPBI	BzABPBI
D_{H_2}	1.25	6.49	24.73	21.67	87.60	24.45	40.03	102.02	105.71	206.32	70.87	12.69
D_{N_2}	0.009	0.01	0.30	0.12	1.06	0.08	0.34	1.48	1.35	4.17	0.47	0.15
D_{O_2}	0.030	0.10	0.96	0.68	3.48	0.50	1.12	4.99	5.27	13.19	2.26	0.56
D_{CH_4}	0.003	-	0.11	0.05	0.31	0.04	0.12	0.60	0.57	1.78	0.20	0.06
D_{CO_2}	0.085	0.09	1.29	0.69	3.65	0.65	1.77	4.34	2.69	11.17	2.35	0.38
Diffusivity selectivity												
D_{H_2}/D_{N_2}	139	662	83.5	174.8	82.6	306	119.5	69.2	78.4	49.5	151.1	85.2
D_{H_2}/D_{CO_2}	14.7	70.5	19.2	31.5	24	37.8	22.6	23.5	39.3	18.5	30.1	33.1
D_{O_2}/D_{N_2}	3.3	10.2	3.2	5.5	3.3	6.2	3.3	3.4	3.9	3.2	4.8	3.8
D_{CO_2}/D_{N_2}	9.4	9.4	4.3	5.5	3.4	8.0	5.3	2.9	2.0	2.7	5.0	2.6
D_{CO_2}/D_{CH_4}	28	-	12.0	14.9	11.8	18	14.6	7.2	4.7	6.3	11.5	6.3

^a Expressed in 10^{-8} cm²/s.

Figure 5.13a represents the plot of $\ln D$ versus $1/v_f$ of *N*-substituted PBI. The R^2 values were > 0.7 for H_2 , N_2 , O_2 and CO_2 , respectively, except for CH_4 , where, R^2 was lower (0.66). These values of linear correlation coefficient were obtained after excluding the data for BzABPBI, which otherwise resulted in lowering these values. The relation could not be evaluated for all methylene trimethylsilyl substituted PBIs due to inability to estimate v_f . As could be seen from a plot of diffusion coefficient versus kinetic diameter of gases (Figure 5.13b), diffusion coefficient increased in the order of kinetic diameter. The correlation was excellent as the R^2 values were > 0.90 for all the *N*-substituted PBIs.

Variation in solubility and diffusivity coefficient indicated that after the substitution, diffusivity coefficient for a particular gas increased to a larger extent than the increase in solubility coefficient. In other words, substitutions were predominantly effective towards varying diffusivity coefficient. The extent of increase in diffusion coefficient was more significant for the cases of *4-tert*-butylbenzyl substitution, which led to increase in gas diffusivity for various gases by 43 - 118 folds for DBzPBI-I and 8 - 52 folds for DBzPBI-BuI; as compared to respective diffusivity values of parent PBI-I and PBI-BuI. On the other hand, methyl, *n*-butyl or methylene trimethylsilyl substitution led to 1.1 - 35.7 folds and 2.2 - 18.4 folds increase in gas diffusion coefficient for PBI-I and PBI-BuI, respectively. This increase in diffusivity was followed by decrease in diffusivity selectivity. The CO_2 based selectivities were decreased by just 50 - 60% in the case of *N*-substituted PBI-I, while it decreased by 10 - 80% for *N*-substituted PBI-BuI. It was noted that D_{O_2}/D_{N_2} in *N*-substituted PBI-I remained either same (as in DBPBI-I or DBzPBI-I) or increased by 1.4 - 3.1 times. The D_{H_2}/D_{CO_2} were also increased by 1.3 - 4.8 times in *N*-substituted PBI-I in comparison to parent PBI-I.

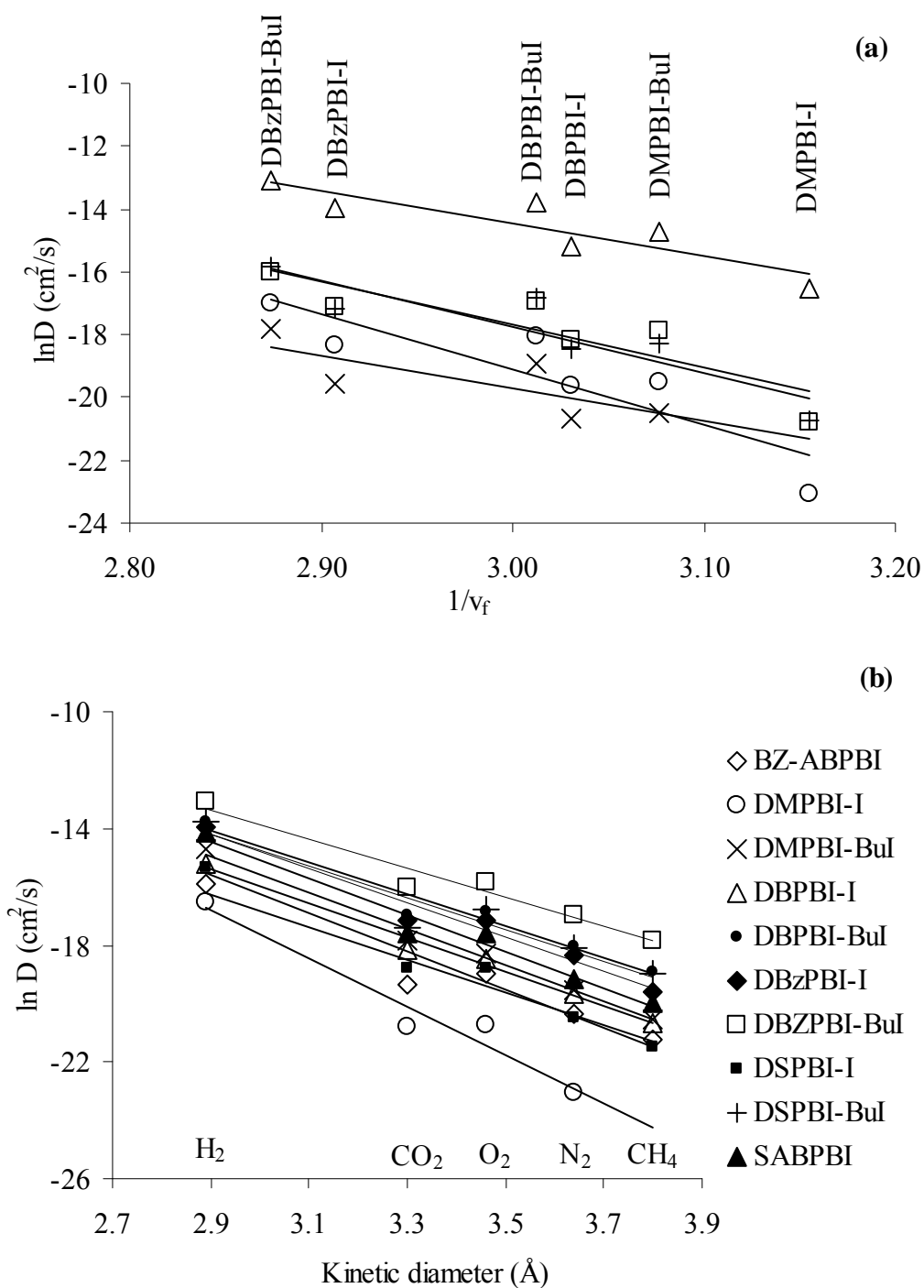


Figure 5.13. Correlation of Diffusion coefficient of gases in N -substituted PBI with (a) v_f (Δ : H₂, \circ : N₂, +: O₂, \times : CH₄, \square : CO₂) and (b) kinetic diameter of H₂, CO₂, O₂, N₂ and CH₄

Chapter 6

Investigations in polymeric forms of ionic liquids (PILs) based on polybenzimidazoles: Emphasis on CO₂ permeation properties

6.1. Synthesis

6.1.1. *N*-quaternization of PBI to obtain polymeric forms of ionic liquids (PIL)s

N-quaternization of PBI-I or PBI-BuI was done in a single step by in-situ formation of the Na-salt using NaH, followed by the addition of small excess of methyl iodide (4.2 molar equivalents). An immediate formation of a precipitate was observed at the ambient temperature, which slowly dissolved after the temperature was elevated to 80 °C and maintained for 24 h. This elevation of temperature to effect the dissolution was performed in order to ensure the complete substitution. Formed solution remained clear and homogeneous after the temperature was lowered to the ambient. It was then precipitated in a mixture of toluene and acetone. This mixture was needed to be used since partial solubility was observed in individual solvents viz., acetone, methanol and water; which otherwise could have been the obvious choices as the non-solvent. The obtained polymer after vacuum drying was purified by dissolving in a solvent (DMF/DMSO) and reprecipitation in the mixture of toluene and acetone. The yields of these reactions were > 90%. The percent substitution for *N*-quaternization reactions is discussed below for individual cases.

N-quaternization of ABPBI was needed to perform at 170 °C (rather than at 80 °C as in cases of PBI-I and PBI-BuI) using 1.1 molar equivalents of NaH in DMSO. It is known that ABPBI is insoluble in DMSO and could be dissolved only in acidic solvents such as methanesulfonic acid, sulfuric acid, phosphoric acid, polyphosphoric acid, etc. [Asensio (2005)]. A complete dissolution in DMSO could occur only after prolonged stirring at 170 °C for 5 h in presence of NaH. The solution remained homogeneous after cooling it to the ambient. This shows that the Na-salt formation itself needed harsher

conditions owing to the poor solubility of ABPBI in DMSO. This behaviour could be attributed to the rigid backbone of ABPBI. The addition of methyl iodide (2.2 molar equivalents) to thus formed Na-salt of ABPBI was done at 40 °C for 15 minutes. A precipitate was formed, which dissolved when the temperature was elevated to 80 °C and further maintained for 24 h in order to ensure complete substitution. The reaction mixture was cooled to the ambient temperature and then precipitated in the mixture of toluene and acetone. The yield of this reaction was ~ 80%.

6.1.2. Estimation of degree of substitution

¹H-NMR of PILs containing iodide as the counter ion are shown in Figure 6.1. It was noted that the peak for imidazole proton (N-H) was absent, which appeared at δ 13.2 in the case of unsubstituted PBI-I or PBI-BuI. Owing to insolubility of ABPBI in DMSO, its ¹H-NMR spectrum could not be recorded. Quantitative *N*-quaternization could also be supported based on the integration of the protons of methyl group appearing in the range δ 4.2 - 4.5. It was concluded that TMPBI-I-I and TMPBI-BuI-I were completely quaternized. The degree of substitution for DMABPBI-I was ~ 92% based on the integration of methyl protons. Upon magnification of the region δ 13 - 14.5 of its NMR spectrum (Figure 6.1) a small hump was noted at δ 13.9 ppm, attributable to protons of unreacted N-H groups. The integration of this peak amounts to about 7% of the total N-H group per repeat unit remained unreacted.

The purified quaternized PBI were estimated for iodide content by volumetric titration following the Volhard's method (Section 3.7). The iodide content thus estimated was correlated to the molar percent degree of substitution in the reaction of *N*-quaternized PBIs. TMPBI-I-I showed 98.8%, while TMPBI-BuI-I showed 98.5% substitution. These values are in good agreement with those obtained by ¹H-NMR analysis. Thus substitution reaction proceeded almost quantitatively in these two cases.

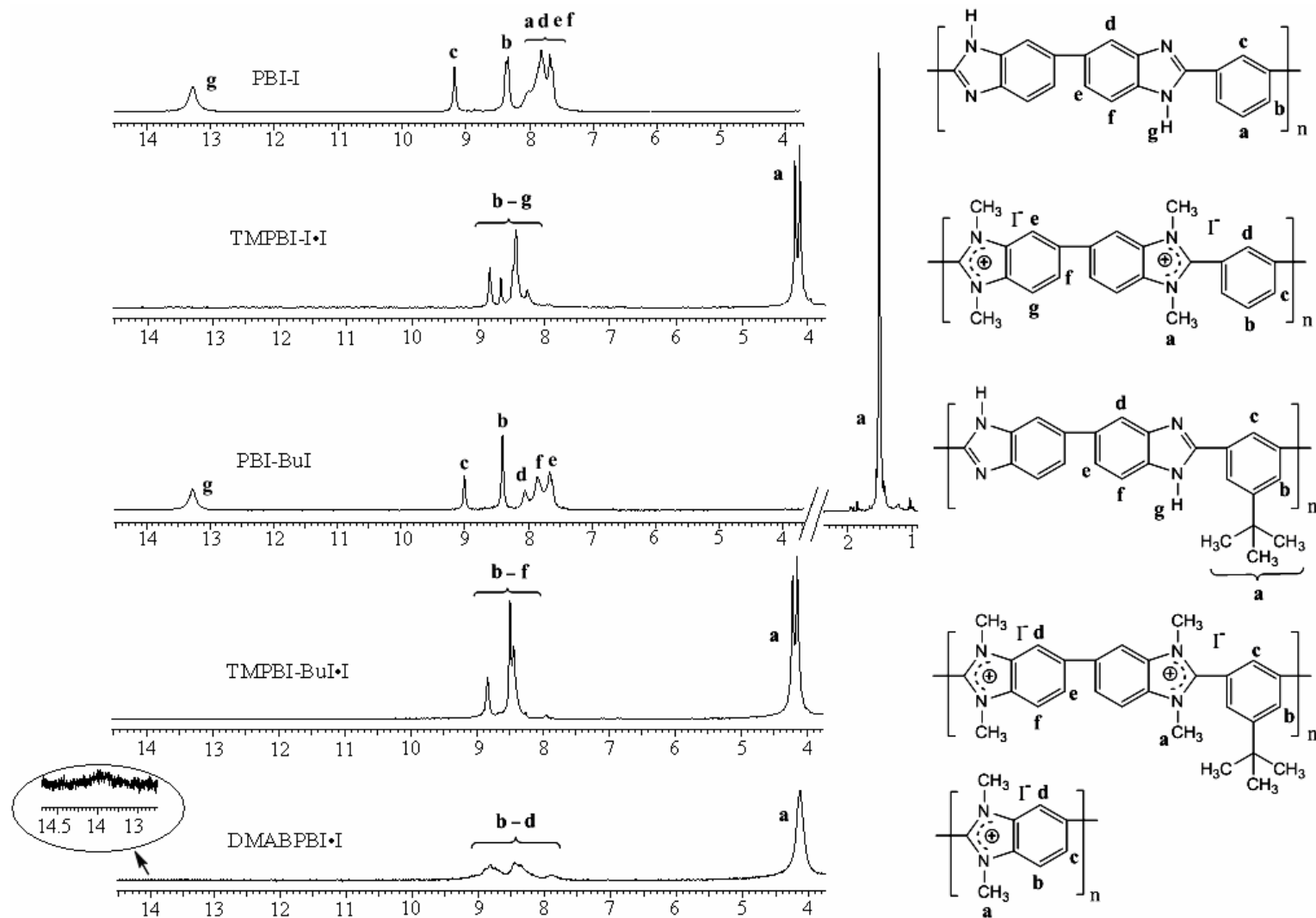


Figure 6.1. $^1\text{H-NMR}$ spectra of PILs

In the case of DMABPBI·I, degree of substitution by Volhard's method was found to be 118% (while, $^1\text{H-NMR}$ analysis showed 92% substitution). Since this value was higher than the theoretical value, repeated purification of DMABPBI·I by dissolution in DMF followed by reprecipitation in methanol was performed. The value still remained unchanged, and thus subsequent Soxhlet extraction using methanol: water mixture for 72 h was performed. Even after such rigorous processing, the iodide content was found to be stable at 118%. This surplus iodide than expected could have been originated from methyl iodide taken in excess during *N*-quaternization reaction.

6.1.3. Anion exchange

Exchange of iodide of all the *N*-quaternized PBIs (TMPBI·I·I, TMPBI·BuI·I and DMABPBI·I) by either BF_4^- or Tf_2N^- was performed at ambient. In case of BF_4^- -exchange reactions using AgBF_4 , visual observations based on immediate formation of AgI precipitate after the AgBF_4 addition provided an indication for the exchange. In view of polymeric nature of the cationic species, the reaction mixture was further stirred for 24 h in order to ensure maximum possible exchange. In the case of chloride replacement of poly[*p*-vinylbenzyltrimethyl ammonium chloride] by BF_4^- using NaBF_4 in acetonitrile, 5 molar equivalents of NaBF_4 was needed in order to achieve appreciable exchange of 95.3% [Bhole (2007c)]. Marcilla et al. (2004) reported that poly(*I*-vinyl-3-alkyl imidazolium) halides in water mixed with an excess of an aqueous solution of hydrophobic salts ($\text{CF}_3\text{SO}_3\text{Li}$, LiClO_4 , NaBF_4 , NaPF_6 , $(\text{CF}_3\text{SO}_2)_2\text{NLi}$, and $(\text{CF}_3\text{CF}_2\text{SO}_2)_2\text{NLi}$) resulted in precipitation of a new polymer as a result of the anion-exchange reaction [Marcilla (2004)]. In present case, AgBF_4 salt was chosen since there was only a little choice on manipulation of solvent (type and composition) based on the solubility of *N*-quaternized PBI containing iodide counter ion. With AgBF_4 , irreversible nature of reaction by virtue of AgI precipitate formation would assure complete exchange of anion. The yields of AgI precipitate were $\geq 95\%$ for all the cases. Besides this, none of the exchanged polymer (now containing BF_4^- anion) showed presence of any residual iodide in it when titrated with 0.01 M AgNO_3 solution. Thus, it could be concluded that all of the iodide was quantitatively exchanged by BF_4^- .

In case of exchange using Li- Tf_2N , the byproduct LiI was found to be soluble in the solution. The homogeneous solution after stirring for 24 h was poured on to the

stirred water to precipitate the polymer. Obtained polymer was collected on Buchner and repeatedly washed with water. The filtrate was analyzed for iodide content in it. This analysis showed that the exchange in case of TMPBI-I·Tf₂N, TMPBI-BuI·Tf₂N and DMABPBI·Tf₂N was 83%, 86% and 23%, respectively. The inability of quantitative exchange could be attributed to dissolved state of the byproduct LiI, which could be in equilibrium with PIL having Tf₂N⁻ as the counter ion. On the contrary, BF₄⁻ exchange was quantitative due to the formation of AgI precipitate. The equilibrium nature of this exchange reaction was further supported by the low exchange in case of DMABPBI·Tf₂N, though 1.2 molar equivalents of Li-Tf₂N was used. Owing to the lower exchange, this polymer was not used further.

6.2. Physical properties

6.2.1. Solvent solubility

The solvent solubility of these PBIs was evaluated with 1% (w/v) polymer concentration as a criterion and the results are summarized in Table 6.1. It is known that PBI has poor solvent solubility. PBI-I is soluble only in DMF, DMAc, DMSO and NMP [Iwakura (1964c), Lyoo (2000), Klaehn (2007)], while ABPBI is soluble only in acidic solvents like methanesulfonic acid, sulfuric acid, phosphoric acid and polyphosphoric acid [Asensio (2005)]. Though the backbone of PILs remained the same as that of PBI, the substitution by an alkyl group inducing ionic character and the presence of anion improved the organic solvent solubility of these PILs while retaining solubility in acids. Though most of the PILs were easily soluble in CH₃SO₃H, H₂SO₄ and H₃PO₄, those with iodide as the counter ion left an insoluble residue settling at the bottom of flask. The anion of PIL had its own effect on solubility. For example, all PILs with Tf₂N⁻ as a counter ion were freely soluble in polar aprotic solvents, viz. cyclohexanone, acetone and acetonitrile. PILs with BF₄⁻ and I⁻ though were insoluble in cyclohexanone and acetone, TMPBI-I·BF₄ and TMPBI-BuI·BF₄ were soluble in acetonitrile. PILs with iodide as the counter ion were partly soluble in CF₃COOH, while those with BF₄⁻ and Tf₂N⁻ anion were easily soluble in this solvent. *N*-quaternization of ABPBI rendered solubility in DMF, DMAc, DMSO and NMP. All these PILs were insoluble in common volatile solvents, viz., chloroform, tetrachloroethane, toluene and methanol.

Table 6.1. Solvent solubility of PILs

Solvent	DMF	DMAc	DMSO	NMP	Cyclo hexanone	Acetone	1,4- Dioxane	CH ₃ CN	HCOOH	CF ₃ COOH	CH ₃ SO ₃ H	H ₂ SO ₄	H ₃ PO ₄
TMPBI-I· I	±	±	++	++	-	-	-	-	++	±	SR	SR	SR
TMPBI-I· BF ₄	++	+	++	+	-	-	-	++	++	++	++	++	++
TMPBI-I· Tf ₂ N	++	++	++	++	++	++	±	++	++	++	++	++	+
TMPBI-BuI· I	++	±	++	++	-	-	±	-	++	±	SR	SR	SR
TMPBI-BuI· BF ₄	++	++	++	++	-	-	-	++	++	++	++	++	++
TMPBI-BuI· Tf ₂ N	++	++	++	++	++	++	-	++	++	++	++	++	+
DMABPBI· I	++	++	++	++	-	-	±	-	±	±	SR	SR	SR
DMABPBI· BF ₄	+	±	+	+	-	-	-	-	±	++	++	++	++

++: Soluble at ambient; +: Soluble after heating at 80 °C for 24 h; ±: Partially soluble or swelling after heating at reflux temperature; SR: Soluble with residue settling at the bottom of clear supernatant solution; -: Insoluble at reflux temperature.

6.2.2. Spectral characterizations and density

For all PILs, scanning FTIR at ambient temperature showed a broad peak at $\sim 3610\text{ cm}^{-1}$, attributable to the sorbed moisture (Figure 6.2a). However, the intensity of this peak was generally higher for PILs with iodide as the counter ion and was lower for those with hydrophobic BF_4^- or Tf_2N^- as the counter ion. This peak disappeared when the scans were recorded at $150\text{ }^\circ\text{C}$ as shown in Figure 6.2b. As a result of *N*-substitution, broad band present in unsubstituted PBI at $2400 - 3400\text{ cm}^{-1}$ originating from N-H stretching [Musto (1991, 1993), Hu (1993), Brook (1993)] disappeared. Peaks for benzimidazole in the range of $1500 - 1650\text{ cm}^{-1}$ attributable to C=C/C=N stretching vibrations (1612 cm^{-1}) as well as ring modes are characteristic of conjugation between benzene and imidazole ring [Musto (1993)]. These peaks were observed in present cases also. In case of PILs with BF_4^- as the counter ion, a peak at $\sim 1050\text{ cm}^{-1}$ was seen, which was attributed to the B-F stretching vibration [Suarez (1996), Yu (2006)]. On the other hand, for PILs with Tf_2N^- as the counter ion, peaks at $\sim 1330\text{ cm}^{-1}$ and 612 cm^{-1} were attributed to the asymmetric stretching and bending mode vibrations of sulfone group, respectively [Pennarun (2005)]. In these cases, a broad band at $1130 - 1240\text{ cm}^{-1}$ attributable to the symmetric stretching vibrations of C-F [Choi (1997), Pennarun (2005)] was also seen.

WAXD analysis of these PILs (Figure 6.3) indicated that all of them were amorphous in nature. Two prominent amorphous peaks in the ABPBI based PILs and PILs with Tf_2N^- as the counter ion were observed, indicating two different types of predominant chain packing arrangements in the polymer matrix. The *d*-spacing (d_{sp}) corresponding to the amorphous peak maxima in WAXD spectra are given in Table 6.2. The nature of anion exhibited its own effect on the d_{sp} of the PILs. The d_{sp} in a series of PIL based on a particular PBI increased in the order of variation in their anion as $\text{I}^- < \text{BF}_4^- < \text{Tf}_2\text{N}^-$. This follows the order of increasing number of atoms in the anion, thus the increasing volume. It could have been worth to estimate the fractional free volume of these PILs based on measured density [Van Krevelen (1997)], which could not be attempted due to unavailability of van der Waal's volume of these anions.

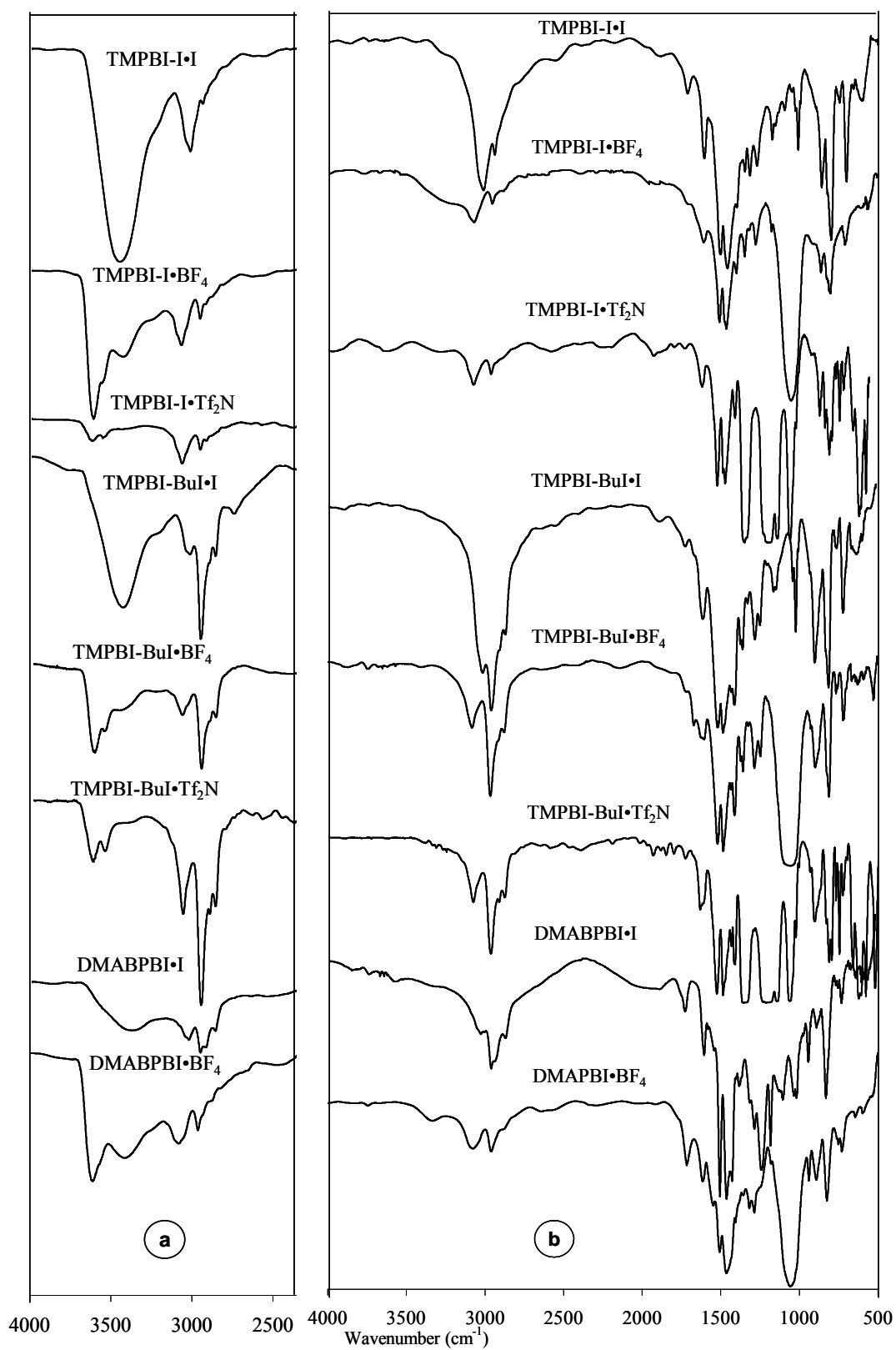


Figure 6.2. FT-IR spectra of PILs at (a) ambient and (b) 150 °C

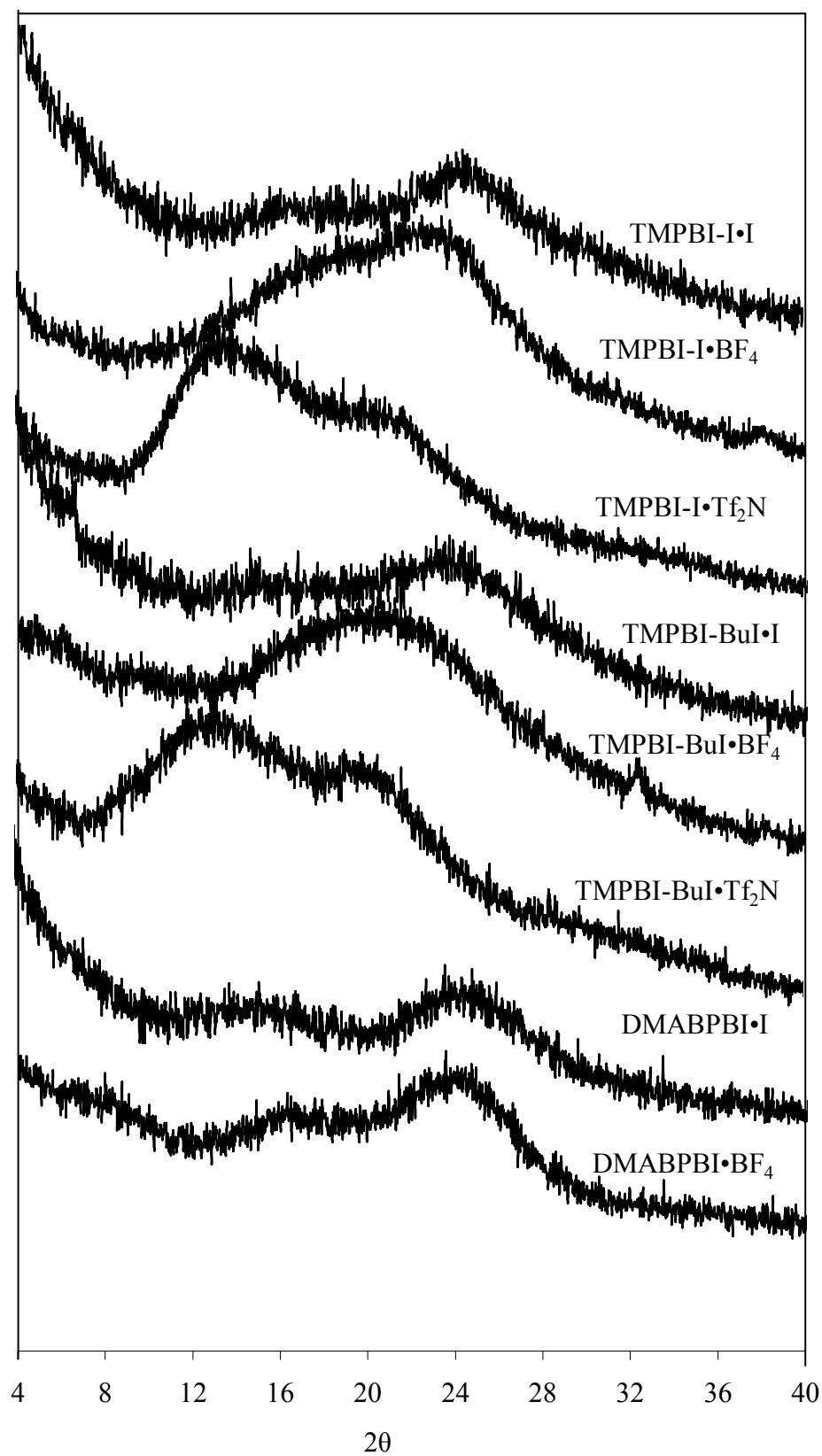


Figure 6.3. Wide angle X-ray diffraction spectra of PILs

Except for DMABPBI-I and ABPBI, density of all the PBIs was determined by floatation method. For DMABPBI-I, the density was highest in the series (Table 6.2) and appropriate solvent-pair with least solvent sorption in the polymer matrix for density determination could not be found. Thus, its density was determined using specific gravity bottle. Due to insolubility of ABPBI in organic solvents, fibrous ABPBI was used for its density determination by specific gravity bottle. In order to find the deviation between the density obtained by the above two methods, the density of PBI-I was determined following these methods. The density obtained using specific gravity bottle was 1.325 g/cm^3 , which is in good agreement with the one obtained by floatation method as 1.331 g/cm^3 .

Table 6.2. Physical properties of PILs

Polymer	$\eta_{\text{inh}}^{\text{a}}$ (dL/g)	d_{sp}^{c} (Å)	ρ^{d} (g/cm ³)	TGA analysis	
				IDT ^e (°C)	W ₉₀₀ ^f (%)
PBI-I	0.85	4.05	1.331	600	67
TMPBI-I·I	3.3	3.69, 5.54	1.598	340	48.2
TMPBI-I·BF ₄	3.3	3.75	1.397	372	43
TMPBI-I·Tf ₂ N	3.2	4.17, 6.91	1.569	460	32.7
PBI-BuI	1.0	4.04, 4.69	1.193	525	65
TMPBI-BuI·I	3.1	3.71	1.469	250	41.8
TMPBI-BuI·BF ₄	3.5	4.27	1.312	374	42
TMPBI-BuI·Tf ₂ N	3.4	4.48, 6.86	1.489	465	33.5
ABPBI	1.8 ^b	3.01	1.437	620	44.7
DMABPBI·I	4.4	3.66	2.023	215	34
DMABPBI·BF ₄	4.3	3.71, 5.44	1.486	325	49

^a: Inherent viscosity determined using 0.2 g/dL solution in DMSO at 35 °C; ^b: Inherent viscosity determined using 0.2 g/dL solution in conc. H₂SO₄ at 35 °C; ^c: *d*-spacing obtained from wide angle X-ray diffraction spectra; ^d: Density measured at 35 °C; ^e: Initial decomposition temperature; ^f: Char yield at 900 °C.

The densities of all PILs were higher than their parent unsubstituted PBIs. This could be attributed to the closer chain packing owing to ionic interactions and the presence of halides in the anion. Closer chain packing is qualitatively supported by the WAXD analysis, since the d_{sp} did not increase considerably inspite of added bulk of the anions. The density within a series of PIL (based on particular PBI) increased in the order of anion as $\text{BF}_4^- < \text{Tf}_2\text{N}^- \approx \text{I}^-$.

6.2.3. Solution viscosity

The inherent viscosity of PILs in the concentration range of 0.025 - 0.2 g/dL in DMSO was found to be larger than their parent PBIs (PBI-I and PBI-BuI). Due to insolubility of ABPBI in any of the organic solvents, its viscosity was measured in H_2SO_4 for the comparison. Dilute solutions of these PILs showed polyelectrolyte behavior. As could be seen from Figure 6.4, these PILs exhibited an increase in inherent viscosity with decreasing polymer concentrations. This abnormal behaviour of viscosity of polyelectrolytes is well known, attributable to the chain expansion at lower concentration [Fuoss (1948a, 1948b, 1948c) Eisenberg (1954), Yammanka (1990), Moinard (2005)]. When the polymer concentration decreases, the macroions expand like a rod with the increase of intramolecular repulsive forces. This increased intramolecular repulsive forces are due to weakening of the screening of the fixed charges on the macromolecules by counterions in the solution [Eisenberg (1954), Moinard (2005)]. Stretching and coil expansion due to the dilution of polymer solution are consequences in case of flexible polyelectrolytes [Fuoss (1948a), Eisenberg (1954), Yammanka (1990), Moinard (2005)]. Present cases of PILs based on rigid polybenzimidazoles also showed the polyelectrolyte effect. The rigid polyelectrolytes, which can not change their shapes significantly such as poly(*p*-phenylene) is also known to show the polyelectrolyte effect [Ballauff (2004)]. In case of poly(*p*-phenylene), this effect was caused by long-range electrostatic repulsion of the dissolved macroion rather than due to conformational changes [Ballauff (2004)]. Poly (N_1, N_3 -dimethylbenzimidazolium) salt (PBI quaternized by methyl iodide) is reported to show polyelectrolyte behavior in DMSO and the mixture of DMSO and water (1:1) [Hu (1993)]. In present case, parent unsubstituted PBIs (PBI-I, PBI-BuI) since are not charged, did not show polyelectrolyte effect as could be seen from Figure 6.4.

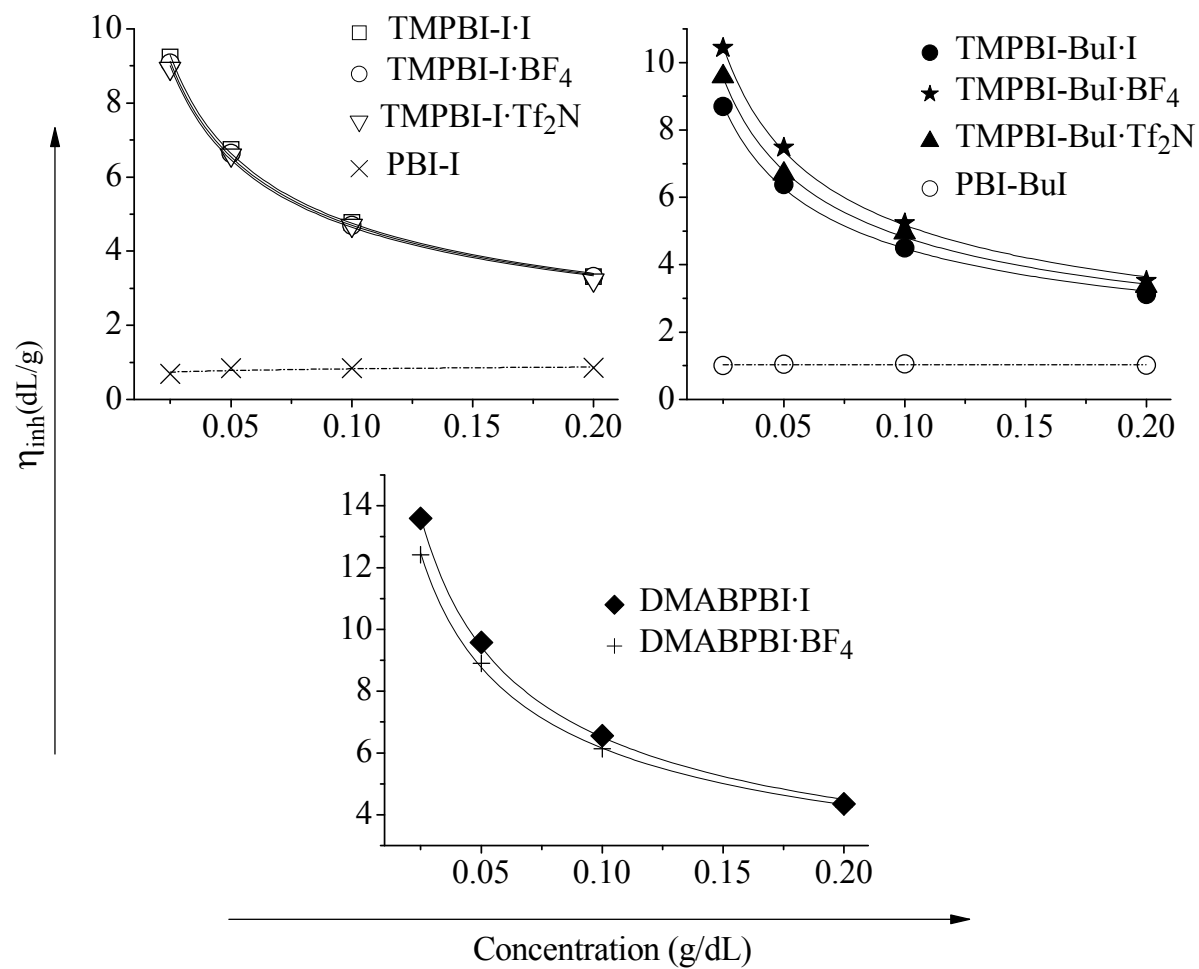


Figure 6.4. Viscosity of PILs as a function of polymer concentration in DMSO at 35 °C

Their inherent viscosity behaviour with concentration was linear. Since ABPBI is insoluble in DMSO, the viscosity with varying concentration could not be measured. It is known that unsubstituted PBI-I in acidic solvents such as H_2SO_4 [Neuse (1982)], HCOOH [Kojima (1980), Neuse (1982)] show polyelectrolyte effect. Thus viscosity of ABPBI in H_2SO_4 was not measured while varying concentrations. Furthermore, the inherent viscosity of PILs at varying concentration was also found to be proportional to the square root of polymer concentration (Figure 6.5) obeying the Fuoss Equation for polyelectrolytes [Fuoss (1948a), Bhowmik (2008)]

$$(\eta_{\text{inh}})^{-1} = \frac{1}{A} + \left(\frac{B}{A}\right)c^{0.5} \quad (6.1)$$

where, A and B are constants; η_{inh} and c are inherent viscosity and concentration of polymer in DMSO, respectively.

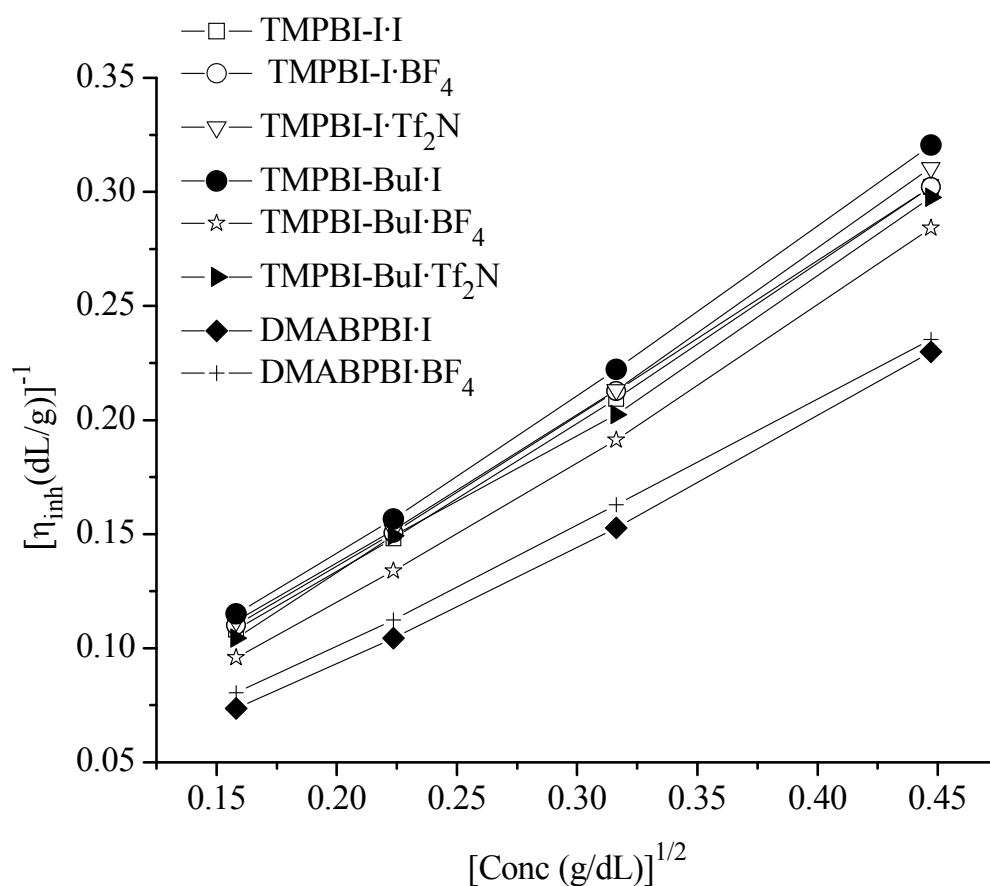


Figure 6.5. Fuoss plot of PILs in DMSO at 35 °C

6.2.4. Thermal properties

The nature of anion had a significant effect on the thermal stability of present PILs (Table 6.2). As also could be seen from thermograms (Figure 6.6), with the same polycation and varying the anion, thermal stability of PILs decreased following the order of anions as $\text{Tf}_2\text{N}^- > \text{BF}_4^- > \text{I}^-$. In the case of ionic liquids, thermal stability is known to depend on the nature of counter ion [Ngo (2000), Pringle (2003)]. In a study on thermal stabilities for several imidazolium based ionic liquids with varying anions viz. Tf_2N^- , BF_4^- , halide ions (Cl^- , Br^- , I^-), etc.; it was found that halide anions drastically reduced the thermal stability of ionic liquids than the other anions [Ngo (2000)]. Similarly, low molecular weight ionic liquids containing fluorinated anion Tf_2N^- showed higher thermal stability than the corresponding non-fluorinated bis(methanesulfonyl)amide anion [Pringle (2003)]. Thus, even though the present PILs exhibited lower thermal stability than their parent PBI, stability upto 465 °C was appreciable. Glass transition temperature of these PILs in DSC thermograms could not be detected even after repeated cycle of heating and cooling.

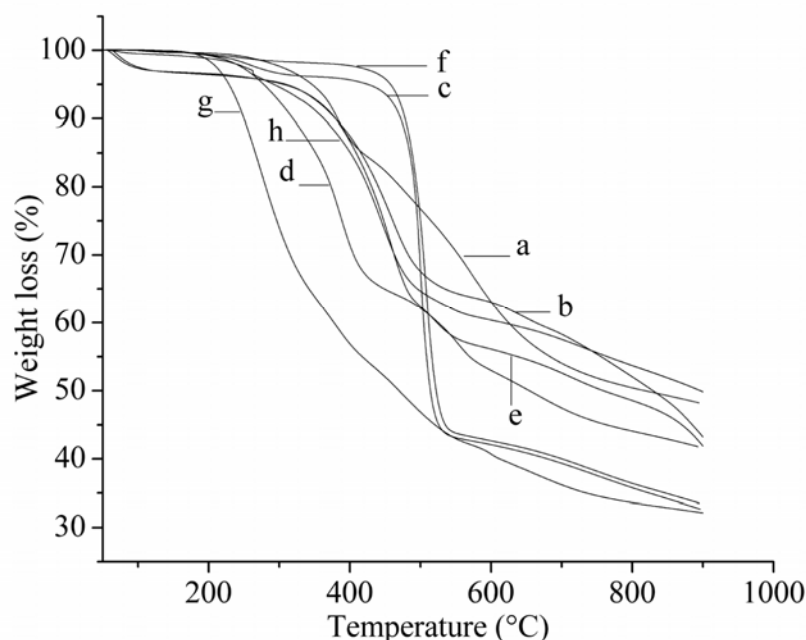


Figure 6.6. TGA spectra of PILs (a: TMPBI-I·I; b: TMPBI-I·BF₄; c: TMPBI-I·Tf₂N; d: TMPBI-BuI·I; e: TMPBI-I·BF₄; f: TMPBI-I·Tf₂N; g: DMABPBI-I·I; h: DMABPBI-I·BF₄)

6.3. Permeation properties

6.3.1. Sorption properties

Sorption isotherms for present PILs obtained at 35 °C using pure gases (H₂, N₂, CH₄ and CO₂) showed a typical dual-mode nature (Figure 6.7), as usually observed for glassy polymers and described by Equation 4.1. As seen from the Figure 6.7, sorption of different gases increased in the order: H₂ < N₂ < CH₄ < CO₂. This follows the trend of increasing order of inherent condensabilities of these gases (for example, critical temperature (T_c) increases in the order -239.85 °C < -146.95 °C < -82.45 °C < 31.05 °C for H₂, N₂, CH₄ and CO₂ respectively). In case of TMPBI-I and TMPBI-BuI based PILs, the CO₂ sorption was more when BF₄⁻ was the counter ion than that of I⁻ or Tf₂N⁻ as the counter ion. Sorption of other gases (H₂, N₂ and CH₄) for all these PILs varied in a narrow range. Their sorption in a series of PILs based on a particular PBI generally decreased in the order of anions as I⁻ > BF₄⁻ > Tf₂N⁻. After PIL formation of ABPBI, significant increase in the CO₂ sorption was observed, than that of other gases, which could be correlated to the possible increase in free volume because of added bulk of anions. ABPBI based PIL with Tf₂N⁻ as the counter ion could not be studied since the degree of exchange was low as given in Section 6.1.3.

The dual-mode sorption parameters k_D, C'_H and b were estimated by the non-linear regression analysis of experimentally determined gas sorption data at varying pressures upto 20 atm (Table 6.3). The Henry's solubility coefficient k_D, ascribed to the gas dissolution in rubbery state was lower for all the non-polar gases in these PILs indicating their glassy nature. The Langmuir affinity constant b is the ratio of rate constants of sorption and desorption processes [Schultze (1991)] and characterizes the sorption affinity for particular gas-polymer system [Kanehashi (2005)]. C'_H is the hole-filling constant, which presents the maximum amount of penetrant sorbed into microvoids or free volume of the glassy polymer matrix [Vieth (1976), Kanehashi (2005)]. Both, C'_H and b increased with the increasing order of gas condensabilities for any particular PIL. These parameters were significantly higher for CO₂ than that for other gases, especially for CH₄ for almost all the PILs studied.

PILs based on ABPBI showed a significant increase in C'_H for CO₂ and CH₄ than that of unsubstituted case. This was correlated to the significant increase in d_{sp}, which is

indicative of increased free volume. Unfortunately no quantitative information could be available about the packing density of these materials, especially on fractional free volume. The multiple peaks in WAXD spectra in these cases were not indicative enough.

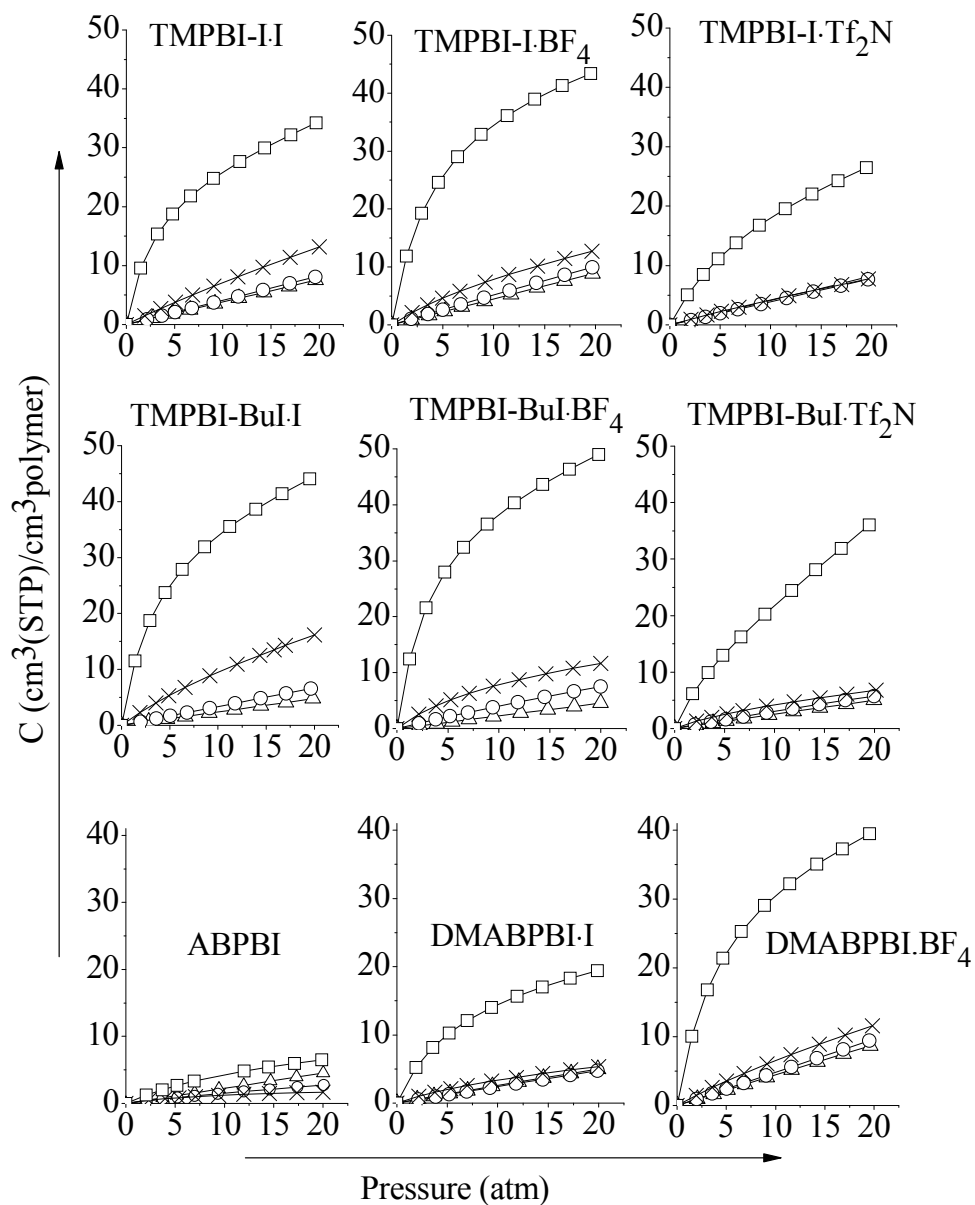


Figure 6.7. Sorption isotherms for PILs at 35 °C (Δ : H₂, \circ : N₂, \times : CH₄, \square : CO₂)

Table 6.3. Dual-mode sorption parameters^a

(a) Dual-mode sorption parameters for PBI-I based PIL									
Gas	TMPBI-I·I			TMPBI-I·BF ₄			TMPBI-I·Tf ₂ N		
	k _D	C' _H	b	k _D	C' _H	b	k _D	C' _H	b
H ₂	0.382	0.12	3.5x10 ⁻⁴	0.448	0.43	1.7x10 ⁻⁵	0.411	0.78	4.6x10 ⁻⁵
N ₂	0.412	0.81	1x10 ⁻⁴	0.454	3.37	0.022	0.390	1.17	7x10 ⁻⁴
CH ₄	0.494	7.01	0.045	0.360	8.55	0.099	0.317	2.81	0.06
CO ₂	0.236	34.81	0.238	0.414	45.56	0.250	0.521	23.0	0.126
(b) Dual-mode sorption parameters for PBI-BuI based PIL									
Gas	TMPBI-BuI·I			TMPBI-BuI·BF ₄			TMPBI-BuI·Tf ₂ N		
	k _D	C' _H	b	k _D	C' _H	b	k _D	C' _H	b
H ₂	0.240	0.63	3x10 ⁻⁵	0.228	0.176	4.8x10 ⁻⁴	0.253	0.18	3x10 ⁻⁴
N ₂	0.335	0.71	0.001	0.295	3.30	0.048	0.244	1.62	0.060
CH ₄	0.473	11.21	0.074	0.200	11.27	0.108	0.210	3.47	0.148
CO ₂	0.645	37.19	0.282	0.633	42.60	0.302	1.386	10.57	0.295
(c) Dual-mode sorption parameters for ABPBI based PIL									
Gas	ABPBI			MABPBI·I			MABPBI·BF ₄		
	k _D	C' _H	b	k _D	C' _H	b	k _D	C' _H	b
H ₂	0.226	0.761	1.2x10 ⁻⁴	0.213	1.575	4x10 ⁻²	0.443	4.06	7.7x10 ⁻⁵
N ₂	0.103	1.115	0.083	0.217	1.01	0.036	0.483	3.08	1x10 ⁻⁴
CH ₄	3x10 ⁻¹¹	2.566	0.0936	0.115	4.82	0.085	0.335	10.78	0.042
CO ₂	0.082	8.216	0.0731	0.223	19.33	0.172	0.448	37.7	0.224

^a k_D is expressed in cm³ (STP)/cm³ polymer. atm, C'_H is expressed in cm³ (STP)/cm³ polymer, while b is expressed in atm⁻¹.

Table 6.4 presents solubility coefficient and solubility selectivity at 20 atm. Except for PILs based on Tf_2N^- as anion, the solubility coefficient for CO_2 for other PILs was found to increase in comparison to the respective coefficient for parent unsubstituted PBIs (PBI-I, PBI-BuI and ABPBI). It could be seen that this increased CO_2 sorption led to increase in $S_{\text{CO}_2}/S_{\text{N}_2}$ in all the PILs. This increase was by 19 - 21% for PILs based on PBI-I; 61 - 66% for PILs based on PBI-BuI and 71 - 76% for PILs based on ABPBI. In other words, sorption of condensable gas CO_2 was increased to a larger extent than that of non-condensable gas, N_2 . This indicates promises of PILs in enhancing CO_2 sorption capacity. In cases of PBI-I based PILs, the $S_{\text{CO}_2}/S_{\text{CH}_4}$ selectivity increased only marginally due to simultaneous increase in CH_4 sorption. However, PBI-BuI based PILs showed considerable increase in $S_{\text{CO}_2}/S_{\text{CH}_4}$, inspite of very small variation in CO_2 solubility coefficient.

For ABPBI based PILs, solubility coefficient for all the gases increased than that for unsubstituted ABPBI. This was attributed to the decrease in chain packing density. The unsubstituted ABPBI has very low d_{sp} of 3.01 Å. After the PIL formation, an increase in d_{sp} (Table 6.2) suggested that added bulk of anion made the polymer chains to pack looser, which led to increase in the sorption of all the gases. This enhancement was comparatively larger for CO_2 (2.9 - 6 folds). This led to a large increase in $S_{\text{CO}_2}/S_{\text{N}_2}$ selectivity, while $S_{\text{CO}_2}/S_{\text{CH}_4}$ was slightly decreased, due to simultaneous increase in CH_4 sorption.

Table 6.4. Solubility coefficient (S)^a and solubility selectivity (S_A/S_B) of PILs

Solubility Coefficient	PBI-I	TMPBI-I·I	TMPBI-I·BF ₄	TMPBI-I·Tf ₂ N	PBI·BuI	TMPBI·BuI·I	TMPBI·BuI·BF ₄	TMPBI·BuI·Tf ₂ N	ABPBI	DMABPBI·I	DMABPBI·BF ₄
S_{H_2}	0.37	0.38	0.45	0.41	0.33	0.40	0.23	0.25	0.23	0.25	0.44
S_{N_2}	0.40	0.41	0.51	0.38	0.57	0.34	0.38	0.29	0.14	0.24	0.48
S_{CH_4}	0.45	0.66	0.64	0.39	1.04	0.81	0.58	0.34	0.08	0.27	0.58
S_{CO_2}	1.42	1.73	2.19	1.34	2.24	2.22	2.46	1.84	0.33	0.97	1.99
Solubility selectivity											
S_{H_2}/S_{N_2}	0.93	0.93	0.88	1.08	0.58	1.18	0.61	0.86	1.64	1.04	0.92
S_{H_2}/S_{CO_2}	0.26	0.23	0.21	0.31	0.15	0.18	0.09	0.14	0.70	0.26	0.22
S_{N_2}/S_{CH_4}	0.89	0.62	0.80	0.97	0.55	0.42	0.66	0.85	1.75	0.89	0.83
S_{CO_2}/S_{N_2}	3.53	4.22	4.29	3.53	3.93	6.53	6.47	6.34	2.36	4.04	4.15
S_{CO_2}/S_{CH_4}	3.16	2.62	3.42	3.44	2.15	2.74	4.24	5.41	4.13	3.59	3.43

^a Expressed in cm³ (STP)/cm³ polymer.atm.

6.3.2. Gas permeability and diffusivity

Permeability coefficient for H₂, N₂, CH₄ and CO₂ and ideal selectivities for various gas pairs are given in Table 6.5. *N*-quaternization of PBI led to an increase in gas permeability, the effect being more prominent for PBI-I than for PBI-BuI. For PBI-I based PILs, the gas permeability for light gases (He, H₂) was increased upto 17 folds and for heavy gases (N₂, CH₄ and CO₂) it was increased upto 78 folds than that of unsubstituted PBI-I. On the other hand, for PILs based on PBI-BuI, the increase in gas permeability was just upto 13 folds. This variation in permeability enhancement can be explained based on the higher initial v_f of PBI-BuI than that for PBI-I. After *N*-quaternization of PBI-BuI, bulk of added methyl group and anions may not be able to significantly loosen chain packing as they could do in case of PBI-I based PILs, owing to initial closely packed polymer backbone of PBI-I. The gas permeability data for ABPBI could not be generated since its membrane preparation from aprotic solvent could not be made possible. It is known that the films prepared using acid as the solvent exhibit considerable crystallinity [Sannigrahi (2006)]. Thus membrane preparation using methanesulfonic acid or formic acid could have been possible, crystallinity effects could not have been avoided. However, after PIL formation of ABPBI, gas permeability for DMABPBI-I for various gases was high enough to be recorded. The permeability for a given gas in DMABPBI·BF₄ was higher than that of its iodide counterpart owing to the bulk of the anion.

It can be seen from Table 6.5 that the nature of anion had a considerable effect on the gas permeability, which increased in the order of anions as $I^- < BF_4^- < Tf_2N^-$ for a particular series of PIL based on a PBI. Similar to gas sorption behavior, effect of anions towards increasing gas permeability than the parent PBI was predominant in case of PBI-I based PILs than for the PBI-BuI based PILs. This was due to the higher initial v_f of PBI-BuI than PBI-I, wherein, the effect of substituent methyl group and anion in disrupting the chain packing was predominant for the later cases. Among all anions, the effect of Tf₂N⁻ by virtue of its bulk was higher in increasing the gas permeability of PILs. For TMPBI-I·Tf₂N and TMPBI-BuI·Tf₂N, the gas permeability was increased by 17 - 78 folds and 1.7 - 13 folds as compared to PBI-I and PBI-BuI, respectively.

Table 6.5. Permeability coefficient (P)^a and permselectivity (P_A/P_B)^b of PILs

Permeability Coefficient	PBI-I	TMPBI-I-I	TMPBI-I-BF ₄	TMPBI-I-Tf ₂ N	PBI-BuI	TMPBI-BuI-I	TMPBI-BuI-BF ₄	TMPBI-BuI-Tf ₂ N	DMABPBI-I	DMABPBI-BF ₄
P _{He}	1.05	1.53	7.56	17.7	10.1	5.0	9.07	26	1.63	5.49
P _{H₂}	0.6	1.36	5.51	10.3	10.7	6.3	6.91	18.3	1.58	2.53
P _{N₂}	0.0048	0.003	0.048	0.35	0.06	0.06	0.20	0.78	0.0052	0.019
P _{CH₄}	0.0018	-	0.013	0.14	0.05	0.05	0.10	0.42	0.0025	0.012
P _{CO₂}	0.16	0.25	1.02	8.2	1.91	1.84	4.80	17.9	0.13	0.42
Permselectivity										
P _{He} /P _{H₂}	1.8	1.1	1.4	1.7	0.9	0.8	1.3	1.4	1.0	2.2
P _{He} /P _{N₂}	219	494	158	51	168	83	45	33	314	289
P _{He} /P _{CH₄}	583	-	582	126	202	100	91	62	652	458
P _{H₂} /P _{N₂}	125	439	115	29	178	105	35	24	304	133
P _{H₂} /P _{CH₄}	333	-	424	74	214	126	69	44	632	211
P _{H₂} /P _{CO₂}	3.8	5.4	5.4	1.3	5.6	3.4	1.4	1.0	12.2	6.0
P _{CO₂} /P _{N₂}	33	81	21	23	32	31	24	23	25	22
P _{CO₂} /P _{CH₄}	89	-	79	59	38	37	48	43	52	35
P _{N₂} /P _{CH₄}	2.7	-	3.7	2.5	1.2	1.2	2	1.9	2.1	1.6

^a: Determined at 20 atm upstream pressure, expressed in Barrer (1 Barrer = 10⁻¹⁰ cm³(STP).cm/cm².s.cm Hg); ^b: Ratio of pure gas permeability.

Table 6.6. Diffusivity coefficient (D)^a and diffusivity selectivity (D_A/D_B) of PILs

Diffusivity Coefficient	PBI-I	TMPBI-I·I	TMPBI-I·BF ₄	TMPBI-I·Tf ₂ N	PBI-BuI	TMPBI-BuI·I	TMPBI-BuI·BF ₄	TMPBI-BuI·Tf ₂ N	DMABPBI·I	DMABPBI·BF ₄
D_{H_2}	1.25	2.70	9.34	19.13	24.45	19.94	23.05	55.21	4.81	4.33
D_{N_2}	0.009	0.006	0.07	0.69	0.08	0.14	0.41	2.05	0.017	0.031
D_{CH_4}	0.003	-	0.02	0.27	0.04	0.04	0.13	0.94	0.007	0.015
D_{CO_2}	0.085	0.112	0.35	4.7	0.65	0.63	1.48	7.38	0.102	0.159
Diffusivity selectivity										
D_{H_2}/D_{N_2}	139	450	133	27.7	306	142	56.2	26.9	282.9	140
D_{H_2}/D_{CO_2}	14.7	24.1	27	4.1	37.6	31.7	15.6	7.5	47.2	27.2
D_{N_2}/D_{CH_4}	3.0	-	3.5	2.6	2.0	3.5	3.2	2.2	2.4	2.1
D_{CO_2}/D_{N_2}	9.4	18.7	5.0	6.8	8.0	4.5	3.6	3.6	6.0	5.1
D_{CO_2}/D_{CH_4}	28	-	17.5	17.4	16.3	15.8	11.4	7.9	14.6	10.6

^a Expressed in 10^{-8} cm²/s.

An increase in permeability though was associated with a decrease in selectivity in some cases, this decrease was not monotonous. Except for TMPBI-I-I, though He or H₂ based selectivities were decreased for all PILs, the decrease was more pronounced for Tf₂N⁻ based PILs. For TMPBI-I·Tf₂N and TMPBI-Bul·Tf₂N, He or H₂ based selectivities decreased upto 78% and 87% respectively, in comparison to the parent unsubstituted PBI. $P_{\text{CO}_2}/P_{\text{N}_2}$ was decreased by 3 - 28% in PBI-Bul based PILs, while PBI-I based PILs showed 11 - 36% decrease in CO₂ based selectivities ($P_{\text{CO}_2}/P_{\text{N}_2}$ and $P_{\text{CO}_2}/P_{\text{CH}_4}$). Comparatively smaller fall in CO₂ based selectivity can be explained based on preferred higher sorption of CO₂ in PILs as discussed in the Section 6.3.1. However for PBI-Bul based PILs, the $P_{\text{CO}_2}/P_{\text{CH}_4}$ was increased upto 26%.

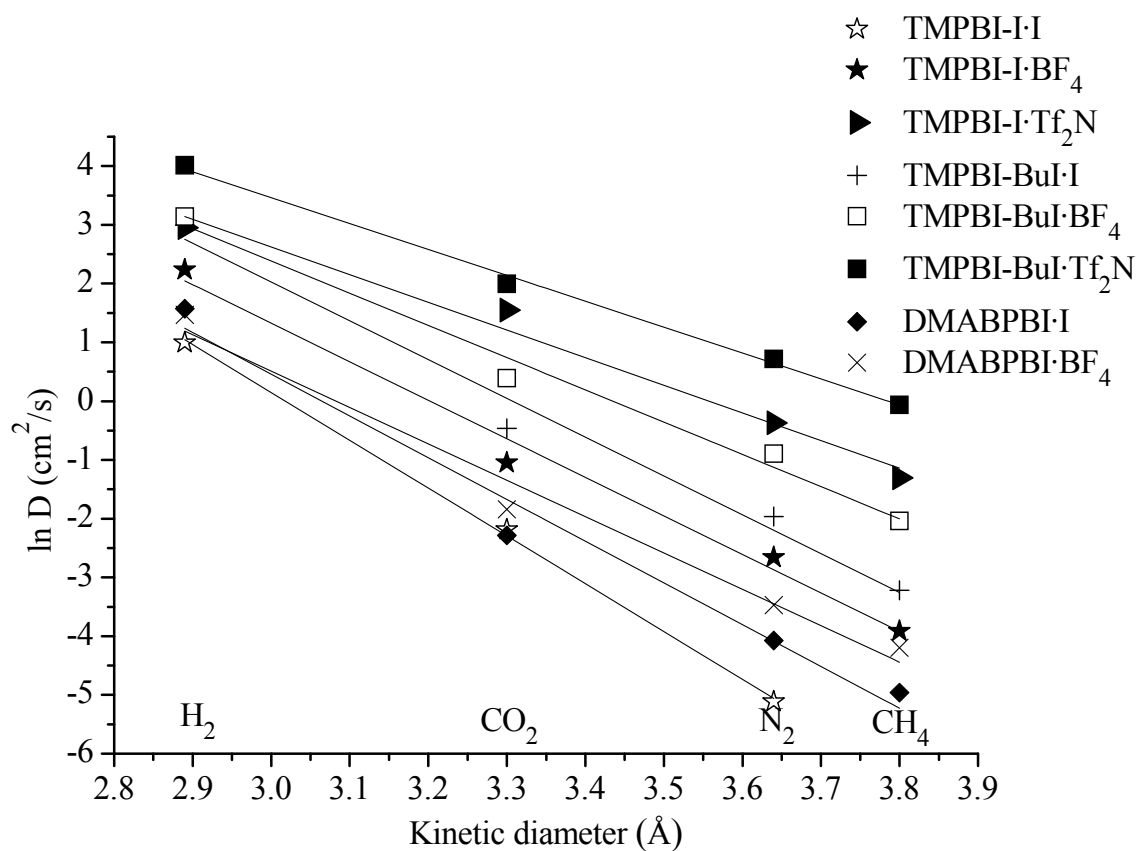


Figure 6.8. Correlation of diffusion coefficient with kinetic diameter (Å) of gases in PILs at 35 °C

The permeability coefficient for a particular gas along with its solubility coefficient at 20 atm was used to estimate diffusivity coefficient using Equation 6.2 and is tabulated in Table 6.6.

$$P_A = D_A S_A \quad (6.2)$$

Comparison of diffusivity and solubility coefficients with their parent PBIs showed that the former increased to a greater extent than the later. The diffusivity coefficient was found to increase in the order of anions $I^- < BF_4^- < Tf_2N^-$, same as that for permeability coefficient. As seen from the Figure 6.8, the diffusivity coefficient was found to correlate well with the kinetic diameter of gases. It can also be observed from Figure 6.8 that the diffusion coefficient for the Tf_2N^- based PILs was the highest. For PBI-I based PILs, the diffusion coefficient for light gas H_2 was increased by 2.2 - 15.3 folds and for N_2 , CH_4 and CO_2 , it was increased upto 90 folds as compared to PBI-I. However for PBI-BuI based PILs the diffusion coefficient for H_2 was slightly decreased and for N_2 , CH_4 and CO_2 , it was increased upto 25.6 folds as compared to PBI-BuI. The diffusivity selectivity D_{N_2}/D_{CH_4} was found to increase upto 17% for PBI-I based PILs and upto 75% for PBI-BuI based PILs. Significant decrease in H_2 based diffusivity selectivities (D_{H_2}/D_{N_2} , D_{H_2}/D_{CO_2}) was observed for PILs with Tf_2N^- as the counter ion. However, CO_2 based diffusivity selectivities showed marginal decrease.

From the comparison of diffusivity, solubility and permeability coefficients, it could be concluded that in general, after PIL formation, CO_2 based permeation properties were enhanced as compared to the parent unsubstituted PBIs. TMPBI-I· BF_4 and TMPBI-I· Tf_2N showed 6.4 and 51.3 folds increase in CO_2 permeability respectively. This was coupled with a small decrease in P_{CO_2}/P_{N_2} and P_{CO_2}/P_{CH_4} by 11 - 36% than that of PBI-I. Similarly, TMPBI-BuI· BF_4 and TMPBI-BuI· Tf_2N showed 2.5 and 9.4 times higher CO_2 permeability than the parent PBI-BuI. This was associated with a small decrease of ~ 28% in P_{CO_2}/P_{N_2} and upto 26% increase in P_{CO_2}/P_{CH_4} selectivities, as compared to the parent PBI-BuI. The effect of variation in counter ion towards enhancement of CO_2 permeation properties can also be seen from the placement of these PILs on Robeson's upper bound for P_{CO_2} versus P_{CO_2}/P_{CH_4} (Figure 6.9). This enhanced CO_2 permeation

characteristics depict the potentials of PBI based PILs to be used for CO₂ based separation.

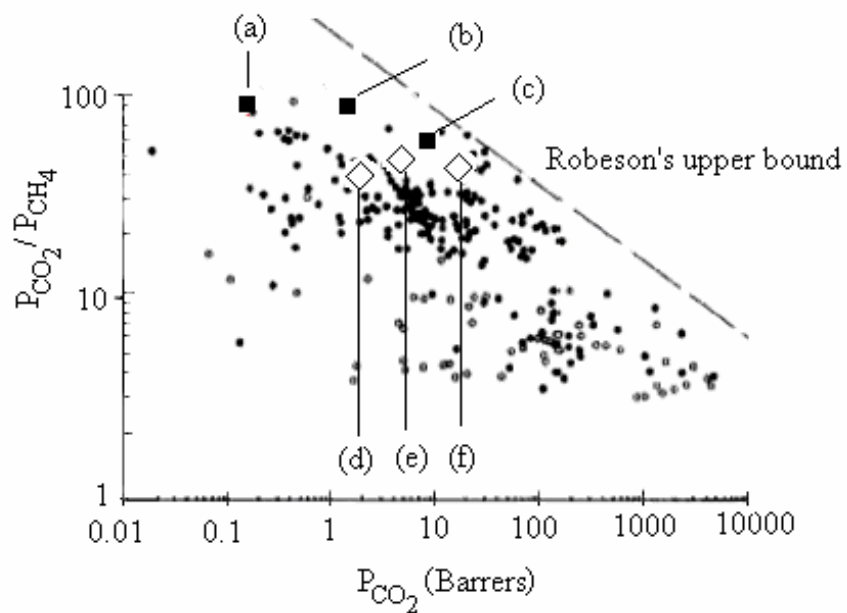


Figure 6.9. Occurrence of PBI-I based PILs(■) and PBI-BuI based PILs (□) on Robeson's plot [Robeson (1991)] (a) PBI-I; (b) TMPBI-I·BF₄; (c) TMPBI-I·Tf₂N; (d) PBI-BuI; (e) TMPBI-BuI·BF₄; (f) TMPBI-BuI·Tf₂N

Chapter 7

Conclusions

A series of polybenzimidazoles (PBI) were prepared based on 3,3'-diaminobenzidine (DAB) and substituted aromatic dicarboxylic acids. All PBIs were amorphous and exhibited high degradation temperature (> 400 °C). An introduction of *tert*-butyl group in PBI-BuI, hexafluoroisopropylidene group in PBI-HFA, bromine in PBI-BrT and PBI-DBrT enhanced solvent solubility of these PBIs. O₂ and H₂ permeability increased in the order: PBI-T < PBI-BrT < PBI-I < PBI-2,6Py < PBI-DBrT < PBI-BuI < PBI-HFA; while the $\alpha(\text{H}_2/\text{O}_2)$ selectivity followed almost a reverse order. Though the selectivity in substituted PBIs lowered than that of unsubstituted PBI-I, they were 2 - 3 times higher than the conventional gas separation materials like polyarylate and polysulfone. This observation put forth the need for further investigation on developing structure – gas property relationship in PBI family to draw an advantage of otherwise known excellent physical properties of PBI (thermochemical and mechanical stability) to be used as a gas separation membrane material.

Incorporation of hexafluoroisopropylidene or *tert*-butyl group in PBI led to a decrease in packing density (as revealed by increased d_{sp} and v_f), a small reduction in thermal stability and enhanced solvent solubility. Initial explorations on gas permeation properties of PBIs obtained with substituted acid moiety revealed that the bulky *tert*-butyl group in PBI-BuI and hexafluoroisopropylidene group in PBI-HFA led to the excellent combination of physical and gas permeation properties as compared to base case of PBI-I. For PBI-BuI and PBI-HFA, H₂ and O₂ permeability was increased by 16.9 - 40 times than that of PBI-I. Thus PBI-BuI and PBI-HFA were chosen for detailed investigation of gas sorption and permeation properties using gases of interest viz., H₂, He, N₂, O₂, CH₄ and CO₂.

A comparison of sorption properties of PBI-HFA or PBI-BuI with that of PBI-I showed that an increase in sorption of CO₂ and CH₄ was more than that for other gases. The predicted diffusivity coefficients of CO₂, N₂ and CH₄ in PBI-I correlated well with

fractional free volume and solubility parameter of polymers with regression coefficient of > 0.9 . The PBI-I permeability for CO_2 , N_2 and CH_4 were estimated from these predicted diffusivity and experimentally determined solubility.

For various gases, increase in permeability for PBI-HFA and PBI-BuI in comparison to PBI-I was 10 - 40 times, while reduction in selectivities for various gas pairs was 77% or less; which placed them near Robeson's upper bound. Solubility coefficients for PBI-I, PBI-BuI and PBI-HFA correlated well with the Lennard-Jones force constant (ϵ/κ) of gases and fractional free volume (v_f) of polymers. The diffusivity of various gases and H_2 and O_2 based diffusivity selectivity were increased. PBI-BuI possessed better diffusivity based selectivities than that for PBI-HFA, which holds additional flexibility due to the bridge position of HFA.

N-substitution of PBI-I (base case), PBI-BuI (bulky substitution) and ABPBI (rigid backbone) using selective alkyl groups led to enhanced solvent solubility, lowering in solution viscosity (due to elimination of H-bonding), density and thermal stability. The substitution by *4-tert*-butylbenzyl, methylene trimethylsilyl or *n*-butyl group on PBI-I and PBI-BuI rendered solubility even in chlorinated solvents (CHCl_3 and TCE). Permeability of various gases increased with general lowering in selectivity for various gas pairs. From the estimation of dual-mode sorption parameters, solubility and diffusivity coefficient it was revealed that the nature of PBI and the substituent used for *N*-substitution plays a crucial role in depicting permeation properties. Variation in T_g was more predominant in controlling sorption for various substituted PBI-I and PBI-BuI, while variation in v_f was more predominant in cases of ABPBI substitution.

In *N*-substituted PBI-I and PBI-BuI, decrease in gas sorption was ascribed to the decrease in C'_H , which could be correlated to the difference between glass transition temperature and experimental temperature ($T_g - 35$) °C. *N*-substitution of ABPBI led to substantial increase in gas sorption as well as diffusion, as a result of increased v_f . The solubility coefficients in all the *N*-substituted PBIs were found to correlate well with Lennard-Jones force constant (ϵ/k). The diffusivity coefficient for a particular gas increased to a larger extent than the increase in solubility coefficient. The effect of *4-tert*-butylbenzyl substitution was more significant than the methyl, *n*-butyl or methylene trimethylsilyl substitution for increasing the diffusivity, and thus permeability. A

remarkable increase in permeability for *N*-substituted PBI-I (3 - 129 times) than that of PBI-BuI (1.2-27 times) was attributed to the higher initial v_f of PBI-BuI. When compared with unsubstituted cases, both these substituted PBIs showed significant decrease in permselectivities based on He or H₂ upto 87% and modest decrease for CO₂ based selectivities of upto about 69% due to smaller increase in CO₂ permeability, in comparison to the increase in permeability for other gases. The diffusion coefficient and permeability coefficient was found to correlate well with physical properties such as kinetic diameter of gases and v_f of the polymers.

A novel class of film forming polymeric forms of ionic liquids (PILs) were synthesized by *N*-quaternization of PBIs and subsequent anion exchange of I⁻ with BF₄⁻ and Tf₂N⁻. TMPBI-I·Tf₂N⁻ and TMPBI-BuI·Tf₂N⁻ were easily soluble in polar aprotic solvents, viz. cyclohexanone, acetone and acetonitrile. Quaternization of ABPBI rendered solubility in DMF, DMAc, DMSO and NMP. All the PILs exhibited polyelectrolyte behaviour in solution, as typically observed for ionomers. The densities of all PILs were higher than their parent unsubstituted PBIs. Thermal stability of the PILs followed the trend of anions as Tf₂N⁻ > BF₄⁻ > I⁻.

The sorption of CO₂ was more in PILs with BF₄⁻ as the counterion than that of I⁻ or Tf₂N⁻ as the counter ion. This increase in CO₂ sorption led to an increase in S_{CO_2}/S_{N_2} selectivity by 19 - 21% for PILs based on PBI-I; 61 - 66% for PILs based on PBI-BuI and 71 - 76% for PILs based on ABPBI. Marginal increase in S_{CO_2}/S_{CH_4} for PBI-I based PILs and considerable increase for PBI-BuI based PILs was noted. However, for ABPBI based PILs the S_{CO_2}/S_{CH_4} was slightly decreased due to simultaneous increase in CH₄ sorption.

The diffusivity coefficient was increased to a greater extent than the solubility coefficient for various PILs, and increased in the order of anions as I⁻ < BF₄⁻ < Tf₂N⁻. The diffusivity coefficient was found to correlate well with the kinetic diameter of gases. The gas permeability increased with the order of anions of PILs as I⁻ < BF₄⁻ < Tf₂N⁻, similar to the order of d_{sp} of the corresponding PILs. The He or H₂ based selectivities were decreased significantly (upto 87%); while, CO₂ based selectivities showed marginal decrease (upto 36%) due to preferred CO₂ sorption in comparison to parent unsubstituted PBI. For PBI-BuI based PILs, the P_{CO_2}/P_{CH_4} was increased upto 26%. Though

substitution caused large increase in permeability of all gases, preferred CO₂ sorption in these PILs resulted in comparatively smaller decrease in CO₂ based selectivities, than that based on other gases. It was observed that the successive variation in anions made these PILs to lie near Robeson's upper bound. This enhanced CO₂ permeation characteristics without much reduction in thermal properties along with improved solvent solubility depicts the potential of PBI based PILs to be used for CO₂ based separation.

References

- Aaron D., Tsouris C., *Sep. Sci. Tech.*, **2005**, 40, 321-348.
- Adrova N.A., Koton M.M., Dubnova A.M., Moskvina Ye.M., Pokrovskii Ye.I., Fedorova Ye.F. *Vysokomol soyed.*, **1965**, 7, No. 2, 305 - 307.
- Al Marzouqi M.H., Abdulkarim M.A., Marzouk S.A., El-Naas M.H., Hasanain H.M., *Ind. Eng. Chem. Res.* **2005**, 44, 9273 - 9278.
- Ali S.H., Merchant S.Q., Fahim M.A., *Sep. Purif. Tech.*, **2002**, 27, 121 - 136.
- Anderson J.L., Dixon J.K., Brennecke J.F., *Acc. Chem. Res.*, **2007**, 40, 1208 - 1216.
- Ariza M.J., Jones D.J., Rozière J., *Desalination*, **2002**, 147, 183 - 189.
- Armor J.N., *Appl. Cat.*, **1989**, 49, 1 - 25.
- Asensio J.A., Borrós S., Gómez-Romero P., *J. Membr. Sci.*, **2004**, 241, 89 - 93.
- Asensio J.A., Gómez-Romero P., *Fuel Cells*, **2005**, 5, 336 - 343.
- Asensio J.A., Borros S., Gomez-Romero P., *J. Polym. Sci.; Part A: Polym. Chem.*, **2002**, 40, 3703-3710.
- Baker R.W., *Membrane Technology and Applications*, 2nd Ed., Wiley, New York, **2004**.
- Ballauff M., Blaul J., Guillaume B., Rehahn M., Traser S., Wittemann M., Wittmeyer P., *Macromol. Symp.*, **2004**, 211, 1 - 24.
- Banihashemi A., Fabbro D., Marvel C.S., *J. Polym. Sci., Part A-1*, **1969**, 7, 2293 - 2303.
- Banihashemi A., Kiaizadeh F., *Makromol. Chem.*, **1980**, 181, 325 - 331.
- Bara J.E., Gabriel C.J., Lessmann S., Carlisle T.K., Finotello A., Gin D.L., Noble R.D., *Ind. Eng. Chem Res.*, **2007a**, 46, 5380 - 5386.
- Bara J.E., Lessmann S., Gabriel C.J., Hatakeyama E.S., Noble R.D., Gin D.L., *Ind. Eng. Chem. Res.* **2007b**, 46, 5397 - 5404.
- Bara J.E., Gabriel C.J., Hatakeyama E.S., Carlisle T.K., Lessmann S., Noble R.D., Gin D.L., *J. Membr. Sci.*, **2008a**, 321, 3 - 7.
- Bara J.E., Lessmann S., Gabriel C.J., Hatakeyama E.S., Noble R.D., Gin D.L., *Ind. Eng. Chem. Res.*, **2008b**, 46, 5397 - 5404.
- Bara J.E., Hatakeyama E.S., Gabriel C.J., Zeng X., Lessmann S., Gin D.L., Noble R.D., *J. Membr. Sci.*, **2008c**, 316, 186 - 191.
- Barbari T.A., *J. Polym. Sci. Part B. Polym. Phys.*, **1997**, 35, 1737 - 1746.

Barbari T.A., Koros W.J., Paul D.R., *J. Polym. Sci., Part B: Polym. Phys.*, **1988**, 26, 729.

Barrer R.M., *Diffusion in and through solids*, Cambridge University Press, London **1951**.

Barrer R.M., *J Membr. Sci.*, **1984**, 18, 25 - 35.

Barrer R.M., *Trans Faraday Sci.*, **1939**, 35, 628 - 643.

Bates E.D., Mayton R.D., Ntai I., Davis J.H., *J. Am. Chem. Soc.*, **2002**, 124, 926 - 927.

Belohlav L.R., *Angew. Makromol. chemie.*, **1974**, 40, 465 - 483.

Benamor A., Aroua M.K., *Fluid Phase Equilibria*, **2005**, 231, 150 - 162.

Berens A.R., Hopfenberg H.B., *J. Membr. Sci.*, **1982**, 10, 283 - 303.

Berry G.C., Fox T.G., *Adv. Polym. Sci.*, **1968**, 5, 261 - 357.

Berthod A., Ruiz-Ángel M.J., Carda-Broch S., *J. Chromatogr. A*, **2008**, 1184, 6 - 18.

Bhide B.D., Voskericyan A., Stern S.A., *J. Membr. Sci.*, **1998**, 140, 27 - 49.

Bhole Y.S., Karadkar P.B., Kharul U.K., *Eur. Polym. J.*, **2007a**, 43, 1450 - 1459.

Bhole Y.S., Karadkar P.B., Kharul U.K., *J. Polym. Sci.; Part B: Polym. Phys.*, **2007b**, 45, 3156 - 3168.

Bhole Y.S., *Ph.D. dissertation*, **2007c**, University of Pune, India.

Bhowmik P.K., Kamatam S., Han H., Nedeltchev A.K., *Polymer*, **2008**, 49, 1748 - 1760.

Blanchard L.A., Hancu D., Beckman E.J., Brennecke J.F., *Nature*, **1999**, 399, 28 - 29.

Blasig A., Tang J., Hu X., Tan S.P., Shen Y., Radosz M., *Ind. Eng. Chem. Res.*, **2007a**, 46, 5542 - 5547.

Blasig A., Tang J., Hu X., Shen Y., Radosz M., *Fluid Phase Equilib.* **2007b**, 256, 75 - 80.

Blauwhoff P.M.M., Versteeg G.F., Van Swaaij W.P.M., *Chem. Eng. Sci.*, **1984**, 39, 207 - 225.

Bondi A., *J. Phys. Chem.*, **1964**, 68, 441 - 451.

Bonfanti C., Lanzini L., Roggero A., Sisto R., *J. Polym. Sci.; Part A: Polym. Chem.*, **1994**, 32, 1361 - 1369.

Bouchet R., Siebert E., *Solid State Ionics*, **1999**, 118, 287 - 299.

Brand R.A., Bruma M., Kellman R., Marvel C.S., *J. Polym. Sci. Polym. Chem. Ed.*, **1978**, 16, 2275 - 2284.

Bredesen R., Jordal K., Bolland O., *Chem. Engg. Proc.*, **2004**, 43, 1129 - 1158.

Breed L.W., Wiley J.C., *J. Polym. Sci. Polym. Chem. Ed.*, **1976**, 14, 83 - 92.

Brock T., Sherrington D.C., Tang H.G., *Polymer*, **1991**, 32, 353 - 357.

- Brock T., Sherrington D.C., *Polymer*, **1992**, 33, 1773 - 1777.
- Brooks N.W., Duckett R.A., Rose J., Ward I.M., *Polymer*, **1993**, 34, 4038 - 4042.
- Burrell H., Solubility parameter values, in Brandrup J. and Immergut E.H., (Eds.), *Polymer Handbook*, 2nd Ed., John Wiley, New York, **1975**, pp 338 - 340.
- Cabasso I., Yuan Y., Johnson F.E., *U.S. Patent*, **2005**, US 6987163.
- Cadena C., Anthony J.L., Shah J.K., Morrow T.I., Brennecke J.F., Maginn E.J., *J. Am. Chem. Soc.*, **2004**, 126, 5300 - 5308.
- Caja J., Dunstan T.D.J., Ryan D.M., Katovic, V, Proc. in Proceedings of the 12th International Symposium on Molten Salts, P. C. Trulove, H. C. De Long, G. R.Stafford, S. Dekai, Editors, **PV 99-41**, pp 150, *Electrochem. Soc. Proc. Ser.*, Pennington, NJ, **2000**
- Caja J., Dunstan T.D.J., May M., Krall H., Katovic, V Meet. Abstract, *Electrochem. Soc.*, **2006**, 602, 2024.
- Cao C., Wang R., Chung T.S., Liu Y., *J. Membr. Sci.*, **2002**, 209, 309 - 319.
- Caro J., Noack M., Kölsch P., Schäfer R., *Micro. Mesopor. Matr.*, **2004**, 38, 3-24.
- Carollo A., Quartarone E., Tomasi C., Mustarelli P., Belotti F., Magistris A., Maestroni F., Parachini M., Garlaschelli L., Righetti P.P., *J. Power Sources*, **2006**, 160, 175 - 180.
- Cassidy, P.E., *Thermally Stable Polymers*, Dekker, New York, **1980**.
- Chakraborty A.K., Astarita G., Bischoff K.B., *Chem. Eng. Sci.*, **1986**, 41, 997 - 1003.
- Chanda M., Rempel G.L., *React. Polym.*, **1989a**, 11, 165 - 176.
- Chanda M., Rempel G.L., *React. Polym.*, **1989b**, 27, 3237 - 3250.
- Chanda M., Rempel G.L., *React. Polym.*, **1990a**, 12, 83 - 94.
- Chanda M., Rempel G.L., *React. Polym.*, **1990b**, 13, 103-119.
- Chanda M., Odriscoll K.F., Rempel G.L., *React. Polym.*, **1987a**, 5, 157 - 169.
- Chanda M., Odriscoll K.F., Rempel G.L., *React. Polym.*, **1987b**, 7, 25 - 35.
- Chanda M., Rempel G.L., *React. Polym.*, **1991/1992**, 16, 29 - 39.
- Chanda M., Rempel G.L., *React. Polym.*, **1992**, 17, 159 - 174.
- Charati S.G., Houde A.Y., Kulkarni S.S., Kulkarni M.G., *J. Polym. Sci. Polym. Phys. Ed.*, **1991**, 29, 921 - 931.
- Chen H., Kovvali A.S., Sirkar K.K., *Ind. Eng. Chem. Res.*, **2000**, 39, 2447 - 2458.

Chen H., Obsuskovic G., Majumdar S., Sirkar K.K., *J. Membr. Sci.*, **2001**, 183, 75 - 88.

Chen N., Tien C-F., Patton S.M., Langsam M. Burgoyne W.F. *Polym. Mater. Sci. Eng.*, **1993**, 69, 161 - 163.

Chenevey E.C., Conciatori A.B., Chatham N.J., *US Patent*, **1969**, US 3433772.

Chern R.T., Sheu F.R., Jia L., Stannett V.T., Hopfenberg H.B., *J. Membr. Sci.*, **1987**, 35, 103 - 115.

Chern R.T., Provan C.N., *Macromolecules*, **1991**, 24, 2203 - 2207.

Chivers R.A., Moore D.R., *Polymer*, **1994**, 35, 110 - 116.

Choe E.-W, Choe D.D., *Polymeric Materials Encyclopedia*; Salamone J.C. (Ed.); CRC Press: New York, **1996**, Vol. 7, pp. 5619 - 5637.

Choe E.W., *J. Appl. Polym. Sci.*, **1994**, 53, 497 - 506.

Choi E.-J., Hill D.J., Kim K.Y., O'Donnell J.H., Pomery P.M., *Polymer*, **1997**, 38, 3669 - 3676.

Chowdhury G., Vujosevic R., Matsura T., Laverty B., *J. Appl. Polym. Sci.*, **2000**, 77, 1137 - 1143.

Chuang S.-W., Hsu S.L.-C., Liu Y.-H., *J. Membr. Sci.*, **2007**, 305, 353 - 363.

Chung T.S., Ren J., Wang R., Li D.F., Liu Y., Pramoda K.P., Cao C., Loh W.W., *J. Membr. Sci.*, **2003**, 214, 57 - 69.

Chung T.-S., A critical Review of Polybenzimidazoles in, *Polymer Reviews*, **1997**, 37, 277 - 301.

Coleman M.R., Koros W.J., *J. Membr. Sci.*, **1990**, 50, 285 - 297.

Coleman M.R., Koros W.J., *J. Polym. Sci.; Part B: Polym. Phys.*, **1994**, 32, 1915 - 1926.

Connell J.W., Hergenrother P.M., Smith J.G., *US Patent*, **1994**, US 5317078.

Connell J.W., Hergenrother P.M., Smith J.G., *US Patent*, **1996**, US 5554715.

Connell J.W., Hergenrother P.M., Smith J.G., *US Patent*, **1997**, US 5637670.

Costello L.M., Koros W.J., *J. Polym. Sci.; Part B: Polym. Phys.*, **1994**, 32, 701 - 713.

Cot L., Ayral A., Durand J., Guizard, Hovnanian N., Julbe A., Larbot A., *Solid State Sci.*, **2000**, 2, 313-334.

Dai Y., Guiver M.D., Robertson G.P., Kang Y.S., Lee K.J., Jho J.Y., *Macromolecules*, **2004**, 37, 1403 - 1410.

D'Alelio G.F., *US Patent*, **1963**, US 3763107.

Danesi P.R., Reichley-Yinger L., Rickert P.G., *J. Membr. Sci.*, **1987**, 31, 117-145.

Dang T.D., Arnold F.E., *US Patent*, **1994**, US 5312876.

Dawans F., Reichel B., Marvel C.S., *J. Polym. Sci., Part A*, **1964**, 2, 5005 - 5016.

de Sales J.A., Patrício P.S.O., Machado J.C., Silva G.G., Windmüller D., *J. Membr. Sci.*, **2008**, 310, 129 - 140.

Dortmundt, D. and K. Doshi, "Recent Developments in CO₂ Removal Membrane Technology," *UOP LLC*, Des Plaines, Illinois, **1999**.

Dudgeon C.D., Vogl O., *J. Polym. Sci. Polym. Chem. Ed.*, **1978**, 16, 1831 - 1852.

Dudley C.N., Schöberl B., Sturgill G.K., Beckham H.W., Rezac M.E., *J. Membr. Sci.*, **2001**, 191, 1 - 11.

Duval J.-M., Folkers B., Mulder M.H.V., Desgrandchamps G., Smolders C.A., *J. Membr. Sci.*, **1993**, 80, 189-198.

Edlund D.J., Pledger W.A., *J. Membr. Sci.*, **1993**, 77, 255-264.

Eisenberg H., Pouyet J., *J. Polym. Sci.*, **1954**, 13, 85 - 91.

Földes E., Fekete E., Karasz F.E., Pukanszky B., *Polymer*, **2000**, 41, 975 - 983.

Fortunato R., Afonso C.A.M., Reis M.A.M., Crespo J.G., *J. Membr. Sci.*, **2004**, 242, 197 - 209.

Foster R.T., Marvel C.S., *J. Polym. Sci.; Part A: Gen. Papers*, **1965**, 3, 417 - 421.

Fuoss R.M., *J. Polym. Sci.*, **1948a**, 3, 603 - 604.

Fuoss R.M., *J. Polym. Sci.*, **1948b**, 3, 602 - 603.

Fuoss R.M., Strauss U.P., *J. Polym. Sci.*, **1948c**, 3, 246 - 263.

Gabelman A., Hwang S.-T., *J. Membr. Sci.*, **1999**, 159, 61 - 106.

Garcia C., Tiemblo P., Lozano A.E., Abajo J., de la Campa J.G., *J. Membr. Sci.*, **2002**, 205, 73-81.

Gerber A.H., *J. Polym. Sci. Polym. Chem.*, **1973**, 11, 1703 - 1719.

Gerber A.H., *US Patent*, **1976**, US 3943125.

Ghosal K., Freeman B.D., *Polym. Adv. Tech.*, **1994**, 5, 673 - 697.

Ghosal K., Chern R.T., Freeman B.D., *Macromolecules*, **1996**, 29, 4360 - 4369.

Ghosal K., Chern R.T., *J. Membr. Sci.*, **1992**, 72, 91 - 97.

Ghosal K., Freeman B.D., *Polym. Adv. Tech.*, **1993**, 5, 673 - 697.

Gieselman M.B., Reynolds J.R., *Macromolecules* **1992**, 25, 4832 - 4834.

- Gieselman M.B., Reynolds J.R., *Macromolecules* **1993**, 26, 5633 - 5642.
- Glipa X., Haddad M.E., Deborah J.J., Rozière, *Solid State Ionics*, **1997**, 97, 323 - 331.
- Goldberg D.E., Genetic algorithms in search, optimization and machine learning, Addison-Wesley, Reading, MA **1989**.
- Gómez-Romeroa P., Asensio J.A., Borrós S., *Electrochimica Acta*, **2005**, 50, 4715 - 4720.
- Gordon B., Kumpf R.J., Painter P.C., *J. Polym. Sci.; Part A: Polym. Chem.*, **1988**, 26, 1689 - 1696.
- Gray, D.N., Rouch, L.L., Strauss, E.L., *Polym. Prepr.*, **1967**, 8, 1138.
- Gülmüs S.A., Yilmaz L., *J. Polym. Sci.; Part B: Polym. Phys.*, **2007**, 45, 3025 - 3033.
- Guo H., Zhu G., Li H., Zou X., Yin X., Yang W., Qiu S., Xu R., *Angew. Chem.*, **2006**, 45, 7053 - 7056.
- Gür T.M., *J. Membr. Sci.*, **1994**, 93, 283 - 289.
- Hacarlioglu P., Toppare L., Yilmaz L., *J Appl. Polym. Sci.*, **2003**, 90, 776 - 785.
- Hachisuka H., Takizawa H., Tsujita Y., Takizawa A., Kinoshita T., *Polymer*, **1991**, 32, 2382 - 2386.
- Hachisuka H., Tsujita Y., Takizawa A., Kinoshita T., *Polymer*, **1988**, 29, 2050 - 2055.
- Handa Y.P., Roovers J., Moulinie P., *J. Polym. Sci., Part B: Polym. Phys.*, **1997**, 35, 2355-2362.
- Hardy L., Espuche E., Seytre G., Stevenson I., *J. Appl. Polym. Sci.*, **2003**, 89, 1849 - 1857.
- He R., Li Q., Bach A., Jensen J.O., Bjerrum N.J., *J. Membr. Sci.*, **2006**, 277, 38 - 45.
- He Y., Inoue Y., *Polym. Int.*, **2000**, 49, 623 - 626.
- Hedberg F., Marvel C.S., *J. Polym. Sci. Polym Chem. Ed.*, **1974**, 12, 1823 - 1828.
- Hellums M.W., Koros W.J., Husk G.R., Paul D.R., *J. Membr. Sci.*, **1989**, 46, 93 - 112.
- Hensema E.R., Sena M.E.R., Mulder M.H.V., Smolders C.A. *Gas Sep. Purif.*, **1994**, 8, 149-160.
- Higgins J., Marvel C.S., *J. Polym. Sci. A-1*, **1970**, 8, 171 - 177.
- Hirayama Y., Kase Y., Tanihara N., Sumiyama Y., Kusukia Y., Haraya K., *J. Membr. Sci.*, **1999**, 160, 87 - 99.
- Hook R.J., *Ind. Eng. Chem Res.*, **1997**, 36, 1779 - 1790.

Houde A.Y., *Ph.D. dissertation*, **1991**, University of Pune, India.

Hu C.-C., Chang C.-S., Ruaan R.-C., Lai J.-Y., *J. Membr. Sci.*, **2003**, 226, 51 - 61.

Hu M., Pearce E., Kwei T.K., *J. Polym. Sci.; Part A: Polym. Chem.*, **1993**, 31, 553 - 561.

Hu X., Tang J., Blasig A., Shen Y., Radosz M., *J. Membr. Sci.*, **2006**, 281, 130 - 138.

Huang J., Zou J., Ho W.W.S., *Ind. Eng. Chem. Res.*, **2008**, 47, 1261 - 1267.

Imai Y., Uno K., Iwakura Y., *Makromol. Chem.*, **1965**, 83, 179 - 187.

Inbasekaran M.N., Mullins M.J., World Patent, **1993**, WO 9314071.

Ismail A.F., Lorna W., *Separ. Purif. Techn.*, **2002**, 27, 173 - 194.

Iwakura Y., Uno K., Imai Y., Fukui., *Makromol. Chem.*, **1964a**, 77, 41 - 50.

Iwakura Y., Uno K., Imai Y., *Makromol. Chem.*, **1964b**, 77, 33 - 40.

Iwakura Y., Uno K., Imai Y., *J. Polym. Sci. Part A-2*, **1964c**, 2605 - 2615.

Iwakura Y., Suginami-ku, Uno K., Imai Y., *US Patent*, **1967**, US 3313783.

Jadhav A.S., Jayarani P., Kulkarni S.S., Vernekar S.P., *US Patent*, **1997**, US 5606000.

Jayakody J.R.P., Chung S.H., Durantino L., Zhang H., Xiao L., Benicewicz B.C., Greenbauma S.G., *J. Electrochem. Soc.*, **2007**, 154, B242 - B246.

Jia M., Peinemann K.-V., Behling R.-D., *J. Membr. Sci.*, **1991**, 57, 289-292.

Joly C., Le Cerf D., Chappey C., Langevin D., Muller G., *Sepr. Purif. Tech.*, **1999**, 16, 47 - 54.

Jorgensen B.S., Young J.S., Espinoza B.F., *US Patent*, **2004**, US 0261616.

Jouanneau J., Mercier R., Gonon L., Gebel G., *Macromolecules*, **2007**, 40, 983 - 990.

Kalnin I.L., Breckenridge G.J., *US Patent*, **1978**, US 4113683.

Kane J., *Polym. Prep.*, **1990**, 31, 709 - 710.

Kanehashi S., Nagai K., *J. Membr. Sci.*, **2005**, 253, 117 - 138.

Karadkar P.B., Kharul U.K., Bhole Y.S., Badhe Y.B., Tambe S.S., Kulkarni B.D., *J. Membr. Sci.*, **2007**, 303, 244-251.

Karadkar P.B., *M.E. Thesis*, **2006**, Nagpur University, India.

Kawakami H., Anzai J., Nagaoka S., *J. Appl. Polym. Sci.*, **1995**, 57, 789 - 795.

Kawakami J.H., Muruganandam N., Brode G.L., *US Patent*, **1991**, US 5055114.

Kemperman A.J.B., Rolevink H.H.M., Bargeman D., van den Boomgaard Th., Strathmann H., *J. Membr. Sci.*, **1998**, 138, 43 - 55.

Kemperman A.J.B., Bargeman D., Boomgaard T., Strathmann H., *Sep. Sci. Technol.*, **1996**, 31, 2733-2762.

Kesting R.E., Fritzsche A.K., *Polymeric gas separation membranes*, Wiley, New York **1993**.

Kharul U.K., Kulkarni S.S., *Macromol. Chem. Phys.*, **1997**, 198, 1909 - 1919.

Kharul U.K., Kulkarni S.S., Kulkarni M.G., Houde A.Y., Charati S.G., Joshi S.G., *Polymer*, **1998**, 39, 2011 - 2022.

Kharul U.K., Kulkarni S.S., *Bull. Mater. Sci.*, **1994**, 17, 1071 - 1077.

Kharul U.K., Kulkarni S.S., *US Patent*, **2002**, US 6420511.

Khulbe K.C., Matsuura T., Lamarche G., Kim H.J., *J. Membr. Sci.*, **1997**, 135, 211 - 223.

Kim H.-S., Kim Y.-H., Ahn S.-K., Kwon S.-K., *Macromolecules*, **2003**, 36, 2327 - 2332.

Kim H.-J., Cho S.Y., An S.J., Eun Y.C., Kim J.-Y., Yoon H.-K., Kweon H.-J., Yew K.H., *Macromol. Rapid Comm.*, **2004**, 25, 894 - 897.

Kim T.H., Koros W.J., Husk G.R., O'Brien K.C., *J. Membr. Sci.*, **1988**, 37, 45 - 62.

Kim T.-H., Koros W.J., Husk G.R., *J. Membr. Sci.*, **1989**, 46, 43 - 56.

Kim T.-H., Lim T.-W., Lee J.-C., *J. Power Sources*, **2007a**, 172, 172 - 179.

Kim T.-H., Lim T.-W., Park Y.-S., Shin K., Lee J.-C., *Macromol. Chem. Phys.* **2007b**, 208, 2293 - 2302.

Kim T.-H., Kim S.-K., Lim T.-W., Lee J.-C., *J. Membr. Sci.*, **2008a**, 323, 362 - 370.

Kim T.-H., Eun Y.-C., Cho S.-Y., Kweon H.-J., *US Patent*, **2008b**, US 7388035.

Kim Y.-S., Yang S.-M., *Sep. Purif. Tech.*, **2000**, 21, 101 - 109.

Klaehn J.R., Luther T.A., Orme C.J., Jones M.G., Wertsching A.K., Peterson E.S., *Polym. Prep.*, **2005**, 46, 708 - 709.

Klaehn J.R., Luther T.A., Orme C.J., Jones M.G., Wertsching A.K., Peterson E.S., *Macromolecules*, **2007**, 40, 7487 - 7492.

Kojima T., *J. Polym. Sci., Polym. Phys. Ed.*, **1980**, 18, 1685 - 1695.

Kokelenberg H., Marvel C.S., *J. Polym. Sci., Part A-1*, **1970**, 8, 3199 - 3209.

Koros W.J., *J. Polym. Sci. Polym. Phys. Ed.*, **1985**, 23, 1611 - 1628.

Koros W.J., Fleming G.K., *J. Membr. Sci.*, **1993**, 83, 1 - 80.

Koros W.J., Mahajan R., *J. Membr. Sci.*, **2000**, 175, 181 - 196.

Korshak V.V., Rusanov A.L., Tugushi D.S., *Polymer*, **1984**, 25, 1539 - 1548.

- Korshak V.V., Gverdtsiteli I.M., Kipiani L.G., Tugushi D.S., *Polym. Sci. U.S.S.R.*, **1979**, 21, 133 - 138.
- Korshak V.V., Teplyakov M.M., Fedorova R.D., *J. Polym. Sci., Part A-1: Polym. Chem.*, **1971**, 9, 1027-1043.
- Kovacs H.N., Delman A.D., Simms B.B., *J. Polym. Sci.; Part A-1: Polym. Chem.*, **1968**, 6, 2103 - 2115.
- Kovvali A.S., Sirkar K.K., *Ind. Eng. Chem. Res.*, **2001**, 40, 2502 - 2511.
- Kovvali A.S., Sirkar K.K., *Ind. Eng. Chem. Res.*, **2002**, 41, 2287 - 2295.
- Kreuer K.D., Fuchs A.M. Ise., Spaeth M., Maier J., *Electrochim. Acta*, **1998**, 43, 1281-1288.
- Kulprathipanja, S., Neuzil R.W., Li N.N., *US Patent*, US 4740219, **1988**.
- Kumins C.A., Kwei T.K., Free-volume and other theories,, in Crank J. and Park G.S. (Eds.), *Diffusion in Polymers*, Academic Press, New York, **1968**, pp. 107.
- Leinonen S.-M., Sherrington D.C., *J. Chem. Res.*, **1999**, 572 - 573
- Levine H.H., *Encycl. Polym. Sci. Tech.*, **1969**, 11, pp 188.
- Li J.-L., Chen B.-H., *Sepr. Purif. Tech.*, **2005**, 41, 109 - 122.
- Li Q., Hjuler H.A., Bjerrum N.J., *J. Appl. Electrochem.*, **2001**, 31, 773 - 779.
- Li Q., He R., Jensen J.O., Bjerrum N.J., *Chem. Mater.*, **2003**, 15, 4896 - 4915.
- Li Q., He R., Jensen J.O., Bjerrum N.J., *Fuel cell*, **2004a**, 4, 147 - 159.
- Li Q., He R., Berg R.W., Hjuler H.A., Bjerrum N.J., *Solid State Ionics*, **2004b**, 168, 177 - 185.
- Lin H., Freeman B.D., Toy L., Bondar V., Gupta R., Pas S., Hill A., *ACS National Meeting Book of Abstracts*, **2004**, 228, Poly-447.
- Lin W.-H., Chung T.-S., *J. Membr. Sci.*, **2001**, 186, 183 - 193.
- Litynski J.T., Klara S.M., McIlvried H.G., Srivastava R.D., *Environmental International*, **2006**, 32, 128 - 144.
- Liu J.-F., Jönsson J. Å, Jiang G.-B., *Trends in Analytical Chemistry*, **2005**, 24, 20 - 27.
- Liu Y., Pan C.Y., Ding M.X., Xu J.P., *J. Appl. Polym. Sci.*, **1999**, 73, 521 - 526.
- Loeb and Sourirajan, *Advan. Chem. Ser.*, **1962**, 38, 117.
- Loría-Bastarrachea M.I., Aguilar-Vega M., *J. Appl. Polym. Sci.*, **2007**, 103, 2207 - 2216.

- Lu G.Q., Diniz da Costa J.C., Duke M., Giessler S., Socolow R., Williams R.H., Kreutz T., *J. Coll. Inter. Sci.*, **2007**, 314, 589 – 603.
- Lyoo W.S., Choi J.H., Han S.S., Yoon W.S., Park M.S., Ji B.C., Cho J., *J. Appl. Polym. Sci.*, **2000**, 78, 438 - 445.
- Mahajan R., Koros W.J., *Ind. Eng. Chem. Res.*, **2000**, 39, 2692 - 2696.
- Mandal B.P., Biswas A.K., Bandyopadhyay S.S., *Chem. Eng. Sci.*, **2003**, 58, 4137 - 4144.
- Marcilla R., Blazquez J.A., Rodriguez J., Pomposo J.A., Mecerreyes D., *J. Polym. Sci.; Part A: Polym. Chem.*, **2004**, 42, 208 - 212.
- Masuda T., Isobe E., Higashimura T., *J. Am. Chem. Soc.*, **1983**, 105, 7473 - 7474.
- McCaig M.S., Paul D.R., *Polymer*, **1999**, 40, 7209 - 7225.
- McGonigle E.-A., Liggat J.J., Pethrick R.A., Jenkins S.D., Daly J.H., Hayward D., *J. Polym. Sci.; Part B: Polym. Phys.*, **2004**, 42, 2916 - 2929.
- McHattie J.S., Koros W.J., Paul D.R., *Polymer*, **1991a**, 32, 840 - 850.
- McHattie J.S., Koros W.J., Paul D.R., *Polymer*, **1992**, 33, 1701 - 1711.
- McHattie J.S., Koros W.J., Paul D.R., *Polymer*, **1991b**, 32, 2618 - 2625.
- Mearns P., *J. Am. Chem. Soc.*, **1954**, 76, 3415 - 3422.
- Mecerreyes D., Grande H., Miguel O., Ochoteco E., Marcilla R., Cantero I., *Chem. Mater.*, **2004**, 16, 604-607.
- Meindersma G.W., Kuczynski M., *J. Membr. Sci.*, **1996**, 113, 285-292.
- Mi Y., Stern S.A., Trohalaki S., *J. Membr. Sci.*, **1993**, 77, 41 - 48.
- Michaels A.S., Bixler H.J., *J. Polym. Sci.*, **1961**, 50, 393 – 412
- Mikawa M., Nagaoka S., Kawakami H., *J. Membr. Sci.*, **2002**, 208, 405 - 414.
- Milford G.N., *US Patent*, **1983**, US 4394500.
- Mitsubishi K., Marvel C.S., *J. Polym. Sci., Part A*, **1965**, 1661 - 1663.
- Moinard D., Borsali R., Taton D., Gnanou Y., *Macromolecules*, **2005**, 38, 7105 - 7120.
- Moon S., Schwartz A.L., Hecht J.K., *J. Polym. Sci.; Part A-1: Polym. Chem.*, **1970**, 8, 3665 - 3666.
- Mulder M., *Basic principles of membrane technology*, Kluwer Academic Publisher, Dordrecht, **1998**.
- Mulvaney J.E., Marvel C.S., *J. Polym. Sci.*, **1961**, 50, 541 - 547.

Muruganandam N., Koros W.J., Paul D.R., *J. Polym. Sci.; Part B: Polym. Phys.*, **1987**, 25, 1999 - 2026.

Musto P., Wu L., Karasz F.E., MacKnight W.J., *Polymer*, **1991**, 32, 3 - 11.

Musto P., Karasz F.E., MacKnight W.J., *Polymer*, **1993**, 34, 2934 - 2945.

Nakajima H., Ohno H., *Polymer*, **2005**, 46, 11499 - 11504.

Nakajima T., Marvel C.S., *J. Polym. Sci. ; Part A-1 : Polym. Chem.*, **1969**, 7, 1295 - 1298.

Narayan T.V.L., Marvel C.S., *J. Polym. Sci.; Part A-1: Polym. Chem.*, **1967**, 5, 1113 - 1118.

Neuse E., *Adv. Polym. Sci.*, **1982**, 47, 1 - 42.

Neuse E.W., Horlbeck G., *Polym. Eng. Sci.*, **1977**, 17, 821 - 827.

Neuse E.W., Loonat M.S., *Macromolecules*, **1983**, 16, 128 - 136.

Ngo H.L., LeCompte K., Hargens L., McEwen A.B., *Thermochimica Acta*, **2000**, 357/358, 97 - 102.

Nunes S.P.N., Peinemann K.V., *Membrane technology in the chemical industry*, Wiley-VCH, Weinheim, New York, **2001**.

Ohashi H., Ohya H., Aihara M., Negishi Y., Semenova S.I., *J. Membr. Sci.*, **1998**, 146, 39-52.

Ohfuji Y., Eguchi T., *US Patent*, **1972**, US 3655632.

Ohno H., Yoshizawa M., Ogihara W., *Electrochim. Acta*, **2004**, 50, 255 - 261.

Olivier-Bourbigou H., Magna L., *J. Mol. Cat. A: Chem.*, **2002**, 182/183, 419 – 437

Pace R.J., Datyner A., *J. Polym. Sci. Polym. Phys. Ed.*, **1979**, 17, 437 - 451.

Paul D.R., Koros W.J., *J. Polym. Sci., Polym. Phys. Ed.*, **1976**, 14, 675 - 685.

Paul D.R. and Yampol'skii Y.P., *Polymeric gas separation membranes*, CRC Press, Boca Raton, FL, **1993**.

Pennarun P.-Y., Jannasch P., *Solid State Ionics*, **2005**, 176, 1849 - 1859.

Peron J., Ruiz E., Jones D.J., Rozière J., *J. Membr. Sci.*, **2008**, 314, 247 - 256.

Pesiri D.R., Jorgensen B., Dye R.C., *J. Membr. Sci.*, **2003**, 218, 11 - 18.

Pessan L.A., Koros W.J., *J. Polym. Sci.; Part B: Polym. Phys.*, **1993**, 31, 1245 - 1252.

Petropoulos J.H., *J. Polym. Sci. Part A-2*, **1970**, 8, 1797 - 1801.

Pez G.P., Carlin R.T., Laciak D.V., Sorensen J.C., *US Patent*, **1988**, US 4761164.

Phillips, M.A., *J. Chem. Soc.*, **1930**, 1409- 1419.

Pinnau I., He Z., Morisato A., *J. Membr. Sci.*, **2004**, 241, 363 - 369.

Pixton M.R., Paul D.R., *Macromolecules*, **1995a**, 28, 8277 - 8286.

Pixton M.R., Paul D.R., *J. Polym. Sci.; Part B: Polym. Phys.*, **1995b**, 33, 1353 - 1364.

Plummer L., Marvel C.S., *J. Polym. Sci., Part A*, **1964**, 2, 2559 - 2569.

Polotskaya G.A., Acranova S.A., Cazdina N.V., Kuznetsov Y.P., Nesterov V.V., *J. Appl. Polym. Sci.*, **1996**, 62, 2215 - 2218.

Polotskaya G.A., Agranova S.A., Antonova T.A., Elyashevich G.K., *J. Appl. Polym. Sci.*, **1997**, 66, 1439 - 1443.

Prince A.E., Ridge B.N.J., *US Patent*, **1970a**, US 3551389.

Prince A.E., Ridge B.N.J., *US Patent*, **1970b**, US 3509108.

Pringle J.M., Golding J., Baranyai K., Forsyth C.M., Deacon G.B., Scott J.L., MacFarlane D.R., *New J. Chem.*, **2003**, 27, 1504 - 1510.

Pu H., Liu G., *Polym. Int.*, **2005**, 54, 175 - 179.

Pu H., *Polym. Int.*, **2003**, 52, 1540 - 1545.

Qing S., Huang W., Yan D., *Eur. Polym. J.*, **2005a**, 41, 1589 - 1595.

Qing S., Huang W., Yan D., *J. Polym. Sci.; Part A: Polym. Chem.*, **2005b**, 43, 4363.

Qing S., Huang W., Yan D., *React. Funct. Polym.*, **2006**, 66, 219 - 227.

Quinn R., Appleby J.B., Pez G.P., *J. Membr. Sci.*, **1995**, 104, 139 - 146.

Ramachandran N., Aboudheir A., Idem R., Tontiwachwuthikul P., *Ind. Eng. Chem Res.*, **2006**, 45, 2608 - 2616.

Raucher D., Sefcik M.D., *ACS Symp.*, **1983**, Ser. No. 223, pp 11.

Reddy T.A., Srinivasan M., *J. Polym. Sci.; Part A: Polym. Chem.*, **1988**, 26, 1051 - 1061.

Reimers M.J., Cibulsky M.J., Barbari T.A., *J. Polym. Sci.; Part B: Polym. Phys.*, **1993**, 31, 537-543.

Robeson L.M., *J. Membr. Sci.*, **1991**, 62, 165 - 185.

Roszbach V., Oberlein G., *Thermostable polyheterocyclics in: Handbook of Polymer Synthesis*, Kricheldorf H.R. (Eds), Marcel Dekker, New York, **1991**, pp. 1197 - 1280.

Sada E., Kumazawa H., Xu P., Nishigaki M., *J. Membr. Sci.*, **1988**, 37, 165 - 179.

Sada E., Kumazawa H., Xu P., *J. Membr. Sci.*, **1987**, 35, 117 - 122.

- Saegusa Y., Horikiri M., Nakurmura S., *Macromol. Chem. Phys.*, **1997**, 198, 619 - 625.
- Sannigrahi A., Arunbabu D., Murali Sankar R., Jana T., *J. Phy. Chem. B*, **2007**, B 111, 12124 - 12132.
- Sannigrahi A., Arunbabu D., Jana T., *Macromol. Rapid Comm.*, **2006**, 27, 1962 - 1967.
- Sartori G., Savage D.W., *Ind. Eng. Chem Res.*, **1983**, 22, 239 - 249.
- Scariah K.J., Krishnamurthy V.N., and Rao K.V.C., *J. Polym. Sci.; Part A: Polym. Chem.*, **1987**, 25, 2675 - 2687.
- Schild H.G., Kolb E.S., Mehta P.G., Ford M., Gaudiana R.A., *Polymer*, **1994**, 35, 1222-1228.
- Scholes C.A., Kentish S.E., Stevens G.W., *Recent Patents on Chem. Eng.*, **2008**, 1, 52-66.
- Schultze J.D., Zhou Z., Springer J., *Die Angewandte Makromolekulare Chemie*, **1991**, 185/186, 265 - 274.
- Scovazzo P., Kieft, J., Finan D.A., Koval C., DuBois D., Noble R., *J. Membr. Sci.*, **2004**, 238, 57 - 63.
- Scurto A.M., Aki S.N.V.K., Brennecke J.F., *J. Am. Chem. Soc.*, **2002**, 124, 10276 - 10277.
- Sefcik M.D., Schaefer J., May F.L., Raucher D., Dub S.M., *J. Polym. Sci. Polym. Phys. Ed.*, **1983**, 21, 1041 - 1054.
- Seymour R.B., Carraher Jr. C.E., *Structure property relationship in polymers*, Plenum press, New York, **1984**.
- Smid J., Albers J.H.M., Kusters A.P.M., *J. Membr. Sci.*, **1991**, 64, 121-128.
- Spillman R.W, Economics of gas separation membranes, *Chem. Eng. Prog.*, **1989**, 85, 41 - 62.
- Srinivasan P.R., Mahadevan V., Srinivasan M., *J. Polym. Sci. Polym. Chem.*, **1982**, 20, 3095 - 3105.
- Staudt-Bickel C., Koros W.J., *J. Membr. Sci.*, **1999**, 155, 145 - 154.
- Sterescu D.M., Bolhuis-Versteeg L., Van der Vegt N.F.A., Stamatialis D.F., Wessling M., *Macromol. Rapid Comm.*, **2004**, 25, 1674 - 1678.
- Stern S.A., Industrial Applications of Membrane Processes: The Separation of Gas Mixtures, in *Membrane Processes for Industry*, Proceedings of the Symposium, Southern Research Institute, Birmingham, AL, pp. 196 - 217, **1966**.

Stern S.A., Mullhaupt J.T., Gareis P.J., *AIChE J.*, **1969**, 15, 64 - 73.

Stern S.A., Frisch H.L., *Ann. Rev. Mater. Sci.*, **1981**, 11, 523

Stern S.A., Saxena V., *J. Membr. Sci.*, **1980**, 7, 47 - 59.

Stern S.A., Mi Y., Yamamoto H., St. Clair A.K., *J. Polym. Sci. Polym. Phys. Ed.*, **1989**, 27, 1887 - 1909.

Stern S.A., Mauze G.R., Frisch H.L., *J. Polym. Sci.: Polym. Phys. Ed.*, **1983**, 21, 1275 - 1298.

Stern S.A., *J. Membr. Sci.*, **1994**, 94, 1 - 65.

Stern S.A., Gareis P.J., Sinclair T.F., Mohr P.H., *J. Appl. Polym. Sci.*, **1963**, 7, 2035 - 2051.

Story B.J., Koros W.J., *J. Appl. Polym. Sci.*, **1991**, 42, 2613 - 2626.

Story B. J., Koros W.J., *J. Membr. Sci.*, **1992**, 67, 191 - 210.

Strathman H., Membrane separation process, *J. Membr. Sci.*, **1981**, 9, 121 - 189.

Suarez P.A.Z., Dullius J.E.L., Einloft S., De Souza R.F., Dupont J., *Polyhedron*, **1996**, 15, 1217 - 1219.

Takeuchi H., Takahashi K., Goto W., *J. Membr. Sci.*, **1987**, 34, 19 - 31.

Tanaka K., Okano M., Toshino H., Kita H., and Okamoto K-I., *J. Polym. Sci.; Part B: Polym. Phys.*, **1992**, 30, 907 - 914.

Tanaka K., Islam Md. N., Kido M., Kita H., Okamoto K., *Polymer*, **2006**, 47, 4370 - 4377.

Tang J., Sun W., Tang H., Radosz M., Shen Y., *Macromolecules*, **2005a**, 38, 2037 - 2039.

Tang J., Tang H., Sun W., Plancher H., Radosz M., Shen Y., *Chem. Commun.*, **2005b**, 3325 - 3327.

Tarasevich M.R., Karichev Z.R., Bogdanovskaya V.A., Kuznetsova L.N., Efremov B.N., Kapustin A.V., *Russian J. Electrochem.*, **2004**, 40, 653-656.

Thomas W., *Chem Rev.*, **1999**, 99, 2071 - 2083.

Toi K., Morel G., Paul D.R., *J. Appl. Polym. Sci.*, **1982**, 27, 2997 - 3005.

Trischler F.D., Kjoller K.J., Levine H.H., *J. Appl. Polym. Sci.*, **1967**, 11, 1325 - 1331.

Trischler F.D., Calif. S.D., *U.S. Patent*, **1971**, US 3578644.

Trischler F.D., Levine H.H., *J. Appl. Polym. Sci.*, **1969**, 13, 101 - 106.

- Tsujita Y., *Prog. Polym. Sci.*, **2003**, 28, 1377 - 1401.
- Tsur Y., Levine H.H., Levy M., *J. Polym. Sci. Polym. Chem.*, **1974**, 12, 1515 - 1529.
- Uhlmann D.R., Renninger G., Kritchevsky G., Vander Sande J., *J. Macromol. Sci. Phys.;*
Part B, **1976**, 153 - 172.
- Vaidya P.D., Kenig E.Y., *Chem. Eng. Technol.*, **2007**, 30, 1467 - 1474.
- Van Amerongen G.J., *J. Appl. Polym. Sci.*, **1950**, 5, 307 - 332.
- Van Krevelen DW., *Properties of polymers: Correlation with chemical structure*,
Amsterdam: Elsevier Science, **1997** (Chapter 7).
- Varma I.K., Veena C., *J. Polym. Sci., Polym. Chem. Ed.*, **1976**, 14, 973 - 980.
- Veith W.R., Howell J.M., Hsieh J.H., *J. Membr. Sci.*, **1976**, 1, 177 - 220.
- Versteeg G.F., Van Swaaij W.P.M., *Chem. Eng. Sci.*, **1988**, 43, 573 - 585.
- Victor J.G., Torkelson J.M., *Macromolecules*, **1987**, 20, 2241 - 2250.
- Vieth W.R., Tam P.M., Michaels A.S., *J. Colloid and Interface Sci.*, **1966**, 22, 360 - 370.
- Vieth W.R., Howell J.M., Hsieh J.H., *J. Membr. Sci.*, **1976**, 1, 177 - 220.
- Vogel H., Marvel C.S., *J. Polym. Sci.*, **1961**, 50, 511 - 539.
- Vogel H., Marvel C.S., *J. Polym. Sci. ; Part A: Gen. Papers*, **1963**, 1, 1531 - 1541.
- Vogel H., Marvel C.S., *US Patent*, **1966**, US 26065.
- Wainright J.S., Wang J.-T., Weng D., Savinell R.F., Litt M., *J. Electrochem. Soc.*,
1995, 142, 121 - 123.
- Wang J., Song Y., Zhang C., Ye Z., Liu H., Lee M-H, Wang D., Ji J., *Macromol. Chem.*
Phys., **2008**, 209, 1495 - 1502.
- Wang R., Li D.F., Zhou C., Liu M., Liang D.T., *J. Membr. Sci.*, **2004**, 229, 147 - 157.
- Wang Z., Chen T., Xu J., *J. Appl. Polym. Sci.*, **2002**, 83, 791 - 801.
- Washiro S., Yoshizawa M., Nakajima H., Ohno H., *Polymer*, **2004**, 45, 1577 - 1582.
- Way J.D., Noble R.D., *Facilitated Transport*, in Ho W.S.W., Sirkar K.K. (Eds.),
Membrane Handbook, Van Nostrand, Reinhold, NY, **1992**, pp 833 - 866.
- Wilks B.R., Chung W.J., Ludovice P.J., Rezac M.E., Meakin P., Hill A.J., *J. Polym. Sci.*,
Part B: Polym. Phys., **2006**, 44, 215 - 233.
- Wolfe J.F., *Encycl. Polym. Sci. Eng.*, **1987**, 11, 601 - 635.
- Xiao L., Zhang H., Jana T., Scanlon E., Chen R., Choe E.-W., Ramanathan L.S., Yu S.,
Benicewicz B.C., *Fuel Cells*, **2005**, 5, 287 - 295.

- Xiao L., Zhang H., Choe E.-W., Scanlon E., Ramanathan L.S., Benicewicz B.C., *ACS Division of Fuel Chemistry, Preprints*, **2003a**, 48, 447 - 448.
- Xiao L., Zhang H., Jana T., Scanlon E., Chen R., Choe E.-W., Ramanathan L.S., Yu S., Benicewicz B.C., *Fuel Cells*, **2005**, 5, 287 - 295.
- Xiao L., Zhang H., Choe E.-W., Scanlon E., Ramanathan L.S., Benicewicz B.C., *Abstracts of Papers, 225th ACS National Meeting, New Orleans, US*, **2003b**, Fuel-211.
- Xu H., Chen K., Guo X., Fang J., Yin J., *J. Membr. Sci.*, **2007**, 288, 255 - 260.
- Yamaguchi I., Osakada K., Yamamoto T., *Macromolecules*, **2000**, 33, 2315 - 2319.
- Yamaguchi I., Osakada K., Yamamoto T., *Macromolecules*, **1997**, 30, 4288 - 4294.
- Yamanaka J., Matsuoka H., Kitano H., Hasegawa M., Ise N., *J. Am. Chem. Soc.*, **1990**, 112, 587 - 592.
- Yu B., Zhoua F., LiuG., Liang Y., Huck W.T.S., LiuW., Supplementary material for *Chem. Comm.*, **2006**, 22, 2356 - 2358.
- Zao H., *Chem. Eng. Comm.*, **2006**, 193, 1660 - 1677.
- Zhang H., Chen R., Ramanathan L.S., Scanlon E., Xiao L., Choe E.-W., Benicewicz B.C., *ACS Division of Fuel Chemistry, Preprints*, **2004**, 49, 588 - 589.
- Zhang J., Hou X., *J. Membr. Sci.*, **1994**, 97, 275 - 282.
- Zhang J., Xiaohuai H., *Gaofenzi Xuebao*, **1995**, 3, 278 - 283.
- Zimmerman C.M., Singh A., Koros W.J., *J. Membr. Sci.*, **1997**, 137, 145 - 154.
- Zolandz R.R., Fleming G.K., Gas permeation theory and applications, in: Ho W.S.W., Sirkar K.K. (Eds.), *Membrane Handbook*, Van Nostrand Reinhold, New York, **1992**, pp. 25 - 53, 78 - 94.

Synopsis of the thesis:
**“STRUCTURE - GAS PERMEATION PROPERTY CORRELATIONS IN
POLYBENZIMIDAZOLES AND RELATED POLYMERS”**

by
Santosh C. Kumbharkar
Polymer Science and Engineering Division, National Chemical Laboratory,
Dr. Homi Bhabha Road, Pune- 411 008

Preamble

Gas separation using polymeric membranes is a fast growing area of membrane technology owing to its competitiveness over conventional methods like cryogenic or PSA. It has lower capital / operating costs and processing flexibility. New material investigations aiming at improved permeation properties (combined high permeability and selectivity) is reported in the literature for various families of polymers (polyimides¹, polysulfones², polycarbonate³, etc.), blends of polymers⁴, composites with small organics⁵, etc. Most of these materials need operational temperatures to be lower and controlled atmosphere to retain their performance. To meet stringent challenges, material with not only better permeation properties, but also with better processing capability and stability towards harsher operational conditions need to be investigated.

Polybenzimidazole (PBI) is widely demonstrated as the proton exchange membrane material for fuel cell⁶, where it is known to be stable at high temperatures and oxidative environment. These characteristics suggest potentials of PBI to be used as the gas separation membrane material where harsher chemical / temperature environments are involved. Most of the polymeric membranes for such applications require cooling of the gas mixture to ambient temperatures. Significant economic benefits could be realized if these separations are performed at elevated temperatures. PBI, as a family of polymers

could be best suited for such applications which would retain its thermo-chemical and mechanical stability at elevated temperatures and high pressures; while maintaining its permeation properties to acceptable levels (where common polymers usually show lowering in selectivity). Moreover, PBI could be used in presence of reactive or acid gases like NH_3 , H_2S or CO_2 . A major draw-back of PBI is that it has very low gas permeability. This may be the reason for the less attention drawn towards gas permeability investigations in PBI. There are only couple of references available describing permeation properties of PBI. It was thought that through appropriate structural architecture, permeability of PBI can be improved without large sacrifice on its thermo-chemical stability, and becomes the objective of the present work. Initially, permeability of a series of PBIs obtained by condensation of 3,3'-diaminobenzidine with aromatic dicarboxylic acids having different types of substituent was examined; followed by N-substitution and quaternization of PBI. Structure-gas permeation property relationship in PBI and these related polymers was studied to explore their potentials. The work done towards achieving this goal has been presented into following chapters in this thesis.

Chapter 1: Introduction

This chapter briefly reviews applications of gas separation using polymeric membranes and their advantages over the conventional processes. Rational for the work describes requirement of gas separation membrane materials and potentials of PBI to be used for this purpose. Scope of the work is followed by aims and objectives. This chapter ends with organization of the thesis.

Chapter 2: Literature survey

This chapter begins with theoretical aspects of gas permeation. Factors affecting gas permeation properties in polymeric membranes are briefly described. This is followed by effects of systematic structural variation on gas permeation properties in different family of polymers. In view of importance of CO₂ separation in current scenario and possible applicability of PBI for this purpose, materials specifically used for CO₂ separation are reviewed. At the end of the chapter, permeation and physical properties of PBI and synthetic aspects are reviewed.

Chapter 3: Experimental

This chapter deals with PBI synthesis, procedures used for polymer characterization, sorption and gas permeation analysis. Experimental procedures optimized during synthesis of different PBIs with structural variations in acid moiety while keeping diamine same, viz., 3,3'-diaminobenzidine (DAB) is described. The protocol set for preparation of N-substituted PBI and quaternization of nitrogen of imidazole moiety in PBI with appropriately chosen alkyl iodides is given. After quaternization, exchange of iodide anions with select anions, those are known to improve CO₂ sorption in ionic liquids was performed. Dense membrane preparation followed by characterization of physical properties that are known to affect gas permeation is presented. The methods and equipments used for gas sorption and permeation analysis are described.

Results and discussion is divided into 3 chapters as given below.

Chapter 4: Variations in acid moiety of PBI based on DAB: Synthesis, characterization and investigation of gas permeation properties

In order to examine effects of substitution site, substituent polarity and its bulk, a series of PBI was synthesized while varying the acid moiety (where various substitutions can be systematically addressed). In the series, the tetramine was kept same as 3,3'-diaminobenzidine (DAB). This chapter presents results obtained and discussion on these initial structure-permeability explorations with select gases (H_2 and O_2). This investigation revealed that only 5-*tert*-butylisophthalic acid (PBI-BuI) and 4,4'-(hexafluoroisopropylidene)bis(benzoic acid) based PBI (PBI-HFA) offered acceptable permeability, though all other PBIs exhibited 2 to 6 times higher selectivity than for the common polymers like polysulfone and polyarylate. Thus, investigations with these two polymers, along with PBI based on isophthalic acid (PBI-I) were continued for the determination of physical properties, sorption and permeation of gases of industrial significance (He, H_2 , O_2 , N_2 , CH_4 and CO_2). Incorporation of hexafluoroisopropylidene and *tert*-butyl groups led to decreased chain packing. PBI based on 4,4'-(hexafluoroisopropylidene)bis(benzoic acid) and 5-*tert*-butyl isophthalic acid exhibited 10–40 times higher permeability, while changes in selectivities for industrially important pairs ranged from modest decrease of 75% or less, than that of PBI based on isophthalic acid. Occurrence of permeation characteristics (especially P_{H_2} and P_{H_2}/P_{N_2}) near Robeson's upper bound, high thermal stability and good solvent solubility achieved by these structural modifications depicted the potential of this family of polymers as gas separation membrane material.

Chapter 5. Effects of N-substitution on physical and gas permeation properties of resulting polybenzimidazoles

N-H group of PBI was substituted by appropriately chosen alkyl halides. Results and discussion based on physical and gas permeation properties of this class of polymers are presented in this chapter. N-substitution was done with three selected PBIs viz., PBI-I (base case), PBI-BuI (bulky substitution) and ABPBI (rigid backbone) based on 3,4-diaminobenzoic acid. Synthesis and characterization of physical properties are discussed, followed by gas sorption and permeation properties.

N-alkylated PBIs containing methyl, butyl, methyltrimethylsilyl and *tert*-butylbenzyl group were obtained by reacting Na-salt of PBI and respective alkyl halide. The nature of substituent (bulk and flexibility) showed its own effect on permeation properties of resulting N-substituted PBI. In comparison to the parent PBI, N-methyl substituted PBIs exhibited increase in permeability upto ~ 3 times for various gases, while reduction in selectivity was upto ~ 40 % for various gas pairs. On the other hand, corresponding increase in permeability caused by bulky methyl-trimethylsilyl and *tert*-butylbenzyl substitution was upto ~ 100 times. Gas sorption analysis revealed that these variations were largely contributed by changes in penetrant diffusivity, rather than solubility in polymer matrix.

Chapter 6. Investigations in polymeric forms of ionic liquids, (PILs) based on polybenzimidazoles: Emphasis on CO₂ permeation properties

This chapter deals with quaternization of nitrogen of imidazole ring belonging to PBI. High CO₂ sorption in ionic liquids is known. Tang et al.⁷ have demonstrated that polymeric forms of ionic liquids too show high CO₂ sorption. Polymers demonstrated by

Tang et al. have aliphatic backbone, while most of the ionic liquids demonstrated in the literature (which show high CO₂ sorption) are based on imidazolium salts. It was thought that PBI can be converted in to polymeric forms of ionic liquids (PIL) by N-quaternization of imidazole ring of PBI, followed by anion exchange. These PILs were obtained from three promising PBIs (PBI-I, PBI-BuI and ABPBI), while anions studied were iodide [I⁻], tetrafluoro borate [BF₄⁻] and bis(trifluoromethane)sulfonimide [Ntf₂⁻]. The uplift of CO₂ sorption was highest for ABPBI based PILs, followed by for PBI-I and PBI-BuI based PILs.

Chapter 7. Conclusions

This chapter summarizes the results obtained and conclusions of this work.

References

- 1) M.R. Coleman, W.J. Koros, J. Membr. Sci. 50 (1990) 285.
- 2) J.S. Mchattie, W.J. Koros, D.R. Paul, Polymer 33 (1992) 1701.
- 3) M.W. Hellums, W.J. Koros, G.R. Husk, D.R. Paul, J. Membr. Sci.46 (1989) 93.
- 4) B.S. Kirkland, D.R. Paul, Polymer 49 (2008) 507.
- 5) G.J. Francisco, A. Chakma, X. Feng, J. Membr. Sci. 303 (2007) 54.
- 6) R. He, Q. Li, A.Bach, J.O. Jensen, N.J. Bjerrum, J. Membr. Sci. 277 (2006) 38.
- 7) J. Tang, W. Sun, H. Tang, M. Radosz, Y. Shen, Macromolecules 38 (2005) 2037.

Signature of the Candidate

(Mr. S.C. Kumbharkar)

Signature of the Research Guide

(Dr. U. K. Kharul)

Publications

- 1) **S.C. Kumbharkar**, P.B. Karadkar, U.K. Kharul, "Enhancement of gas permeation properties of polybenzimidazoles by systematic structure architecture", *J. Membr. Sci.* **286** (2006) 161-169
- 2) **S.C. Kumbharkar**, Md. Nazrul Islam, R.A. Potrekar, U.K. Kharul, "Variation in acid moiety of polybenzimidazoles: Investigations toward their applicability as proton exchange and gas separation membrane materials", Revision submitted to *Polymer*.
- 3) **S.C. Kumbharkar**, U.K. Kharul, "Effects of *N*-substitution of PBI on physical and gas permeation properties of resulting polybenzimidazoles", to be communicated.
- 4) **S.C. Kumbharkar**, U.K. Kharul, "Investigations in polymeric forms of ionic liquids (PILs) based on polybenzimidazoles: Emphasis on CO₂ permeation properties", Under preparation.

Presentations in conferences

- 1) **S.C. Kumbharkar**, U.K. Kharul - Gas permeability investigations in substituted polybenzimidazoles; Oral presentation at 8th *International Conference on Catalysis in Membrane Reactors (ICCMR8)* held at CGCRI, Kolkata; 18 - 21 Dec. 2007.
- 2) **S.C. Kumbharkar**, P.B. Karadkar, U.K. Kharul - Gas separation properties of polybenzimidazoles; Presented at 9th *National conference of Polymers for Advanced Technologies; 'MACRO 2006'* held at National Chemical Laboratory, Pune; 17 - 20 Dec. 2006.
- 3) Md. N. Islam, R. Kannan, **S.C. Kumbharkar**, U.K. Kharul, P.C. Ghosh, K. Vijaymohan, S.P. Vernekar; Proton Exchange Membranes Based on Polybenzimidazole: Performance Evaluation for Hydrogen Oxygen Fuel Cells; Presented at 9th *National conference of Polymers for Advanced Technologies; 'MACRO 2006'* held at National Chemical Laboratory, Pune; 17 - 20 Dec. 2006.
- 4) **S.C. Kumbharkar**, P.M. Chincholkar, R.A. Potrekar, U.K. Kharul; Presented at National Seminar on "*Membrane Science & Technology: Challenges & Opportunities*", held at RRL, Jorhat; February 12 - 13, 2004.
- 5) **S. C. Kumbharkar**, R. A. Potrekar, U.K.Kharul; third prize for Poster Presentation held at NCL; Organized by Society of Polymer Science; Pune Chapter 26th July 2004.